# QUANTIFYING THE COLOUR APPEARANCE OF DISPLAYS

**Youngshin Kwak**

A thesis submitted in partial fulfilment of the requirements of the University of Derby for the degree of Doctor of Philosophy

June 2003

# Thesis Redaction Requirements

**Thesis Title**: *Quantifying the colour appearance of displays*

**Author:** *Youngshin Kwak*

**Date:** *2003*

**Please redact the following / features aspects of this thesis:**

**Whole pages**

**Part pages**

**Chapters**

**Images /Captions**
*Fig 2-1 on page 8*

**Other**
*Fig 2-3 on page 10*
*Fig 2-5 on page 14*
*Fig 2-13 on page 30*
*Table 2-1 on page 31*

**Copyright Officer**

**(signed)** C Bell **Date** 18.12.13

**Pp**_____

For queries please contact Interlending: University of Derby 01332 591204

# Contents

# List of Tables

# List of Figures

# Abstract

The LUTCHI data are the main colour appearance data used as the basis of many colour appearance models including CIECAM97s. It was shown in the LUTCHI data that projected colours are very different from reflective colours however there are relatively fewer data for projected colours than for reflective colours. In this study, it is intended to expand the colour appearance data of projected and self-luminous colours. The additional colours would then help investigate the performance of existing colour appearance models and, if necessary, enable the derivation of a new model to improve performance for projected and self-luminous colours.

Before the colour appearance study, firstly the performances of the instruments and the displays used in the study were investigated. It was found that LCD displays perform very differently from CRT monitors. Two mathematical characterisation models for LCD displays were developed named S-Curve Model I and S-Curve Model II.

The new colour appearance data set, CII-Kwak, was accumulated by a series of psychophysical experiments. The magnitude estimation technique was applied with the same experimental set-up as for LUTCHI experiments. The CII-Kwak data set has 20 phases with a total of 28,608 estimations covering various displays, luminance of a reference white, background luminance factors, surround conditions and stimulus sizes.

Based on the CII-Kwak and the LUTCHI data set, the colour appearance phenomena were analysed. It was found that there are systematic colour appearance changes by the viewing factors investigated. Also eight colour appearance models were tested using the CII-Kwak and LUTCHI data sets. CIECAM97s-based models performed similarly well, but all models tested failed to predict several colour appearance changes, especially under dark surround conditions, which lead to suggest a new colour appearance model to have a better performance for colour appearance predictions.

The Kwak03 model was derived from the CIECAM02 with several major modifications such as the cone signal ratios and the omission of the dynamic function. The Kwak03 model was shown to outperform all the other colour appearance models tested and also to be capable of predicting all colour appearance phenomena found in this study with good accuracy.

# Acknowledgements

This thesis is the culmination of four years of PhD study. It could not have been produced without support and advice from many people around me. I would like to take this opportunity to express my gratitude to them.

First of all, I would like to thank my supervisors, Professor Lindsay W. MacDonald and Professor M. Ronnier Luo for their guidance throughout my research. It was a particularly instructive experience to learn two different supervising styles at the same time, which made the perfect combination for the progress of my studies. I should also like to thank Professor MacDonald especially, for giving me an opportunity to study at CII with him. I will always think that I was lucky to meet him in South Korea five years ago.

In addition, I would like to thank Dr. Robert W. G. Hunt, not only for his personal comments on my research, which were always very valuable, but also for his work in colour appearance modelling, which is awesome in its extent and depth. While I was writing this thesis, I came to realise how much of the basis for colour appearance modelling is grounded in his research.

Of course, I should not forget to mention the observers who took part in my experiments. A total of 33 people volunteered to do my experiments. Half of my study is based on their effort and the time they gave up for me. I really appreciate their patience in spending so much time in a dark room, and most importantly, their being glad to do my experiments.

I would like to thank all the students and staff at CII for their friendship and help, with special thanks to my office mates, with whom I spent most of my time.

Finally I send my love and thanks to my family and friends in Korea, who have taught me that I can be happy and feel very supported whatever I do or wherever I go, because they have a strong faith in me and will be there for me all the time.

# Chapter 1
# Introduction

## 1.1 Background

In 1973 Wyszecki described the basic and advanced colorimetry [Wysz1973, Fair1997 p.63]. Similarly Hunt stated that 'future historians may distinguish three phases in the development of colorimetry: matching, differences, and appearance' [Hunt1977a]. Since then, the development of colour science has been following the steps they predicted.

The first stage of colorimetry is colour specification, which provides nominal values to a given colour providing a tool to predict whether or not two colours will match in a given condition. This stage corresponds to Wyszecki's basic colorimetry. The CIE colour specification system, normally designated as CIE Colorimetry, was established for this purpose for the first time in 1931; it has not been changed much since then (see Section 2.4). In many industrial applications, it is more important to define the colour difference between two colours rather than to give mere numbers to represent them; this marks the second phase of colorimetry: colour difference equations. In 1976, the CIE recommended two standard colour difference equations, CIELAB and CIELUV. The CIELAB formula has been widely used and many advanced formulae have been developed based on its space [Luo1999].

The third phase of colorimetry is concerned with colour appearance, i.e. describing what colours look like. This phase is called advanced colorimetry, defined according to Wyszecki as the method of assessing the appearance of colour stimuli presented to

observers in the complicated surroundings of everyday life. This is considered the ultimate goal of colorimetry.

Various colour appearance models have been developed over the years (see Section 2.8). Current colour appearance models require tristimulus values, the outcome of the first phase of CIE colorimetry, as input data. The output of the models are numbers corresponding to the perceived colour attributes such as lightness, chroma, hue etc. It was in 1997 that the colour appearance model, CIECAM97s, was recommended by CIE for the first time. In 2002, the second recommendation, CIECAM02, followed based on the several revisions of CIECAM97s. The third phase of colorimetry, however, is still in its early stages. In spite of rigorous research into colour appearance modelling, current models still have limitations. The performance of a model is primarily limited by the experimental data available to derive and test it. Currently the LUTCHI data set is the only colour appearance data set available for directly developing colour appearance models (see Section 2.6).

## 1.2 Aims of the Investigation

The intention of this thesis is to take another small step towards the ultimate goal of colorimetry. Its purpose is to accumulate new colour appearance data and derive a new colour appearance model with better performance than the previous models. Its particular focus is the colour appearance of displays. The role of the display is becoming more and more important in modern life, with the fast development of display technology and the increasing role of colour management systems in applying these displays. A reliable colour appearance model is vital to colour management systems.

The aims of the investigations were (1) to accumulate a comprehensive set of colour appearance data for self-luminous and projected colours, (2) to compare and analyse the parameters affecting colour appearance, (3) to test the ability of various colour spaces and models to predict the present and earlier data, and (4) to derive new colour appearance model accurately to predict the available experimental data.

The new colour appearance data, CII-Kwak, were rendered compatible with the LUTCHI data by applying the same experimental techniques. The CII-Kwak data set

covers the appearance of display colours made with an LCD projector, a 35-mm slide projector, an LCD monitor and a CRT monitor. The impact of colour appearance changes created by various viewing parameters was also investigated. These parameters included luminance level, background luminance factor and surround condition. The CII-Kwak data set comprises 20 phases with a total of 28,608 visual assessments.

The emphasis of this study was to quantify the colour appearance change by viewing parameters. For testing the performance of colour appearance models, not only the errors in fitting the colour appearance data but also the predictions of colour appearance phenomena were investigated. A new colour appearance model, Kwak03, was also developed to give better performance in predicting colour appearance phenomena, especially for the effect of colour appearance change by luminance level and background luminance factor.

## 1.3 Thesis Outline

The flow chart shown below represents the process used in this study from accumulating colour appearance data to deriving a new colour appearance model. The structure of this thesis is based on this chart. The nine chapters detail the aims of the investigation. An overview of each chapter is given below.

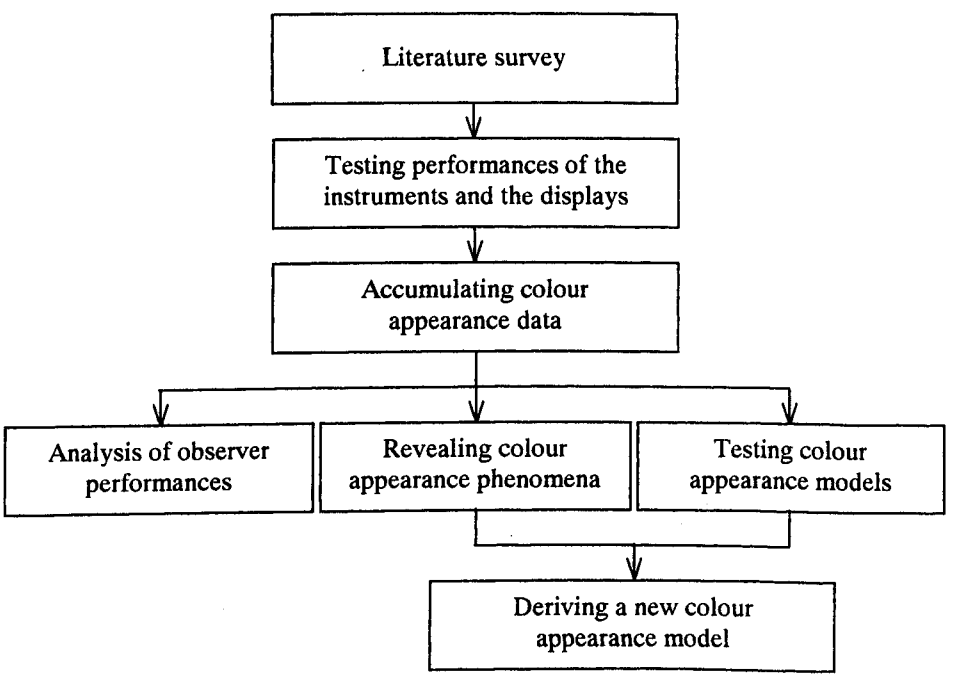

Chapter 2 reviews the background information related to this subject. It first introduces the structure and mechanism of human vision, psychophysical experimental techniques and CIE colorimetry, and then reviews colour appearance phenomena and models.

Chapter 3 describes the performances of the displays and the colour measurement instruments used in this study. New mathematical characterisation models, S-Curve Model I and S-Curve Model II, were also developed and are reported for LCD monitors and projectors.

Chapter 4 describes the details of the CII-Kwak colour appearance data set including the experimental set-up, scaling methods and data analysis methods.

Chapter 5 describes the observer performances in terms of repeatability and accuracy. Other factors affecting the observer responses during the experiments are also discussed, for example previous experiments on colour appearance and the number of observers participating in the experiment.

Chapter 6 describes the colour appearance phenomena found in the CII-Kwak and LUTCHI data sets. The data were analysed in terms of the systematic colour appearance changes due to the luminance levels, background luminance factors, surround conditions and size of viewing field.

Chapter 7 describes the performance of eight colour appearance models tested using the CII-Kwak data set and part of the LUTCHI data. The models tested were CIELAB, LLAB, RLAB, Hunt94, CIECAM97s, FC, Fairchild and CIECAM02.

Chapter 8 describes a new colour appearance model, Kwak03, which was derived from the CII-Kwak and LUTCHI data sets. The structure and each computation step of the model are given in this chapter.

Chapter 9 summarises the findings of this study and discusses future directions for the development of colour appearance research.

## 1.4 Publications

Eleven papers, consisting of 2 journal papers and 9 conference papers, have been published with results from the author's study and are listed below.

1. Y. Kwak and L. MacDonald, Characterisation of a desktop LCD projector, *Displays*, **21**, 179-194, (2000)

2. Y. Kwak and L. W. MacDonald, M. R. Luo, Quantifying colour appearance for projected images, *Proc. 2000 AIC Meeting Seoul*, Seoul, Korea, (Nov. 2000)

3. L. W. MacDonald and Y. Kwak, Characterisation of an LCD projection display, *Proc. SID@EID*, London, (Nov. 2000)

4. Y. Kwak and L. W. MacDonald, Method for characterising the LCD projector, *Proc. IS&T/SPIE's 13th Annual Symposium on Electronic Imaging: Science and Technology, Projection Displays*, San Jose, California USA, (Jan. 2001)

5. Y. Kwak, L. W. MacDonald and M. R. Luo, Colour appearance comparison between LCD projector and LCD monitor colours, *Proc. 2001 AIC,* Rochester, USA, (Jun. 2001)

6. Y. Kwak and L. W. MacDonald, Accurate prediction of colours on liquid crystal displays, *Proc. 9th Color Imaging Conference,* Scottsdale, USA, (Nov. 2001)

7. Y. Kwak, L. W. MacDonald and M. R. Luo, Colour appearance estimation under cinema viewing conditions, *Proc. CGIV'2002 First European Conference on Color in Graphics, Imaging and Vision*, Poitiers, France, (Apr. 2002)

8. Y. Kwak, L. W. MacDonald and M. R. Luo, Mesopic colour appearance, *Proc. IS&T/SPIE's 15th Annual Symposium on Electronic Imaging: Science and Technology, Human Vision and Electronic Imaging VIII*, Santa Clara, California USA, (Jan. 2003)

9. Y. Kwak, C. Li and L. MacDonald, Controling color of liquid-crystal displays, *Journal of the SID*, **11/2**, (2003)

10. Y. Kwak, L. W. MacDonald and M. R. Luo, New colour appearance model – Kwak03 , *11th Color Imaging Conference,* Scottsdale, USA (2003)

11. Y. Kwak, L. W. MacDonald and M. R. Luo, Modelling the lightness predictor under mesopic vision based on CIECAM02, *11th Color Imaging Conference,* Scottsdale, USA (2003)

# Chapter 2
# Literature Survey

## 2.1 Introduction

As stated in Chapter 1, the purpose of this thesis includes collecting new colour appearance data and colour appearance modelling. It is necessary, in order to follow the author's study, to have a general understanding of colour science. In this chapter, the background information needed elsewhere in this thesis is introduced. An outline of the chapter is given below.

Firstly, the physiological aspects of human colour vision are introduced, followed by the psychophysical experimental techniques used for studying colour science. CIE colorimetry, which is the fundamental for colour specification, and colour measurement instruments are described.

The last four sections cover the topics directly related to the collection of new colour appearance data sets and the development of new colour appearance models. At the outset, the terminology used in relation to the colour appearance modelling is introduced. Then the primary colour appearance data used for deriving the latest colour appearance models, the LUTCHI data set, are introduced, and the descriptions of the colour appearance phenomena follow. The particular focus is on the colour appearance change by the luminance level of the reference white, background luminance factor and surround condition. Finally the structures and the equations of eight colour appearance models are introduced: CIELAB, RLAB, LLAB, Hunt94, CIECAM97s, Fairchild, FC and CIECAM02.

## 2.2 Human Colour Vision

In this section, physiological aspects of human colour vision are introduced, focusing on the aspects needed for colour appearance modelling.

### 2.2.1 Construction of the Eye

Construction of the eye is introduced here based on Section 1.3 of 'Measuring Colour' written by Hunt [Hunt1998]. Figure 2–1 shows the cross-sectional diagram of the human eye [Hunt1998, Section 1.3]. The visual stimulus enters through the cornea, where most of the refracting power is provided by its curved surface. The lens then controls the power by changing its shape according to the viewing distance of the stimulus. The cornea and lens acting together form a small inverted image of the outside world on the retina, the light-sensitive layer of the eye. The iris has a hole in the centre called the pupil. The size of the pupil changes according the amount of light entering the eye. It increases from 2mm in diameter in bright light up to a maximum of 8mm in diameter in dim light. The changing pupil size provides some compensation for changes in the level of illumination, expanding the luminance range that the human eye can perceive. The retina, containing photoreceptors, lines the back of the eye.

*Figure 2–1 Cross-sectional diagram of the human eye [Hunt1998, Fig. 1.2. in p.20]*

Photoreceptors are not uniformly distributed on the retina, causing the non-uniform visual sensitivity over its area. Colour vision is limited to stimuli seen within about 40° of the visual axis [Hurv1981 p.21]. The ability to see colour is best in the area called the fovea, gradually deteriorating at the outer part of retina until it is virtually monochromatic and used mainly for the detection of movement. The fovea lies about 4° to one side, as shown in Figure 2–1, and comprises approximately the central 1.5°

diameter of the visual field. At about 10° to the other side of the optical axis is the blind spot, where the nerve fibres connecting the retina to the brain pass through the surface of the eyeball, and where there is no room for photoreceptors.

### 2.2.2 The Retinal Receptors

The human eye has two classes of retinal photoreceptors: the rods and cones, named after their shapes. The most important distinction between rods and cones is in their visual functions. There is only one type of rod in the retina. The function of rods is to give monochromatic vision under low luminance levels. The cones have three types, so called $\rho$, $\gamma$ and $\beta$, which have maximum sensitivities to the short, medium and long wavelengths of the spectrum respectively, and are involved in colour vision at higher luminance levels.

Rods and cones are also different in their spectral sensitivities, as illustrated in Figure 2–2. Currently, there is no standardised spectral sensitivity curves for cones. Three full lines represent the relative sensitivity of 2° cone fundamentals, based on the data by Stockman and Sharpe [Stoc2000], which are defined as linear combinations of the Stiles and Burch [Stil1959] 10° colour matching functions. The broken line represents the spectral sensitivity of the rods obtained by having observers adjust the strength of a beam of light of one wavelength until the sensation it produces has the same intensity as a beam of fixed strength at a reference wavelength [CIE1951]. This curve is also known as the CIE spectral luminous efficiency for scotopic vision, $V'(\lambda)$.

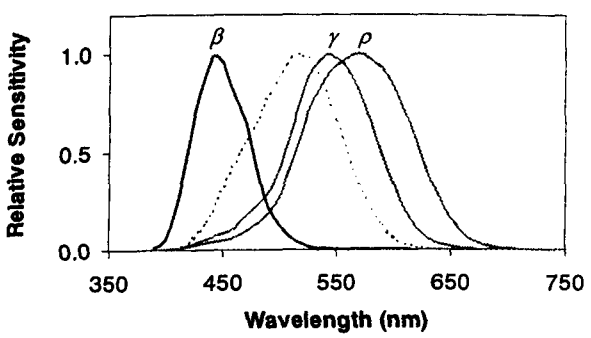


*Figure 2–2 Spectral sensitivity curves for cones (full lines) and rod (broken line) (Refer http://cvrl.ucl.ac.uk/ for the data)*

*Scotopic* vision is in operation when the stimuli have luminances of less than some hundredths of a cd/m$^2$ and only rods are active. Vision served only by cones is called

*photopic* vision and requires luminances of several cd/m$^2$ or more. Vision in which both rods and cones are active is called *mesopic* vision.

As mentioned in the previous section, cones and rods are not uniformly distributed on the retina. Figure 2–3 shows the distribution of the density of photoreceptors as a function of location on the human retina. Data are from Osterberg's study [Oste1935] and the diagram is obtained from the website http://webvision.umh.es/webvision /imageswv/Ostergr.jpeg. The cone density is highest in the fovea and falls rapidly outside. In contrast, there are no rods in the fovea and a maximum in a ring around the fovea at about 4.5 mm or 18° from the fovea [Kolb2003].

***Figure 2–3 Density of rod and cone photoreceptors along the horizontal meridian***

Also, it is known that $\beta$ cones are relatively sparsely populated through the retina and completely absent in the most central area of the fovea. There are far more $\rho$ and $\gamma$ cones than $\beta$ cones. These relative populations of the cones must be considered when combining the cone responses to predict higher-level visual responses. In colour appearance studies, the ratio between $\rho$:$\gamma$:$\beta$ cones has been assumed to be 40:20:1, following the study of Walraven and Bouman [Walr1966, Hunt1998 p.223].

### 2.2.3 Mechanisms of Colour Vision

In this section, the historic development of understanding of the mechanism of colour vision is introduced. The theories given here are summarised from 'Chapter 8. Theories and models of color vision' in 'Color science' written by Wyszecki and Stiles [Wysz1982 p.582,583].

For many years the three-component, or trichromatic, theory of colour vision played a dominant role in colour science and an alternative theory of colour vision, known as

opponent-colour theory, was given relatively little attention. In more recent years, zone theories of colour vision have become widely accepted. They bring together the trichromatic theory and the opponent-colour theory by confining the underlying processes postulated by these theories to two separate but sequential zones.

Trichromatic theory, also known as the Young-Helmholtz three-component theory, was developed based on the work of Maxwell, Young and Helmholtz. It assumes the existence of three independent cone types with different spectral sensitivities and also that the signals generated in these cones are transmitted directly to the brain, where "colour sensations" are experienced that correlate in a simple and direct way to the three cone signals. The theory accounts for the experimental data of foveal colour matching by means of additive mixtures of colour stimuli (see Section 2.4.3), but fails to explain several visually observed phenomena. For example, it cannot explain why an observer sees yellow when a red stimulus is additively mixed with a green stimulus in appropriate proportions. Clearly, yellow is perceived as qualitatively different from each of the two components in the mixture.

The appearance of colour stimuli or colour perception is explained with considerable success by the opponent-colours theory, which was proposed by Hering [Heri1964]. Hering noted that certain hues were never perceived to occur together. A colour perception is never described as reddish-green or yellowish-blue, while combinations of red and yellow, red and blue, green and yellow and green and blue are readily perceived. Hering assumed that there were three types of receptors, but his receptors had bipolar responses to light-dark, red-green and yellow-blue. Such processes count for the visual experience of seeing a variety of, but combination-limited, hues of varying saturation and brightness.

When only considering one theory, neither the trichromatic nor opponent-colour theory could give a satisfactory explanation of several important colour vision phenomena. When merged into a single theory, known as zone theory, however, many colour vision phenomena could be explained, such as colour matching, colour discrimination, colour appearance, chromatic adaptation, and other experiments for observers with both normal and defective colour vision. The recent colour appearance models are also based on zone theory. A schematic illustration of the encoding of cone signals for a zone theory is shown in Figure 2–4.

G. E. Muller is usually credited with being the first to introduce the zone-theory concept [Mull1930, Judd1949, Judd1951]. Essentially, zone theory assumes that in Zone 1 there are located three independent types of cone photoreceptor in which colour vision is initiated through the process of absorption of light in the photopigments of the cones and converted into neural signals. This zone theory complies with the basic assumption of trichromacy in the Young-Helmholtz theory and accounts for the experimental data of colour matching. In Zone 2, the cone signals are coded in a neural network that generates three new signals; one achromatic signal and two antagonistic chromatic signals. This zone complies with the basic assumption of the existence of opponent processes in the Hering theory and accounts for many experimental data of colour appearance.

Subsequent zones (Zone 3 in the diagram) in the visual system are thought likely to exist in which further processing of the signals from Zone 2 takes place, but specific assumptions as to the internal structure and functioning of these zones have yet to be developed. In the final zone of the assumed hierarchal structure of the visual system located in the cortex, the signals are interpreted in the context of other visual information (mainly spatial and temporal) received at the same time and in the context of previously accumulated visual experience (memory).

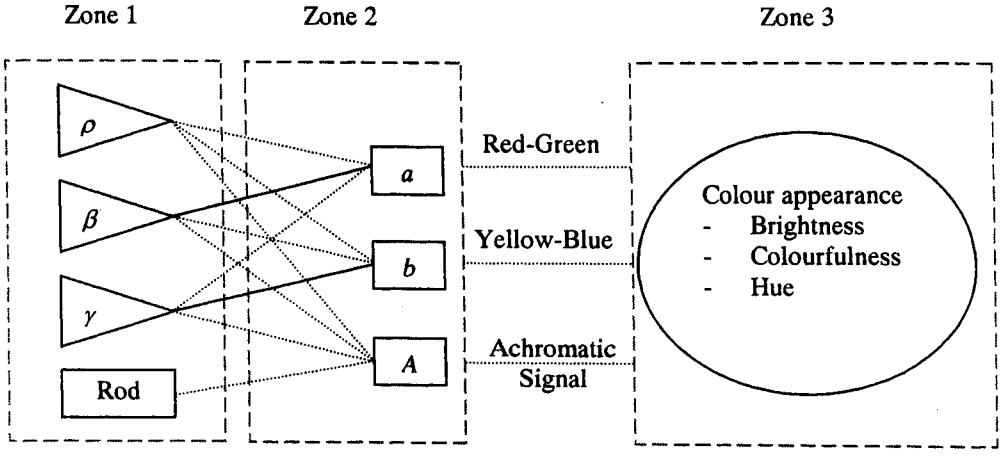


*Figure 2–4 Schematic illustration of the encoding of cone signals for zone theory*

### 2.2.4 Mechanisms of Adaptation

Along with the mechanism of colour signals, another important factor for human vision is the dynamic mechanisms of adaptation that serve to optimise the visual response to a given viewing environment. In particular, luminance and chromatic adaptations play an important role in the development of colour appearance models.

The human eye can function under illumination levels covering at least 10 orders of magnitude, ranging from, for example, a starlit night to a sunny afternoon [Fair1998a p.26]. Instead of having a single response function corresponding to the entire range of illumination levels, the human eye has evolved to have a more efficient system which pursuits the state of the eye to be optimised to a given condition. This process is called luminance or dynamic adaptation. There are several mechanisms contributing to dynamic adaptation. Note that in Section 2.2.1 it was already mentioned that the amount of light entering the eye is controlled by the pupil size, i.e. dilation of the pupil helps to collect more photons for photoreceptors under low luminance levels. Rods also start to work at very low luminance extending the dynamic range. Most importantly, however, dynamic adaptation can be achieved by changing the sensitivity of photoreceptors according to the luminance level of a given scene.

According to Valeton and Norren [Vale1983], there are three sensitivity regulating mechanisms proposed for cones: response compression [Boyn1970], pigment bleaching [Boyn1970] and cellular adaptation [Norm1979]. Response compression is caused by the non-linear relation between stimulus intensity and response of photoreceptors. The pigments of photoreceptors are bleached at very high levels of adaptation and desensitised because fewer quanta from a given stimulus light are absorbed. Cellular adaptation is an active mechanism in the receptor cell that adjusts its operating range to conform to the ambient illumination.

Figure 2–5 illustrates the computational example of shrinking of the range of cone response as luminance level is increased, which is shown by Kaiser and Boynton [Kais1996 p.217]. Curve 1 is for a linear, non-adapting receptor with a fixed pupil. Curve 2 results from the reduction of pupil area. Curve 3 results when the effect of cellular adaptation is combined with pupil response. When the effect of photopigment

bleaching is added Curve 4 results. Receptor response compression brings Curve 4 down to Curve 5. In Section 2.9.4 the Hunt94 colour appearance model illustrates how these mechanisms could be implemented in a colour appearance model.

***Figure 2–5 How four factors are taken into account to shrink the range of cone response [Kais1996 Figure 6.5]***

Chromatic adaptation is a visual mechanism for adapting to changes in the spectral composition from an illuminant entering the eye [Luo2000]. A typical example is a piece of white paper which is seen first in daylight then in tungsten or fluorescent light. Although these lights are completely different, the appearance of the paper remains the same: white. This effect can be thought of as analogous to an automatic white-balance in video cameras. Often it is considered to be the result of independent changes in responsivity of the three types of cone photoreceptors, while dynamic adaptation refers to overall responsivity changes in all of the receptors [Fair1998a p.177].

## 2.3 Psychophysical Experimental Techniques for Colour Science Study

Psychophysics is a scientific method used to study the relationship between stimulus and sensation. It remains a central part of experimental psychology [Gesc1997]. Colour science also requires the understanding of psychophysics since it involves quantifying and understanding the phenomena related to colour perception, one of the human sensations. It is psychophysical techniques that have produced most of our knowledge of human colour vision and colour appearance phenomena. Psychophysical experiments are foundations of CIE colorimetry and colour

appearance models. The psychophysical experiment is also a useful tool to measure image quality, which is a central issue for the development of imaging devices. Image quality means the integrated set of perceptions of the overall degree of excellence of an image [Enge2000]. Fairchild categorised visual experiments into two broad classes [Fair1998a p.44] :

1. Threshold and matching experiments, which are designed to measure visual sensitivity to small changes in stimuli (or perceptual equality).
2. Scaling experiments, which are intended to generate a relationship between the physical and perceptual magnitudes of a stimulus.

Threshold experiments are used to determine the just-noticeable difference (JND) and therefore are useful to measure the visual tolerances such as perceived colour difference. Matching techniques find the stimuli giving the same perception. CIE colorimetry is based on a metameric (see Section 2.4.3) colour matching experiment. Another common use of matching experiment is to find corresponding colours (see Section 2.3.1) for example to derive chromatic adaptation functions.

Scaling experiments directly provide scales of perception that are essential for the development of colour appearance models. The LUTCHI experiments (refer Section 2.7) are examples of the use of scaling technique for colour appearance study.

### 2.3.1 Matching Technique

During a psychophysical experiment using the matching technique, two colours are shown to the observers who are asked to adjust one of the stimuli to match the appearance of the other colour. For example, for CIE colorimetry a given colour is perceptually matched by an additive mixture of red, green and blue lights, which produces a metameric match (see Section 2.4.3).

In the study of chromatic adaptation or colour appearance, it is often necessary to produce a colour match across two different viewing conditions. This is called asymmetric matching. One special case in an asymmetric matching experiment is haploscopic matching [Fair1998a p54, Luo2000]. This technique requires specially designed viewing apparatus, which presents a different adapting stimulus to each of

the observer's two eyes. One eye views a test stimulus in one set of viewing conditions and the other eye simultaneously views a matching stimulus in a different set of viewing conditions. The observer simultaneously views both stimuli and produces a match. For example, a stimulus viewed in daylight illumination might be matched to another stimulus viewed under incandescent illumination. These pairs of colour stimuli that look alike when one is seen in one set of adaptation condition and the other is seen in a different set, are called corresponding colour stimuli [Hunt1998 p.318]. Corresponding colours are used for studying chromatic adaptation. The Hunt Effect and Stevens' experiment on the effect of adaptation were also investigated using this technique (see Section 2.8). The task for haploscopic matching is relatively simple and the results, in general, have higher precision than the other techniques. Its validity, however, is dependent on an assumption in which the adaptation of one eye does not affect the sensitivity of the other eye. This technique also imposes unnatural viewing conditions together with constrained eye movement.

### 2.3.2 Sensory Scaling

Colour appearance models can be developed depending upon the availability of both the stimulus and the sensory response i.e. the perceived quantity of colour appearance. According to Stevens, the methods for constructing psychological scales can be classified into three types: confusion (or discrimination) scaling, partition scaling, and ratio scaling [Stev1960, Gesc1997 p.191]. Each is designed to generate a numerical scale of sensory magnitude, although each requires a different kind of perceptual response from the observer and the resulting scales have different types. Note that there are four types of scales: nominal, ordinal, interval and ratio scales. Nominal scales use the numbers only for classification or identification purposes, like the usage of symbols. An ordinal scale is a set of measurements in which the amount of a specified property of objects or events can be ranked. Only the property of order in the number system can be applied to ordinal scale measurements. If an interval scale has been achieved, the intervals between the scale values represent differences or distances between amounts of the property measured. Thus in an interval scale, both the size of the differences between numbers and their ordinal relationship are meaningful however there is no meaningful zero point on an interval scale. A ratio scale, as well as having the properties of order and distance, has a natural origin to

represent zero amount of a property. In these scales, the ratios of the scale values have meaning [Gesc1997 p.186, Fair1998a p.48].

#### 2.3.2.1. Confusion (Discrimination) Scaling

Confusion (or discrimination) scales of sensation are based on indirect scaling procedures in which sensory magnitudes of stimuli are inferred from measures of stimulus discriminability. Successful confusion scaling results in an interval measurement scale, since discrimination data indicate the differences but not the ratios among sensation magnitudes. Fechner was the first to employ a form of this method in his construction of a psychological scale from difference thresholds. Fechner proposed that sensation magnitude increases with the logarithm of stimulus intensity, which is derived from measurements of just noticeable difference, JND, by considering it a unit of perception [Fech1860, Fech1966]. Later in 1927 Thurstone proposed a mathematical model called the "law of comparative judgement" for constructing a scale from data obtained by paired comparison procedures where each stimulus is compared with all other stimuli [Thur1959].

#### 2.3.2.2. Partition Scaling

Partition scales are obtained by direct scaling procedures in which the observer must make direct judgements of the psychological differences among stimuli. The resulting scales are interval scales because they measure the differences among sensations. There are two main kinds of partition scaling methods, equisection scaling and category scaling [Gesc1997 p.207]. Equisection is a method that requires observers to section the psychological continuum into equal sense distances. In category scaling, the observer is presented with a large number of stimuli and told to assign all of them to a specified number of categories.

The Munsell System [Newh1940,1943, Bern1985, Wybl2000], which is one of the most widely used colour order systems, is based on the partition scaling. Colour order systems mean systematically arranged collections of colour samples. In the Munsell System, colours are arranged to have a constant perceptual difference between any two neighbouring samples for each perceptual attribute.

### 2.3.2.3. Ratio Scaling (using Magnitude Estimation Technique)

It was Stevens [Stev1961] who opposed Fechner's principle and refined the technique of ratio scaling. Stevens proposed that subjective magnitude could be obtained by direct assessments. Stevens' solution to the problem of direct ratio scaling of sensation was simply to present stimuli to observers and ask them to assign numbers to them which seemed to correspond to their sensations. This method is known as magnitude estimation and Stevens' Power Law is based upon the finding that magnitude estimations for a variety of sensory dimensions increase in proportion to the stimulus intensity raised to a power. Stevens claimed that the judgement of subjective magnitude is inherently a noisy phenomenon with large variation between observers, but the Power Law stands out as a first-order relation [Stev1957].

In the experiments involved with magnitude estimation, it is the geometric mean, not the arithmetic mean, that appears to be the appropriate average [Stev1971]. Note that the use of the geometric mean to average the observer responses has a connection with the power law. The power law is stated as $\psi = k\phi^{\alpha}$ where $\psi$ is sensation magnitude, $\phi$ is stimulus intensity, $k$ is an arbitrary constant determining the scale unit, and $\alpha$ is the power exponent which depends on the sensory modality and stimulus conditions. Constant $k$ is also known as the modulus determined by each observer if a standard value is not given. If the Power Law is working, it is clear that average exponent – the average slope between log $\psi$ and log $\phi$ – can be determined by the geometric mean regardless of the different modulus value for each observer.

The magnitude estimation technique has been widely used in the colour science field especially for chromatic adaptation [Isha1970, Naya1972, Rowe1972, Poin1977,1980, Bart1979] and colour appearance study [Stev1958, Luo1991a, 1993a, 1993b, 1997, Kuo1995]. This technique is a preferred method since experiments can be conducted under natural viewing conditions with free eye movement. Experimental results for colour appearance estimation are also directly in relation to those predicted by colour appearance models, and therefore can be used directly to test existing colour appearance models or for deriving new colour models [Luo1991a].

## 2.4 CIE Colorimetry

Colorimetry means the measurement of colour. CIE colorimetry, established in 1931, was the first international standard system to allow the specification of a colour for an average observer and became the foundation of colour science. CIE (Commission Internationale de l'Éclairage) is the international commission on illumination and is responsible for international recommendations for photometry and colorimetry. Measuring colour requires quantifying three components, which are needed to produce the perception of colour: light source, objects and the human visual system. This section deals with how each component is quantified and how they are combined to give final colour measurement data.

Hunt's *Measuring Colour* (3rd Edition), Fairchild's *Colour Appearance Models*, and Wyszecky and Stiles' *Color Science* (2nd Edition) are used as general references for this section on CIE colorimetry [Hunt1998, Fair1997, Wysz1982].

### 2.4.1 Illuminants and Light Sources

A light source is typically measured in term of spectral power distribution, which is a function of wavelength across the visible spectrum. Spectral power is represented by spectral radiance ($W/sr/m^2/nm$), which is the emitted power (energy per unit time) per unit solid angle and per unit area measured in a given direction, at a point in the path of a beam for a given wavelength. The sum of spectral radiance across the spectrum is called radiance ($W/sr/m^2$) [Hunt1998 Appendix9]. A spectroradiometer is commonly used for the measurement of the spectral power distribution of light sources (see Section 2.5).

For standardisation, the CIE distinguishes between illuminants, which are defined in terms of spectral power distributions, and sources, which are defined as physically realisable producers of radiant power. The CIE has established a number of relative spectral power distributions, known as CIE illuminants, for colorimetry. Figure 2–6 shows two CIE Standard Illuminants D65 and A.

Another important quantity often used to represent light sources is the colour temperature. Colour temperature means the temperature of a Planckian radiator (so called black body) whose radiation has the same chromaticity as that of a given

stimulus. Since most light sources are not black body radiators, correlated colour temperature (CCT) is generally used. The CCT of a light source is the colour temperature of a black body radiator that appears to be the closest colour match to the light source in question.

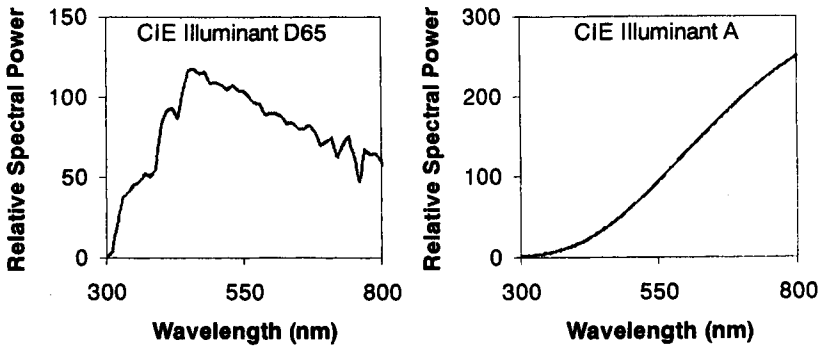


*Figure 2–6 Relative spectral power distributions for CIE illuminants D65 and A*

## 2.4.2 Objects and Standard Measurement Geometry

The second component, which is usually necessary in the formation of a radiant power distribution to the human eye, is an object. Spectral distributions of reflectance and transmittance as a function of wavelength are used for the colour measurement of opaque and transparent objects respectively. Reflectance or transmittance can be measured by comparing the power of incident and reflected or transmitted light, often using the instrument called a spectrophotometer (see Section 2.5).

Note that the reflectance or transmittance of an object is not just a function of wavelength, but also of the illumination and viewing geometry. A glossy sample is a good example of appearance that changes by viewing angle. The CIE has defined four recommended illumination and viewing geometries for reflectance measurements: diffuse/normal (d/0), normal/diffuse (0/d), 45/normal (45/0) and normal/45 (0/45). The designations indicate the illumination geometry before the slash and the viewing geometry following the slash. Note that d/0 and 0/d are optically reversible geometries and so are 45/0 and 0/45.

In the diffuse/normal geometry, the colour sample is illuminated from all angles using an integrating sphere (hollow spheres that are painted white inside) and viewed at an angle near the normal to the surface. In the normal/diffuse geometry, the sample is illuminated from the angle near to its normal and the reflected energy is collected

from all angles using an integrating sphere. In many instruments, an area of the integrating sphere with a gloss trap can be replaced such that the specular component of reflection is excluded and only diffuse reflectance is measured. Such measurements are called 'specular component excluded' measurements; 'specular component included' measurements are made when the entire sphere is intact. Figure 2–7 shows geometries for d/0 specular included (left) and d/0 specular excluded (right).

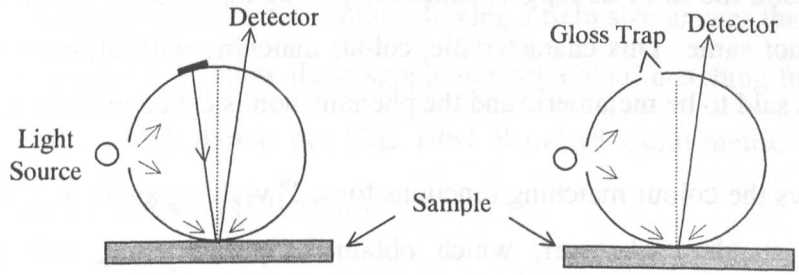


*Figure 2–7 Measurement geometry for d/0 specular included and d/0 specular excluded*

In a 45/0 geometry, the sample is illuminated with one or more beams of light, incident at an angle of 45° from the normal, and measurements are made along the normal and vice versa for 0/45 geometry as shown in Figure 2–8. The 45/0 and 0/45 conditions represent typical viewing of surfaces in directional light and ensure that all components of gloss are excluded from the measurements.

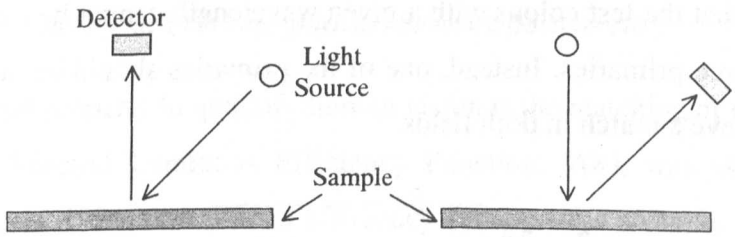


*Figure 2–8 Measurement geometry for 45/0 and 0/45*

### 2.4.3 Standard Observers

For colour vision, the amounts of light observed by the three cone types define the colour of an object or light source that the eye is seeing. Therefore using the sensitivity curves of the three cone types (see Figure 2–2) would be the method to quantify the human eye for colour measurement. The CIE colorimetry system established in 1931, however, needed to use an indirect method to define the standard observer, since the cone spectral sensitivities have never been clearly defined.

For CIE colorimetry, spectral colours were visually matched by an additive mixture of three primaries: monochromatic red, green and blue lights. The test colour to be matched is seen in one half of the field of view, and, in the other half, the observer sees an additive mixture of beams of red, green and blue light. The amounts of red, green, and blue light are then adjusted until the mixture matches the test colour. Note that this colour matching experiment does not produce a spectrally identical colour. Colours would look the same as long as cones are producing the same signals even if the spectra are not same. This characteristic, colour matching with different spectral compositions, is said to be metameric and the phenomenon is called metamerism.

Figure 2–9 shows the colour matching functions for a 2° viewing angle used to derive the CIE 1931 standard observer, which obtained by combining two separate experimental results by J. Guild at the National Physical Laboratory and W.D. Wright at Imperial College. This diagram indicates the amount of the primaries required to match unit amount of power at each wavelength. Units to represent the amount of the primaries are determined so that addition of three primaries matches perceptually with the equi-energy stimulus, $S_E$, of same luminance. The equi-energy stimulus, $S_E$, means the stimulus consisting of equal amounts of power per small constant-width wavelength interval throughout the spectrum [Hunt1998 p.321]. Negative parts in the curves mean that the test colour with a given wavelength cannot be matched with the addition of three primaries. Instead, one of the primaries should be added to the test colour to achieve a match in both fields.

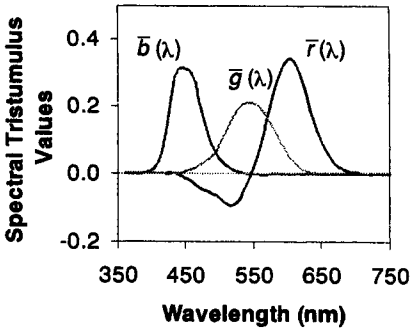


*Figure 2–9 The colour-matching functions for the CIE 1931 Standard Colorimetric Observer*

The colour matching functions, $\bar{r}(\lambda)$ , $\bar{g}(\lambda)$ , $\bar{b}(\lambda)$ in Figure 2–9 were linearly transformed to $\bar{x}(\lambda)$, $\bar{y}(\lambda)$, $\bar{z}(\lambda)$ to avoid the negative parts as shown in Figure 2–10. It also renders the $\bar{y}(\lambda)$ identical to the $V(\lambda)$ function, which will be explained later in

this section. These curves are called the CIE colour matching functions and they define the colour matching properties of the CIE 1931 Standard Colorimetric Observer, often referred to as the 2° observer [CIE1971,1986].

As mentioned in Section 2.2.2, the distribution of photoreceptors across the retina is not uniform, indicating that a match made with a 2° field may not remain a match if the field size is altered. For this reason, in 1964 the CIE recommended a different set of colour matching functions for samples having a field size greater than 4°. Curves in thin lines in Figure 2–10 show these supplementary colour matching functions, $\bar{x}_{10}(\lambda)$, $\bar{y}_{10}(\lambda)$, $\bar{z}_{10}(\lambda)$, which define the CIE 1964 Standard Colorimetric Observer, also known as the 10° observer [CIE1986].

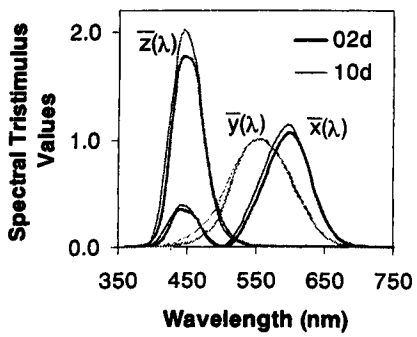


*Figure 2–10 The CIE colour matching functions for the 1931 Standard Colorimetric Observer (02°) and for the 1964 Supplementary Standard Observer (10°)*

Another important property to quantify human vision is the matching of brightness. In 1924, the CIE Spectral Luminous Efficiency Function, $V(\lambda)$, was established for photopic vision. In 1951, a luminous efficiency function for scotopic vision (rods) known as $V'(\lambda)$ was defined by the CIE [CIE1924,1951].

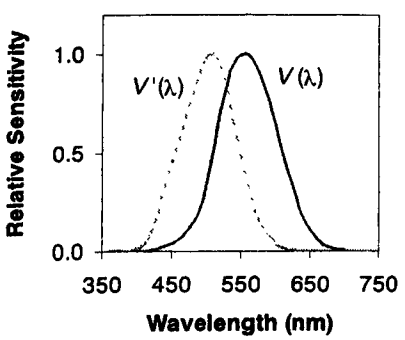


*Figure 2–11 CIE scotopic, V'(λ), and photopic, V(λ), luminous efficiency functions*

Figure 2–11 shows both scotopic and photopic luminous efficiency functions. Note that they are relative functions of wavelength. The $V'(\lambda)$ curve is obtained by a matching experiment, i.e. having observers adjust the strength of a beam of lgiht of one wavelength until the sensation produces the same intensity as a beam of fixed strength of a reference wavelength. Relative sensitivity can then be calculated by comparing the intensities. If the variable beam has twice the strength, sensitivity will be half of a reference light. For the $V(\lambda)$ curve, the experimental technique called flicker photometry was used. In flicker photometry, the criterion of equality of luminance of two stimuli is the disappearance of the flicker produced by presenting them alternately to the eye at a certain minimum frequency.

The $V(\lambda)$ and $V'(\lambda)$ functions are the basis of photometry. In radiometry, light is measured with equal sensitivity to all wavelengths. The perceived brightness of each wavelength, however, is affected by the sensitivity of the human eye, $V(\lambda)$ and $V'(\lambda)$. In photometry, these two functions are used as weighting factors to determine which of any two lights, whatever their spectral composition, will appear under the same conditions to have the greater intensity. Eq. ( 2-1 ) summarises the equation to calculate photopic and scotopic luminance. Luminance is the photopic correspondence of radiance.

$$\text{Photopic Luminance} \quad L = 683 \cdot \int V(\lambda) \cdot P(\lambda) \cdot d\lambda \quad (\text{unit}: \text{cd/m}^2) \qquad (2\text{-}1)$$

$$\text{Scotopic Luminance} \quad L' = 1700 \int V'(\lambda) \cdot P(\lambda) \cdot d\lambda$$

where $P(\lambda)$: Spectral Power (W/sr/m$^2$/nm)

### 2.4.4 Tristimulus Values

The colour of a stimulus can be represented as three numbers called tristimulus values $X$, $Y$, $Z$ using the three CIE colour matching functions in the same way as to calculate luminance via the CIE spectral luminous efficiency function. Eq. ( 2-2 ) shows the equations to calculate tristimulus values where $k$ is a constant and $P(\lambda)$ is the power of wavelength $\lambda$. For a reflective sample, $P(\lambda)$ is defined as the product of the spectral reflectance, $R(\lambda)$, (or transmittance, $T(\lambda)$ for transmitting materials) and the spectral power distribution of the light source or illuminant of interest, $S(\lambda)$. That is $P(\lambda) = R(\lambda) \cdot S(\lambda)$ for reflective material and $P(\lambda) = T(\lambda) \cdot S(\lambda)$ for transmissive material. $\bar{x}(\lambda)$,

$\bar{y}(\lambda)$, $\bar{z}(\lambda)$ and $\bar{x}_{10}(\lambda)$, $\bar{y}_{10}(\lambda)$, $\bar{z}_{10}(\lambda)$ are the colour matching functions for 2° and 10° standard observers.

$$X = k\int P(\lambda)\cdot\bar{x}(\lambda)\cdot d\lambda, \quad Y = k\int P(\lambda)\cdot\bar{y}(\lambda)\cdot d\lambda, \quad Z = k\int P(\lambda)\cdot\bar{z}(\lambda)\cdot d\lambda \qquad (2\text{-}2)$$

$$X_{10} = k\int P(\lambda)\cdot\bar{x}_{10}(\lambda)\cdot d\lambda, Y_{10} = k\int P(\lambda)\cdot\bar{y}_{10}(\lambda)\cdot d\lambda, Z_{10} = k\int P(\lambda)\cdot\bar{z}_{10}(\lambda)\cdot d\lambda$$

If $P(\lambda)$ represents the spectral radiance (W/sr/m$^2$/nm) of a light source or a colour sample and $k$ is 683 (lm/W), $Y$ is luminance (cd/m$^2$) since $\bar{y}(\lambda)$ is identical to the $V(\lambda)$ function. When this is the case, the symbols $X_L$, $Y_L$, $Z_L$ are used and called absolute tristimulus values. For convenience, however, $k$ can be chosen to make $Y_L$=100 for a perfect reflecting diffuser i.e. an ideal isotropic diffuser with a reflectance (or transmittance) equal to unity (or the reference white in the scene). Tristimulus values normalised in this way are called relative tristimulus values and use symbols $X$, $Y$, $Z$. In this case, $Y$ is called the luminance factor.

For the measurement of the relative tristimulus values of a reflective material using a spectrophotometer, a relative spectral power distribution is used for $S(\lambda)$, which is normalised by having an arbitrary value of 100 at 560nm with the values of other wavelengths converted to ratios relative to this reference value. The constant $k$ for the relative tristimulus values of a reflective material is given in Eq. ( 2-3 ).

For relative tristimulus values of a reflective material

$$k = \frac{100}{\int P(\lambda)\cdot[\bar{y}(\lambda) \text{ or } \bar{y}_{10}(\lambda)]\cdot d\lambda} \qquad (2\text{-}3)$$

where $P(\lambda) = S(\lambda)\cdot R(\lambda)$

$S(\lambda)$ : relative spectral power of the light source

$R(\lambda)$ : reflectance of the object (0 ~ 1)

## 2.4.5 Chromaticity

Another convenient way to represent tristimulus values is to use chromaticity co-ordinates as shown in Eq. ( 2-4 ). Chromaticity co-ordinates map all colours into a two-dimensional space, which is preferred because of its convenience. Note that $x$+$y$+$z$=1, therefore using only two chromaticity co-ordinates, such as $x$ and $y$, with one tristimulus value can recover the full tristimulus values $X$, $Y$, $Z$.

$$x = \frac{X}{X+Y+Z}, \quad y = \frac{Y}{X+Y+Z}, \quad z = \frac{Z}{X+Y+Z} \qquad (2\text{-}4)$$

The left diagram in Figure 2–12 shows the CIE $x$, $y$ chromaticity diagram. The curved line in the diagram shows where the spectral colours lie and is named the spectrum locus. The straight line connecting the two ends of the spectrum is known as the purple boundary. The area enclosed by the spectrum locus and the purple boundary encloses the domain of all visible colours, since all perceivable colours existing in nature are the combinations of spectral colours and any mixture of two spectral colours in this additive system is located on the line joining the two points representing the two original spectral colours.

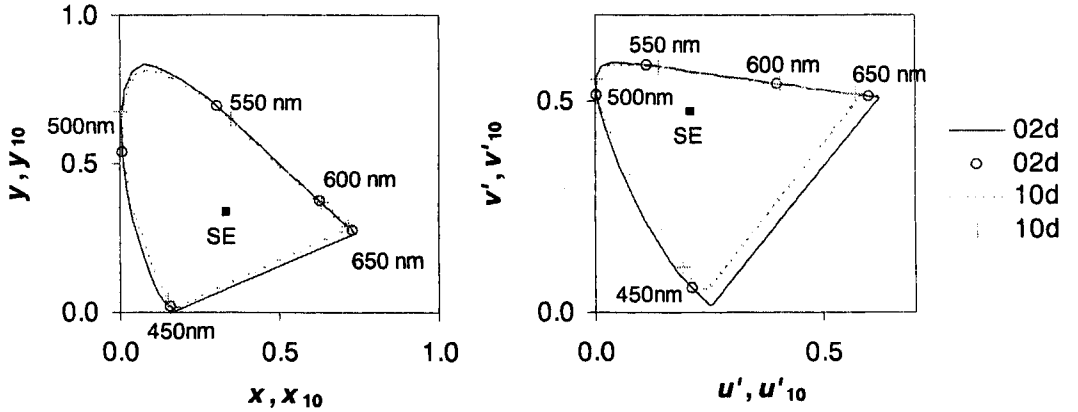


*Figure 2–12 The CIE x, y and u', v' chromaticity diagrams showing the spectrum locus and equi-energy stimulus for 2° and 10° observers*

Although the $x$,$y$ chromaticity diagram has been widely used, it has a serious disadvantage: the very non-uniform colour distribution in its space. Therefore another effort was made to establish a more uniform chromaticity diagram, which is known as the CIE 1976 Uniform Chromaticity Scales (UCS) diagram, defined by Eq. ( 2-5 ). The CIE $u'$, $v'$ chromaticity diagram is shown the right diagram in Figure 2–12 with the spectral locus and equi-energy stimulus for 2° and 10° observers.

$$u' = \frac{4X}{X+15Y+3Z}, \quad v' = \frac{9Y}{X+15Y+3Z} \qquad (2\text{-}5)$$

## 2.4.6 Limitation of CIE Colorimetry

The CIE colorimetry system has been successfully applied over the years by providing a mathematical tool for specifying a colour. This system can determine if

any two colour stimuli would match or not under a given set of viewing conditions. If the tristimulus values are identical, two colours will be observed as identical by the "standard" observer. However it is well known that the appearance of a colour is affected not only by its own spectral composition but also by viewing conditions such as background colour, etc. For example, a grey colour patch on a white background looks darker than the same patch on a black background. This phenomenon is known as simultaneous contrast and cannot be predicted by CIE colorimetry. A colour appearance model is needed to extend CIE colorimetry to provide a method for assessing the colour appearance under distinct viewing conditions.

## 2.5 Colour Measuring Instruments

CIE tristimulus values are obtained by colour measuring devices, which can be divided into three types: colorimeter, spectrophotometer and spectroradiometer. Colorimeters directly measure colorimetric quantities whereas spectrophotometers and spectro-radiometers calculate colorimetric quantities from spectral data measured across the visible spectrum, i.e. in the wavelength range from 380 to 780nm using Eq. ( 2-2 ) [Bern2000 Ch. 3].

In colorimeters, light is simultaneously collected by three detectors, which are covered with carefully designed colour filters so that their spectral sensitivities are similar to the CIE colour matching functions. Spectrophotometers are designed to measure spectral reflectance or transmittance in the visible region of the spectrum between about 380 and 780 nm. The main components of all spectrophotometers are a light source, an optical system for defining the geometric conditions of measurement (see Section 2.4.2 for CIE geometry), some means of dispersing light, and a detector and signal processing system that converts light into signals suitable for analysis [Bern2000 Ch. 3, Hunt1998 Ch. 5].

A spectroradiometer is an instrument designed to measure radiometric quantities (irradiance, radiance) in a narrow spectral bandpass as a function of wavelength. A tele-spectroradiometer is one of the spectroradiometers that was used in the author's study. It has the advantage of being able to measure the colour of a distant object from its usual observing position under its usual viewing conditions [Zwin1996]. A basic spectroradiometer contains a dispersing element (diffracting grating) and a detector.

For a scanning spectroradiometer, a photo detector is sequentially exposed to the different wavelength bands across the visible spectrum while an array of photosensitive elements makes all the measurements across the spectrum simultaneously for a multichannel spectroradiometer [Hunt1998 p.108, Hans1997].

The critical factors for designing a spectroradiometer are wavelength range, spectral bandwidth, wavelength sampling increment, dynamic range and measurement area [Hans1997]. Wavelength range should cover the visible spectrum and the measurement area determines the minimum sample size to measure. Dynamic range is limited by the performance of the detector. Choosing the optimum spectral bandwidth is a compromise between signal (a wider bandwidth gives higher signal, and thus better signal-to-noise ratio) and spectral resolution. Wider bandwidths may lead to errors in the calculation of tristimulus values. Ideally the wavelength sampling increment should be identical to the bandwidth to avoid over- or under-sampling.

## 2.6 Colour Appearance Terminology

The factors influencing colour appearance include colour appearance attributes and the spatial structure of the viewing field. In this section, definitions of colour appearance attributes are summarised first and then the description of visual areas in the observing field. Colour appearance terminology used throughout this thesis also follows the definitions introduced in this section.

### 2.6.1 Definitions of Colour Appearance Attributes

Colour appearance attributes can be categorised into three groups: achromatic, chromatic and hue. The definitions of each are introduced below, based on the CIE International Lighting Vocabulary [CIE1987, Hunt1998 Appendix 9].

**Achromatic Attributes**

| | |
|---|---|
| Brightness | Attribute of a visual sensation according to which an area appears to emit more or less light. |
| Lightness | The brightness of an area judged relative to the brightness of a similarly illuminated are that appears to be white or highly transmitting. |

**Chromatic Attributes**

| | |
|---|---|
| Colourfulness | Attribute of a visual sensation according to which an area appears to exhibit more or less of its hue. |
| Chroma | The colourfulness of an area judged in proportion to the brightness of a similarly illuminated area that appears to be white or highly transmitting. |
| Saturation | Colourfulness of an area judged in proportion to its brightness. |

**Hue**

| | |
|---|---|
| Hue | Attribute of a visual sensation according to which an area appears to be similar to one or to proportions of two, of the perceived unique hues i.e. red, yellow, green, and blue. |

Note that each dimension of a colour perception except hue has more than one attribute. However they correspond to the same perception but only differ in their definitions. Brightness and colourfulness are the attributes representing the absolute strength of the perception while lightness and chroma are calculated (or normalised) relative to the brightness or colourfulness of a reference colour. In other words, lightness and chroma do not apply to unrelated colours but only to related colours since they need one or more colours in the viewing field. Unrelated colour means a colour perceived to be in isolation from other colours while related colour is perceived to be in relation to other colours.

It is important to understand and standardise the concepts of the colour appearance attributes since earlier studies on colour appearance used these terms slightly differently, which could lead to confusion when interpreting the results. For example, it was a difficult and controversial subject about which concepts and terms should be used for the strength of chromatic response by which hue is recognised. However after the concept of "colourfulness" was suggested by Hunt [Hunt1977a, Pointer1978], and subsequently demonstrated by Pointer to be easily understood by observers [Pointer1978, 1980], the terms "colourfulness", "chroma" and "saturation" became standardised and widely used in the colour science field.

## 2.6.2 Visual Areas in The Observing Field

The appearance of a colour is greatly affected by the environment around it. For related colours, Hunt recognised five different visual fields [Hunt1991,1995, 1998], which have been widely adopted for colour appearance study. Descriptions of these five areas are given below and Figure 2–13 illustrates their relationships.

| | |
|---|---|
| Stimulus | The colour element considered. Typically a uniform patch of about 2° angular subtense. |
| Proximal field | The immediate environment of the stimulus, extending for about 2° from the edge of the stimulus in all or most directions. |
| Background | The environment of the stimulus, extending typically for about 10° from the edge of the proximal field in all, or most directions. When the proximal field is the same colour as the background, the latter is regarded as extending from the edge of the stimulus. |
| Surround | The field outside the background. |
| Adapting field | The total environment of the stimulus, including the proximal field, the background, and the surround, and extending to the limit of vision in all directions. |

***Figure 2–13 The regime of fields used in colour appearance models (adapted from Hunt [Hunt1995 p.739])***

The stimulus and background are described in terms of the tristimulus values. If the stimulus has an angular subtense of more than 4°, the tristimulus values for the CIE 10° observer are used otherwise those for the CIE 2° observer are applied. For the current generation of colour appearance models, the proximal field is not used, but it will be necessary to model simultaneous contrast in the future.

The surround is used as a categorical term for practical use. For colour appearance models, the surround is defined as the relative ratio of the luminance of the adapting field to the luminance of a stimulus [Fair1998a p.275, Moro2000]. In CIECAM97s [Luo1998], surround conditions are categorised into four groups: average, dim, dark and cut-sheet, as summarised in Table 2-1. Colour appearance models derived after CIECAM97s normally use three categories, average, dim and dark without the 'cut-sheet' condition.

*Table 2-1 List of the CIECAM97s surrounds (Table1 in [Moro2000])*

In CIECAM97s, 'average surround' means that the surround luminance is similar to the average luminance of all colours in the viewing field, i.e. having a relative surround luminance of greater than 20% of the luminance of the scene white, as is typically the case when surface colours are viewed. 'Dim surround' means that the surround luminance is appreciably less than the average luminance of the viewing field, i.e. 0% to 20%, as is typically the case when viewing television. 'Dark surround' means that the surround luminance is very low compared to the average luminance of the viewing field, i.e. close to 0%, as is typically the case when viewing film projected in a darkened room. 'Cut-sheet' means the conditions typical for viewing cut-sheet film against a back-lit illumination [Luo1998, Fair1998a p.275, Moro2000].

## 2.7 LUTCHI Colour Appearance Data Set

The LUTCHI data set is a large body of psychophysical experimental data for describing colour appearance. Each data file consists of relative tristimulus values and observer judgements of visual lightness (or brightness), colourfulness and hue, together with information about reference white, background and surround condition. According to the official web site of the LUTCHI data [LUTCHI], the main body of

the results was obtained from two consecutive research projects funded by the British Government's Alvey (1987-1989) and IEATP (1990-1992) programmes. The data were produced at the Loughborough University of Technology Computer-Human Interface Research Centre and are hence named the LUTCHI colour appearance data. Subsequently, two new data sets were also accumulated: Kuo & Luo, and BIT. These data sets were also included to form the full LUTCHI Colour Appearance Data Set.

The data were used to refine the Hunt colour appearance model [Hunt1991, 1994] and to derive the LLAB colour appearance model [Luo1996, Morov1996]. Most importantly, this data set was used for the development of the CIE colour appearance model, CIECAM97s [CIE1998, Luo1998]. Many colour appearance models developed after CIECAM97s, such as CAMs2 [Li2000], Fairchild [Fair2001], FC [Hunt2002], CIECAM02 [Moro2002], are also based on the LUTCHI data. The data have also been used to test various colour appearance models [Luo1991b].

The data set is divided into eight groups according to the experimental viewing conditions as shown in Table 2-2 and has a total of 59 phases. The same experimental technique was applied to all experimental groups. During the experiments, a series of test colours with decoration colours in the peripheral area were shown under various viewing conditions. Observers were asked to estimate the lightness, colourfulness and hue of each test colour using a magnitude estimation method. LUTCHI data show the averaged visual assessment results. Arithmetic means were calculated for lightness and hue and geometric means were used for colourfulness and brightness [Luo991a].

Group R-HL and R-LL [Luo1991a] experiments were conducted using reflective samples under various viewing conditions. Since the same physical samples were used throughout the whole experiments, the results directly show colour appearance change by illuminant, luminance level and background parameters. For Group CRT [Luo1991a], CRT monitor colours were made to have the same chromaticities as those for R-LL to investigate the difference between luminous and reflective colours. Group R-VL [Luo1993a] was conducted using reflective colours and had 12 phases covering a large luminance range including mesopic luminance levels. The first 6 phases gave lightness, colourfulness and hue data while other 6 phases gave brightness results instead of lightness for the same colour samples. Group LT and

35mm were for colour appearance of transmissive samples, i.e. cut-sheet film and 35-mm slides [Luo1993b, Wang1994].

The experimental group BIT was complied by the Beijing Institute of Technology, China for the colour appearance of unrelated colours [Luo1997]. Group R-Textile was conducted with textile samples [Kuo1995].

| Group | Media | No. of Phases | Light Source | Reference White ($cd/m^2$) | Back-ground | No. of Observers | No. of Colours (per phase) | No. of Estima-tions |
|---|---|---|---|---|---|---|---|---|
| R-HL | Reflective | 6 | D50, D65, WF, A | ~ 250 | White, Grey, Black | 6 or 7 | ~100 | 11,970 |
| R-LL | Reflective | 6 | | ~ 40 | | | | 11,970 |
| CRT | Self-luminous | 11 | | ~ 40, 20 | | | | 19,390 |
| LT | Cut-sheet transparency | 10 | D50 | 325 ~ 2259 | Grey | 7 or 8 | 98 | 21,748 |
| 35mm | 35mm projection | 6 | 4000 K | 47~113 | Grey | 5 or 6 | ~ 99 | 9,093 |
| R-VL | Reflective | 12 | 5000 K | 0.4~843 | Grey | 4 | 40 | 5,760 |
| R-Textile | Reflective (Textile) | 3 | D65, A, TL84 | 250, 540 | Grey | 5 | 240 | 10,770 |
| BIT | Reflective /Self-lum. | 5 | D65 | 90, 3.6 | Black | 6 | 120, 90 (CRT) | 10,440 |

***Table 2-2 Summary of LUTCHI data sets***

## 2.8 Colour Appearance Phenomena

As explained in Section 2.2.4, the human eye can adapt to the changing environment and this process helps us to have more consistent visual information. However this compensation is not perfect. For example, we can distinguish between cloudy and sunny days in spite of the dynamic adaptation. Also there are spatial interactions between the visual information collected by the photoreceptors across the retina making the colour appearance change according to the background or surround.

In this section, colour appearance phenomena are introduced, i.e. colour appearance change by luminance level, background, surround conditions and chromaticity of the illuminant. Note that understanding the changes in colour appearance produced by the viewing parameters is essential for developing a model of colour appearance.

### 2.8.1 Colour Appearance Change by Different Luminance Levels

The first phenomenon considered is how colour appearance will be changed if the overall luminance level of an image is shifted – higher or lower.

#### 2.8.1.1. Lightness Change by Different Luminance Levels

Groups R-HL, R-LL and R-VL in the LUTCHI data set, which were introduced in the previous section, contain colour appearance data covering high and low luminance levels. Comparing R-HL (252 cd/m$^2$) and R-LL (44 cd/m$^2$) experiments showed that dark colours appear lighter in high-level luminance than in low-level luminance [Luo1991a], which was also shown in R-VL experiments [Luo1993a]. This experimental result indicates lower lightness contrast under higher luminance since the lightness of the reference white was set to 100 regardless of its luminance level. The term 'contrast' means 'the rate of change of the relative luminance of image elements of a reproduction as a function of the relative luminance of the same image elements of the original image' [Fair1995].

There is another experimental result contradicting the LUTCHI data. Bartleson and Breneman [Bart1967] asked observers to estimate the brightness of several areas within a printed image and a projected image of a photographic transparency under various luminance levels. They found that contrast increased for higher luminance level.

#### 2.8.1.2. Purkinje Shift

A notable phenomenon related to the lightness change by luminance level is the Purkinje shift. As introduced in Section 2.4.3, in photopic vision only cone cells are functioning but as the luminance level decreases the rod cells start to contribute and eventually only rods are functioning for scotopic vision. The luminous efficiency functions of scotopic and photopic vision are shown in Figure 2–11 (p. 23), which indicates two distinctive patterns. Therefore as vision changes from the photopic to the scotopic state, there is a shift in peak spectral sensitivity toward shorter wavelengths. This shift, called the Purkinje shift, reduces the brightness of a predominantly longer wavelength colour stimulus relative to that of a predominantly

shorter wavelength colour stimulus when the luminances are reduced in the same proportion from photopic to mesopic or scotopic levels without changing the respective relative spectral power dstributions of the stimuli involved [Hunt1998 p.327, Fair1998a p.81].

### 2.8.1.3. Colourfulness Change by Different Luminance Levels (Hunt Effect)

It is well known that colourfulness increases with luminance. This phenomenon is called the Hunt effect, which was named from a study 'Light and dark adaptation and the perception of color' [Hunt1952]. In that study the corresponding colours between two different adaptation conditions were established using the haploscopic matching technique.

During the experiment, different adaptation levels were presented to the left eye with a series of test colours in the centre while the adaptation level of the right eye was set to the reference level. The different adaptation levels were obtained by inserting neutral filters to cover the whole viewing field of the left eye including the adapting field outside and the test colour in the centre. Hence test colours had exactly the same relative luminance levels compared to the adapting field regardless of its absolute luminance.

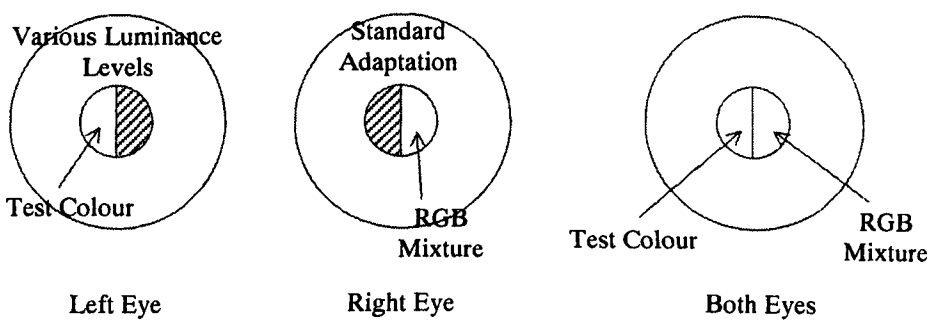


*Figure 2–14 The viewing field of the experiment for the Hunt effect*

Observers were asked to match the test colours shown to the left eye by mixing red, green and blue lights shown to the right eye adapted to the reference luminance level. Figure 2–14 shows the viewing field shown to each eye with the fused viewing field that observers saw with both eyes. The results demonstrated that as the adapting

luminance is lowered the match made on the right eye becomes less chromatic. In other words, higher luminance level induces higher colourfulness.

The Hunt effect was confirmed by Breneman's study [Bren1987], which applied a matching technique with a complex visual field, and by the LUTCHI study for groups R-HL, R-LL and R-VL. The LUTCHI data used colour patches in a viewing booth [Luo1991a, Luo1993a].

### 2.8.2 Colour Appearance Change by Different Background Luminance Factors

In this section, the colour appearance change on a test colour by the change of background luminance factor is introduced. Changing the background luminance factor also affects the adaptation luminance level, but the luminance of a test colour is not changed while the luminance of the background colour surrounding the test colour is changed.

The colour appearance change due to the background is known as simultaneous contrast. If the angular subtense of the colour is not too small (greater than about half a degree), the colour tends to appear more like the opposite of the background following the opponent-colour theory. In other words, colours on dark backgrounds appear lighter and those on light backgrounds appear darker. A red background makes colours look greener and a green background induces red and a similar opponent relationship applies between yellow and blue backgrounds [Hunt1977b, Fair1998a p.135]. However, if the colour is seen at a very small angular subtense, and particularly if it is in the form of an intricate pattern on the background, the spreading effect usually occurs, which makes the colour appear more like the surround [Hunt1977b].

In the next subsections, achromatic and chromatic changes by the background are further discussed. Only the effect of a neutral background is considered here.

#### 2.8.2.1. Brightness/Lightness Change by Different Background Luminance Factors

In J.C. Stevens and S.S. Stevens' paper on 'Brightness Function: Effects of Adaptation' [Steve1963], a change of brightness according to adaptation was investigated with an observer's eyes differently adapted using the magnitude estimation technique. The left eye was dark-adapted and the right eye was adapted to a constant luminance. For the right eye, surrounding the target was a large adaptation field, which was white cardboard illuminated by projector lamps.

In the experiment, the observer's eyes were first dark adapted for 10 min. Then for 3 min the left eye continued to dark adapt, while the right eye adapted to a luminance level that was constant for a given experiment. When a test stimulus was presented to either eye, the adaptation lights were extinguished and the observer assigned a number in proportion to the apparent brightness. The observer's right eye was adapted to 97dB (800 cd/m$^2$), 79 dB (25 cd/m$^2$), 63 dB (0.64 cd/m$^2$) or to darkness. In each experiment, 4 to 7 test stimuli of various luminances (44~104 dB corresponding to 0.008~7995 cd/m$^2$) were presented alternately to the right and left eyes.

The experimental results showed that, under lower adapting luminance, a stimulus appears brighter and the brightness contrast decreases. The Stevens and Stevens experimental result can be interpreted as a higher brightness/lightness contrast induced by an increase of background luminance factor. Note that unlike the experiment for revealing the Hunt effect, the same test colours were used for all adaptation levels for the Stevens and Stevens experiment, which is similar to changing background luminance level while the test colours remain the same.

The increase of lightness contrast for the lighter background was confirmed in the LUTCHI data [Luo1991a].

#### 2.8.2.2. Colourfulness Change by Different Background Luminance Factors

The effect of colourfulness change by the background luminance factor was investigated by Pitt and Winter [Pitt1974]. Observers were asked to adjust a luminous colour against a black background to match a colour filter back-illuminated by a

transparency illuminator in a darkened room. The experimental conditions were described as light and dark surround in the original paper, but it was more like a light and a dark background viewed under a dark surround condition according to the definition in Section 2.6.2 [Fair1995].

Pitt and Winter found that the dark background required observers to generate a colour of higher purity in order to match the colour having a light background. In other words, light background induces higher colourfulness. Also their experimental results showed that, in addition to the increase of colourfulness required for the dark backgrounded colours, their luminances also had to be reduced to make them match a colour in the light background. This finding agrees with the experimental results discussed in Section 2.8.2.1.

Groups R-HL, R-LL and CRT in the LUTCHI data set have experimental phases with white, grey and black backgrounds. The original report on the LUTCHI data concluded that there is a colourfulness reduction for both the white and black background compared to a grey background [Luo1991a]. However the original data analysis did not consider the difference of the measurement data. When considering the change of tristimulus values by the background colour, it is found that the visual LUTCHI data also confirm that colours against a lighter background appear more colourful (see Section 6.4.2).

Contrary to the above findings, Hunt predicted the opposite effect such that a darker background induces higher colourfulness as a result of higher lightness since brighter colours appear more colourful according to the Hunt effect. Also, Hunt observed that for a dark background dark colours appear more colourful and lighter colours appear less colourful [Hunt1994]. Note that most of the colour appearance models introduced in Section 2.9 predict a colourfulness increment for darker background.

### 2.8.3 Colour Appearance Change by Different Surround

In this section the surround effects on colour appearance are reviewed. Definitions of the surround conditions were given in Section 2.6.2 and only the experimental results satisfying the definitions are reviewed here. The effect on hue is not considered because in the present study only neutral surrounds were used.

### 2.8.3.1. Lightness Change by Different Surround

Hunt explained that the effects of the dim and dark surrounds make pictures lighter than those appearing under an average surround. But this effect occurs to a greater extent in dark areas than in light areas of the picture; hence the dark surround lowers the apparent contrast [Hunt1995 p.93, Bren1962]. A reduction of lightness contrast for dark surround also can be found in several other experiments [Bart1967, Bren1977].

### 2.8.3.2. Colourfulness Change by Different Surround

Breneman [Bren1977] examined the effect of surround on colourfulness by judging the relative saturation of test colours with the same hue and apparent brightness in average and dark surround conditions. Note that Breneman used the term 'saturation' to denote the attribute of perception, which should actually be 'colourfulness' according to the definition given in Section 2.6.1 since observers were asked to judge the absolute chromatic property between different viewing conditions.

The experiment was conducted using three different techniques for two exploratory experiments and one principal experiment. The first experiment was conducted using haploscopic viewing. Observers viewed the light surround with the left eye and the dark surround with the right eye. Munsell colour chips with visually equal brightness were shown in both fields and the observer was asked to judge which of the two colours appeared to be more colourful (described as 'saturated' in the paper) and to express the apparent colourfulness of the lesser as a percentage of the greater. For the second exploratory experiment, a matching technique was applied with the same viewing conditions. Breneman found that the first experimental results showed no effect while the second experiment showed that 19% higher chromatic purity ($P = \left[(u'-u'_0)^2 + (v'-v'_0)^2\right]^{1/2}$) was necessary to match a colour in the dark surround ($u'$, $v'$) with that in the light surround condition ($u'_0$, $v'_0$). Because of the different results between the two experiments and the problems found in the matching experiment, a more extensive experiment followed.

For the third experiment, i.e. the principal experiment, the technique of the first experiment was used again. However this time an alternative binocular method was

applied instead of the haploscopic method. The observer alternately viewed the two fields moving his head from side to side until he had evaluated the relative colourfulness of the colour stimuli. This experiment found that a 4% increase in purity was needed for the dark-surround viewing condition. This result means that a colour will look more colourful under average surround than under dark surround conditions.

Breneman left the conclusion as an open question since the effect found was small and could have resulted from an experimental bias. However, as noted by Fairchild, the results in the third experiment, which was designed to reduce the experimental bias found from the previous two experiments, indicated that there was a small but significant effect for each colour investigated, namely that a dark surround decreased perceived colourfulness [Bren1977 Fig. 3, Fair1995].

### 2.8.4 Colour Appearance Change by Different Illuminants (Helson-Judd Effect)

The most important phenomenon related to the colour appearance change by illuminant is chromatic adaptation, which was briefly introduced in Section 2.2.4. However the detailed phenomena related to chromatic adaptation are not reviewed here since it is outside the scope of the present study. Note that some chromatic adaptation models are introduced in Section 2.9 as a part of colour appearance models.

The other effect due to illuminant is the Helson-Judd effect, which is a tendency in coloured illumination for light colours to be tinged with the hue of the illuminant and for dark colours to be tinged with the complementary hue. This was first illustrated by Helson in 1938 [Hunt1998 p.322, Hels1938]. The Hunt and Nayatani *et al.* models predict this effect quite strongly but Fairchild argued in his book 'Color Appearance Models' that the Helson-Judd effect cannot be observed with complex stimuli [Fair1997 p.148]. Also this effect was not found at all in the LUTCHI visual data.

## 2.9 Colour Appearance Models

The CIE Technical Committee 1-34 (TC1-34) set out to define a colour appearance model as being a model that should at least include predictors of the relative colour appearance attributes of lightness, chroma, and hue. For a model to provide reasonable predictors of these attributes, it must include some form of a chromatic adaptation transform. More complex models may also include predictors of brightness and colourfulness or to model luminance-dependent effects such as the Hunt effect [Fair1997 p.217].

In this section eight colour appearance models, which were used in the author's study, are introduced. These are CIELAB, RLAB, LLAB, Hunt94, CIECAM97s, FC, Fairchild and CIECAM02.

### 2.9.1 The CIELAB Uniform Colour Space

The CIE 1976 $L^*a^*b^*$ colour space, or CIELAB, is one of the uniform colour spaces recommended by CIE. Input data are the tristimulus values of a stimulus ($XYZ$) and a reference white ($X_nY_nZ_n$). The predicted colour appearance attributes are lightness $L^*$, chroma $C^*_{ab}$ and hue angle $h_{ab}$. Eq. ( 2-6 ) shows the equations. Note that CIELAB $L^*$, $a^*$ and $b^*$ normalise the tristimulus values to those of reference white ($X/X_n$, $Y/Y_n$, $Z/Z_n$), which is a modified form of the von Kries chromatic-adaptation transform [vonK1902, 1911].

$$L^* = 116 \cdot f(Y/Y_n) - 16 \qquad (2\text{-}6)$$

$$a^* = 500 \cdot [f(X/X_n) - f(Y/Y_n)]$$

$$b^* = 200 \cdot [f(Y/Y_n) - f(Z/Z_n)]$$

$$\text{where } f(x) = x^{1/3} \quad \text{for } x > 0.008856$$

$$= 7.787 \cdot x + 16/116 \quad \text{for } x \le 0.008856$$

$$C^*_{ab} = \sqrt{(a^*)^2 + (b^*)^2}$$

$$h_{ab} = \tan^{-1}(b^*/a^*) \quad \text{[degrees]}$$

CIELAB $L^*$, $a^*$ and $b^*$ represent three axes in a three dimensional uniform colour space, in which the colour difference of two colours is equal to the Euclidean distance between two points representing the colours. In CIELAB space, colour difference $\Delta E^*_{ab}$ is calculated using Eq. ( 2-7 ). $\Delta L^*$, $\Delta a^*$ and $\Delta b^*$ are the differences between two colours in the $L^*$, $a^*$ and $b^*$ dimensions respectively.

$$\Delta E^*_{ab} = \left[(\Delta L^*)^2 + (\Delta a^*)^2 + (\Delta b^*)^2\right]^{1/2} \qquad (2\text{-}7)$$

## 2.9.2 The RLAB Model

The RLAB model [Fair1993,1994,1996] comprises two main parts: chromatic adaptation and a uniform colour space similar to CIELAB space, which is used to calculate colour appearance predictors.

Input data for the RLAB model are:

| | | | |
|---|---|---|---|
| Relative tristimulus values of test stimulus | $X$ | $Y$ | $Z$ |
| Relative tristimulus values of the white point | $X_n$ | $Y_n$ | $Z_n$ |
| The absolute luminance of a white object in the scene | $Y_{Ln}$ (cd/m$^2$) | | |
| Model Parameters | $D$ | $\sigma$ | |

The RLAB has two parameters $D$ and $\sigma$. The $D$ factor allows various proportions of cognitive discounting-the-illuminant, which is 1.0 for hard-copy image, 0.0 for soft-copy displays or an intermediate value (0.5 when no visual data are available) for projected images in completely darkened rooms. Parameter $\sigma$ varies depending on the categorised surround condition, which is 1/2.3, 1/2.9 or 1/3.5 for dark, dim and average surround respectively.

Equations for RLAB are given in Eq. ( 2-8 ) and Eq. ( 2-9 ). Eq. ( 2-8 ) shows the chromatic adaptation process by which input tristimulus values ($XYZ$) in a test condition are transformed to the corresponding colours ($X_{ref}Y_{ref}Z_{ref}$) under the RLAB reference viewing condition (illuminant D65, 2° observer, 318 cd/m$^2$, discounting-the-illuminant: $D$=1.0). The chromatic adaptation transformation (the matrix **A**) is derived using the cone signals ($LMS$) in the Hunt-Pointer-Estevez cone space [Hunt1985]. The matrix **M** transforms the tristimulus values to the cone signals.

It is notable that RLAB considers cognitive chromatic adaptation (so called 'discounting-the-illuminant') separately from the sensory mechanism. Discounting-the-illuminant is the cognitive ability of observers to interpret the colours of objects based on the illuminated environment in which they are viewed. The von Kries type chromatic adaptation is used for sensory mechanism. Degrees of sensory and cognitive adaptation are determined by the factors $p$ and $D$ respectively.

In Eq. ( 2-9 ), tristimulus values under the reference condition are used to construct the three co-ordinates for colour space, $L^R$, $a^R$ and $b^R$, which are analogous to CIELAB $L^*$, $a^*$ and $b^*$ respectively. Chroma $C^R$ and hue angle $h^R$ are calculated from the RLAB space in the same way as for CIELAB. RLAB also provides hue composition, $H^R$, and saturation, $s^R$, predictors.

Note that RLAB compensates the colour appearance change by surround using model parameter $\sigma$ but with no consideration of background effect. Also it is notable that luminance of reference white is only used to decide the degree of chromatic adaptation. There is no compensation for the colour appearance change by the change of luminance level.

**Step 1. Chromatic Adaptation**

$$\begin{vmatrix} L \\ M \\ S \end{vmatrix} = M \cdot \begin{vmatrix} X \\ Y \\ Z \end{vmatrix} \quad \text{where} \quad M = \begin{vmatrix} 0.3897 & 0.6890 & -0.0787 \\ -0.2298 & 1.1834 & 0.0464 \\ 0.0 & 0.0 & 1.0000 \end{vmatrix} \tag{2-8}$$

$$\begin{vmatrix} X_{ref} \\ Y_{ref} \\ Z_{ref} \end{vmatrix} = R \cdot A \cdot \begin{vmatrix} L \\ M \\ S \end{vmatrix} \quad \text{where} \quad A = \begin{vmatrix} a_L & 0.0 & 0.0 \\ 0.0 & a_M & 0.0 \\ 0.0 & 0.0 & a_S \end{vmatrix}$$

$$a_K = \frac{p_K + D \cdot (1.0 - p_K)}{K_n}, \quad K = L, M, S$$

$$p_K = \frac{1.0 + Y_n^{1/3} + k_E}{1.0 + Y_n^{1/3} + 1.0/k_E} : \text{The proportion of complete von Kries adaptation}$$

$$k_E = \frac{3.0 \cdot K_n}{L_n + M_n + S_n} \qquad L_n, M_n, S_n : L, M, S \text{ of the reference white}$$

$$R = (A_{ref} \cdot M)^{-1} = \begin{vmatrix} 1.9569 & -1.1882 & 0.2313 \\ 0.3612 & 0.6388 & 0.0 \\ 0.0 & 0.0 & 1.0000 \end{vmatrix}$$

**Step 2. Opponent-colour dimensions and colour appearance predictors**

Lightness $L^R = 100 \cdot (Y_{ref})^{\sigma}$

$$a^R = 430 \cdot \left[ (X_{ref})^{\sigma} - (Y_{ref})^{\sigma} \right], \quad b^R = 170 \cdot \left[ (Y_{ref})^{\sigma} - (Z_{ref})^{\sigma} \right] \qquad (2\text{-}9)$$

Hue angle $h^R = \tan^{-1}(b^R / a^R)$ [degrees]

Hue Composition $H^R$ : calculated via linear interpolation of the values in the conversion table

Chroma $C^R = \sqrt{(a^R)^2 + (b^R)^2}$

Saturation $s^R = C^R / L^R$

| $h^R$ | R (%) | Y (%) | G (%) | B (%) | $H^R$ | |
|---|---|---|---|---|---|---|
| 24 | 100 | 0 | 0 | 0 | 0 | R |
| 90 | 0 | 100 | 0 | 0 | 100 | Y |
| 162 | 0 | 0 | 100 | 0 | 200 | G |
| 180 | 0 | 0 | 78.6 | 21.4 | 221 | B79G |
| 246 | 0 | 0 | 0 | 100 | 300 | B |
| 270 | 17.4 | 0 | 0 | 82.6 | 317 | R83B |
| 0 | 82.6 | 0 | 0 | 17.4 | 383 | R17B |
| 24 | 100 | 0 | 0 | 0 | 400 | R |

***Table 2-3 Conversion table from hue angle to hue composition for RLAB***

## 2.9.3 The LLAB Model

The LLAB model [Luo1996, Morov1996] has a similar structure as the RLAB model, which includes a chromatic adaptation transform and a uniform colour space. Unlike the RLAB model, LLAB first calculates colour appearance predictors after a chromatic adaptation transformation and a uniform colour space is then constructed using predicted lightness, chroma and hue angle. LLAB takes into account the colour appearance changes by background luminance factor and also the luminance level, which enable the prediction of colourfulness.

The LLAB model requires the input information of luminance level of the reference white, background and surround conditions along with the relative tristimulus values in the test colours. Input data for the LLAB model are shown below. Also four model parameters need to be predetermined according to the viewing conditions as shown in Table 2-4.

| | | | |
|---|---|---|---|
| Relative tristimulus values of the test stimulus | $X$ | $Y$ | $Z$ |
| Relative tristimulus values of the reference white under the test condition | $X_o$ | $Y_o$ | $Z_o$ |
| Relative tristimulus values of the reference white under the reference condition ($S_E$) | $X_{or}$ | $Y_{or}$ | $Z_{or}$ |
| The absolute luminance of the reference white under the test condition | $L$ (cd/m$^2$) | | |
| Background luminance factor under the test condition | $Y_b$ | | |

Model parameters (determined by surround condition)

Incomplete adaptation factor : $D$

Surround induction factor : $F_S$

Lightness induction factor : $F_L$

Colourfulness induction factor : $F_C$

| Surround Condition | $D$ | $F_S$ | $F_L$ | $F_C$ |
|---|---|---|---|---|
| Average surround ( > 4° ) | 1.0 | 3.0 | 0.0 | 1.00 |
| Average surround ( < 4° ) | 1.0 | 3.0 | 1.0 | 1.00 |
| Dim surround | 0.7 | 3.5 | 1.0 | 1.00 |
| Cut-sheet | 1.0 | 5.0 | 1.0 | 1.10 |
| Dark surround | 0.7 | 4.0 | 1.0 | 1.00 |

***Table 2-4 The surround parameters used in the LLAB model***

Eq. ( 2-10 ) shows the equations for chromatic adaptation. The output of this procedure are the corresponding colours in the reference condition with the equi-energy illuminant $S_E$. In the LLAB model, the BFD chromatic adaptation transform [Lam1985] is adopted. After chromatic adaptation, preliminary opponent dimensions using modified CIELAB co-ordinates ($L_L$, $A$, $B$) are calculated and appearance correlates are specified as shown in Eq. ( 2-11 ). Predicted colour appearance attributes are lightness ($L_L$), chroma ($C_L$), colourfulness ($Ch_L$), saturation ($S_L$), hue angle ($h_L$) and hue quadrature ($H_L$). Then the final opponent signals $L_L$, $A_L$ and $B_L$ are calculated using lightness predictor ($L_L$), colourfulness predictor ($Ch_L$) and hue angle ($h_L$). Equations for the opponent signals are shown in Eq. ( 2-12 ).

Note that the background effect is only considered in the lightness predictor using the $z$ function and the luminance level effect is only considered in the colourfulness predictor. Thus LLAB cannot predict the lightness contrast change by luminance level. Also there is no direct compensation of colourfulness change by background. Note

however that the colourfulness predictor is a function of the lightness predictor, which contains the background effect.

## Step 1. Chromatic Adaptation

$$\begin{vmatrix} R \\ G \\ B \end{vmatrix} = M \cdot \begin{vmatrix} X/Y \\ Y/Y \\ Z/Y \end{vmatrix} \quad \text{where } M = \begin{vmatrix} 0.8951 & 0.2664 & -0.1614 \\ -0.7502 & 1.7135 & 0.0369 \\ 0.0389 & -0.0685 & 1.0296 \end{vmatrix} \qquad (2\text{-}10)$$

$$R_r = [D \cdot (R_{or}/R_o) + 1 - D] \cdot R, \quad G_r = [D \cdot (G_{or}/G_o) + 1 - D] \cdot G$$

$$\text{if } B > 0, \quad B_r = [D \cdot (B_{or}/B_o^{\beta}) + 1 - D] \cdot B^{\beta} \quad \text{whre } \beta = (B_{or}/B_o)^{0.0834}$$

$$\text{else} \qquad B_r = -[D \cdot (B_{or}/B_o^{\beta}) + 1 - D] \cdot |B|^{\beta}$$

$$\begin{vmatrix} X_r \\ Y_r \\ Z_r \end{vmatrix} = M^{-1} \cdot \begin{vmatrix} R_r Y \\ G_r Y \\ B_r Y \end{vmatrix}$$

## Step 2. Colour appearance predictors

Lightness $L_{I} = 116 \cdot [f(Y_r/100)]^z - 16 \quad \text{where } z = 1 + F_{L} \cdot (Y_b/100)^{1/2}$ (2-11)

$$A = 500 \cdot [f(X_r/100) - f(Y_r/100)], \quad B = 200 \cdot [f(Y_r/100) - f(Z_r/100)]$$

$$\text{if } x > 0.008856 \quad f(x) = x^{1/F_3}$$

$$\text{else } f(x) = \left[ \left(0.008856^{1/F_3} - 16/116\right)/0.008856 \right] \cdot x + 16/116$$

Chroma $Ch_{I} = 25 \cdot \ln(1 + 0.05 \cdot C) = 25 \cdot \ln\left(1 + 0.05 \cdot \sqrt{A^2 + B^2}\right)$

Colourfulness $C_{I} = Ch_{I} S_M S_C F_C$

$$\text{where } S_M = 0.7 + 0.02 \cdot L_{I} - 0.0002 \cdot L_{I}^2$$

$$S_C = 1.0 + 0.47 \cdot \log L - 0.057 \cdot (\log L)^2$$

Saturation $S_{I} = Ch_{I}/L_{I}$

Hue angle $h_{I} = \tan^{-1}(B/A)$ [degrees]

Hue quadrature $H_{I} = H_{I1} + (H_{I2} - H_{I1}) \cdot (h_{I} - h_{I1})/(h_{I2} - h_{I1})$

where $h_{I1}, h_{I2}$ : nearest unique hue angles having lower and higher values than $h_{I}$

$H_{I1}, H_{I2}$ : $H_{I}$ values corresponding to $h_{I1}$ and $h_{I2}$

| $h_L$ | R (%) | Y (%) | G (%) | B (%) | $H_L$ | |
|---|---|---|---|---|---|---|
| 25 | 100 | 0 | 0 | 0 | 0 | R |
| 62 | 50 | 50 | 0 | 0 | 50 | R50Y |
| 93 | 0 | 100 | 0 | 0 | 100 | Y |
| 118 | 0 | 50 | 50 | 0 | 150 | Y50G |
| 165 | 0 | 0 | 100 | 0 | 200 | G |
| 202 | 0 | 0 | 50 | 50 | 250 | G50B |
| 254 | 0 | 0 | 0 | 100 | 300 | B |
| 322 | 50 | 0 | 0 | 50 | 350 | B50R |

*Table 2-5 Conversion table from hue angle to hue quadrature for LLAB*

**Step 3. Opponent-colour dimensions**

$$L_{L} = 116 \cdot [f(Y_r/100)]^{z} - 16 \qquad (2\text{-}12)$$

$$A_{L} = C_{L} \cdot \cos(h_{L})$$

$$B_{L} = C_{L} \cdot \sin(h_{L})$$

## 2.9.4 The Hunt94 Model

The Hunt94 model is one of the most extensive, complete and complex colour appearance models to date. The Hunt colour appearance model has been created by R. W. G. Hunt from some of his earlier chromatic-adaptation studies [Hunt1952] up through its rigorous development in the 1980s and 1990s [Hunt1982, 1985, 1987, 1991, 1994]. Hunt94 is a Hunt model revised in 1994 (see Chapter 31 of 'Reproduction of Colour' for full details of Hunt94) [Hunt1995].

This model is based on the zone theory of colour vision. Although the starting data of Hunt94 are tristimulus values, they are soon transformed to cone signals, which are then converted to opponent colour signals after the process of adaptation. The opponent signals are used to construct colour appearance predictors, which account for the colour appearance change by the luminance level, background and surround conditions. Also Hunt94 includes a rod signal in the achromatic predictors requiring scotopic luminance information.

Input data for the Hunt94 are:

| | | | |
|---|---|---|---|
| Relative tristimulus values of test stimulus | $X$ | $Y$ | $Z$ |
| Relative tristimulus values of the reference white | $X_w$ | $Y_w$ | $Z_w$ |

| | |
|---|---|
| Photopic luminance of the adapting field | $L_A$ (cd/m$^2$) |
| Background luminance factor | $Y_b$ |
| Scotopic luminance of the adapting field | $L_{AS}$ (scotopic cd/m$^2$) |
| Scotopic luminance relative of test colour to the reference white | $S/S_w$ (if unavailable, use $Y/Y_w$) |
| Surround parameters | $N_c$ $N_b$ |
| Background parameters | $N_{cb}$ $N_{bb}$ |

Photopic luminance of the adapting field is normally taken as 1/5 of that of the reference white. If the measurement data are not available, the scotopic luminance of the adapting field, $L_{AS}$, can be approximated from the photopic adapting luminance, $L_A$, and correlated colour temperature, $T$, using the equation, $L_{AS}=2.26 \cdot L_A \cdot [T/4000-0.4]^{1/3}$. Also the relative scotopic luminance of a test colour can be substituted by the relative photopic luminance. Hunt94 has two surround and two background induction factors for chromatic ($N_c$, $N_{cb}$) and achromatic ($N_b$, $N_{bb}$) components respectively. Surround parameters, $N_c$ and $N_b$, which need to be predetermined according to the viewing conditions, are shown in Table 2-6.

| Surround Conditions | $N_c$ | $N_b$ |
|---|---|---|
| Small areas in uniform backgrounds and surrounds | 1.0 | 300 |
| Normal scenes | 1.0 | 75 |
| Dim surround | 1.0 | 25 |
| Cut-sheet | 0.7 | 25 |
| Dark surround | 0.7 | 10 |

***Table 2-6 The surround parameters used in the Hunt94 model***

The first step to implementing Hunt94 is to transform the tristimulus values to three cone signals, $\rho$, $\gamma$, $\beta$ in the Hunt-Pointer-Estevez cone space. This transformation is normalised such that the equi-energy illuminant, $S_E$, has equal $\rho$, $\gamma$, $\beta$ values. Subsequently these signals are transformed to the adapted colour signals, $\rho_a$, $\gamma_a$, $\beta_a$, by the non-linear cone response function, which is based on the physiological measurement of cone response of primate vision [Boyn1970, Vale1983]. Section 2.9.4.1 summarises the procedure for calculating the adapted cone signals from the input tristimulus values.

Note that the cone response function contains four factors, i.e. colour bleaching, dynamic adaptation, chromatic adaptation and Helson-Judd effect. These are determined by the luminance level and the chromaticity of the reference white. The cone response function with colour bleaching factor and dynamic adaptation factor models the sensitivity regulating mechanisms introduced in Section 2.2.4.

The next step is to formulate the opponent type signals, which are the achromatic signal and colour difference signals, as shown in Section 2.9.4.2. Note that achromatic signal is a linear combination of three cone signals and one rod signal. The ratios between $\rho_a$, $\gamma_a$, $\beta_a$, are set to 40:20:1 according to the study of Walraven and Bouman [Walr1966].

Section 2.9.4.3 shows the colour appearance predictors of Hunt94. $J_p$ is the lightness predictor for the projected colours [Luo1993b]. The chroma predictor is especially revised from the previous version of Hunt model to take into account the lightness dependency of the chroma change by the background luminance factor [Hunt1994, see Section 2.8.2.2].

### 2.9.4.1. Adaptation

$$\begin{vmatrix} \rho \\ \gamma \\ \beta \end{vmatrix} = M_{II} \cdot \begin{vmatrix} X \\ Y \\ Z \end{vmatrix} \quad \text{where } M_{II} = \begin{vmatrix} 0.38971 & 0.68898 & -0.07868 \\ -0.22981 & 1.18340 & 0.04641 \\ 0.00000 & 0.00000 & 1.00000 \end{vmatrix}$$

$$\rho_a = B_\rho \cdot \left[ 40 \cdot \frac{(F_L F_\rho \rho/\rho_w)^{0.73}}{(F_L F_\rho \rho/\rho_w)^{0.73} + 2} + \rho_D \right] + 1$$

$$\gamma_a = B_\gamma \cdot \left[ 40 \cdot \frac{(F_L F_\gamma \gamma/\gamma_w)^{0.73}}{(F_L F_\gamma \gamma/\gamma_w)^{0.73} + 2} + \gamma_D \right] + 1$$

$$\beta_a = B_\beta \cdot \left[ 40 \cdot \frac{(F_L F_\beta \beta/\beta_w)^{0.73}}{(F_L F_\beta \beta/\beta_w)^{0.73} + 2} + \beta_D \right] + 1$$

where

Cone bleaching factor: $B_\rho$, $B_\gamma$, $B_\beta$

$$B_\rho = \frac{10^7}{10^7 + 5 \cdot L_A \cdot (\rho_w/100)}, \quad B_\gamma = \frac{10^7}{10^7 + 5 \cdot L_A \cdot (\gamma_w/100)}, \quad B_\beta = \frac{10^7}{10^7 + 5 \cdot L_A \cdot (\beta_w/100)}$$

Dynamic adaptation factor: $F_L$

$$F_L = 0.2 \cdot k^4 \cdot (5L_A) + 0.1 \cdot (1 - k^4)^2 \cdot (5L_A)^{1/3} \quad , \quad k = 1/(5L_A + 1)$$

Chromatic adaptation factor: $F_\rho, F_\gamma, F_\beta$

$$F_\rho = \frac{1 + L_A^{1/3} + h_\rho}{1 + L_A^{1/3} + 1/h_\rho} \quad , \quad F_\gamma = \frac{1 + L_A^{1/3} + h_\gamma}{1 + L_A^{1/3} + 1/h_\gamma} \quad , \quad F_\beta = \frac{1 + L_A^{1/3} + h_\beta}{1 + L_A^{1/3} + 1/h_\beta}$$

where $h_\rho = \frac{3 \cdot \rho_w}{\rho_w + \gamma_w + \beta_w}$ , $h_\gamma = \frac{3 \cdot \gamma_w}{\rho_w + \gamma_w + \beta_w}$ , $h_\beta = \frac{3 \cdot \beta_w}{\rho_w + \gamma_w + \beta_w}$

Helson-Judd effect factor: $\rho_D$, $\gamma_D$, $\beta_D$

$$\rho_D = 40 \cdot \frac{(F_L F_\gamma \cdot Y/Y_w)^{0.73}}{(F_L F_\gamma \cdot Y/Y_w)^{0.73} + 2} - 40 \cdot \frac{(F_L F_\rho \cdot Y/Y_w)^{0.73}}{(F_L F_\rho \cdot Y/Y_w)^{0.73} + 2}$$

$$\gamma_D = 0$$

$$\beta_D = 40 \cdot \frac{(F_L F_\gamma \cdot Y/Y_w)^{0.73}}{(F_L F_\gamma \cdot Y/Y_w)^{0.73} + 2} - 40 \cdot \frac{(F_L F_\beta \cdot Y/Y_w)^{0.73}}{(F_L F_\beta \cdot Y/Y_w)^{0.73} + 2}$$

### 2.9.4.2. Opponent Colour Signals

Achromic Signal $A = N_{bb} \cdot \left[ A_a - 1 + A_S - 0.3 + (1^2 + 0.3^2)^{1/2} \right]$ where $N_{bb} = \frac{0.725}{n^{0.2}}$ , $n = \frac{Y_b}{Y_w}$

Photopic: $A_a = 2 \cdot \rho_a + \gamma_a + 0.05 \cdot \beta_a - 3.05$

Scotopic: $A_S = B_S \cdot 3.05 \cdot \left[ 40 \cdot \frac{(F_{LS} S/S_w)^{0.73}}{(F_L F_\rho \rho/\rho_w)^{0.73} + 2} \right] + 0.3$

where $F_{LS} = 3800 \cdot j^2 \cdot \left( \frac{5 \cdot L_{AS}}{2.26} \right) + 0.2 \cdot (1 - j^2)^4 \cdot \left( \frac{5 \cdot L_{AS}}{2.26} \right)^{1/6}$

$$j = \frac{1}{5 \cdot L_{AS}/2.26 + 0.00001}$$

$$B_S = \frac{0.5}{1 + 0.3 \cdot [(5 \cdot L_{AS}/2.26) \cdot (S/S_w)]^{0.3}} + \frac{0.5}{1 + 5 \cdot (5 \cdot L_{AS}/2.26)}$$

Colour Difference Signals $C_1 = \rho_a - \gamma_a$ , $C_2 = \gamma_a - \beta_a$ , $C_3 = \beta_a - \rho_a$

### 2.9.4.3. Colour Appearance Predictors

#### Chromatic Predictors

Yellowness - Blueness $M_{YB} = 100\frac{(C_2 - C_3)}{9} e_s \frac{10}{13} N_c N_{cb} F_t$

Redness - Greenness $M_{RG} = 100 \cdot \left(C_1 - \frac{C_2}{11}\right) \cdot e_s \frac{10}{13} N_c N_{cb}$

where $e_s = e_1 + (e_2 - e_1)\frac{h_s - h_1}{h_2 - h_1}$,

$$N_{cb} = 0.725 \cdot \left(\frac{Y_w}{Y_b}\right)^{0.2}, F_t = \frac{L_A}{L_A + 0.1}$$

Saturation $s = \frac{50 \cdot M}{\rho_a + \gamma_a + \beta_a}$

where $M = \left(M_{YB}{}^2 + M_{RG}{}^2\right)^{1/2}$ : Chromatic Response

Chroma $C_{94} = 2.44 \cdot s^{0.69} \cdot (Q/Q_w)^{Y_b/Y_w} \cdot \left(1.64 - 0.29^{Y_b/Y_w}\right)$

Colourfulness $M_{94} = C_{94} \cdot F_L^{0.15}$

#### Achromatic Predictors

Brightness $Q = \left[7 \cdot \left(A + \frac{M}{100}\right)\right]^{0.6} N_1 - N_2$ where $N_1 = \frac{(7A_w)^{0.5}}{5.33 \cdot N_b^{0.13}}$, $N_2 = \frac{7A_w N_b^{0.362}}{200}$

Lightness $J = 100 \cdot \left(\frac{Q}{Q_w}\right)^z$, $z = 1 + \left(\frac{Y_b}{Y_w}\right)^{0.5}$

Modified lightness for projected transparecies

$$J_p = J'' \cdot \left\{1.14 \cdot \left[1 - \left(\frac{J''}{100}\right)^3\right] + \left(\frac{J''}{100}\right)^5\right\} \text{ where } J'' = 100 \cdot \left(\frac{Q}{Q_w}\right)^{1.2}$$

#### Hue Predictors

Hue angle $h_s = \tan^{-1}\left[\frac{(C_2 - C_3)/9}{C_1 - C_2/11}\right]$ [degrees]

Hue quadrature $H = H_1 + \frac{100 \cdot (h_s - h_1)/e_1}{(h_s - h_1)/e_1 + (h_2 - h_s)/e_2}$

Table 2-7 shows the hue angle, $h_s$, and eccentricity, $e_s$, of the four unique hues. Note that $e_1$ and $h_1$ are the values of $e_s$ and $h_s$, respectively for the unique hues having the nearest lower values of h and $e_2$ and $h_2$ are the values for the unique hues having the nearest higher value of $h$.

| Unique Hue | Red | Yellow | Green | Blue |
|---|---|---|---|---|
| Hue angle $h_s$ | 20.14 | 90.00 | 164.25 | 237.53 |
| Eccentricity $e_s$ | 0.8 | 0.7 | 1.0 | 1.2 |

***Table 2-7 The hue angle and eccentricity of the unique hues for the Hunt94 model***

## 2.9.5 The CIECAM97s Model

CIECAM97s [CIE1998, Luo1998, Hunt1998 Chapter12] is the first recommended colour appearance model agreed by CIE Technical Committee TC 1-34 in May 1997. The CIECAM97s model also follows the zone theory of colour vision. The input tristimulus values are transformed to the cone signals after chromatic and dynamic adaptation. Then these adapted cone signals are used to construct three opponent colour signals, which are used for the colour appearance predictors.

Input data for the CIECAM97s are:

| | |
|---|---|
| Relative tristimulus values of test stimulus | $X$ $Y$ $Z$ |
| Relative tristimulus values of the reference white | $X_w$ $Y_w$ $Z_w$ |
| Reference white in reference conditions | $X_{wr}=100$ $Y_{wr}=100$ $Z_{wr}=100$ |
| Photopic luminance of the adapting filed (normally taken as 1/5 of the lumininace of reference white) | $L_A$ (cd/m$^2$) |
| Background luminance factor | $Y_b$ |
| Surround Parameters (See Table 2-8) | $F$ $c$ $F_{LL}$ $N_c$ |
| Background parameters | $N_{cb}$ $N_{bb}$ |

| Surround Condition | $F$ | $c$ | $F_{LL}$ | $N_c$ |
|---|---|---|---|---|
| Average Surround ( > 4° ) | 1.0 | 0.69 | 0.0 | 1.0 |
| Average Surround ( < 4° ) | 1.0 | 0.69 | 1.0 | 1.0 |
| Dim surround | 0.9 | 0.59 | 1.0 | 1.1 |
| Dark surround | 0.9 | 0.525 | 1.0 | 0.8 |
| Cut-sheet | 0.9 | 0.41 | 1.0 | 0.8 |

***Table 2-8 The surround parameters used in the CIECAM97s model***

The procedures for CIECAM97s are divided into three groups: adaptation, opponent-colour signals and colour appearance prediction. Section 2.9.5.1 gives the adaptation process, i.e. the transformation of input tristimulus values under the test viewing conditions to the adapted cone signals under the reference viewing conditions. This adaptation process consists of chromatic adaptation and dynamic adaptation.

Note that the chromatic adaptation transform used in the LLAB model is also adopted in the CIECAM97s with an additional function for calculating the degree of adaptation, $D$. Using this step, tristimulus values ($XYZ$) under the test viewing condition are transformed to the tristimulus values ($X_cY_cZ_c$) of corresponding colours under the reference condition. Then the corresponding tristimulus values ($X_cY_cZ_c$) are transformed to the cone signals ($\rho\ \gamma\ \beta$) in the Hunt-Pointer-Estevez cone space followed by dynamic adaptation using cone response functions similar to those used for the Hunt94 model (see Section 2.9.4.1). The output signals ($\rho_a\ \gamma_a\ \beta_a$) are the adapted cone signals according to the luminance level of the image.

Section 2.9.5.2 shows the opponent colour signals, which represent achromatic signal, $A$, redness-greenness, $a$, and yellowness-blueness, $b$. The achromatic signal is calculated as a combination of three cones while the colour difference signals $a$ and $b$ are calculated by combining the differences of cone signals. The calculations of colour appearance predictors are given in Section 2.9.5.3.

CIECAM97s predicts the lightness contrast change by background and surround conditions. Luminance level affects lightness contrast in the dynamic adaptation process using the cone response function. Chromatic predictors, i.e. saturation, chroma and colourfulness, are modelled to be functions of background, surround and also luminance level (the Hunt Effect).

### 2.9.5.1. Chromatic and Dynamic Adaptation (CIECAM97s)

**Chromatic Adaptation**

$$\begin{vmatrix} R \\ G \\ B \end{vmatrix} = M_{CMCCAT97} \cdot \begin{vmatrix} X/Y \\ Y/Y \\ Z/Y \end{vmatrix} \quad \text{where } M_{CMCCAT97} = \begin{vmatrix} 0.8951 & 0.2664 & -0.1614 \\ -0.7502 & 1.7135 & 0.0367 \\ 0.0389 & -0.0685 & 1.0296 \end{vmatrix}$$

$$R_C = \left[D \cdot \left(\frac{R_{WR}}{R_W}\right) + 1 - D\right] \cdot R \;,\; G_C = \left[D \cdot \left(\frac{G_{WR}}{G_W}\right) + 1 - D\right] \cdot G \;,\; B_C = \left[D \cdot \left(\frac{B_{WR}}{B_W{}^p}\right) + 1 - D\right] \cdot |B|^p$$

$$D = F - \frac{F}{1 + 2 \cdot L_A^{1/4} + L_A^2/300} \;,\quad p = \left(\frac{B_W}{B_{WR}}\right)^{0.0834}$$

$$\begin{vmatrix} X_C \\ Y_C \\ Z_C \end{vmatrix} = M^{-1}_{CAMCAT97} \begin{vmatrix} R_C Y \\ G_C Y \\ B_C Y \end{vmatrix}$$

**Dynamic Adaptation**

$$\begin{vmatrix} \rho \\ \gamma \\ \beta \end{vmatrix} = M_{II} \cdot \begin{vmatrix} X_C \\ Y_C \\ Z_C \end{vmatrix} \quad \text{where } M_{II} = \begin{vmatrix} 0.38971 & 0.68898 & -0.07868 \\ -0.22981 & 1.18340 & 0.04641 \\ 0.00000 & 0.00000 & 1.00000 \end{vmatrix}$$

$$\rho_a = 40\frac{(F_L \rho/100)^{0.73}}{(F_L \rho/100)^{0.73} + 2} + 1 \;,\; \gamma_a = 40\frac{(F_L \gamma/100)^{0.73}}{(F_L \gamma/100)^{0.73} + 2} + 1 \;,\; \beta_a = 40\frac{(F_L \beta/100)^{0.73}}{(F_L \beta/100)^{0.73} + 2} + 1$$

$$\text{where } F_L = 0.2 \cdot k^4 \cdot (5L_A) + 0.1 \cdot (1 - k^4)^2 \cdot (5L_A)^{1/3} \;,\; k = 1/(5L_A + 1)$$

### 2.9.5.2. Opponent Colour Signals (CIECAM97s)

Achromic Signal $A = [2 \cdot \rho_a + \gamma_a + 0.05 \cdot \beta_a - 2.05] \cdot N_{bb}$ where $N_{bb} = \frac{0.725}{n^{0.2}}$ , $n = \frac{Y_b}{Y_w}$

Redness - Greenness $a = \rho_a - \frac{12}{11} \cdot \gamma_a + \frac{1}{11} \cdot \beta_a$

Yellowness - Blueness $b = \frac{1}{9}(\rho_a + \gamma_a - 2 \cdot \beta_a)$

### 2.9.5.3. Colour Appearance Predictors (CIECAM97s)

Lightness $J = 100 \cdot \left(\frac{A}{A_w}\right)^{cz}$ , $z = 1 + F_{LL} \cdot \left(\frac{Y_b}{Y_w}\right)^{0.5}$

Brightness $Q = \frac{1.24}{c} \cdot \left(\frac{J}{100}\right)^{0.67} \cdot (A_W + 3)^{0.9}$

Saturation $$s = N_c \cdot N_{cb} \frac{5000 \cdot e \cdot \sqrt{a^2 + b^2} \cdot (10/13)}{\rho_a + \gamma_a + (21/20) \cdot \beta_a}$$

$$e = e_1 + (e_2 - e_1)\frac{h - h_1}{h_2 - h_1}, \quad N_{cb} = 0.725 \cdot \left(\frac{Y_w}{Y_b}\right)^{0.2}$$

Chroma $$C = 2.44 \cdot s^{0.69} \cdot (J/100)^{0.67 \cdot n} \cdot (1.64 - 0.29^n)$$

Colourfulness $$M = C \cdot F_L^{0.15}$$

Hue angle $$h = \tan^{-1}(b/a) \quad \text{[degrees]}$$

Hue quadrature $$H = H_1 + \frac{100 \cdot (h - h_1)/e_1}{(h - h_1)/e_1 + (h_2 - h)/e_2}$$

where $h_1, h_2$ : nearest unique hue angles with lower and higher values than $h$

$e_1, e_2$ : eccentricity $e$ corresponding to unique hues $h_1$ and $h_2$

$H_1$ : $H$ value corresponding to $h_1$

| Unique Hue | Red | Yellow | Green | Blue |
|---|---|---|---|---|
| Hue angle $h$ | 20.14 | 90.00 | 164.25 | 237.53 |
| Eccentricity $e$ | 0.8 | 0.7 | 1.0 | 1.2 |

***Table 2-9 The hue angle and eccentricity of the unique hues for the CIECAM97s, Fairchild and FC model***

### 2.9.5.4. Shortcomings of the CIECAM97s Model

After the establishment of CIECAM97s, some problems with its performance were found and several revised models were suggested such as CAM97s2, Fairchild or FC, eventually leading to the latest CIE recommended model, CIECAM02 [Moro1998, Li2000, Fair2001, Luo2000, Luo2002, Moro2002].

There are three main shortcomings in CIECAM97s. Firstly, the lightness scale, $J$, does not become zero even for a perfect black stimulus. Note that the achromatic signal, $A$ (given in Section 2.9.5.2), always includes a value, $N_{bb}$, for a black stimulus ($X$=$Y$=$Z$=0) indicating that the lightness of an ideal black is not zero and increases under lower luminance level (lower $A_w$) [Moro1998, Luo1999, Luo2000]. Secondly the surround parameter, $N_c$, which decides the colour gamut change by the surround condition, has an anomaly. As shown in Table 2-8, $N_c$ has its highest value (i.e. highest chroma or colourfulness), for a dim surround followed by an average and dark

surround. Parameter $N_c$ for a dim surround should have a value between that of an average and dark surround [Moro1998, Luo1999, Luo2000]. Thirdly, it is found that the hue and saturation of CIECAM97s vary if a colour of a given chromaticity has a changing luminance factor, which is undesirable in imaging applications [Hunt2003].

The revised models were designed to fix the shortcomings of CIECAM97s and also to improve the performance and simplify the equations. In particular, the revised models were simplified by removing the non-linearity of the chromatic adaptation transform of the blue channel (see Section 2.9.5.1), which makes CIECAM97s uninvertible [Finl1999, 2000, Li2000, 2002].

## 2.9.6 Fairchild

The Fairchild Model is one of the modified CIECAM97s models derived by M. D. Fairchild [Fair2001]. Although the basic structure remains the same, several equations are modified and simplified to give better performance. The Fairchild model has the same input data as CIECAM97s.

| | | | |
|---|---|---|---|
| Relative tristimulus values of test stimulus | $X$ | $Y$ | $Z$ |
| Relative tristimulus values of the reference white | $X_w$ | $Y_w$ | $Z_w$ |
| Reference white in reference conditions | $X_{wr}=100$ | $Y_{wr}=100$ | $Z_{wr}=100$ |
| Photopic luminance of the adapting field (normally taken as 1/5 of the lumininace of reference white) | $L_A$ (cd/m$^2$) | | |
| Background luminance factor | $Y_b$ | | |
| Surround Parameters (See Table 2-10) | $F$ | $c$ | $N_c$ |
| Background parameters | $N_{cb}$ | $N_{bb}$ | |

However there are several changes in the model parameters. Firstly the $F_{LL}$ parameter has been removed from CIECAM97s because it only functioned for large stimuli that are not found in imaging applications. Secondly the $N_c$ parameter was adjusted so that a dim surround has a middle value between those for average and dark surround as shown in Table 2-10. Also Fairchild suggested allowing intermediate surround compensation rather than having a limited number of categorical parameters. The $c$ parameter can be used as a continuous variable and the $N_c$ parameter is selected as a function of the $c$ parameter as shown in the following diagram.

| Surround Conditions | $F$ | $c$ | $N_c$ |
|---|---|---|---|
| Average Surround | 1.0 | 0.69 | 1.0 |
| Dim surround | 0.9 | 0.59 | 0.95 |
| Dark surround | 0.9 | 0.525 | 0.8 |

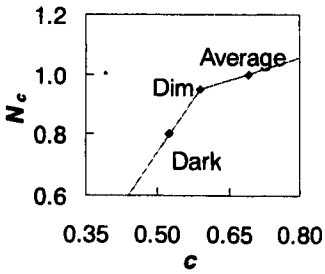


***Table 2-10 The surround parameters used in the Fairchild model***

The equations used to implement the Fairchild model are grouped into the adaptation process, the opponent colour signals and the colour appearance predictors in sections 2.9.6.1, 2.9.6.2 and 2.9.6.3 respectively. For the chromatic adaptation process in Section 2.9.6.1, the non-linearity of the blue channel found in CIECAM97s is removed and a newly optimised matrix, $\mathbf{M}_{Fairchild}$, is introduced to transform *XYZ* to spectrally sharpened *RGB* space.

The change made to the opponent signals in Section 2.9.6.2 is a value subtracted from the achromatic signal formulae. It has been changed from 2.05 for the CIECAM97s to 3.05 following the correction made by Li *et al.* for the CAM97s2 model [Li2000]. Also the chroma predictor was modified in Section 2.9.6.3 to reduce the chroma scale of CIECAM97s at low chroma levels [Moro1998, Wybl2000, Newm2000]. Note that unique hues used to calculate hue quadratures have not been changed from CIECAM97s.

### 2.9.6.1. Chromatic and Dynamic Adaptation (Fairchild)

#### Chromatic Adaptation

$$\begin{vmatrix} R \\ G \\ B \end{vmatrix} = M_{Fairchild} \cdot \begin{vmatrix} X \\ Y \\ Z \end{vmatrix} = \begin{vmatrix} 0.8562 & 0.3372 & -0.1934 \\ -0.8360 & 1.8327 & 0.0033 \\ 0.0357 & -0.0469 & 0.0112 \end{vmatrix} \cdot \begin{vmatrix} X \\ Y \\ Z \end{vmatrix}$$

$$R_C = \left[ D \cdot \left( \frac{R_{WR}}{R_W} \right) + 1 - D \right] \cdot R \;,\; G_C = \left[ D \cdot \left( \frac{G_{WR}}{G_W} \right) + 1 - D \right] \cdot G \;,\; B_C = \left[ D \cdot \left( \frac{B_{WR}}{B_W} \right) + 1 - D \right] \cdot B$$

$$D = F - \frac{F}{1 + 2 \cdot L_A^{1/4} + L_A^2 / 300}$$

$$\begin{vmatrix} X_C \\ Y_C \\ Z_C \end{vmatrix} = M_{Fairchild}^{-1} \begin{vmatrix} R_C \\ G_C \\ B_C \end{vmatrix}$$

### Dynamic Adaptation

$$\begin{vmatrix} R' \\ G' \\ B' \end{vmatrix} = M_{II} \cdot \begin{vmatrix} X_C \\ Y_C \\ Z_C \end{vmatrix} \quad \text{where } M_{II} = \begin{vmatrix} 0.38971 & 0.68898 & -0.07868 \\ -0.22981 & 1.18340 & 0.04641 \\ 0.00000 & 0.00000 & 1.00000 \end{vmatrix}$$

$$R_a' = 40\frac{(F_L R'/100)^{0.73}}{(F_L R'/100)^{0.73}+2}+1 \;,\; G_a' = 40\frac{(F_L G'/100)^{0.73}}{(F_L G'/100)^{0.73}+2}+1 \;,\; B_a' = 40\frac{(F_L B'/100)^{0.73}}{(F_L B'/100)^{0.73}+2}+1$$

where $F_L = 0.2\cdot k^4\cdot(5L_A)+0.1\cdot(1-k^4)^2\cdot(5L_A)^{1/3}$ , $k = 1/(5L_A+1)$

## 2.9.6.2. Opponent Colour Signals (Fairchild)

Achromic Signal $A = \left[2\cdot R_a' + G_a' + 0.05\cdot B_a' - 3.05\right]\cdot N_{bb}$ where $N_{bb} = \dfrac{0.725}{n^{0.2}}$ , $n = \dfrac{Y_b}{Y_w}$

Redness - Greenness $a = R_a' - \dfrac{12}{11}\cdot G_a' + \dfrac{1}{11}\cdot B_a'$

Yellowness - Blueness $b = \dfrac{1}{9}\left(R_a' + G_a' - 2\cdot B_a'\right)$

## 2.9.6.3. Colour Appearance Predictors (Fairchild)

Lightness $J = 100\left(\dfrac{A}{A_w}\right)^{cz}$ , $z = 1+\left(\dfrac{Y_b}{Y_w}\right)^{0.5}$

Brightness $Q = \dfrac{1.24}{c}\cdot\left(\dfrac{J}{100}\right)^{0.67}\cdot(A_W+3)^{0.9}$

Saturation $s = N_c\cdot N_{cb}\dfrac{5000\cdot e\cdot\sqrt{a^2+b^2}\cdot(10/13)}{\rho_a+\gamma_a+(21/20)\cdot\beta_a}$

$$e = e_1 + (e_2-e_1)\frac{h-h_1}{h_2-h_1}, \quad N_{cb} = 0.725\cdot\left(\frac{Y_w}{Y_b}\right)^{0.2}$$

Chroma $C = 0.7487\cdot s^{0.973}\cdot(J/100)^{0.945\cdot n}\cdot\left(1.64-0.29^n\right)^{1.41}$

Colourfulness $M = C\cdot F_L^{0.15}$

Hue angle $h = \tan^{-1}(b/a)$ [degrees]

Hue quadrature $H = H_1 + \dfrac{100\cdot(h-h_1)/e_1}{(h-h_1)/e_1+(h_2-h)/e_2}$

* Refer *Table* 2-9 for the unique hue angle, $h$, and eccentricity, $e$, data

## 2.9.7 The FC Model

The FC model [Hunt2002] is also a revised version of CIECAM97s by modifying the Fairchild model. It has the same structure as the CIECAM97s and Fairchild models but with several changes in details. The FC model follows the same input data and model parameters as the Fairchild model (see the previous Section 2.9.6 for the details of input data and the model parameters). The formulae for the FC model are introduced in Section 2.9.7.1, 2.9.7.2 and 2.9.7.3 for the adaptation, opponent signals and colour appearance predictors respectively.

As shown in Section 2.9.7.1, the FC model uses the same linearised chromatic adaptation for the blue channel as the Fairchild model but with a new optimised *XYZ*-to-*RGB* transformation matrix known as CMCCAT2000 [Li2002]. Also note that a new $D$ factor is proposed for the degree of chromatic adaptation.

The main differences between the FC and the Fairchild models are shown in Section 2.9.7.3 for the calculation of colour appearance predictors. Firstly lightness has a modified $z$ function, which controls the lightness contrast change by the background luminance factor. The chroma predictor for FC is the same with CIECAM97s. Note that CIECAM97s and FC are based on the LUTCHI data sets while the Fairchild scale was based upon the Munsell data to formulate chromatic predictors. Another main difference in FC model is the new saturation predictor, which was derived from the visual data on the magnitude estimation of saturation obtained by Juan [Juan2000].

### 2.9.7.1. Chromatic and Dynamic Adaptation (FC)

**Chromatic Adaptation**

$$\begin{vmatrix} R \\ G \\ B \end{vmatrix} = M_{CMCCAT2000} \cdot \begin{vmatrix} X \\ Y \\ Z \end{vmatrix} \quad \text{where } M_{CMCCAT2000} = \begin{vmatrix} 0.7982 & 0.3389 & -0.1371 \\ -0.5918 & 1.5512 & 0.0406 \\ 0.0008 & -0.0239 & 0.9753 \end{vmatrix}$$

$$R_C = \left[D \cdot \left(\frac{R_{WR}}{R_W}\right) + 1 - D\right] \cdot R \ , \ G_C = \left[D \cdot \left(\frac{G_{WR}}{G_W}\right) + 1 - D\right] \cdot G \ , \ B_C = \left[D \cdot \left(\frac{B_{WR}}{B_W}\right) + 1 - D\right] \cdot B$$

$$D = F \cdot [0.08 \cdot \log_{10}(L_A) + 0.76]$$

$$\begin{vmatrix} X_C \\ Y_C \\ Z_C \end{vmatrix} = M^{-1}_{CAMCAT2000} \begin{vmatrix} R_C \\ G_C \\ B_C \end{vmatrix}$$

### Dynamic Adaptation

$$\begin{vmatrix} \rho \\ \gamma \\ \beta \end{vmatrix} = M_{II} \begin{vmatrix} X_C \\ Y_C \\ Z_C \end{vmatrix} \quad \text{where } M_{II} = \begin{vmatrix} 0.38971 & 0.68898 & -0.07868 \\ -0.22981 & 1.18340 & 0.04641 \\ 0.00000 & 0.00000 & 1.00000 \end{vmatrix}$$

$$\rho_a = 40\frac{(F_L\rho/100)^{0.73}}{(F_L\rho/100)^{0.73}+2}+1 \;,\; \gamma_a = 40\frac{(F_L\gamma/100)^{0.73}}{(F_L\gamma/100)^{0.73}+2}+1 \;,\; \beta_a = 40\frac{(F_L\beta/100)^{0.73}}{(F_L\beta/100)^{0.73}+2}+1$$

$$\text{where } F_L = 0.2\cdot k^4\cdot(5L_A)+0.1\cdot\left(1-k^4\right)^2\cdot(5L_A)^{1/3} \;,\; k = 1/(5L_A+1)$$

## 2.9.7.2. Opponent Colour Signals (FC)

Achromic Signal $A = [2\cdot\rho_a+\gamma_a+0.05\cdot\beta_a-3.05]\cdot N_{bb}$ where $N_{bb} = \frac{0.725}{n^{0.2}}$ , $n = \frac{Y_b}{Y_w}$

Redness - Greenness $a = \rho_a - \frac{12}{11}\cdot\gamma_a + \frac{1}{11}\cdot\beta_a$

Yellowness - Blueness $b = \frac{1}{9}(\rho_a+\gamma_a-2\cdot\beta_a)$

## 2.9.7.3. Colour Appearance Predictors (FC)

Lightness $J = 100\cdot\left(\frac{A}{A_w}\right)^{cz}$ , $z = 0.85+\left(\frac{Y_b}{Y_w}\right)^{0.5}$

Brightness $Q = \frac{1.24}{c}\cdot\left(\frac{J}{100}\right)^{0.67}\cdot(A_W+3)^{0.9}$

Chroma $C = 2.44\cdot t^{0.69}\cdot(J/100)^{0.67\cdot n}\cdot\left(1.64-0.29^n\right)$

$$\text{where } t = N_c\cdot N_{cb}\frac{5000\cdot e\cdot\sqrt{a^2+b^2}\cdot(10/13)}{\rho_a+\gamma_a+(21/20)\cdot\beta_a}$$

$$e = e_1+(e_2-e_1)\frac{h-h_1}{h_2-h_1}, N_{cb} = 0.725\cdot\left(\frac{Y_w}{Y_b}\right)^{0.2}$$

Colourfulness $M = C\cdot F_L^{0.15}$

Saturation $s = (M/Q)^{0.5}$

Hue angle $h = \tan^{-1}(b/a)$ [degrees]

Hue quadrature $H = H_1+\frac{100\cdot(h-h_1)/e_1}{(h-h_1)/e_1+(h_2-h)/e_2}$

* Refer *Table* 2-9 for the unique hue angle, *h*, and eccentricity, *e*, data

### 2.9.8 The CIECAM02 Model

CIECAM02 is the latest CIE standard colour appearance model proposed by the CIE TC 8-01 in 2002 [Moro2002]. This new model retains the basic structure of CIECAM97s but with many revisions to remove the shortcomings of CIECAM97s mentioned in Section 2.9.5.4. In this section, the CIECAM02 model is divided into three stages: chromatic and dynamic adaptation, opponent colour signals and the prediction of colour appearance. These are introduced in sections 2.9.8.1, 2.9.8.2 and 2.9.8.3 respectively.

The input data of CIECAM02 are the same as those of CIECAM97s but the surround parameters are modified as shown in Table 2-11. Input data and parameters are summarised below.

| | | | |
|---|---|---|---|
| Relative tristimulus values of test stimulus | $X$ | $Y$ | $Z$ |
| Relative tristimulus values of the reference white | $X_w$ | $Y_w$ | $Z_w$ |
| Reference white in reference conditions | $X_{wr}=100$ | $Y_{wr}=100$ | $Z_{wr}=100$ |
| Photopic luminance of the adapting field (normally taken as 1/5 of the lumininace of reference white) | $L_A$ (cd/m$^2$) | | |
| Background luminance factor | $Y_b$ | | |
| Surround parameters (See Table 2-11) | $F$ | $c$ | $N_c$ |
| Background parameters | $N_{cb}$ | $N_{bb}$ | |

| Surround Conditions | $F$ | $c$ | $N_c$ |
|---|---|---|---|
| Average Surround | 1.0 | 0.69 | 1.0 |
| Dim surround | 0.9 | 0.59 | 0.95 |
| Dark surround | 0.8 | 0.525 | 0.8 |

***Table 2-11 The surround parameters used in the CIECAM02 model***

In the chromatic adaptation stage, the non-linearity of the blue channel in CIECAM97s was removed, which required a new *RGB* space, and a modified CMCCAT2000 called CAT02 was chosen for the *XYZ*-to-*RGB* transformation matrix. Also a new function, $D$, for incomplete adaptation and a new eccentricity function, $e$, were adopted.

In CIECAM02, a modification was made to the cone response functions for dynamic adaptation such that the hue and saturation do not vary if the luminance factor changes for a colour of a given chromaticity [Hunt2003]. For the opponent colour

signals, the achromatic signal was modified to yield zero for a stimulus having $Y$=0. All of the colour appearance predictors except hue for CIECAM02 are modified from CIECAM97s.

### 2.9.8.1. Chromatic and Dynamic Adaptation (CIECAM02)

**Chromatic Adaptation**

$$\begin{vmatrix} R \\ G \\ B \end{vmatrix} = M_{CAT02} \cdot \begin{vmatrix} X \\ Y \\ Z \end{vmatrix} \quad \text{where } M_{CAT02} = \begin{vmatrix} 0.7328 & 0.4296 & -0.1624 \\ -0.7036 & 1.6975 & 0.0061 \\ 0.0030 & 0.0136 & 0.9836 \end{vmatrix}$$

$$R_C = \left[ D \cdot \left( \frac{R_{WR}}{R_W} \right) + 1 - D \right] \cdot R \ , \ G_C = \left[ D \cdot \left( \frac{G_{WR}}{G_W} \right) + 1 - D \right] \cdot G \ , \ B_C = \left[ D \cdot \left( \frac{B_{WR}}{B_W} \right) + 1 - D \right] \cdot B$$

$$D = F \cdot \left[ 1 - \frac{1}{3.6} \cdot e^{\frac{-L_A - 42}{92}} \right]$$

$$\begin{vmatrix} X_C \\ Y_C \\ Z_C \end{vmatrix} = M_{CAT02}^{-1} \begin{vmatrix} R_C \\ G_C \\ B_C \end{vmatrix}$$

**Dynamic Adaptation**

$$\begin{vmatrix} R' \\ G' \\ B' \end{vmatrix} = M_H \begin{vmatrix} X_C \\ Y_C \\ Z_C \end{vmatrix} \quad \text{where } M_H = \begin{vmatrix} 0.38971 & 0.68898 & -0.07868 \\ -0.22981 & 1.18340 & 0.04641 \\ 0.00000 & 0.00000 & 1.00000 \end{vmatrix}$$

$$R'_a = 400 \frac{(F_L R'/100)^{0.42}}{(F_L R'/100)^{0.42} + 27.3} + 0.1 \ , \ G'_a = 400 \frac{(F_L G'/100)^{0.42}}{(F_L G'/100)^{0.42} + 27.3} + 0.1$$

$$B'_a = 400 \frac{(F_L B'/100)^{0.42}}{(F_L B'/100)^{0.42} + 27.3} + 0.1$$

$$\text{where } F_L = 0.2 \cdot k^4 \cdot (5L_A) + 0.1 \cdot (1 - k^4)^2 \cdot (5L_A)^{1/3} \ , \ k = 1/(5L_A + 1)$$

### 2.9.8.2. Opponent Colour Signals (CIECAM02)

$$\text{Achromic Signal } A = \left[ 2 \cdot R'_a + G'_a + 0.05 \cdot B'_a - 0.305 \right] \cdot N_{bb} \quad \text{where } N_{bb} = \frac{0.725}{n^{0.2}} \ , \ n = \frac{Y_b}{Y_w}$$

$$\text{Redness - Greenness} \quad a = R'_a - \frac{12}{11} \cdot G'_a + \frac{1}{11} \cdot B'_a$$

$$\text{Yellowness - Blueness} \quad b = \frac{1}{9} \left( R'_a + G'_a - 2 \cdot B'_a \right)$$

### 2.9.8.3. Colour Appearance Predictors (CIECAM02)

Lightness $$J = 100 \cdot \left(\frac{A}{A_w}\right)^{cz} \quad , \quad z = 1.48 + \left(\frac{Y_b}{Y_w}\right)^{0.5}$$

Brightness $$Q = \frac{4}{c} \cdot \sqrt{\frac{J}{100}} \cdot (A_W + 4) \cdot F_L^{0.25}$$

Chroma $$C = t^{0.9} \cdot \sqrt{J/100} \cdot \left(1.64 - 0.29^n\right)^{0.73}$$

where $$t = \frac{e \cdot \sqrt{a^2 + b^2}}{R_a' + G_a' + (21/20) \cdot B_a'} \quad , \quad N_{cb} = 0.725 \cdot \left(\frac{Y_w}{Y_b}\right)^{0.2}$$

$$e = \frac{12500}{13} \cdot N_c \cdot N_{cb} \cdot \left[\cos\left(h\frac{\pi}{180} + 2\right) + 3.8\right]$$

Colourfulness $$M = C \cdot F_L^{0.25}$$

Saturation $$s = 100 \cdot (M/Q)^{0.5}$$

Hue angle $$h = \tan^{-1}(b/a) \quad \text{[degrees]}$$

Hue quadrature $$H = H_1 + \frac{100 \cdot (h - h_1)/e_1}{(h - h_1)/e_1 + (h_2 - h)/e_2}$$

| Unique Hue | Red | Yellow | Green | Blue |
|---|---|---|---|---|
| Hue angle $h$ | 20.14 | 90.00 | 164.25 | 237.53 |
| Eccentricity $e$ | 0.8 | 0.7 | 1.0 | 1.2 |

***Table 2-12 The hue angle and eccentricity of the unique hues for the CIECAM02 model***

## 2.10 Conclusions

In this chapter the previous studies relevant to the author's study have been reviewed. The direction of current development in colour appearance models suggests firstly that new colour appearance data should be collected in a form compatible with the LUTCHI data. Note that CIECAM97s and subsequent models based on CIECAM97s, including CIECAM02, were all designed to give better fitting to LUTCHI data. Collecting new data compatible with LUTCHI helps to extend the available colour appearance data set with the same format. Secondly using CIECAM02 as a basis is the best strategy for deriving a new model, because it currently has the best features available from the revised models, which were intended to correct the shortcomings of CIECAM97s.

# Chapter 3
# Device Characterisation

## 3.1 Introduction

Colour appearance data sets comprise two parts corresponding to the physical and perceptual properties of test colours. The perceptual property of a colour means how it appears to the human vision and data are accumulated via psychophysical experiments, which will be discussed in the following chapters. This chapter is focused on the physical property of a colour, which is determined by the characteristics of the imaging device (or physical medium) used for displaying colours and the colour measurement instrument.

The author's study involved four display devices, namely a CRT and an LCD monitor, an LCD projector and a 35mm slide projector. The colours were measured using a PR-650 spectroradiometer. It is important to understand the characteristics of each display or measuring device used in the study. In this chapter, the performances of three tele-spectroradiometers (TSR) are compared and then the characteristics of digital displays are discussed.

## 3.2 Comparison between Three Spectroradiometers

A colour appearance data collected by the author was measured using a PhotoResarch PR-650 tele-spectroradiometer (TSR), which is different from the instrument used for the LUTCHI data and other colour appearance studies. Colorimetric data of the LUTCHI study were measured using a Bentham TSR and a Minolta TSR CS-1000 was used for the Juan&Luo data set [Juan2000]. In this section, the results are reported of an investigation into the performance of three TSRs: PR-650

(PhotoResearch), Bentham and CS-1000 (Minolta). The specifications of the spectroradiometers tested are listed in Table 3-1. Refer to Section 2.5 for the principles of a spectroradiometer.

| | PR-650 | CS-1000 | Bentham |
|---|---|---|---|
| | Multi-channel Spectroradiometer | Multi-channel Spectroradiometer | Scanning Spectroradiometer |
| Spectral Range | 380 - 780 nm | 380 - 780 nm | 0 – 1400 nm (Grating: 1200L/mm) |
| Wavelength Resolution | < 3.5 nm/pixel | 0.9 nm/pixel | 0.5 nm |
| Spectral Bandwidth | 8 nm | 5 nm | 5 nm |
| Photodetector Element | 128 elements | 512 elements | --- |
| Luminance Range ($cd/m^2$) | 3.4 – 17,000 | 0.01 – 8,000 | ~ 7,000 |
| Spectral Accuracy | ± 2 nm | ± 0.03 nm | ± 0.2 nm |
| Luminance Accuracy (A) | ± 4 % ± 1 | ± 4 % ± 1 | |
| Chromaticity Accuracy | ± 0.0015x<br>± 0.001y | ± 0.0015x<br>± 0.001y | |
| Traceability | NIST | JIS/DIN | NPL |

***Table 3-1 The specifications of the three spectroradiometers***

Three kinds of measurement results are compared to test the performances. These are the Bentham calibration lamp (a filament lamp measured by NPL), a white tile presented under three different sources, i.e. D65, A and CWF (Cool White Fluorescent) simulators and a Macbeth colour checker chart under a D65 simulator. Measuring the Bentham calibration lamp was used to test the accuracy of each instrument and measuring the white tile was used to measure a light source indirectly. Finally the Macbeth colour checker chart was used to examine the performance for measuring reflective colours.

### 3.2.1 Measurement of the Bentham Calibration Lamp

The Bentham calibration lamp is used to calibrate the Bentham TSR. The lamp is measured by NPL (National Physical Laboratory) regularly to maintain the accuracy of the measurements and their traceability to national standards. Therefore it was decided to use the Bentham calibration lamp to check the accuracy of each spectroradiometer in terms of the luminance and chromaticity. Note that using Bentham lamp does not guarantee wavelength accuracy since it is only a luminance gauge (e.g. there could be a wavelength shift). Figure 3–1 shows the spectral distribution of the lamp based on the measurement data from NPL.

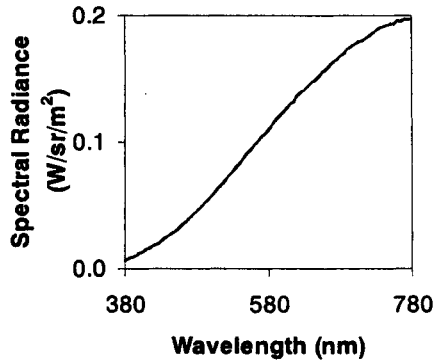


*Figure 3–1 Spectral distribution of the Bentham Calibration Lamp (NPL data)*

The lamp was operated for at least 30 minutes before measurements commenced and the distance between lamp and the object lens of the spectroradiometer was set to 1m. Figure 3–2 shows the measurement geometry. Table 3-2 shows the measurement results. Absolute tristimulus values were calculated from the measured spectral radiance using 2° standard colour matching functions. Also colour differences between the instruments were shown using CIELAB $\Delta E^*_{ab}$ with NPL data as the standard.

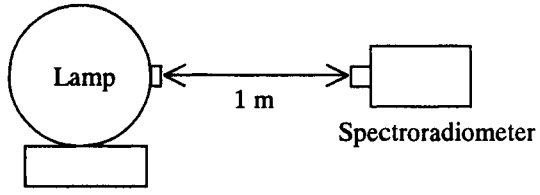


*Figure 3–2 Measurement geometry for the accuracy test of the spectroradiometers*

| | Radiance W/(sr·m²) | $Y_L$ (cd/m²) | $x$ | $y$ | $u$ | $v$ | $\Delta E^*_{ab}$ |
|---|---|---|---|---|---|---|---|
| NPL | 42.46 | 7002 ±1.6% | 0.4493 ±0.0017 | 0.4123 ±0.0003 | 0.2550 ±0.0009 | 0.3509 ±0.0003 | |
| Bentham | 42.72 | 7018 | 0.4492 | 0.4123 | 0.2549 | 0.3509 | 0.12 |
| PR-650 | 42.44 | 6805 | 0.4531 | 0.4131 | 0.2570 | 0.3515 | 2.81 |
| CS-1000 | 42.13 | 6847 | 0.4530 | 0.4135 | 0.2568 | 0.3516 | 2.81 |

*Table 3-2 Bentham Calibration Lamp measurement results*

The Bentham TSR results agree well with NPL data as expected since it was calibrated with the same lamp before starting the measurement. CS-1000 and PR-650 do not fit within the tolerances of NPL result but give similar performance to each other. This becomes clearer when spectral radiance differences are compared as shown in Figure 3–3, which shows the relative spectral radiance difference against the wavelength together with the equation to calculate relative spectral radiance difference.

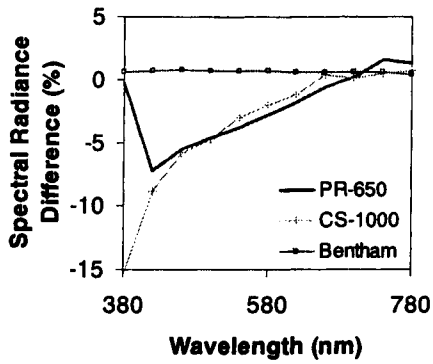


$$\text{Spectral Radiance Difference}(\lambda) = \frac{p_{PR-650 \text{ or } CS-1000}(\lambda) - p_{NPL}(\lambda)}{p_{NPL}(\lambda)} \times 100$$

where $p(\lambda)$: Spectral Radiance

*Figure 3–3 Spectral radiance differences between NPL and spectroradiometers*

The differences between the Bentham and the other two instruments could be caused by their calibration standards. The Bentham TSR measurements are traceable to the NPL standard. PhotoResearch and Minolta instruments, however, are traceable to the NIST (National Institute of Standards and Technology) and JIS/DIN standard respectively.

### 3.2.2 Measurement of a White Tile under Three kinds of Light Sources (D65, A, CWF Simulators)

Measuring the radiance of a white tile inside a light booth was used as an indirect method to measure a light source. Figure 3–4 shows the experimental setting. The 0°/45° illuminant/measurement geometry was used and the distance between the centre of the white tile and the object lens of the spectroradiometer was set to 1m. Light sources used were a D65, an A and a CWF simulator. Each lamp was operated for at least 5 minutes before commencing the measurements. The white tile used in this experiment was a Diffuse White Plastic OP.DI.MA 15/10 made by Gigahertz-Optik.

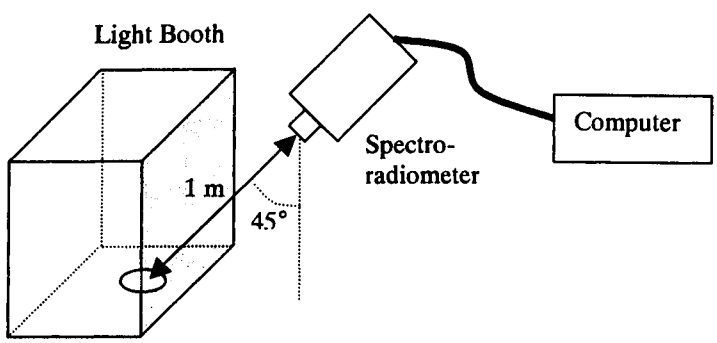


*Figure 3–4 Measurement geometry for the white tile and Macbeth colour chart measurements*

The measured tristimulus values are summarised in Table 3-3. Also CIELAB colour differences $\Delta E^*_{ab}$ were calculated using the each instrument as a standard. The last

three columns in the table show the colour differences calculated using Bentham, PR-650 and CS-1000 data respectively as a reference white.

The white tile measurement results also show similar trends to those found in the lamp measurement data. Measurement results of PR-650 and CS-1000 given in Table 3-3 were similar to each other while Bentham shows a slightly different characteristic from the others. This discrepancy appears again in Figure 3–5 and Figure 3–6, which represent the spectral radiance distributions and chromaticities of the light sources measured by each instrument respectively.

| | | $X_L$ | $Y_L$ (cd/m²) | $Z_L$ | $x$ | $y$ | $\Delta E^*_{ab}$ | | |
|---|---|---|---|---|---|---|---|---|---|
| | | | | | | | Bentham | PR | CS |
| D65 | Bentham | 427.3 | 452.0 | 509.4 | 0.308 | 0.326 | 0.00 | 3.84 | 3.39 |
| | PR-650 | 402.5 | 425.8 | 459.0 | 0.313 | 0.331 | 3.68 | 0.00 | 0.15 |
| | CS-1000 | 409.0 | 433.0 | 467.3 | 0.312 | 0.331 | 3.27 | 0.67 | 0.00 |
| A | Bentham | 491.0 | 449.2 | 156.0 | 0.448 | 0.410 | 0.00 | 4.97 | 4.27 |
| | PR-650 | 457.3 | 415.3 | 136.7 | 0.453 | 0.411 | 4.72 | 0.00 | 0.38 |
| | CS-1000 | 469.0 | 426.9 | 140.5 | 0.453 | 0.412 | 4.08 | 1.14 | 0.00 |
| CWF | Bentham | 359.8 | 375.6 | 240.0 | 0.369 | 0.385 | 0.00 | 6.95 | 6.45 |
| | PR-650 | 345.2 | 353.7 | 208.0 | 0.381 | 0.390 | 6.58 | 0.00 | 1.09 |
| | CS-1000 | 348.0 | 358.9 | 210.6 | 0.379 | 0.391 | 6.12 | 1.24 | 0.00 |

*Table 3-3 Measurement results of the white tile under D65, A and CWF simulators*

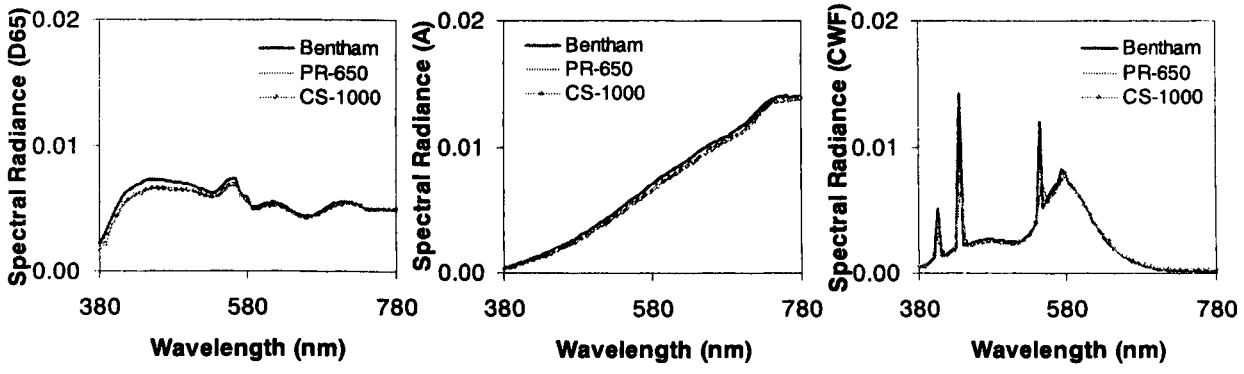


*Figure 3–5 Spectra of three light sources*

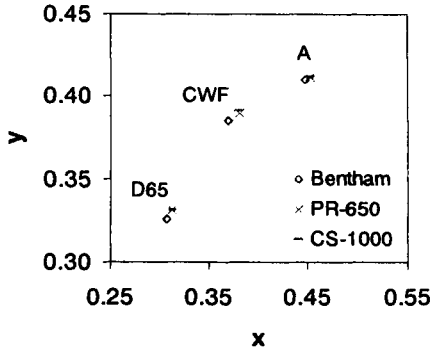


*Figure 3–6 Chromaticities of D65, A and CWF simulators*

Not only the chromaticities but also the luminances showed differences between the TSRs studied. The Bentham TSR has highest luminance followed by CS-1000 and PR-650. Table 3-4 shows the luminance ratio between Bentham and the other two instruments. For measurement of the NPL lamp, the PR-650 and CS-1000 data give 95% and 95.6% of the luminance level of Bentham data respectively. However both the PR-650 and CS-1000 data show decreased ratios for measurement of the white tile compared to the NPL lamp, and the difference between PR-650 and CS-1000 data also becomes larger.

| Luminance Ratio | Bentham (%) | PR-650 (%) | CS-1000 (%) |
|---|---|---|---|
| NPL Lamp | 100 | 97.0 | 97.6 |
| D65 | 100 | 94.2 | 95.8 |
| A | 100 | 92.5 | 95.0 |
| CWF | 100 | 94.2 | 95.5 |

***Table 3-4 Luminance ratio of PR-650 and CS-1000 compared to Bentham data***

Note that the NPL lamp is a tungsten lamp having characteristics similar to the simulator A, but luminance differences between three instruments are largest for simulator A and smallest for NPL lamp. The main difference between NPL lamp and simulator A is luminance level. Luminance of the simulator A is only around 6% of that of NPL lamp. The diagrams in Figure 3–7 show similar analysis results to those in Figure 3–3. This time, measurement data of Bentham was used as the standard since it was the closest to NPL data. Thus spectral radiance differences between data of Bentham and the other two instruments were calculated for NPL lamp and the simulator A.

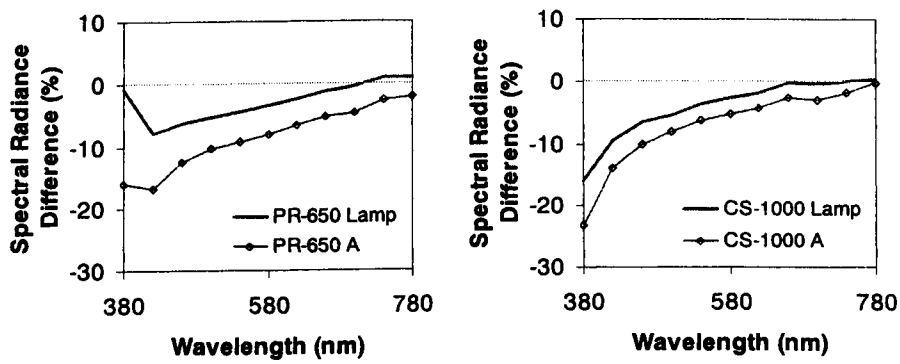


***Figure 3–7 Spectral radiance differences between Bentham vs PR-650 and Bentham vs CS-1000 of NPL lamp and the A simulator***

The left diagram in Figure 3–7 is for PR-650 and the right for CS-1000. Each instrument has similar trends for NPL lamp and simulator A but the differences are larger for the A simulator. This result implies that response curve of the photodetector of each instrument does not have a linear relationship between the instruments investigated. However it is not easy to determine which instrument is most accurate from this analysis since this comparison shows only the relative characteristics between them. The higher difference for short wavelengths might be caused by the lower spectral radiance of NPL lamp and the A simulator.

### 3.2.3 Measurement of the Macbeth ColorChecker under a D65 Simulator

The Macbeth ColorChecker [McCa1976] is widely used in the colour imaging industry and consists of 24 colours. In this study, the 24 colours are used as representative samples of reflective colours to test the performance of spectroradiometers. The same measurement setting as was used to measure a white tile was also used here (see Figure 3–4) under the D65 simulator.

The left diagram in Figure 3–8 shows the chromaticities of 24 colours in an *xy*-diagram. It also shows the same trend that the Bentham TSR gave slightly different results from the other two instruments. In particular the difference is more obvious for the blue area where short wavelengths are dominant.

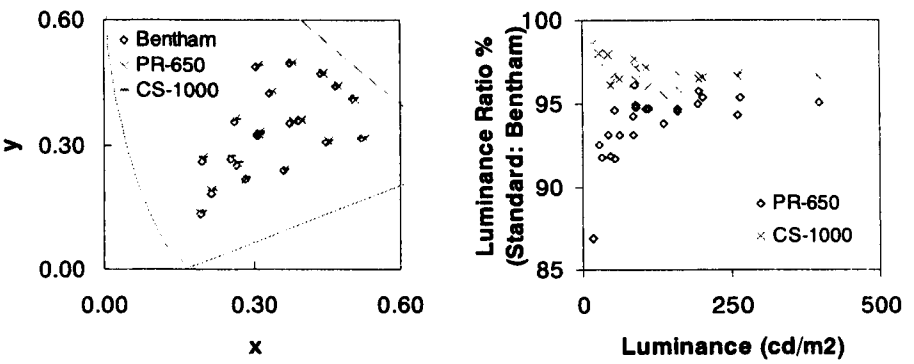


*Figure 3–8 Distribution of chromaticities for the Macbeth ColorChecker Chart and luminance ratios between instruments against the luminance level measured by Bentham*

It was also investigated whether there is a systematic luminance difference between the three TSRs found in the NPL lamp and white diffuser measurements. The right diagram in Figure 3–8 represents the luminance ratio of PR-650 and CS-1000

compared to Bentham. Both the PR-650 and CS-1000 have lower luminances than Bentham however the differences become larger for PR-650 and smaller for CS-1000 respectively under lower luminance levels.

CIELAB values were also calculated to examine the difference of measurement data on colour appearance models. For each instrument, the measurement results of the white diffuser under a D65 simulator were used as a reference white. Table 3-5 lists the CIELAB $\Delta E^*_{ab}$ values between three instruments. Also the coefficient of variation (CV) of $L^*$, $C^*$ and $h$ are shown. The equation to calculate CV is given by Eq. ( 3-1 ), which is used to quantify the discrepancy between the two data sets. If the two data sets are identical, the CV value becomes zero.

$$CV = 100\frac{\sqrt{\sum (p_i - q_i)^2 / n}}{\bar{q}}, \qquad (3\text{-}1)$$

$n = 24$ : number of colours in the Macbeth Colour Checker

$p_i, q_i$ : CIELAB $L^*, C^*$ or $h$ values of $i$th sample of the two TSRs compared

$\bar{q}$ : the mean CIELAB $L^*, C^*$ or $h$ value of a standard TSR

| CIELAB | Bentham | PR-650 | CS-1000 |
|---|---|---|---|
| Bentham | CV (L*/C*/h) / ΔE*ab | 0.65/1.72/1.25 | 0.48/1.44/0.79 |
| PR-650 | 1.3 ± 0.8 (Min:0.2 ~ Max:3.1) | | 0.78/1.44/0.50 |
| CS-1000 | 0.9 ± 0.5 (Min:0.3 ~ Max:2.2) | 0.7 ± 0.4 (Min:0.1 ~ Max:1.5) | |

***Table 3-5 CIELAB ΔE*ab and CV values between the measurement results of Macbeth Colour Checker by three spectroradiometers***

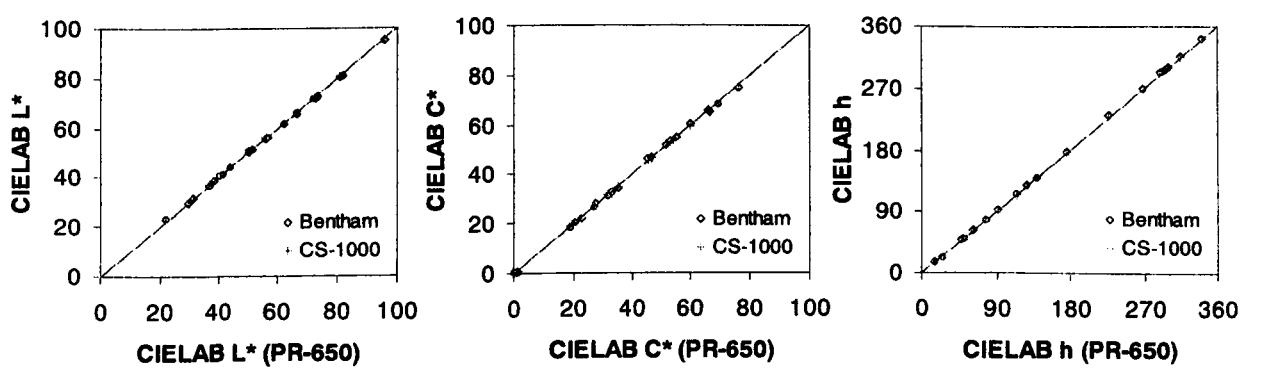


***Figure 3–9 Comparison of CIELAB values between PR-650 and other spectroradiometers***

Figure 3–9 shows the direct comparison of CIELAB values between PR-650 and the other two instruments. In these diagrams, PR-650 is compared with the others since it is the colour measurement device used in the author's study. The CIELAB colour differences $\Delta E^*_{ab}$ are smaller than 1 unit in most cases and most data points shown in Figure 3–9 are located on the 45° lines, implying that the choice of colour measurement instrument should not affect the colour appearance data sets significantly. However CIELAB hue angle comparison (right diagram in Figure 3–9) shows that colour measurement results by Bentham were slightly different from the other instruments for blue colours, which also produced the largest CIELAB colour differences.

## 3.3 Effect of Calibration on the Characteristics of Displays (using LCD Projector)

Calibration of a device means to set up the device (or any other process) so that it gives repeatable performance day in and day out [John1996]. Therefore it is important to examine the current settings of a display before starting any experiment and understand the effect on the output colours of changing a device setting. The settings of a display adjustable by the user include 'Brightness', 'Contrast' and 'Colour temperature' but details are dependent on different manufacturers and models.

In this section, the effect of calibration is investigated using an LCD projector, Sanyo PLC-5605B, which has 'Contrast' and 'Brightness' control buttons allowing the values to be changed from 0 to 63. The nine combinations of minimum (0), middle (32), and maximum (63) values of 'Contrast' and 'Brightness' were tested in terms of the luminance levels and change of primary colours. Note that 'Brightness' and 'Contrast' mean the names of control buttons in a display and do not necessarily follow the definitions of perceptual attributes.

Measurements were performed on a central uniform square patch (h/5×h/5, h: the effective screen height), with the remainder of the display filled with a black background. Experiments were conducted in a dark room with a PR-650 spectroradiometer output to four significant digits.

Table 3-6 gives the luminance measurement results for 9 different settings of 'Contrast' and 'Brightness'. The results show that as 'Brightness' was increased without changing 'Contrast', the luminance values for both black and white colours are also increased. When 'Contrast' was increased without changing 'Brightness', luminance increased for white but decreased for black. This means that the function of the 'Brightness' control is to raise the overall luminance and the role of 'Contrast' is to increase the slope between the brightest and darkest colour as shown in Figure 3–10.

| Setting | | Luminance ($cd/m^2$) | |
|---|---|---|---|
| Contrast | Brightness | Black | White |
| 0 | 0 | 0.5624 | 54.90 |
| 0 | 32 | 0.8404 | 93.16 |
| 0 | 63 | 3.277 | 118.7 |
| 32 | 0 | 0.4101 | 103.0 |
| 32 | 32 | 0.5419 | 152.0 |
| 32 | 63 | 1.509 | 159.8 |
| 63 | 0 | 0.4065 | 139.6 |
| 63 | 32 | 0.4501 | 157.0 |
| 63 | 63 | 0.9283 | 156.6 |

***Table 3-6 Luminance change by 'Contrast' and 'Brightness' setting***

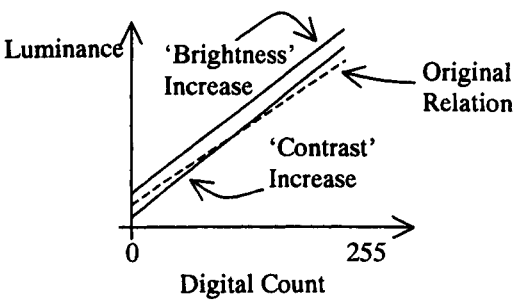


***Figure 3–10 Effect of 'Contrast' and 'Brightness' controls for an LCD projector***

Table 3-6 also indicates that the proper setting of both parameters can give maximum luminance range and it was found that two combinations, 'Brightness' 32, 'Contrast' 32 and 'Brightness' 63, 'Contrast' 32, gave similarly good luminance ranges. However it is not only the maximum and minimum luminance levels that need to be controlled for good image quality but also tone characteristic, which can influence colour rendering ability. Tone characteristic means the relationship between digital input values and output luminance levels.

Figure 3–11 shows tone curves of two 'Contrast'/'Brightness' combinations. The left diagram shows the relationship between normalised digital input values and normalised output luminance. Both combinations show s-shaped curves but the 63/32 curve has lower contrast under high luminance level. Luminance levels are converted to CIELAB $L^*$ values and shown in the right diagram to determine the visual effect of difference between the tone curves. Both diagrams clearly indicate that high luminance colours in the 63/32 setting nearly reach the maximum level, which would make it difficult to distinguish between light colours. It suggests that the high 'Contrast' setting could cause clipping, which means there would be no luminance change by different input values at the extremity. Therefore using the 'Brightness' 32 and 'Contrast' 32 setting is preferred compared to the other combinations for this LCD projector.

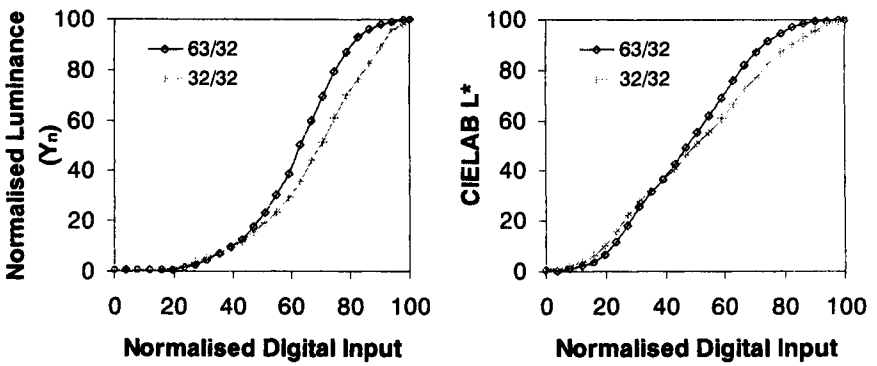


*Figure 3–11 Tone curves of two 'Contrast' and 'Brightness' settings (63/32, 32/32)*

## 3.4 Colour Characteristics of Digital Displays

In this section, the general colour characteristics of CRT and LCD displays are investigated. The tristimulus values of primary colours are first shown and the spectrum and colour gamut of each device are then compared. Subsequently additivity and colour tracking (chromaticity changes of primaries at different intensity levels) of each device are investigated. Table 3-7 lists the six displays tested in this section including one CRT monitor, two LCD projectors and three LCD monitors. Among those six displays, the Barco CRT monitor, Samsung LCD monitor and Sanyo LCD projector were used in the author's study to accumulate colour appearance data.

All measurements were performed on a central uniform square patch (h/5×h/5, h: the effective screen height), against a black background. Experiments were conducted in a dark room. Each display had one hour of warm up time preceding any measurement.

| | Type | Manufacturer | Model |
|---|---|---|---|
| 1 | CRT Monitor | Barco | Calibrator V |
| 2 | LCD Projector | Sanyo | PLC-5605B |
| 3 | | ASK | Impression A10 |
| 4 | LCD Monitor (Flat panel) | Samsung | Sense 820 (Part of laptop computer) |
| 5 | | HP | OmniBook XE3 (Part of laptop computer) |
| 6 | | Sharp | LC-20VM2 |

*Table 3-7 List of the displays used in the experiment*

### 3.4.1 Colorimetric Characteristics

Tables 3-8 to 3-13 list the tristimulus values and chromaticity coordinates of three primary colours, i.e. maximum red (255,0,0), green (0,255,0), and blue (0,0,255), together with white (255,255,255) and black (0,0,0). Note that the measurement results shown in these tables are for the default settings. Their values will be changed depending on the setting of a display as discussed in Section 3.3.

| Barco | $X_L$ | $Y_L$ (cd/m$^2$) | $Z_L$ | $x$ | $y$ | CCT |
|---|---|---|---|---|---|---|
| White | 122.6 | 128.3 | 134.7 | 0.318 | 0.333 | 6201 K |
| Black* | 0.00 | 0.00 | 0.00 | | | |
| Red | 59.31 | 31.59 | 2.868 | 0.633 | 0.337 | |
| Green | 40.41 | 85.82 | 15.28 | 0.286 | 0.606 | |
| Blue | 22.17 | 10.26 | 115.4 | 0.150 | 0.069 | |

* Black was too dark to be measured with PR-650

*Table 3-8 Tristimulus values of primary colours of Barco CRT Monitor*

| Sanyo | $X_L$ | $Y_L$ (cd/m$^2$) | $Z_L$ | $x$ | $y$ | CCT |
|---|---|---|---|---|---|---|
| White | 114.6 | 137.5 | 134.1 | 0.297 | 0.356 | 7073 K |
| Black | 0.3776 | 0.4705 | 0.5471 | 0.271 | 0.337 | |
| Red | 33.45 | 18.1 | 0.6584 | 0.641 | 0.347 | |
| Green | 57.47 | 112 | 5.472 | 0.329 | 0.640 | |
| Blue | 23.99 | 8.145 | 130.1 | 0.148 | 0.050 | |

*Table 3-9 Tristimulus values of primary colours of Sanyo LCD projector*

| ASK | $X_L$ | $Y_L$ (cd/m$^2$) | $Z_L$ | $x$ | $y$ | CCT |
|---|---|---|---|---|---|---|
| White | 411.0 | 495.6 | 558.7 | 0.280 | 0.338 | 8229 K |
| Black | 2.252 | 2.423 | 4.495 | 0.246 | 0.264 | |
| Red | 140.8 | 77.52 | 4.689 | 0.631 | 0.348 | |
| Green | 175.8 | 394.9 | 29.38 | 0.293 | 0.658 | |
| Blue | 99.36 | 28.31 | 533.4 | 0.150 | 0.043 | |

*Table 3-10 Tristimulus values of primary colours of ASK LCD projector*

| Samsung | $X_L$ | $Y_L$ (cd/m$^2$) | $Z_L$ | $x$ | $y$ | CCT |
|---|---|---|---|---|---|---|
| White | 101.0 | 112.5 | 94.20 | 0.328 | 0.366 | 5667 K |
| Black | 0.5031 | 0.541 | 0.8296 | 0.269 | 0.289 | |
| Red | 42.29 | 26.08 | 4.677 | 0.579 | 0.357 | |
| Green | 41.62 | 67.98 | 19.30 | 0.323 | 0.527 | |
| Blue | 17.94 | 19.5 | 72.71 | 0.163 | 0.177 | |

***Table 3-11 Tristimulus values of primary colours of Samsung LCD monitor***

| HP | $X_L$ | $Y_L$ (cd/m$^2$) | $Z_L$ | $x$ | $y$ | CCT |
|---|---|---|---|---|---|---|
| White | 122.4 | 126.7 | 130.9 | 0.322 | 0.333 | 5990 K |
| Black | 0.3335 | 0.3238 | 0.6733 | 0.251 | 0.243 | |
| Red | 53.13 | 31.23 | 6.270 | 0.586 | 0.345 | |
| Green | 47.14 | 77.66 | 20.86 | 0.324 | 0.533 | |
| Blue | 22.31 | 18.10 | 105.4 | 0.153 | 0.124 | |

***Table 3-12 Tristimulus values of primary colours of HP LCD monitor***

| Sharp | $X_L$ | $Y_L$ (cd/m$^2$) | $Z_L$ | $x$ | $y$ | CCT |
|---|---|---|---|---|---|---|
| White | 181.5 | 175.1 | 311.8 | 0.272 | 0.262 | 14154 K |
| Black | 0.6247 | 0.6157 | 1.424 | 0.234 | 0.231 | |
| Red | 81.92 | 43.7 | 8.409 | 0.611 | 0.326 | |
| Green | 56.85 | 111.9 | 21.95 | 0.298 | 0.587 | |
| Blue | 54.90 | 30.94 | 297.0 | 0.143 | 0.081 | |

***Table 3-13 Tristimulus values of primary colours of Sharp LCD monitor***

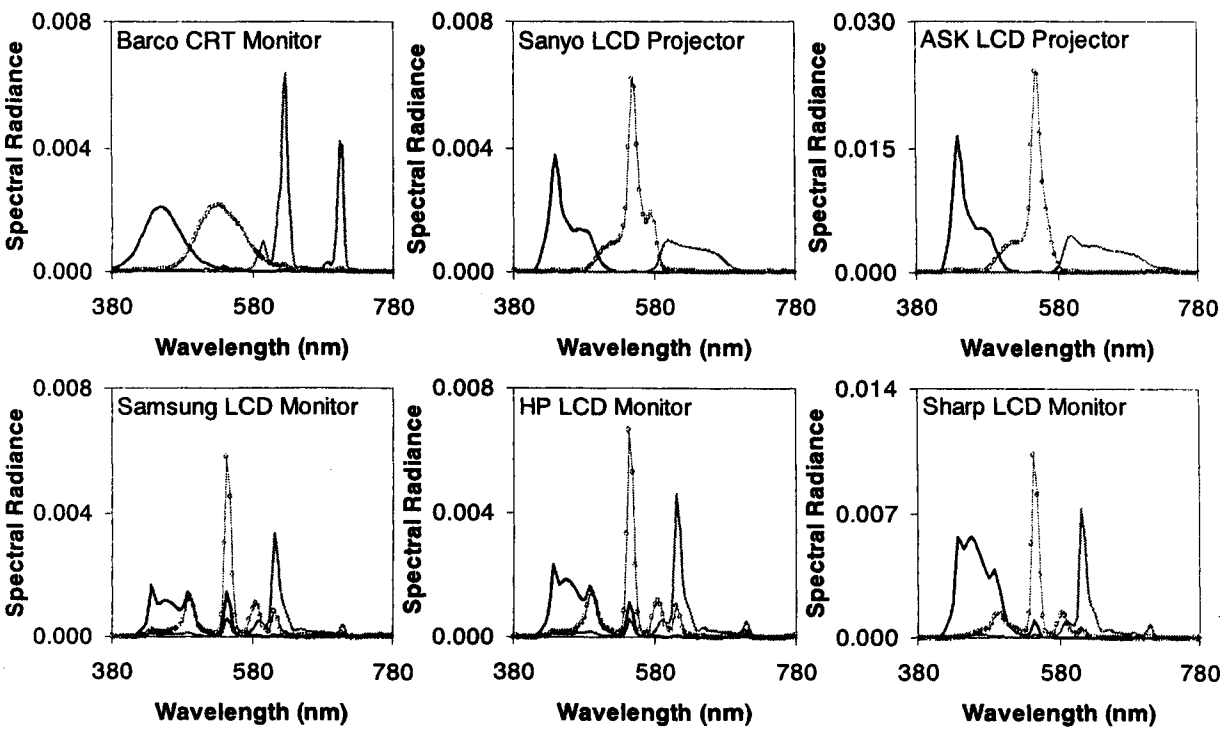


***Figure 3–12 Spectra of primary colours for six displays***

### 3.4.2 Spectral Characteristics

The diagrams in Figure 3–12 show the spectral power distributions of the primary colours of each display. It is clear that each group of devices has characteristic spectral distributions depending on the materials used to generate the colours. Spectra of the Barco CRT monitor show the characteristics of phosphors, whereas spectra of the LCD projectors are from the combination of projection lamp and colour filters. The Sanyo and ASK LCD projectors use different projection lamps, which are metal-halide and UHP respectively, however their spectra are very similar except for a small hump around 580nm for the Sanyo projector. All three LCD monitors have similar spectra produced by the combination of the colour filters and fluorescent back-light, except for the balance between the three channels.

### 3.4.3 Comparing Colour Gamuts

Figure 3–13 shows the colour gamut of each device in an *xy*-diagram. The triangular boundary of the colour gamut is determined by chromaticities of each primary colour. The CRT monitor and LCD projectors tested show similar colour gamuts while the LCD monitors have smaller gamuts than the CRT monitor or LCD projector and also exhibit larger differences between them.

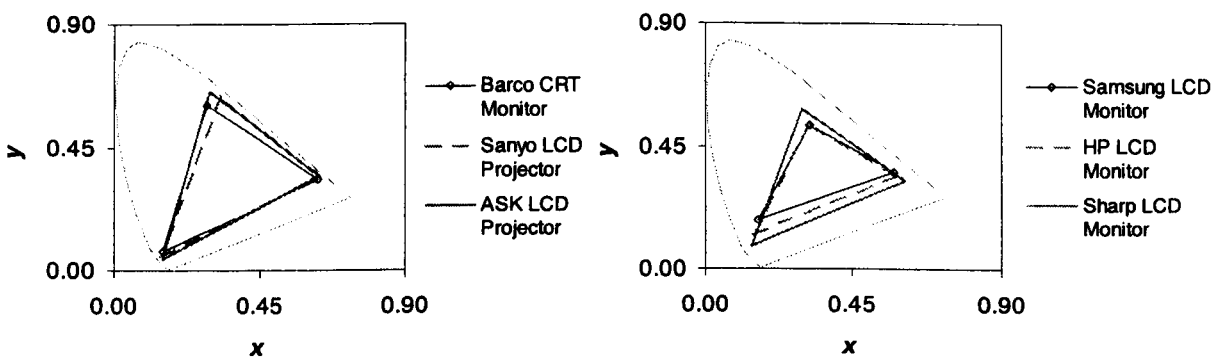


*Figure 3–13 Colour gamuts of displays in xy-space*

### 3.4.4 Additivity Test

Ideally the three channels of a display should be independent of each other. In other words, the output of any one colour channel should not be affected by the signals from the other two channels. This channel independence helps to manage output colour more effectively (refer Section 3.5).

Additivity of a display is tested as a method testing channel independence by evaluating the equivalence between greys and the sums of three channels. Seven digital input values (51, 85, 128, 170, 204, 225 and 255) were chosen between 0 to 255 and the corresponding output tristimulus values of each channel and greys were measured. Eq. ( 3-2 ) shows the equation used to calculate additivity error as a percentage, where $Y_R$, $Y_G$, $Y_B$, $Y_{Black}$, and $Y_{Grey}$, are the tristimulus value $Y$ for the red, green, blue and black together with the added grey by three primaries. Similar equations were applied for $X$ and $Z$ values.

$$\text{Additivity Error}(\%) = \frac{(Y_R + Y_G + Y_B - 2 \cdot Y_{Black}) - Y_{Grey}}{Y_{Grey}} \times 100 \qquad (3\text{-}2)$$

The tristimulus values of the black arise from the light emitted by a display with zero input signals, and these values are always added to colour measurement data. Thus the addition of three channels must have subtracted two times the black values in the equation, since the $Y$ value from black is added three times to the sum of three channels but only once for grey [Fair1998b]. This process to remove the effect of black is called black correction and more details are discussed in the next section.

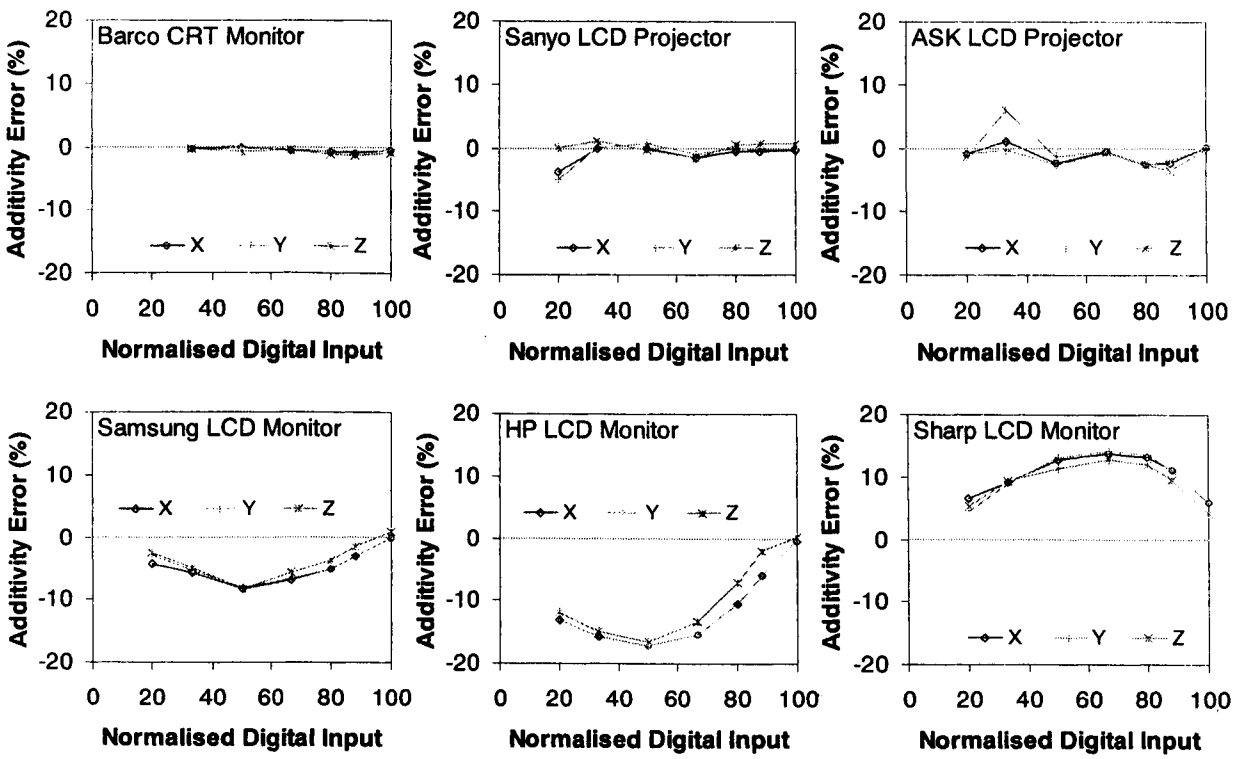


*Figure 3–14 Additivity test*

Figure 3–14 shows the additivity errors represented as a percentage. The Barco CRT monitor showed the best additivity followed by the LCD projectors. All LCD monitors, however, had very poor additivity especially in the mid-range of input values. In the case of the Samsung and HP monitors, grey had higher values than the addition of three channels while the Sharp monitor had the opposite effect that the addition of three channels was larger than the measurement of grey.

### 3.4.5 Colour Tracking (Chromaticity Changes of Primaries)

Colour tracking means the locus of chromaticity changes for primary colours as the input digital values of each channel changes. Thirty-two steps per channel were measured in terms of chromaticities and luminances and the results are plotted in a CIE 1976 UCS diagram ($u'$, $v'$). In the case of the Barco CRT monitor, only digital signal values larger than 80 are considered since colours having small digital values were too dark to measure.

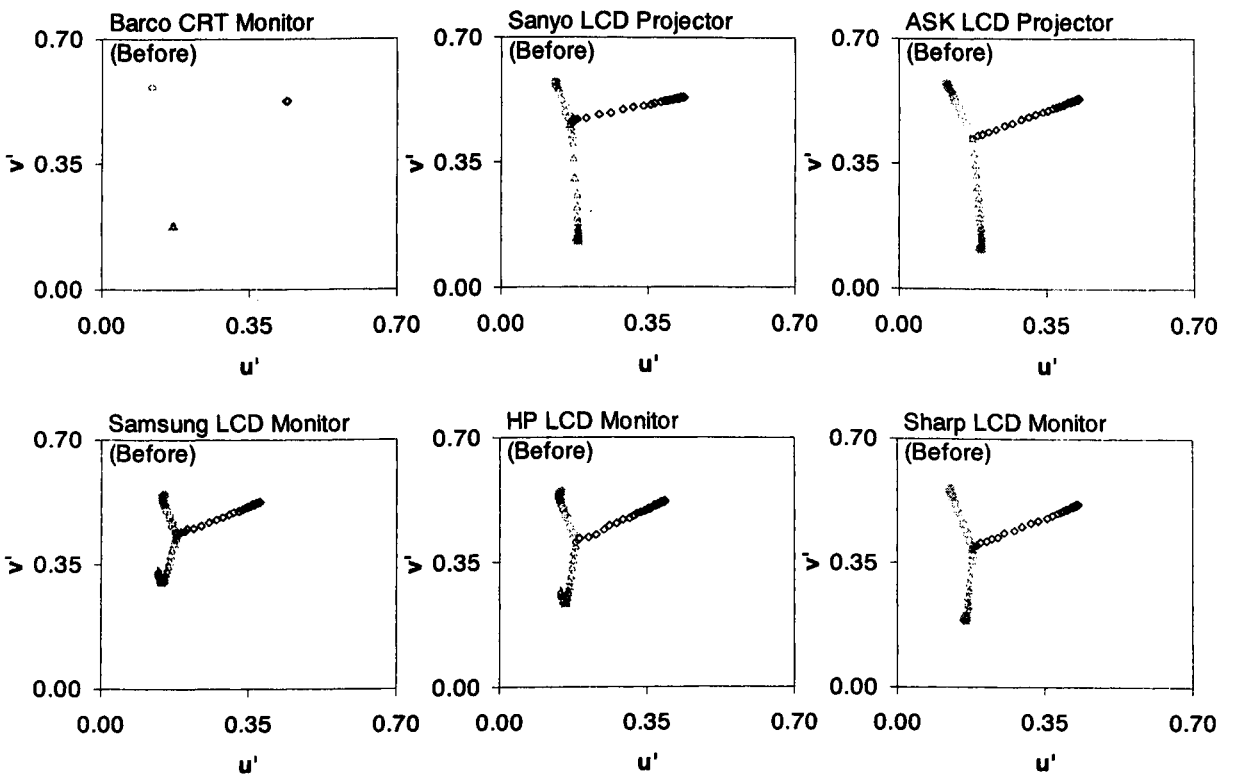


*Figure 3–15 Chromaticity changes of each channel shown in u'v'-space*

Figure 3–15 shows the measurement results. Only the Barco CRT monitor has constant chromaticity values regardless of its input digital values. Chromaticities of all LCD displays follow a line toward the black, which are always included in the

measurement data. (Note that the black of Barco CRT monitor could not be measured therefore did not affect the chromaticities of other colours.) Therefore it was necessary to obtain chromaticities after eliminating black values to understand the colour tracking characteristics of the LCD displays more clearly. The measured tristimulus values of black were subtracted from those of each primary and chromaticies were recalculated using the new tristimulus values. Figure 3–16 shows the final results and it is clear that the chromaticities of three channels for the LCD projector and monitors tested in this section still changed significantly, especially the blue channels, which show the worst performances.

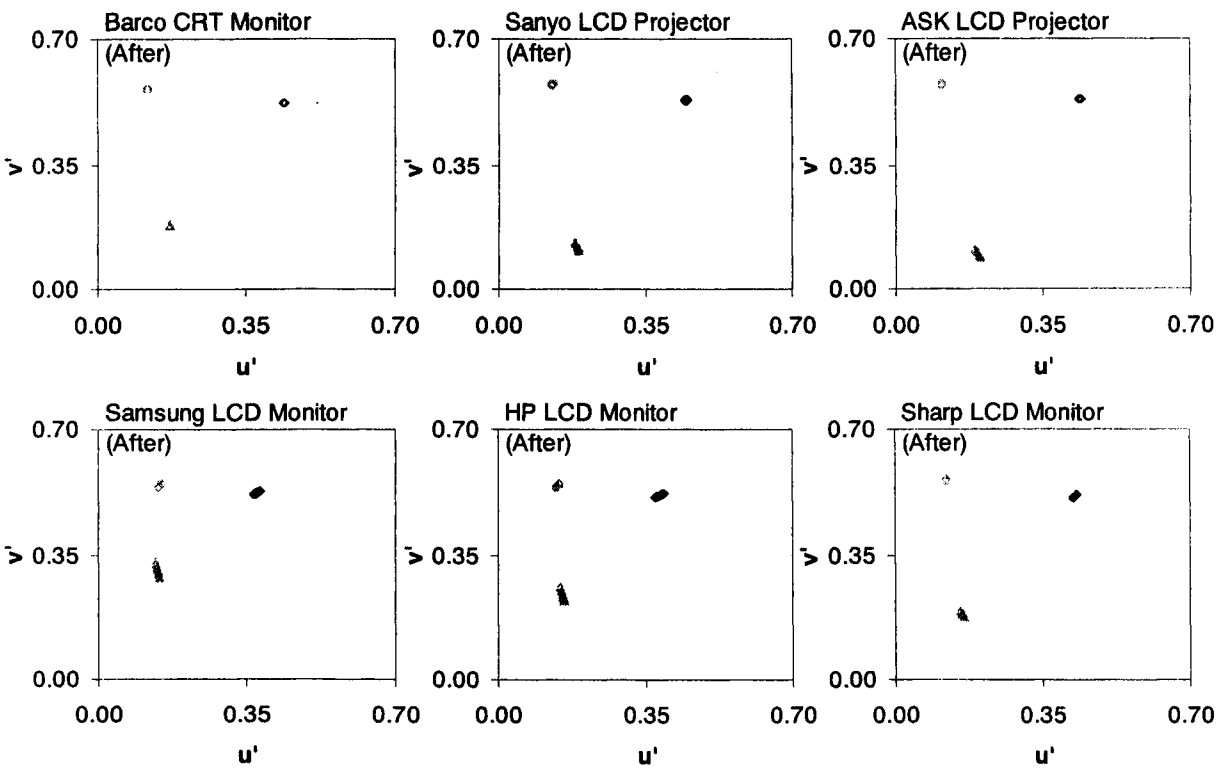


*Figure 3–16 Chromaticity changes of each channel after black correction shown in u'v'-space*

## 3.5 Characterisation Models for Displays

Characterisation of a display defines the relationship between the device signal space and the colour generated, specified in terms of the CIE system [John1996]. The characterisation of a colour-imaging device is an essential procedure in the design of colour reproduction systems [MacD1995]. Proper display characterisation together with a colour appearance model provides a means for accurate colour communication. The ColourTalk system is a good example showing this [Rhod1996]. In the case of conventional CRT displays, theoretical characterisation models are well established

and perform well. However, it has been proven that the GOG model, which is widely used for CRT monitor characterisation, is not suitable for flat panel LCD monitors [Fair1998b].

In this section, mathematical characterisation models are tested for those CRT and LCD displays listed in Table 3-7. Models using look-up-tables (LUT) such as PLCC or cube interpolation are not considered in this study since too many measurements are requires for cube LUTs and PLCC is based on the assumption of chromaticity constancy which is not true for LCDs. For CRT monitors, the GOG model is tested and a new characterisation model is proposed for the LCD displays. Note that tristimulus values $X$, $Y$, $Z$ in this section represent the absolute tristimulus values.

### 3.5.1 Characterisation of CRT Monitor using GOG Model

The GOG model, devised by Berns [Bern1993, Bern1995] for CRT displays, shows the relationship between digital input values and the CIE tristimulus values of light emitted by the phosphors. The GOG model consists of two stages – a non-linear relationship between the digital input values, $d_i$ and three scalars, $R$, $G$, $B$, followed by a linear transformation matrix where the scalars $R$, $G$, $B$ are transformed to CIE tristimulus values $X$, $Y$, $Z$. Eq. ( 3-3 ) shows the non-linear part for the red channel having three model parameters, Gain-Offset-Gamma, which need to be determined from the tone characteristic of the channel. Similar equations are applied for the green ($G$) and blue ($B$) channels. Eq. ( 3-4 ) shows a linear transformation matrix derived from measurements of black and the maximum red, green and blue channel luminances.

$$R = \begin{cases} \left[k_{g,r} \cdot d_r + k_{o,r}\right]^{\gamma_r}, & \left[k_{g,r} \cdot d_r + k_{o,r}\right] \geq 0 \\ 0, & \left[k_{g,r} \cdot d_r + k_{o,r}\right] < 0 \end{cases}$$

where $k_{g,r}$ : Model gain, $\gamma_r$ : Gamma
$k_{o,r}$ : Model offset, $(k_{o,r} = 1 - k_{g,r})$
$d_r$ : Normalised digital input value
$R$ : The Scalar

*(3-3)*

$$\begin{bmatrix} X \\ Y \\ Z \end{bmatrix} = \begin{bmatrix} X_{Black} \\ Y_{Black} \\ Z_{Black} \end{bmatrix} + \begin{bmatrix} X'_{r,\max} & X'_{g,\max} & X'_{b,\max} \\ Y'_{r,\max} & Y'_{g,\max} & Y'_{b,\max} \\ Z'_{r,\max} & Z'_{g,\max} & Z'_{b,\max} \end{bmatrix} \cdot \begin{bmatrix} R \\ G \\ B \end{bmatrix} \qquad (3\text{-}4)$$

where $X' = X - X_{Black}$, $Y' = Y - Y_{Black}$, $Z' = Z - Z_{Black}$

The GOG model assumes two properties of a display, namely channel independence (refer to Section 3.4.4) and the constancy of channel chromaticity (refer to Section

3.4.5). The matrix in Eq. ( 3-4 ) explains why channel independence is assumed to apply in the GOG model. In Eq. ( 3-4 ), output tristimulus values are the sum of three channels. Note that the tristimulus values of maximum red ($X_{r,max}$, $Y_{r,max}$, $Z_{r,max}$), multiplied by scalar $R$ corresponding to digital input, $d_r$, become the tristimulus values of red for the digital value $d_r$ only if the chromaticity of red is not changed by input digital value. The same principle applies for the green and blue channels. Also the scalars $R$, $G$, $B$ may be regarded as 'normalised luminance level' only when the channel chromaticities are constant.

A Barco *Calibrator V* CRT monitor was characterised using the GOG model. A particular objective of this experiment was to examine whether ambient light would affect the performance of the GOG model. This was investigated in preparation for psychophysical experiments using the CRT monitor with and without ambient light (see Section 4.3.4). Therefore it was important to understand any change of performance of a display by ambient light. This experiment was conducted independently from that for Section 3.4 and had a different monitor calibration condition. Note that the measurement data shown in this section are different to those in Section 3.4. Luminance of the monitor was changed by calibration procedure.

Table 3-14 summarises the measured tristimulus values of the primary colours, black and white of the CRT monitor with and without ambient light. Tristimulus values with ambient light are higher than those measured in a dark room as expected. However the tristimulus values after black correction show little difference between them. This means that ambient light causes a certain amount of ambient flare to be added to monitor colours regardless of the input digital values. Figure 3–17 shows the colour gamut of the CRT monitor with and without ambient light. Ambient light increases luminance levels but at the same time decrease the colour gamut of the CRT monitor.

| | Without Ambient Light | | | | | | With Ambient Light | | | | | |
|---|---|---|---|---|---|---|---|---|---|---|---|---|
| | Measured Data | | | After Black Correction | | | Measured Data | | | After Black Correction | | |
| | *X* | *Y* | *Z* | *X'* | *Y'* | *Z'* | *X* | *Y* | *Z* | *X'* | *Y'* | *Z'* |
| White | 89.77 | 92.79 | 107.7 | 89.47 | 92.47 | 107.3 | 92.45 | 95.89 | 110.5 | 89.31 | 92.48 | 107.2 |
| Black | 0.3013 | 0.3155 | 0.3961 | 0.00 | 0.00 | 0.00 | 3.142 | 3.41 | 3.299 | 0.00 | 0.00 | 0.00 |
| Red | 42.44 | 22.62 | 2.31 | 42.14 | 22.30 | 1.91 | 45.26 | 25.73 | 5.239 | 42.12 | 22.32 | 1.94 |
| Green | 29.38 | 62.17 | 11.18 | 29.08 | 61.85 | 10.78 | 32.22 | 65.29 | 14.11 | 29.08 | 61.88 | 10.81 |
| Blue | 18.30 | 8.47 | 94.35 | 18.00 | 8.15 | 93.95 | 21.21 | 11.64 | 97.4 | 18.07 | 8.23 | 94.10 |

***Table 3-14 Tristimulus values for white, black, red, green and blue under with and without ambient light, before and after black point correction***

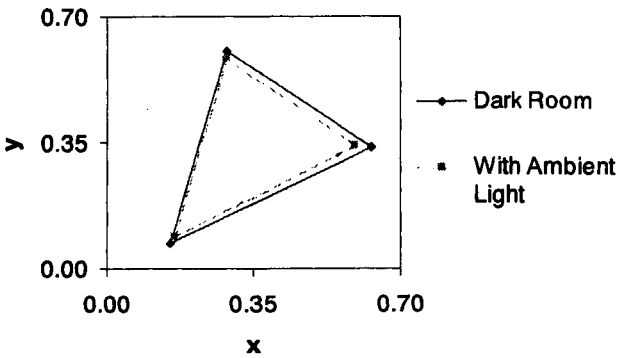


*Figure 3–17 Colour gamut change of CRT monitor by ambient light*

The linear transformation matrices calculated for the GOG model are shown in Eq. ( 3-5 ) for a dark room experiment and in Eq. ( 3-6 ) for the experiment with ambient light using the data in Table 3-14. The constant matrix for the experiment with ambient light is divided into two, i.e. ambient flare and black, based on the source of the light.

$$\begin{bmatrix} X \\ Y \\ Z \end{bmatrix}_{\substack{\text{Dark} \\ \text{Room}}} = \begin{bmatrix} 0.3013 \\ 0.3155 \\ 0.3961 \end{bmatrix}_{\text{Black}} + \begin{bmatrix} 42.14 & 29.08 & 18.00 \\ 22.30 & 61.85 & 8.155 \\ 1.910 & 10.78 & 93.95 \end{bmatrix} \cdot \begin{bmatrix} R \\ G \\ B \end{bmatrix} \qquad (3\text{-}5)$$

$$\begin{bmatrix} X \\ Y \\ Z \end{bmatrix}_{\substack{\text{With} \\ \text{Ambient} \\ \text{Light}}} = \begin{bmatrix} 2.841 \\ 3.095 \\ 2.903 \end{bmatrix}_{\substack{\text{Ambient} \\ \text{Flare}}} + \begin{bmatrix} 0.3013 \\ 0.3155 \\ 0.3961 \end{bmatrix}_{\text{Black}} + \begin{bmatrix} 42.12 & 29.08 & 18.07 \\ 22.32 & 61.88 & 8.230 \\ 1.940 & 10.81 & 94.10 \end{bmatrix} \cdot \begin{bmatrix} R \\ G \\ B \end{bmatrix} \qquad (3\text{-}6)$$

The nine input steps were measured per channel including 0 and 255 to calculate model parameters, i.e. offset and gamma. Firstly a series of $R$, $G$ and $B$ values were calculated from red, green and blue channel measurements respectively using the inverse matrices of Eq. ( 3-5 ) and Eq. ( 3-6 ). Figure 3–18 shows the relationship between input digital values and $R$, $G$ and $B$ values. Diagrams in Figure 3–18 are for the experiment in a dark room. Diagrams for an ambient light experiment, which are not demonstrated here, also showed little difference. All three channels show very similar performances having power functions. This is clearer when the relationship is shown in a log-log scale (right diagram).

Three model parameters gain, offset and gamma in Eq. ( 3-3 ) were calculated to fit the curves in Figure 3–18 using the least squares method, which minimises the square of differences between measured and calculated $R$, $G$, $B$ values. The 'Solver' function

in MS Excel was used for calculation and a constraint is given that the sum of gain and offset is set to 1. The final results are listed in Table 3-15.

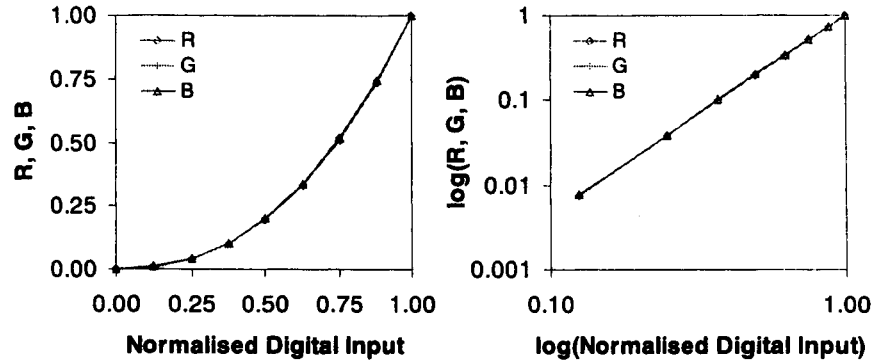


*Figure 3–18 Tone characteristics of a Barco CRT monitor*

| | Dark Room | | | With Ambient Light | | |
|---|---|---|---|---|---|---|
| | Red | Green | Blue | Red | Green | Blue |
| Gain ($k_g$) | 0.988 | 1.018 | 1.014 | 0.981 | 1.012 | 1.012 |
| Offset ($k_o$) | 0.012 | -0.018 | -0.014 | 0.019 | -0.012 | -0.012 |
| Gamma ($\gamma$) | 2.414 | 2.269 | 2.278 | 2.440 | 2.285 | 2.285 |

*Table 3-15 Model parameters of the GOG model for the Barco Calibrator V CRT monitor*

The performance of the GOG model was evaluated using 59 test colours. These comprised all possible combinations of four steps (0, 85, 170 and 255) per channel, excluding primaries, black and white. Measured and predicted tristimulus values were used to calculate CIELAB values and colour differences were calculated between the two data sets. Average $\Delta E^*_{ab}$ values with maximum difference are listed in Table 3-16. Both experimental conditions show similar performances indicating that the performance of the GOG model is not affected by ambient light.

| $\Delta E^*_{ab}$ | Average ± Standard deviation | Maximum |
|---|---|---|
| Dark Room | 0.202 ± 0.105 | 0.477 |
| With Ambient Light | 0.240 ± 0.124 | 0.507 |

*Table 3-16 Performance of the GOG model for the CRT monitor*

## 3.5.2 Characterisation of LCD Displays

In this section, first of all it is investigated whether the GOG model could be used to characterise LC-based displays. At a later stage, new mathematical models for the characterisation, called S-Curve I and S-Curve II, for LC-based displays are proposed.

### 3.5.2.1. Performance of the GOG Model to Characterise LC-based Displays

It was investigated as to whether the GOG model, which was developed for CRT monitors, could be used for LC-based displays. Note that the GOG model uses a power function between digital input values and output luminance levels. Thus the relationships between input digital values and the scalars, $R$, $G$, $B$ were investigated first. For the analysis, the same experimental data used in Section 3.4 are also applied here.

$$\begin{bmatrix} R \\ G \\ B \end{bmatrix} = \begin{bmatrix} X'_{r,\max} & X'_{g,\max} & X'_{b,\max} \\ Y'_{r,\max} & Y'_{g,\max} & Y'_{b,\max} \\ Z'_{r,\max} & Z'_{g,\max} & Z'_{b,\max} \end{bmatrix}^{-1} \cdot \left( \begin{bmatrix} X \\ Y \\ Z \end{bmatrix} - \begin{bmatrix} X_{Black} \\ Y_{Black} \\ Z_{Black} \end{bmatrix} \right) \qquad (3\text{-}7)$$

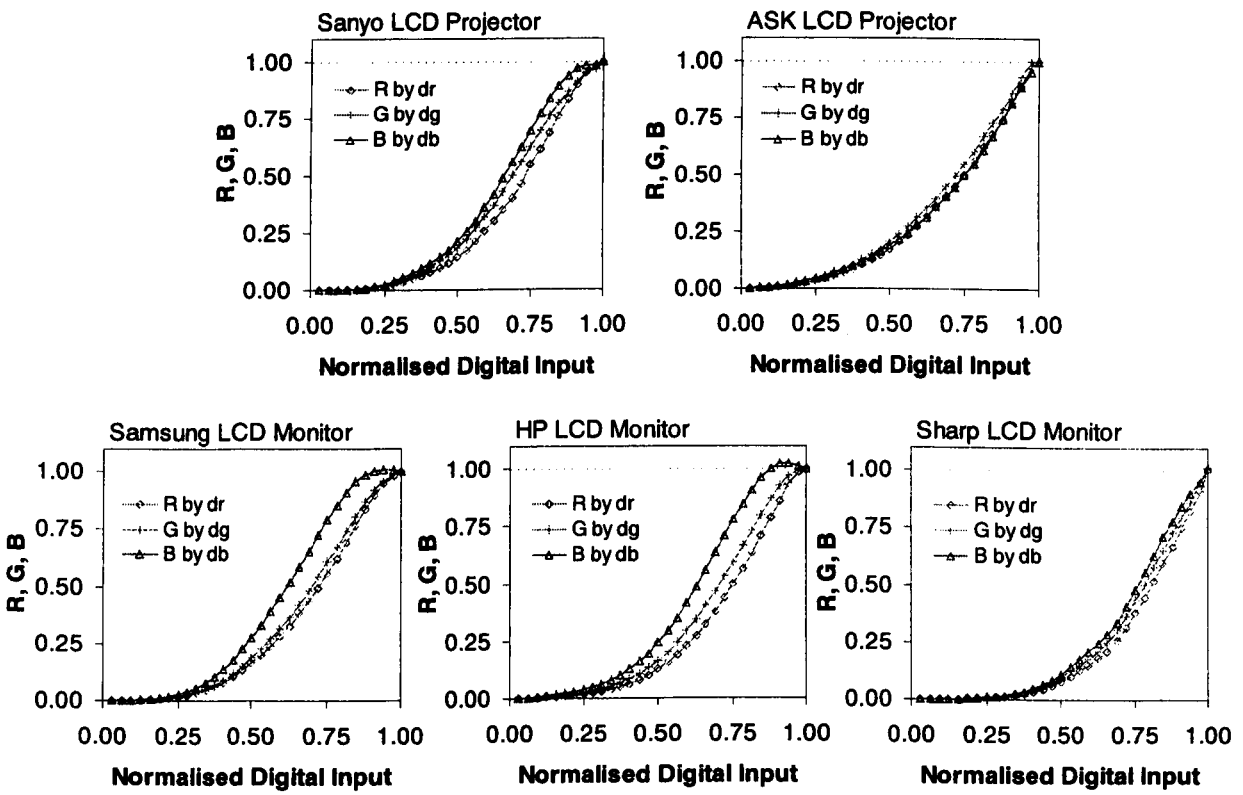


*Figure 3–19 Tone characteristics of LC-based displays*

As mentioned in Section 3.4.5, the tristimulus values of 32 steps per channel were measured and the $R$, $G$, $B$ values were calculated from the tristimulus values using equation ( 3-7 ). $R$ was calculated from the red channel data and $G$ and $B$ from the green and blue channels respectively. Figure 3–19 shows the tone characteristics of five LC displays. It is clear that most of the curves are S-shaped rather than power

functions, suggesting that the GOG model would not provide an accurate method to characterise LCD projector or monitors.

The same strategy for the CRT monitor described in the previous section was used to calculate parameters for the GOG model with nine training colours per channel for two LCD projectors and three LCD monitors. The performance of the GOG model was tested using four data sets, i.e. 32 steps per channel and an array of 59 test colours made by all possible combinations of four steps (0, 85, 170 and 255) for each channel excluding primaries, black and white.

Table 3-17 summarises the performance of the GOG model using CIELAB $\Delta E^*_{ab}$ between the measured and predicted data. Every device shows very poor performance, especially the blue channel, which shows worse performance than the other channels. The ASK LCD projector shows the best performance followed by the Sharp LCD monitor. Note that these two devices have most power function-like tone curves in Figure 3–19. However even for these two displays, the performance of the GOG model is far worse than that for the CRT monitor in the previous section.

| $\Delta E^*_{ab}$ | GOG | | | |
|---|---|---|---|---|
| | Test | Red | Green | Blue |
| Sanyo | 17.39 | 5.14 | 9.00 | 12.25 |
| ASK | 2.11 | 1.47 | 5.57 | 7.00 |
| Samsung | 9.92 | 4.99 | 7.39 | 10.01 |
| HP | 6.71 | 6.51 | 10.54 | 13.23 |
| Sharp | 8.73 | 3.12 | 5.81 | 7.15 |

***Table 3-17 Performance of the GOG model for LCD projectors and monitors***

### 3.5.2.2. Simple LCD Characterisation Model: S-Curve Model I

It was demonstrated that the poor performance of the GOG model for LCD projectors and monitors is due to their S-shaped tone curves. Therefore a new equation is necessary to predict the S-shaped curve in order to give better performance for LCDs. Eq. ( 3-8 ) was proposed for *R*, *G*, *B* values to formulate S-shaped curves instead of the power function in Eq. ( 3-3 ). The characterisation model using this formula instead of power function in GOG model is called S-Curve Model I [Kwak2000, Kwak2003].

$$R = A_r \frac{d_r^{\alpha_r}}{d_r^{\beta_r} + C_r}, \quad G = A_g \frac{d_g^{\alpha_g}}{d_g^{\beta_g} + C_g}, \quad B = A_b \frac{d_b^{\alpha_b}}{d_b^{\beta_b} + C_b} \qquad (3\text{-}8)$$

where $A, \alpha, \beta, C$ : Model Parameters

$d$ : Normalised Digital Input Value

To apply S-Curve Model I, constraints should be considered for the calculation of the parameter to make sure that *R*, *G*, *B* values (1) have a range between 0 and 1 and (2) are monotonic to ensure the existence of an inverse model. Inverse model means finding digital input values corresponding to any given output colour. In other words, there should be one and only one digital value corresponding to a given scalar. The first condition leads to a constraint, $A$=1+$C$, since the scalar has to be 1 at the maximum input value. The second monotonic condition leads to another constraint that the first derivative of Eq. ( 3-8 ) has to be larger than 0 for any input level, which gives the relation, $\alpha C > \beta - \alpha$. These constrains are summarised in Eq. ( 3-9 ) and Eq. ( 3-10 ). The disadvantage of the S-Curve Model I is that Eq. ( 3-8 ) is not analytically reversible unlike the GOG model. Numerical methods are needed.

Put $f(x) = A\frac{x^{\alpha}}{x^{\beta} + C}$, $f'(x)$ = first - order derivative of $f(x)$

1st Constraint : $f(0) = 0$ and $f(1) = \frac{A}{1+C} = 1 \quad \therefore \alpha > 0,\ \beta \geq 0,\ A = 1 + C \qquad (3\text{-}9)$

2nd Constraint $f'(x) = \frac{(\alpha - \beta)x^{\alpha+\beta-1} + \alpha \cdot C \cdot x^{\alpha-1}}{(x^{\beta} + C)^2}$

$f'(x) > 0$ when $x \in (0,1) \qquad \therefore \alpha \cdot C > \beta - \alpha \qquad (3\text{-}10)$

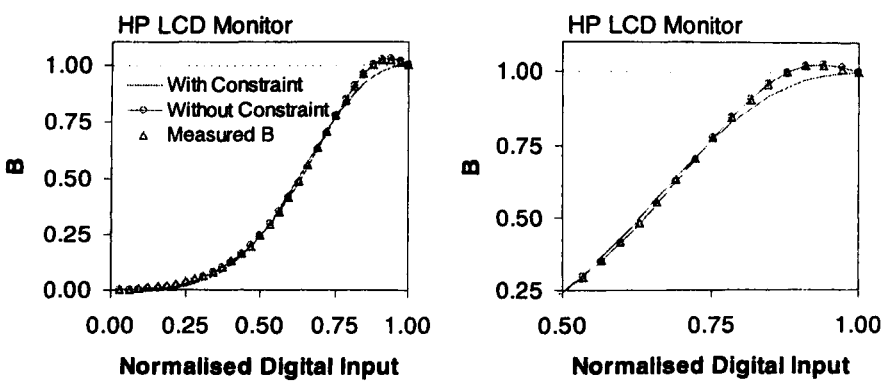


*Figure 3–20 Effect of constraints for the S-Curve Model I (Blue channel for HP LCD Monitor)*

It was later found that the tone characteristic of the HP LCD monitor has an intrinsic problem. The tone curve of the blue channel, which is shown in the middle diagram of the second row in Figure 3–19, has a non-monotonic function i.e. a small hump near the maximum digital input, making two possible input digital values correspond to a given $B$ value. Therefore applying constraints deteriorates the performance of the forward model for the HP LCD monitor, but it is impossible to obtain the inverse model if constraints are not used. Figure 3–20 shows the effect of applying constraints to predict the tone curve of the blue channel for the HP LCD Monitor. The area showing the largest effect of constraints, i.e. high input level, is magnified and shown in the right diagram in Figure 3–20. It is clear that the S-Curve Model I without constraint fits the measurement data very well.

Table 3-18 lists the calculated model parameters of five LC-based displays for the S-Curve Model I. Nine training colours were used per channel, which are the same colours used for the GOG model in the previous section. The least squares method (which minimises the square of difference between measured and calculated $R$, $G$, $B$) was applied to calculate model parameters, which is the same method as for the GOG model. The 'Solver' function in MS Excel was used for calculation. Constraints were applied to every experimental data set.

| | Red Channel | | | | Green Channel | | | | Blue Channel | | | |
|---|---|---|---|---|---|---|---|---|---|---|---|---|
| | $A_r$ | $\alpha_r$ | $\beta_r$ | $C_r$ | $A_g$ | $\alpha_g$ | $\beta_g$ | $C_g$ | $A_b$ | $\alpha_b$ | $\beta_b$ | $C_b$ |
| Sanyo | 3.4 | 3.3 | 10.8 | 2.4 | 2.6 | 3.2 | 7.2 | 1.6 | 1.8 | 3.4 | 6.2 | 0.8 |
| ASK | 27.9 | 2.6 | 19.5 | 26.9 | 13.0 | 2.4 | 31.3 | 12.0 | 2.2 | 2.4 | 0.0 | 1.2 |
| Samsung | 3.4 | 3.2 | 8.7 | 2.4 | 2.6 | 3.2 | 7.3 | 1.6 | 1.4 | 3.6 | 5.0 | 0.4 |
| HP | 4.2 | 3.4 | 10.6 | 3.2 | 2.7 | 3.3 | 8.4 | 1.7 | 1.4 | 3.8 | 5.3 | 0.4 |
| Sharp | 6.3 | 4.0 | 9.6 | 5.3 | 4.0 | 3.9 | 8.6 | 3.0 | 3.2 | 3.8 | 8.9 | 2.2 |

***Table 3-18 Model parameters of 5 LC-based displays for S-Curve Model I***

The performance of the S-Curve Model I is also tested using the same data sets as for the GOG model test, namely 59 test colours and 32 colours per channel. The results are summarised in Table 3-19 using average CIELAB colour difference. S-Curve Model I shows a remarkably improved performance compared to the GOG model in terms of the greatly reduced $\Delta E^*_{ab}$ values. However the blue channel still shows the worst performance for all displays tested.

| $\Delta E^*_{ab}$ | S-Curve I | | | | GOG | | | |
|---|---|---|---|---|---|---|---|---|
| | Test | Red | Green | Blue | Test | Red | Green | Blue |
| Sanyo | 2.76 | 0.99 | 2.31 | 5.25 | 17.39 | 5.14 | 9.00 | 12.25 |
| ASK | 2.01 | 0.82 | 2.85 | 7.59 | 2.11 | 1.47 | 5.57 | 7.00 |
| Samsung | 4.33 | 2.66 | 4.10 | 7.22 | 9.92 | 4.99 | 7.39 | 10.01 |
| HP | 6.67 | 3.64 | 5.46 | 9.95 | 6.71 | 6.51 | 10.54 | 13.23 |
| Sharp | 3.65 | 1.55 | 1.96 | 3.91 | 8.73 | 3.12 | 5.81 | 7.15 |

***Table 3-19 Performance of S-Curve Model I for LCD projectors and monitors***

### 3.5.2.3. Complex LCD Characterisation Model: S-Curve Model II

The only difference between the GOG model and the S-Curve Model I is the non-linear equations for the scalars, *R*, *G*, and *B*. Therefore S-Curve Model I also assumes channel independence and the constancy of channel chromaticity. However in Section 3.4.5, it was clearly shown that the LCDs tested in this study had a significant change of channel chromaticity at different input levels. Note that the blue channel had the most significant change for all displays, corresponding to the worst performance of the blue channel for the S-Curve Model I in Table 3-19.

The effect of chromaticity changes on the model can be shown in the following way. The GOG and S-Curve Model I assume that each channel generates only one kind of scalar. In other words, measurement data of red channel should only generate *R* values and it is assumed that *G* and *B* are not generated. Note that this assumption is based on the chromaticity constancy of channel colours since it is true only when there is no chromaticity change caused by different input values. Therefore the assumption can be investigated by calculating all scalars produced by each channel. The same 32 colours per channel used in Figure 3–19 are used to calculate scalars using Eq. ( 3-11 ).

$$\begin{bmatrix} R_U \\ G_U \\ B_U \end{bmatrix} = \begin{bmatrix} X'_{r,\max} & X'_{g,\max} & X'_{b,\max} \\ Y'_{r,\max} & Y'_{g,\max} & Y'_{b,\max} \\ Z'_{r,\max} & Z'_{g,\max} & Z'_{b,\max} \end{bmatrix}^{-1} \cdot \left( \begin{bmatrix} X_U \\ Y_U \\ Z_U \end{bmatrix} - \begin{bmatrix} X_{Black} \\ Y_{Black} \\ Z_{Black} \end{bmatrix} \right) \qquad (3\text{-}11)$$

where $X_U, Y_U, Z_U$ : Tristimulus Values of Channel Colours

$U = d_r, d_g, d_b$

Figure 3–21 and Figure 3–22 show the scalars $R$, $G$ and $B$ of each channel calculated using Eq. ( 3-11 ) from the measurement data of channel colour for the Barco CRT monitor and Samsung LCD monitor respectively. These two figures clearly show the differences between the two displays. Each channel of the Barco CRT monitor generates one scalar as assumed. On the other hand, all three scalars are generated for each channel (especially for blue channel) of the Samsung LCD monitor, although the sizes of residual scalars are much smaller than the dominant scalar. In this study, they are called residual scalars, which are not generated by either the GOG or S-Curve I models i.e. $G$ and $B$ of red channel ($G_{dr}$, $B_{dr}$), R and B of green channel ($R_{dg}$, $B_{dg}$), R and G of blue channel ($R_{db}$, $G_{db}$).

The residual scalars of the other displays investigated were also calculated and the results are shown in Figure 3–23. The result for the Barco CRT monitor is also shown together in the right diagram of the third row, to be compared with those of the LCDs. Except for the Barco CRT monitor, all other LCDs exhibit similar behaviour.

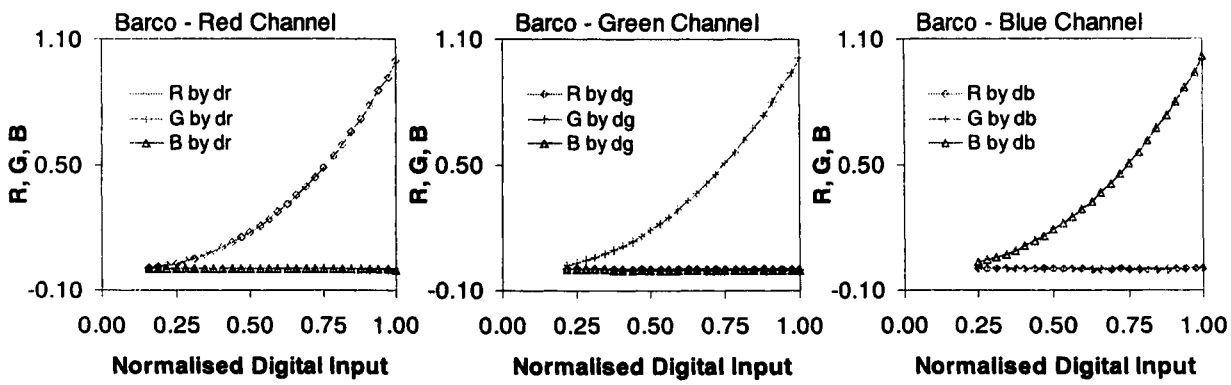


*Figure 3–21 Three scalars R,G,B of each channel for Barco CRT monitor*

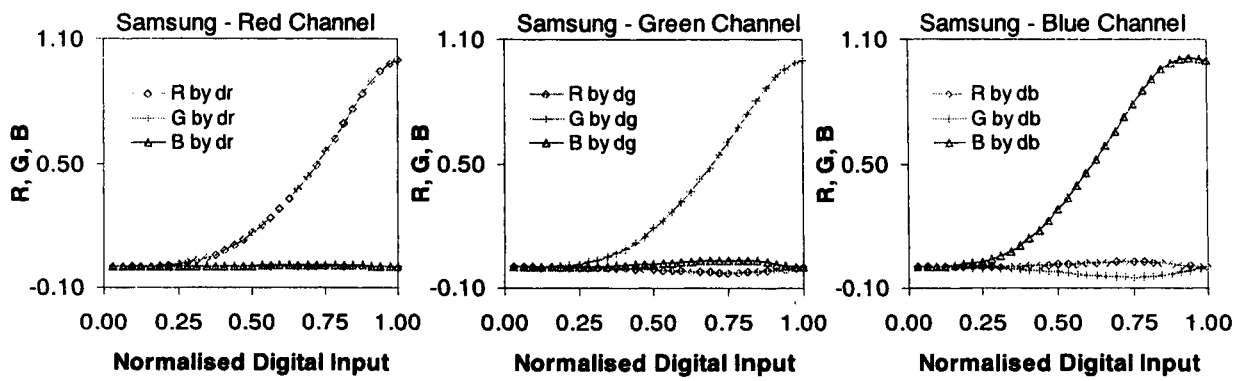


*Figure 3–22 Three scalars R,G,B of each channel for Samsung LCD monitor*

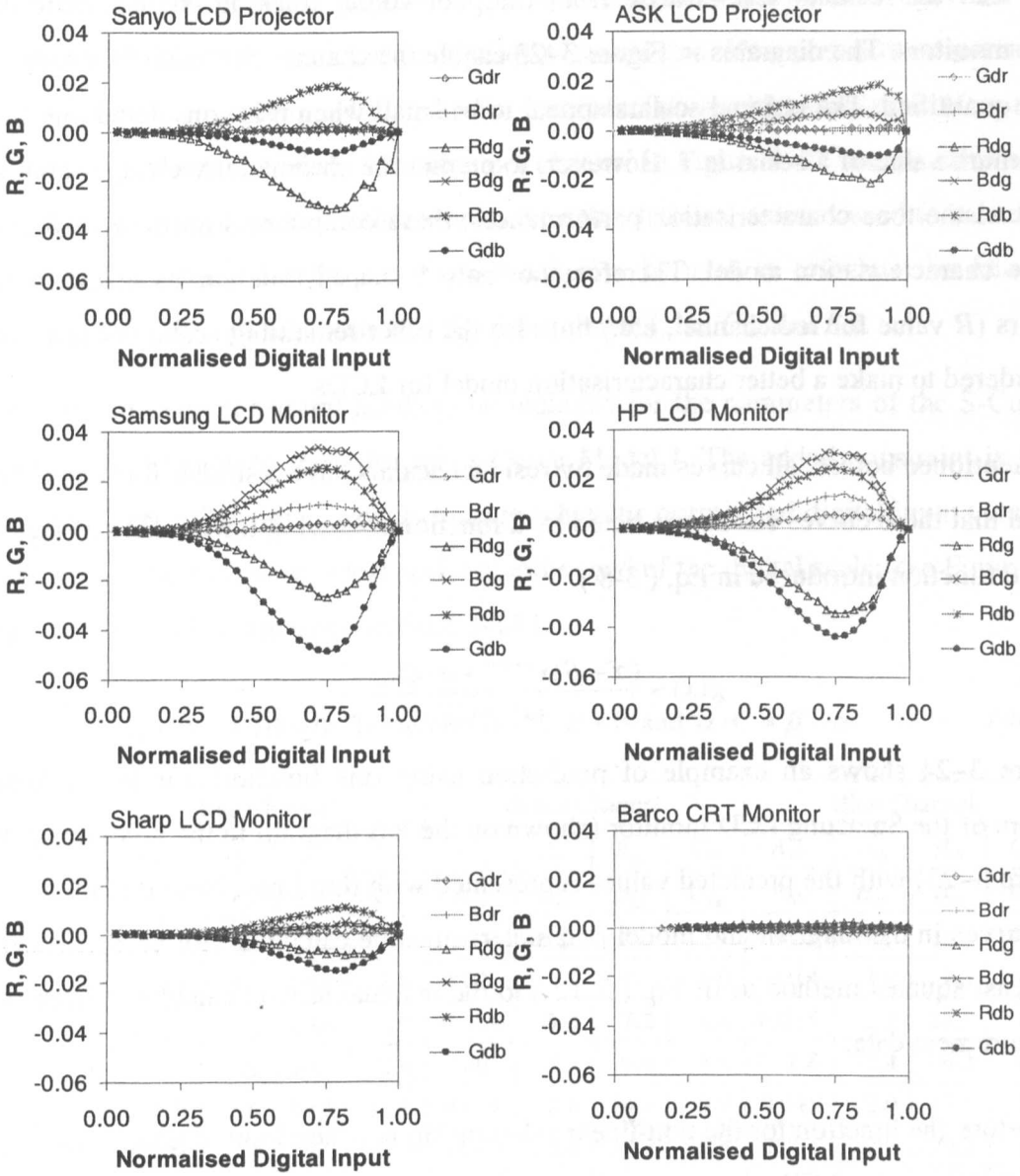


*Figure 3–23 The residual scalars generated by the input signal of each channel*

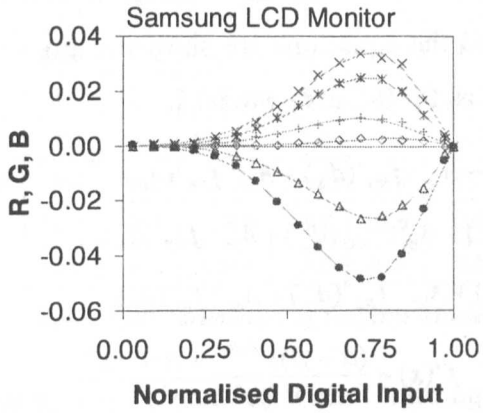


*Figure 3–24 Predictions of residual scalars*

Note that the residual scalars arise from the poor colour tracking characteristic of LCD monitors. The diagrams in Figure 3–23 enable the channel chromaticity changes to be quantified. The residual scalars appear to be small when it is considered that the maximum value of a scalar is 1. However, to predict the chromaticity changes and to improve the tone characterisation performances, these components must be included in the characterisation model. Therefore not only S-shaped tone curves of the main scalars (*R* value for red channel, etc.) but also the other remaining scalars need to be considered to make a better characterisation model for LCDs.

As mentioned before, all curves made by residual scalars have a similar form and it is found that these curves can be predicted by a function following the gradient of the S-Curve function introduced in Eq. ( 3-8 ).

$$g(x) = \frac{(\alpha - \beta)x^{\alpha+\beta-1} + \alpha \cdot C \cdot x^{\alpha-1}}{(x^{\beta} + C)^2} \qquad (3\text{-}12)$$

Figure 3–24 shows an example of prediction using this function, for the residual scalars of the Samsung LCD monitor (shown on the left diagram in the second row in Figure 3–23) with the predicted values represented with thin lines. Note that there are six curves in the diagram and model parameters must be calculated for each curve by the least squares method to fit Eq. ( 3-12 ) to the residual scalars calculated from the measurement data.

Therefore the function for the non-linear relationship between input digital values and the scalars in the LCD characterisation model, S-Curve Model I, was extended by adding extra terms to compensate for the residual scalars having the form of the first derivative of the S-curve function. This new model is called S-Curve Model II [Kwak2000, Kwak2003] and the equations are shown in Eq. ( 3-13 ). Note that the diagonal terms are the same as for S-Curve Model I.

$$\begin{aligned} R &= A_{rr} \cdot f_{RR}(d_r) + A_{rg} \cdot f_{RG}'(d_g) + A_{rb} \cdot f_{RB}'(d_b) \\ G &= A_{gr} \cdot f_{GR}'(d_r) + A_{gg} \cdot f_{GG}(d_g) + A_{gb} \cdot f_{GB}'(d_b) \\ B &= A_{br} \cdot f_{BR}'(d_r) + A_{bg} \cdot f_{BG}'(d_g) + A_{bb} \cdot f_{BB}(d_b) \end{aligned} \qquad (3\text{-}13)$$

$$f(x) = \frac{x^{\alpha}}{x^{\beta} + C}, \quad f'(x) = \frac{(\alpha - \beta)x^{\alpha+\beta-1} + \alpha \cdot C \cdot x^{\alpha-1}}{(x^{\beta} + C)^2}$$

$f'(x)$: first - order derivative of $f(x)$

S-Curve Model II needs 12 parameters per channel since each channel has 3 curves for scalars $R$, $G$, $B$ and each curve requires 4 parameters. However it does not need more training colours than S-Curve Model I to calculate model parameters. Note that the model parameters of three functions per channel in Figure 3–22 can be calculated with the same set of data. In other words, the same training colours used to calculate the parameters for $R$ for the red channel can also be used to calculate the other 8 parameters for the residual scalars in the same channel, i.e. $G_{dr}$ and $B_{dr}$.

Note that an extra constraint needs to be included for the parameters of the S-Curve Model II in addition to those for the S-Curve Model I. The added constraint is that first-order derivative values have to be zero when the normalised digital input value is 0 and 1 since there is no residual scalar at either end of the digital scale (see Figure 3–23). The rules are summarised in Eq. ( 3-14 ).

$$f'(0) = 0, \quad f'(1) = 0 \quad \text{Therefore} \quad \alpha > 1, \ \beta > 0 \ \text{and} \ \alpha \cdot C = \beta - \alpha \qquad (3\text{-}14)$$

| | Red Channel | | | | Green Channel | | | | Blue Channel | | | |
|---|---|---|---|---|---|---|---|---|---|---|---|---|
| R | $A_{rr}$ | $\alpha_{rr}$ | $\beta_{rr}$ | $C_{rr}$ | $A_{rg}$ | $\alpha_{rg}$ | $\beta_{rg}$ | $C_{rg}$ | $A_{rb}$ | $\alpha_{rb}$ | $\beta_{rb}$ | $C_{rb}$ |
| G | $A_{gr}$ | $\alpha_{gr}$ | $\beta_{gr}$ | $C_g$ | $A_{gg}$ | $\alpha_{gg}$ | $\beta_{gg}$ | $C_{gg}$ | $A_{gb}$ | $\alpha_{gb}$ | $\beta_{gb}$ | $C_{gb}$ |
| B | $A_{br}$ | $\alpha_{br}$ | $\beta_{br}$ | $C_b$ | $A_{bg}$ | $\alpha_{bg}$ | $\beta_{bg}$ | $C_{bg}$ | $A_{bb}$ | $\alpha_{bb}$ | $\beta_{bb}$ | $C_{bb}$ |
| Sanyo | **3.4** | **3.3** | **10.8** | **2.4** | -0.026 | 3.7 | 7.3 | 1.0 | 0.014 | 3.8 | 7.4 | 0.9 |
| | 0.001 | 3.2 | 10.8 | 2.3 | **2.6** | **3.2** | **7.2** | **1.6** | -0.035 | 2.2 | 21.5 | 8.7 |
| | -0.000 | 3.0 | 10.8 | 2.6 | 0.002 | 4.4 | 9.4 | 1.1 | **1.8** | **3.4** | **6.2** | **0.8** |
| ASK | **27.9** | **2.6** | **19.5** | **26.9** | -0.035 | 3.4 | 14.6 | 3.2 | 0.045 | 2.9 | 17.3 | 5.0 |
| | 0.001 | 2.0 | 6.0 | 2.0 | **13.0** | **2.4** | **31.3** | **12.0** | -0.031 | 2.8 | 20.0 | 6.2 |
| | -0.001 | 2.0 | 6.0 | 2.0 | 0.013 | 2.9 | 13.4 | 3.6 | **2.2** | **2.4** | **0.0** | **1.2** |
| Samsung | **3.4** | **3.2** | **8.7** | **2.4** | -0.020 | 4.1 | 7.6 | 0.9 | 0.017 | 4.1 | 6.9 | 0.7 |
| | 0.002 | 4.7 | 9.7 | 1.0 | **2.6** | **3.2** | **7.3** | **1.6** | -0.035 | 4.0 | 6.9 | 0.7 |
| | 0.007 | 4.2 | 6.3 | 0.5 | 0.030 | 3.6 | 7.4 | 1.1 | **1.4** | **3.6** | **5.0** | **0.4** |
| HP | **4.2** | **3.4** | **10.6** | **3.2** | -0.031 | 3.9 | 8.7 | 1.2 | 0.019 | 3.9 | 7.4 | 0.9 |
| | 0.008 | 3.3 | 11.7 | 2.5 | **2.7** | **3.3** | **8.4** | **1.7** | -0.034 | 3.9 | 7.6 | 0.9 |
| | 0.008 | 4.2 | 7.1 | 0.7 | 0.026 | 3.8 | 7.8 | 1.1 | **1.4** | **3.8** | **5.3** | **0.4** |
| Sharp | **6.3** | **4.0** | **9.6** | **5.3** | -0.008 | 4.3 | 9.9 | 1.3 | 0.010 | 3.9 | 9.5 | 1.4 |
| | 0.000 | 3.7 | 12.0 | 2.2 | **4.0** | **3.9** | **8.6** | **3.0** | -0.012 | 4.2 | 8.8 | 1.1 |
| | 0.004 | 3.7 | 12.0 | 2.2 | 0.011 | 3.0 | 20.5 | 5.9 | **3.2** | **3.8** | **8.9** | **2.2** |

***Table 3-20 Parameters of S-Curve Model II***

The optimised parameters were calculated with 9 training colours per channel using the least-squares method to minimise the errors between measured and predicted

scalars while satisfying the above rules, which was the same strategy used for GOG and S-Curve Model I. Table 3-20 lists the parameters of displays tested. Bold characters are the parameters used for S-Curve Model I.

The performance of S-Curve Model II is also tested using four test data sets: 59 test colours and 32 steps per channel. Table 3-21 shows the average CIELAB colour differences for S-Curve Model II with those for S-Curve Model I and the GOG model. Clearly the S-Curve Model II outperforms both S-Curve Model I and the GOG model. In particular, the test results using S-Curve Model II for the blue channel show the most significant improvements for all displays compared to S-Curve Model I.

In Table 3-21 it is noticeable that the colour difference errors of the test colour data sets are larger than channel colours (Red, Green, Blue) for most LCDs. This is probably related to additivity failures since the mixture of channels gives poorer performance than single channel colours. Note that S-Curve Model II also assumes channel independence like S-Curve I and GOG model. Only channel chromaticity change was considered in this new model.

| $\Delta E^*_{ab}$ | S-Curve II | | | | S-Curve I | | | | GOG | | | |
|---|---|---|---|---|---|---|---|---|---|---|---|---|
| | Test | Red | Green | Blue | Test | Red | Green | Blue | Test | Red | Green | Blue |
| Sanyo | 2.08 | 0.89 | 1.12 | 1.65 | 2.76 | 0.99 | 2.31 | 5.25 | 17.39 | 5.14 | 9.00 | 12.25 |
| ASK | 1.27 | 0.81 | 1.16 | 2.06 | 2.01 | 0.82 | 2.85 | 7.59 | 2.11 | 1.47 | 5.57 | 7.00 |
| Samsung | 1.57 | 0.76 | 0.67 | 0.71 | 4.33 | 2.66 | 4.10 | 7.22 | 9.92 | 4.99 | 7.39 | 10.01 |
| HP | 4.40 | 1.05 | 1.53 | 2.34 | 6.67 | 3.64 | 5.46 | 9.95 | 12.83 | 6.51 | 10.54 | 13.23 |
| Sharp | 2.81 | 0.74 | 1.21 | 0.68 | 3.65 | 1.55 | 1.96 | 3.91 | 8.73 | 3.12 | 5.81 | 7.15 |

***Table 3-21 Performance results of S-Curve Model II***

| $\Delta E^*_{ab}$ | S-Curve II | | |
|---|---|---|---|
| | Test | Average of Three Channels | Additivity Errors (%) |
| Sanyo | 1.77 | 1.22 | 0.90 |
| ASK | 1.53 | 1.34 | 1.62 |
| Samsung | 1.31 | 0.71 | 4.40 |
| HP | 3.70 | 1.64 | 10.62 |
| Sharp | 2.31 | 0.88 | 10.02 |

***Table 3-22 Effect of additivity on the performance results of S-Curve Model II***

Additivity errors of the three channels shown in Figure 3–14 were averaged using their absolute values and listed in Table 3-22 with the performances of S-Curve

Model II for the test data set and the average of channel colours. This result supports the idea that the poorer performance of the test data set compared to channel colours is caused by poor additivity. The Sharp and HP LCD monitors, showing worst additivity performance, also give the largest difference between the two kinds of data sets, i.e. mixture of channels and individual channel colours.

## 3.6 Summary of Display Characterisation

In this chapter, the performance of colour measurement and display devices were investigated. The data of three tele-spectroradiometers showed a non-linear relationship between them implying that it is important to specify which instrument is used for an experiment. It is recommended to use only one instrument for the whole set of data to have a consistent relationship between the measurement data.

It was shown that the colour characteristics of LCDs are quite different from those of CRT monitors, which lead to the development of new characterisation models, S-Curve Model I and S-Curve Model II, for LCD projectors and monitors.

# Chapter 4
# Psychophysical Experiments

## 4.1 Introduction

The purpose of this experiment was to accumulate a new colour appearance data set, especially under dark surround conditions. The new data set was planned to be compatible with the LUTCHI data set with regard to the experiment with a 35mm-slide projector [Luo1993b]. Therefore these new data should provide a consistent basis for developing colour appearance models for dark surround conditions. In this chapter the experimental set up will be described first, followed by an explanation of the experimental procedure.

Table 4-1 lists the experimental groups of the author's data set called CII-Kwak. It consists of five data groups with a total of twenty phases including three display devices, two surround conditions, three background luminance factors and two stimulus sizes. Luminance levels ranged from 0.1 to 154 cd/m$^2$. During each experiment the lightness, colourfulness and hue of the test colours were assessed by a panel of observers using a magnitude estimation method, making a total of 28,608 estimations for the CII-Kwak data set. All test colours were measured using a PR-650spectroradiometer.

In Table 4-1, Group P represents the viewing conditions for a typical presentation situation. An LCD projector was used in a dark room to display colour patterns. For the Group M experiments, colours were displayed using an LCD flat-panel monitor in a dark room. Group C experiments were performed in a large lecture theatre to simulate cinema viewing conditions, in which test colours were produced using both

an LCD projector and a 35-mm slide projector in a dark room. Group A experiments tested the effect of surround change and used a CRT monitor with and without ambient light. Group F experiments had eight phases covering two stimulus sizes and four luminance levels, the lowest of which extended into the range of mesopic vision. Colours were displayed on a CRT monitor in a dark room. Details of each group are introduced in Section 4.3.

| | Group | Surround | No. of Phases | Light Source | Ref. White | Back-ground | No. of Observers | No. of Colours | No. of Estimations |
|---|---|---|---|---|---|---|---|---|---|
| CII-Kwak | P (Presentation) | Dark | 3 | 7200 K | 19, 154 cd/m$^2$ | Grey Black | 21 | 32 | 6,048 |
| | M (Monitor) | Dark | 3 | 7200 K | ~ 90 cd/m$^2$ | White Grey Black | 11 or 12 | 40 | 4,200 |
| | C (Cinema) | Dark | 4 | 7200, 3900 K | ~ 16 cd/m$^2$ | | 9 or 11 | 40 | 4,800 |
| | A (Ambient) | Dark Average | 2 | 7200 K | ~ 86 cd/m$^2$ | Grey | 11 | 40 | 2,640 |
| | F (Filters) | Dark | 8 | 7200 K | 0.1 ~ 88 cd/m$^2$ | Grey | 10 ~ 12 | 40 | 10,920 |

***Table 4-1 Experimental groups of the CII-Kwak data set***

## 4.2 Viewing Pattern of Test Colours

Figure 4–1 shows the viewing pattern used in the experiment. A similar pattern was also used in the LUTCHI experiment [Luo1991a, Luo1993b]. The borderline of each square is drawn in this figure for legibility. No borderline was used in the real experiment.

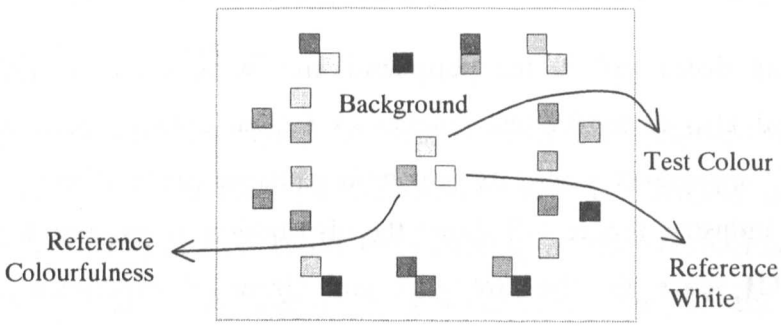


***Figure 4–1 Viewing pattern of the displayed Image***

There were three colour patches in the centre: a test colour, a reference white and a reference colourfulness. The test colour was assessed by the observers whereas the reference white and reference colourfulness were anchor samples to facilitate the

observer's judgements and were not changed during each observation session. However each phase used a different reference colourfulness colour. Section 4.4.1 describes the use of reference colourfulness in the experiments.

Background means the remaining area of the image apart from the 28 colour patches including decoration colours. The colour patches in total cover roughly 8% of the whole image area. The experimental setting was adjusted so that each colour patch subtended to the eyes a viewing field of approximately 1° corresponding to the setting of the Group 35mm experiment in the LUTCHI data set [Luo1993a].

For the group F experiment the viewing pattern was modified slightly to make a large colour patch (See Figure 4–2). The left image shows the "-02" experiment pattern and the right image is for the "-10" experiments. At the same luminance level, only the size of the test colour was changed to subtend either 2° or 10° to the eyes. The same reference colours were used in both cases.

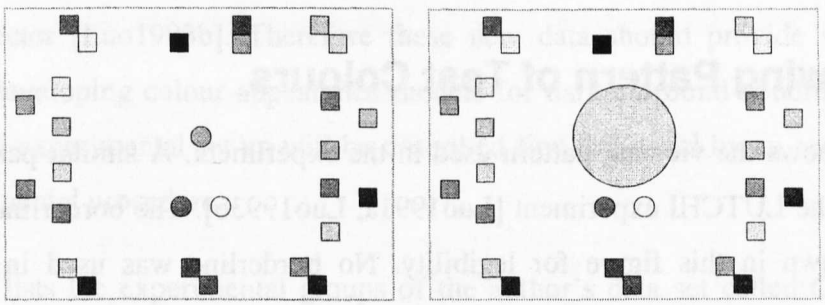

***Figure 4–2 Viewing Patterns for Group F Experiment***

Twenty-five colours distributed in the peripheral area were used to simulate a complex image and also to render test colours as related colours. Note that the experimental colour appearance results using complex images can be directly applied to the graphic arts industry. Figure 4–3 shows the distribution of test and decoration colours in CIELAB space for the Group A and Group F experiments. Other experimental groups also had similar relationships between the distribution of test and decoration colours because the decoration colours with same digital input values were used throughout the whole phases (excluding the experiment with 35-mm slide projector). These diagrams show that the decoration colours were randomly selected to cover all areas of hue and lightness with medium colourfulness.

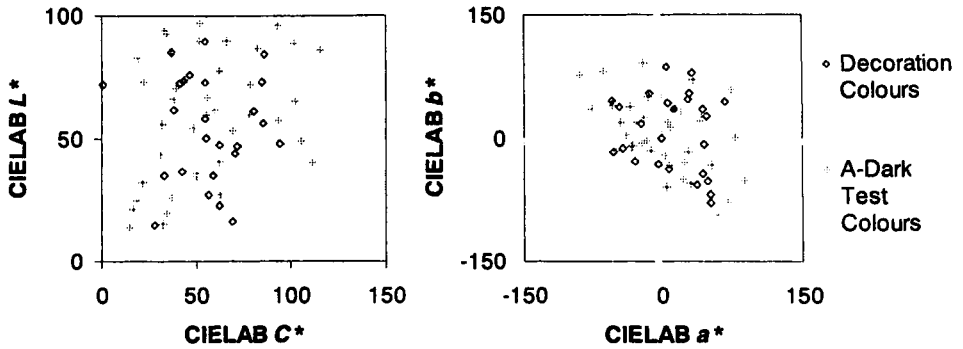


*Figure 4–3 Distribution of decoration colours in CIELAB space (Group A and F)*

A blank screen filled with the background colour was displayed approximately for two seconds between successive test colours to avoid the possibility of an after-image affecting the judgement of the next test colour.

## 4.3 Experimental Settings

Each experiment had a similar experimental set up and procedure. Except for one phase (A-Avg) in which the CRT monitor was illuminated with ambient light, each experiment was performed in a dark room. Light sources other than the screen were completely covered. When the LCD projector was placed in front of observers it was covered with a black cloth to block the light leaking from the vent. In the case of experiments with the CRT monitor, the LED indicator lights from the monitor and the computer were covered and also computer was covered with a black cloth to avoid the light emitted from the rear panel of the computer. Another black cloth was used to cover the surface of the desk supporting the CRT monitor to eliminate reflected light from the surface of the desk.

The distance from test image to the observer was adjusted to be within the recommended distance (3±1 picture heights from the screen) for normal cinema according to ANSI/SMPTE 196M-1986 [ANSI]. A PR-650 spectroradiometer placed in the same position as the observer's eyes was used to measure the colour in terms of colorimetric data. Each experimental setting was regularly checked and each time the test colours were measured to ensure the consistency of colour stimuli in the repeated observation sessions. The colour measurement data reported in this thesis are the average values.

### 4.3.1 Group P Experiment (Presentation Condition)

The Group P represents a typical presentation viewing condition, with a projected image of approximately 1m in width. Projected colours were investigated with two luminance levels and two background luminance factors. The experimental setting is illustrated in Figure 4–4. A Sanyo PLC-5605B LCD projector driven by a Samsung Sense 820 laptop computer was used to project the image onto a white matte screen, which was constructed of plywood painted with Dulux White paint. The projected image size was 117x88 cm. The distance between screen and observer (or spectroradiometer) was 300cm.

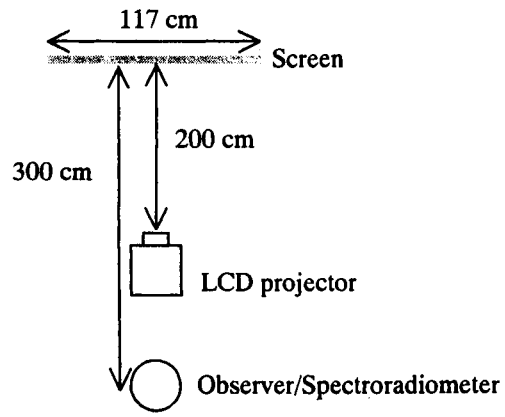


*Figure 4–4 Experimental Geometry for Experiment P*

Table 4-2 gives the details of each phase. The luminance of the reference white of each phase was chosen according to the fact that for projected images, 150 cd/m$^2$ gives excellent image quality for colour pictures and 16.7 cd/m$^2$ is close to the minimal luminance required to achieve an acceptable image quality [Hunt1995 p788]. The low luminance was achieved by using a polyester neutral filter with a density of 0.9 to cover the lens of the projector. The same 21 observers participated all three phases. This was the largest number of observers used in any of the magnitude estimation experiments. The results of this experiment were used to test the effect of the number of observers.

| | Name | Surround | Device | CCT | Ref. White $L_w$ (cd/m$^2$) | Background $Y_b$ (%) | No. of Observers | No. of Samples |
|---|---|---|---|---|---|---|---|---|
| P | P-Grey | Dark | Projector | 7200 K | 154.0 | 18.34 | 21 | 32+10 |
| | P-Black | Dark | Projector | 7200 K | 152.7 | 0.42 | 21 | 32+10 |
| | P-Filter | Dark | Projector | 7200 K | 18.77 | 18.68 | 21 | 32+10 |

*Table 4-2 Experimental Phases of Group P*

Thirty-two test colours were chosen to cover the whole colour gamut of the projector and 10 colours were repeated in each phase to test the repeatability of each observer. Figure 4–5 shows the distributions of the test colours in CIELAB space. Colours having the same digital input values were used throughout all phases, however their chromaticities were not exactly the same. The chromaticity differences between the P-Grey and P-Black phases ($\Delta E^*_{ab}$=6.59) arose from the spatial dependency of the LCD projector. The differences in chromaticities between the P-Grey and P-Filter ($\Delta E^*_{ab}$=3.42) phases may have been caused by the light scattered by the filter in front of the lens used to reduce the luminance. Because of these small colour differences between experimental phases, direct comparison of psychophysical experiment results had intrinsic errors.

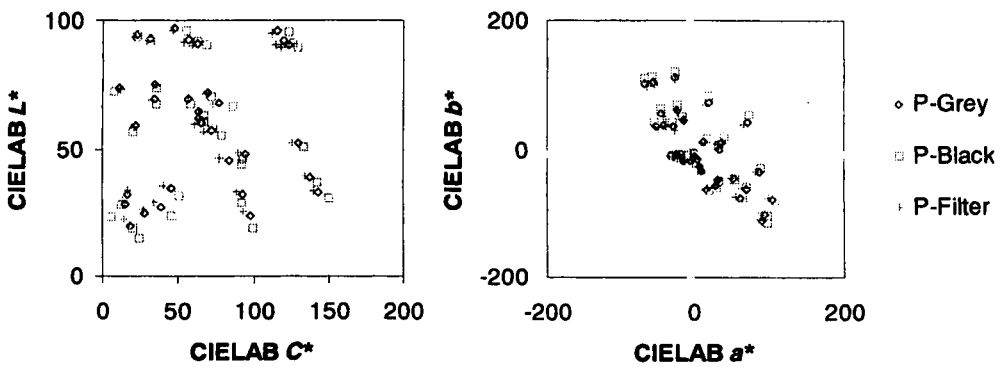


*Figure 4–5 Distribution of test colours of Group P*

## 4.3.2 Group M Experiment (LCD Monitor in a Dark Room)

The Group M experiment was designed to investigate the device dependence of colour appearance. The experiment was performed using an LCD monitor in a dark room and the results were compared with those of Group P – LCD projector. A Samsung Sense 820 laptop computer was used in this experiment. The image size was 28x21 cm. To avoid the angular dependency of the output colours on the LCD screen, the observer's eye position was fixed by means of a viewing frame as shown in Figure 4–6 to the normal direction of the display screen. The distance between monitor and observer (or spectroradiometer) was 70 cm.

Table 4-3 lists the phases in this experiment. The chromaticity of the reference white for the LCD monitor was adjusted to match that of the LCD projector. However the luminance level of the reference white could not be matched because of the limitation

of maximum luminance of the LCD monitor. Forty test colours were used with three different background levels and 10 colours were again duplicated for a repeatability check. The same 10 out of 40 colours were repeated from the Group P experiment.

Figure 4–7 shows the distribution of test colours. There was little difference in colour measurement between different phases implying good spatial independence of the monitor.

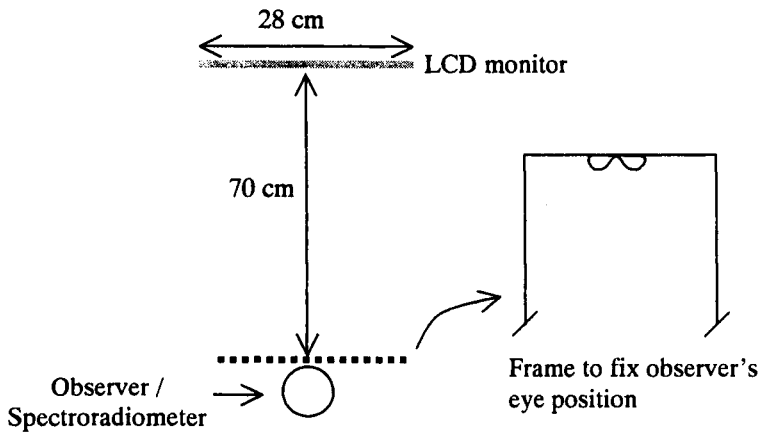


*Figure 4–6 Experimental Geometry for Experiment M*

| | Name | Surround | Device | CCT | Ref. White $L_w$ (cd/m$^2$) | Background $Y_b$ (%) | No. of Observers | No. of Samples |
|---|---|---|---|---|---|---|---|---|
| M | M-Grey | Dark | LCD monitor | 7200 K | 90.33 | 20.65 | 12 | 40+10 |
| | M-Black | Dark | LCD monitor | 7200 K | 89.81 | 0.36 | 11 | 40+10 |
| | M-White | Dark | LCD monitor | 7200 K | 90.22 | 100.0 | 12 | 40+10 |

*Table 4-3 Experimental Phases for Group M*

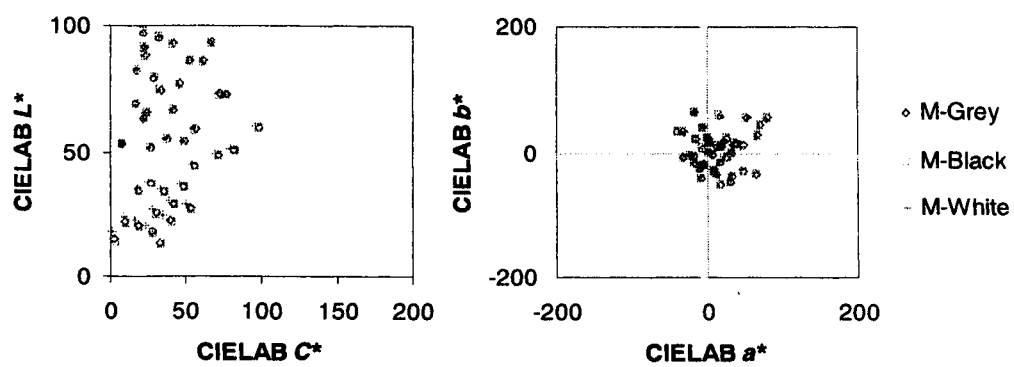


*Figure 4–7 Distribution of test colours of Group M*

### 4.3.3 Group C Experiment (Cinema Conditions)

The Group C experiment involved cinema viewing conditions. The background effect was also tested and compared with that of Group M. Figure 4–8 illustrates the experimental settings. The LCD projector and 35-mm slide projector were used to project large images onto a screen in a darkened lecture theatre. All observers sat within the observer zone and conducted the psychophysical experiment simultaneously. The size of the displayed image was approximately 319x239 cm for the LCD projector and 280x184 cm for the 35-mm slide projector. The maximum angular difference of the observer's seat from the centre was 7.7° and there was little colour difference in measurements of test patches compared to the centre. This implies that sitting in different positions did not affect the stimulus seen by the observers.

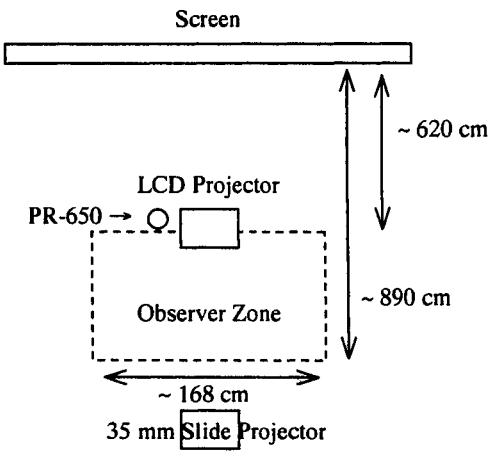


*Figure 4–8 Experimental Geometry for Experiment C*

| | Name | Surround | Device | CCT | Ref. White $L_w$ (cd/m$^2$) | Background $Y_b$ (%) | No. of Observers | No. of Samples |
|---|---|---|---|---|---|---|---|---|
| C | C-Grey | Dark | LCD Projector | 7200 K | 15.68 | 17.37 | 9 | 40+10 |
| | C-White | Dark | LCD Projector | 7200 K | 16.28 | 97.42 | 9 | 40+10 |
| | C-Black | Dark | LCD Projector | 7200 K | 15.00 | 0.00 (0.4) | 11 | 40+10 |
| | C-35mm | Dark | 35mm Slide Projector | 3900 K | 15.42 | 20.38 | 11 | 40+10 |

*Table 4-4 Experimental Phases of Group C*

The experimental phases are summarised in Table 4-4. During each session, 40 colours (see Figure 4–9) were assessed and 10 colours were repeated to investigate observer repeatability (therefore 50 colours were presented in each phase). In the case of the LCD projector experiment, the same 30 test colours were used as in the Group

P experiment and 10 new colours were added. For the 35-mm slide projector experiment, 40 slides were chosen from the original set of 99 slides used in the LUTCHI experiment [Luo1993b].

The luminance of the background for the C-Black phase was too low to be measured by the PR-650 spectroradiometer. However some colour appearance models cannot be used with a background luminance factor of zero. Therefore a value of 0.4% was used to test colour appearance models since the luminance factor of the black background for Group P was 0.4%. Note that Group P and Group C used same LCD projector but the distance between the screen and observers was changed according to the different screen size, which reduced the luminance level of the projected image. The luminance ratio between white and black, however, remained the same.

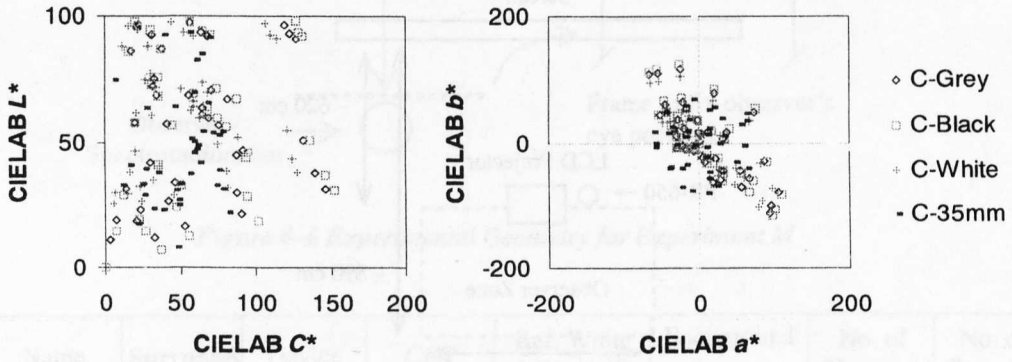


*Figure 4–9 Distribution of test colours for Group C*

### 4.3.4 Group A Experiment (Effect of Ambient Light)

The Group A experiment aimed to investigate the surround effect directly. CRT monitor colours were shown to the observers with and without ambient light. A Barco *Calibrator V* was used to display the colours. Figure 4–10 illustrates the experimental geometry. A fluorescent lamp simulating D65 located in the ceiling was used as a source of ambient light. A white diffuser tile placed in the centre of the monitor was measured for ambient light level. A diffuse reflectance standard (3009/2) provided by Bentham Instruments was used in this study. The ambient level was 52.86 cd/m$^2$, which corresponds to 166 lux.

The experimental conditions in Group A are summarised in Table 4-5. Forty colours were chosen as test colours and ten colours were duplicated to check observer repeatability. The same test colours were used for both phases. The distributions of

the test colours are shown in Figure 4-10 and these figures demonstrate the effect of ambient light on CRT colours, i.e. the ambient light decreases the CIELAB $C^*$ and increases the $L^*$ of CRT colours. Refer to Section 3.5.1 for the colour gamut change by ambient light on a CRT monitor and the effect on the characterisation model.

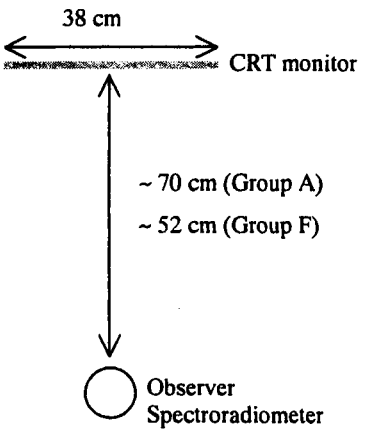


*Figure 4–10 Experimental Geometry for Experiments A and F*

| | Name | Surround | Device | CCT | Ref. White $L_w$ (cd/m$^2$) | Background $Y_b$ (%) | No. of Observers | No. of Samples |
|---|---|---|---|---|---|---|---|---|
| A | A-Dark | Dark | CRT Monitor | 6800 K | 85.77 | 19.82 | 11 | 40+10 |
| | A-Avg | Average | CRT Monitor | 6800 K | 89.13 | 24.00 | 11 | 40+10 |

*Table 4-5 Experimental Phases of Group A*

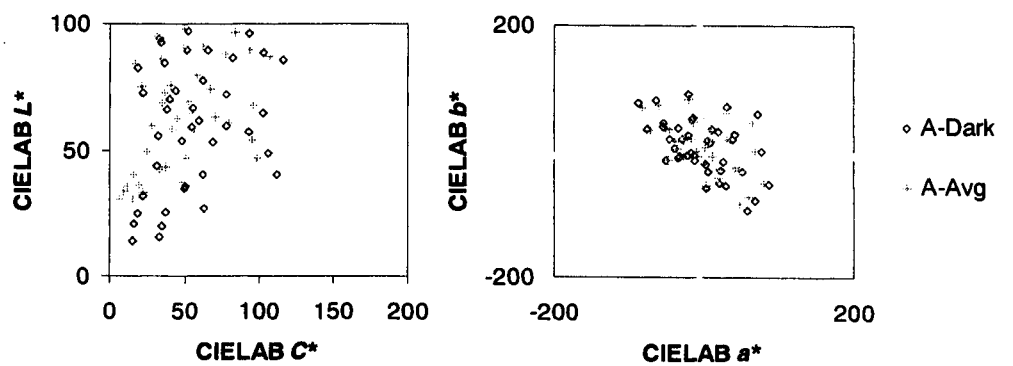


*Figure 4–11 Distribution of test colours for Group A*

## 4.3.5 Group F Experiment (Effects of Luminance and Patch Size)

The Group F experiment consisted of eight phases covering the mesopic and photopic luminance ranges. The effect of patch size was also investigated using test patches with 2° and 10° viewing fields. Phase F0-02 had the same viewing condition as the

Phase A-Dark and most of the colours were repeated. The visual results from these two phases were used to reveal the long-term repeatability of the observers.

A Barco *Calibrator V* monitor was used in a dark room and with a similar setting as the Group A experiment (See Figure 4–10). However the distance between the screen and observers was reduced from 70 cm to 52 cm to make an exact 2° viewing angle instead of 1.4° which was the size used for the previous experiments. Table 4-6 lists the viewing conditions of the experimental phases. The name of phases having "-02", indicates that 2° patches were used and "-10" means that 10° patches were used. The reduction in luminance level was achieved by covering the screen with one, two or three large sheets of neutral density polyester filter, each having density 0.9ND, over the entire monitor faceplate. The density of the filter is defined as $D=\log_{10}(100/T)$ where T is the transmittance expressed as a percentage. 0.9ND means the filter had 12.6% transmittance. The number shown after "Filter" represents the number of neutral filters used. (More filters caused less light from the monitor to reach the observer.)

| | Name | Surround | Device | CCT | Ref. White $Y_w$ | Background $Y_b$ (%) | No. of Observers | No. of Samples |
|---|---|---|---|---|---|---|---|---|
| F | Filter0-02 | Dark | CRT Monitor | 6800 | 87.37 cd/m$^2$ | 19.76 | 12 | 40+10 |
| | Filter0-10 | Dark | CRT Monitor | 6800 | 96.24 | 19.77 | 12 | 40+10 |
| | Filter1-02 | Dark | CRT Monitor | 6700 | 8.856 cd/m$^2$ | 20.86 | 13 | 40+10 |
| | Filter1-10 | Dark | CRT Monitor | 6700 | 9.683 | 20.89 | 12 | 40+10 |
| | Filter2-02 | Dark | CRT Monitor | 6700 | 1.007 cd/m$^2$ | 19.49 | 10 | 40+10 |
| | Filter2-10 | Dark | CRT Monitor | 6700 | 1.099 | 18.96 | 11 | 40+10 |
| | Filter3-02 | Dark | CRT Monitor | 6700 | 0.097 cd/m$^2$ | 19.82 | 11 | 40+10 |
| | Filter3-10 | Dark | CRT Monitor | 6700 | 0.105 | 19.83 | 10 | 40+10 |

***Table 4-6 Experimental Phases of Group F***

In the case of the Filter2 and Filter3 experiments, the luminance levels of some test colours were too low to be measured using the PR-650. Therefore an indirect method was applied to calculate the tristimulus values of those four phases. Firstly the spectral power distribution of the test colour without any filter was measured then tristimulus values of test colour with filters were calculated using the equation below. Only the

equations for $X$ are introduced here in Eq. ( 4-1 ). Similar methods were applied to calculate $Y$ and $Z$.

$$X_{F2} = 683 \cdot \sum_{\lambda=380,\Delta\lambda=4}^{780} p_{F2}(\lambda) \cdot (T(\lambda)/100)^2 \cdot \bar{x}(\lambda) \cdot \Delta\lambda \qquad (4\text{-}1)$$

$$X_{F3} = 683 \cdot \sum_{\lambda=380,\Delta\lambda=4}^{780} p_{F3}(\lambda) \cdot (T(\lambda)/100)^3 \cdot \bar{x}(\lambda) \cdot \Delta\lambda$$

where $p(\lambda)$: Spectral radiance measurement data $W/(sr \cdot m^2 \cdot nm)$

$T(\lambda)$: Transmittance of a filter (%)

The left diagram of Figure 4–12 shows the spectral transmittance of the filter used ($T(\lambda)\cdot 100$), compared with the 12.6% transmittance dashed line. The transmittance was calculated by comparing white colours (maximum digital values) with and without filters. The measured transmittance had only slight fluctuations except for the long wavelength area (longer than 680nm), which showed abnormally higher transmittance. The transmittance curve is depicted with the CIE colour matching functions in the right diagram of Figure 4–12, which shows that the abnormality in long wavelengths has little effect on the measured tristimulus values because of the low values of colour matching functions above 680nm.

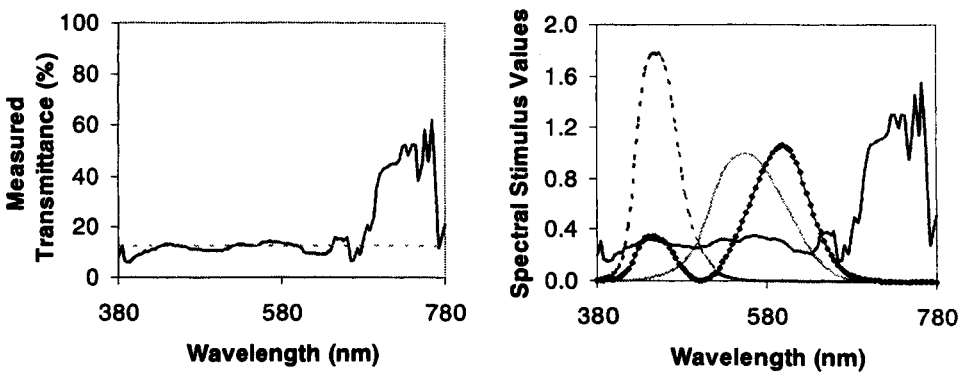


*Figure 4–12 Spectral transmittance of the filter*

It was investigated as to whether the neutral filter is really neutral; in other words, if the neutral filter affects not only the luminance but also the chromaticity of a colour. (Ideally a neutral filter should not affect chromaticity.) The chromaticity of the equi-energy stimulus, $S_E$, with and without the filters was compared to test the performance of the neutral filter as shown in Figure 4–13. The chromaticity of the filters was calculated by applying the transmittance curve to the spectral power distribution of the equi-energy stimulus. For Filter2 and Filter3 the transmittance curves were

applied twice and three times respectively as in ( 4-1 ). Note that the effects of the non-neutral transmittance of the filter are multiplied by applying several filters simultaneously.

Figure 4–13 shows that the chromaticities become more and more shifted from the equi-energy stimulus, $S_E$, towards orange-red as the number of filters is increased. Therefore the input CRT digital signals for Filter1, Filter2 and Filter3 phases had to be adjusted using the GOG model to achieve the same chromaticities as those of the Filter0 (experiment without any filter) phase.

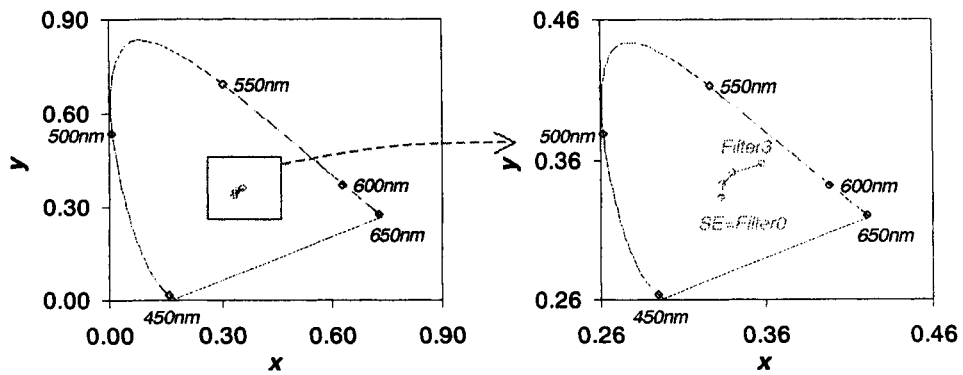


*Figure 4–13 Chromaticity change by the neutral filter*

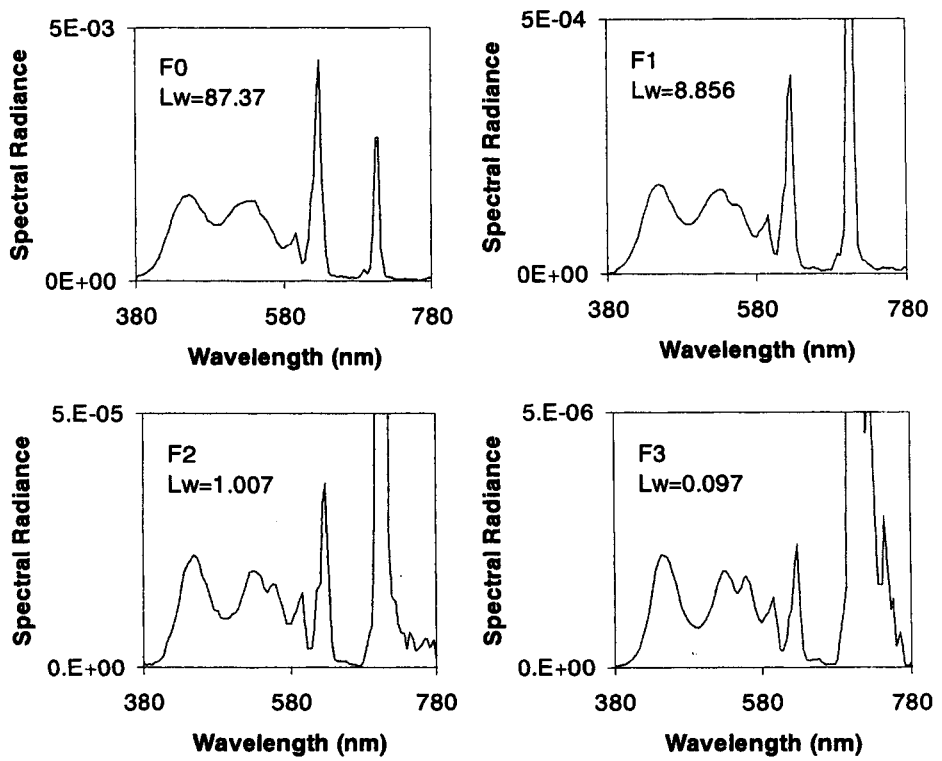


*Figure 4–14 Spectral distributions of reference whites for the group F experiment*

Figure 4–14 shows the spectral power distribution of the reference white at each luminance level, all of which have the same chromaticity. The distribution of the test colours used in Group F experiments is shown in Figure 4–15, indicating that most of the colours were matched between phases.

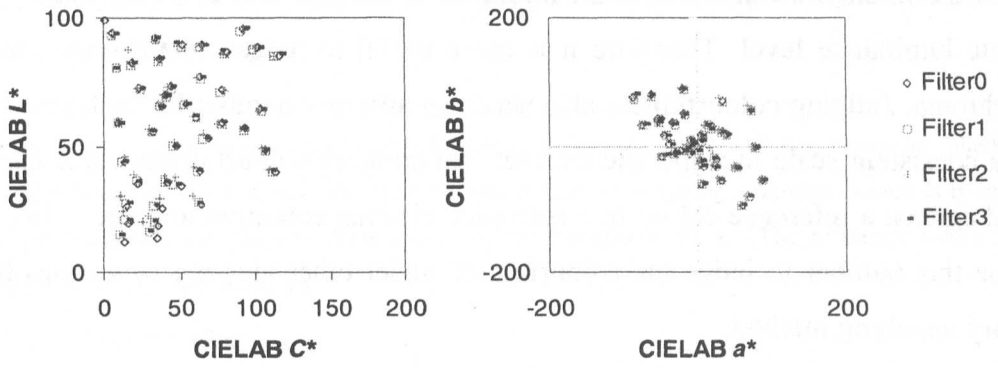


*Figure 4–15 Distribution of test colours for Group F*

## 4.4 Psychophysical Experimental Procedure

### 4.4.1 Experimental Method

The magnitude estimation method was employed to investigate colour appearance, which was the technique used in the LUTCHI experiment. Observers were asked to estimate the lightness, colourfulness and hue of each test colour. Since lightness is a relative scale and colourfulness is an absolute scale, it is often asked why colourfulness is used instead of chroma or why lightness instead of brightness. The simplest answer is that those three attributes are most easily judged by the observers.

Brightness is an absolute attribute but an arbitrary scale would be used for the experiment since there is no anchor point except zero (black). 'Arbitrary scale' means that different observers and experimenters use different numeric ranges therefore it is not possible to compare two independent experimental results directly. On the contrary, lightness is a relative attribute having a fixed scale, since reference white always has maximum lightness of 100 and the lightness of other colours is judged relative to this. Judging lightness gives less information than brightness since lightness does not contain any information of absolute luminance level. However lightness is easy to judge as there is no need to memorise the reference brightness and it is always comparable between different experimental data sets.

A similar analogy can be applied to colourfulness and chroma. Colourfulness is an absolute attribute while chroma is a relative one. However judging chroma is not as simple as lightness because there is no clear fixed chroma reference value as there is for lightness. In other words, judging chroma also needs an 'arbitrary scale' decided by the experimenter but it will lose the information that colourfulness has, namely the absolute luminance level. Therefore it is more useful to judge colourfulness rather than chroma. Judging colourfulness also needs an arbitrary number but at least it can have a consistent scale in a specific data set. An arbitrary colourfulness value can be judged against a reference colour in a reference viewing condition and each observer can use this number to judge the colourfulness under other viewing conditions by a memory matching method.

During psychophysical experiments, the lightness, colourfulness and hue of the test colour were estimated at the same time. This strategy allowed the observers to treat each colour as a whole entity considering the relationship between three attributes. For example if an observer had difficulty in judging hue, it could be connected with a smaller colourfulness value.

### 4.4.2 Observers

Students and staff in the Colour & Imaging Institute were used as observers. They were all volunteers. A total of 33 observers having normal colour vision took part in the author's experiments. There were 11 females and 22 males, 13 Europeans and 20 Orientals. Their ages ranged from 23 to 52. Some observers had experience in using the magnitude estimation method but for most of them it was their first time estimating colour appearance. Each observer participated in 7 sessions on average. Observers' vision was tested for colour deficiency using the Ishihara test.

### 4.4.3 Instruction

Before starting the experiment an instruction sheet was given to the observers, which is introduced in the next paragraph. Also, the definitions of lightness, colourfulness and hue were explained to the observers. (Refer to Section 2.5.1 for the definitions.) Observers were fully informed of their task by reading the instruction sheet and by listening to the experimenter's explanation. A training session, which was conducted

before starting each session (refer to Section 4.4.5), also helped the observer's understanding of the experimental tasks.

> Please sit comfortably and look at the test pattern. You will be shown a series of test colours in a random order. Your task will be to tell me what lightness, colourfulness and hue you see. There is no time limit for each test colour and you can take as long as required until you report your estimations.
>
> **Lightness scaling**
>
> Use the reference white as a standard, which has a lightness of 100, and your imaginary black, which has a lightness of zero. Describe the test colour by assigning a number, which is in the right relationship to the reference white and the imaginary black. (The reference white is displayed in the test pattern.)
>
> **Colourfulness scaling**
>
> Colourfulness is an attribute of a visual sensation according to which an area appears to exhibit more or less of its hue. A neutral colour has no colourfulness, represented by zero on your scale. You are asked to assign a reasonable number to describe the colourfulness of the test colour. This is an open-ended scale since no top limit is set. The colourfulness of the first test colour should always be remembered as 40 so that all subsequent test colours can be related to it. (The first colour is also displayed in the test pattern.)
>
> **Hue scaling**
>
> There are four psychological primaries: red, yellow, green and blue. These four colours can be arranged as points around a circle and lie at opposite ends of $x$ and $y$ axes. You are asked to describe a hue as a proportion of two neighbouring primaries. Firstly, decide whether or not you perceive any hue at all. If not, please reply 'Neutral'. On the other hand if the test colour does not appear neutral then decide which of the four primaries is predominant. Next decide whether or not you see a trace of any other primary hue. If so, identify it. Finally, estimate the proportions in which the two primaries stand, e.g. an orange colour may be 60% yellow and 40% red.

### 4.4.4 Adaptation

Before starting the experiment observers were given time to adapt to the experimental viewing conditions. Adaptation time was varied according to the luminance level involved in the experiment. It lasted around 5 minutes for the high luminance case to 30 minutes for the low luminance phases.

### 4.4.5 Observer Training

There was a training session before commencing each experimental phase. The training was aimed to familiarise the observer with performing the task rather than to teach the observer to follow the specific way of judgement, which could give a bias to the experimental results. Observers were allowed to interpret the concepts of colour attributes according to their own ideas since all observers already knew the definitions based on their varied experience with colour science research. This issue was addressed by S. S. Stevens with regard to observer training. He stated that "there is no need to 'train' the subjects. Indeed, since there is no right or wrong to the subjects' responses, it is not clear what would be meant by training." [Stev1971, p428]

During the training session, three colours were estimated but the responses were not recorded. The viewing condition of the training session was identical to that of the standard phase in each experimental group, namely the experimental phase for which a reference colourfulness was determined for use through all of the phases of each group (see next section). The training session also allowed more time for each observer to memorise the reference colourfulness more naturally.

### 4.4.6 Colourfulness Scaling

Each group of experiments had the same visual scale for colourfulness. Before commencing a new phase, observers were asked to readapt to the experimental condition of the standard phase, followed by performing the training session and memorising the reference colourfulness sample. Subsequently adaptation to the new experimental conditions was carried out. Then observers were asked to estimate the new reference colourfulness sample based on the previous one from memory. This number judged by the observer became a reference number for colourfulness judgement during that session. For the cinema experiments, a slightly different strategy was used. A colour chip was shown in a viewing booth under a D65 simulator and observers were asked to memorise that colour as a reference colourfulness. The same procedure used for the other experimental groups was then followed.

Table 4-7 shows the standard phase for each experimental group. The reference colourfulness of each standard phase was designated as 40. There was no attempt to enforce the same colourfulness scale between different groups of experiments.

| Group | Standard Phase |
|---|---|
| P (Presentation) | P-Grey |
| M (Monitor) | M-Grey |
| C (Cinema) | Colour chip in the viewing booth |
| A (Ambient) | A-Dark |
| F (Filters) | Filter2-02/10 |

***Table 4-7 The standard phase of each experimental group***

### 4.4.7 Recording of the Observer Responses

The observer's visual task was not constrained, i.e. not fixated on the test patch, and there was no limit on the time for estimating each test patch. Observer responses were recorded by the experimenter except for Group C – cinema condition experiment. During the Group C experiment, all observers conducted the experiment simultaneously and were asked to write down their individual responses on paper.

## 4.5 Data Analysis Method

The data analysis was carried out using the same method used by Luo et al. [Luo1991a], which was based on previous studies of colour appearance using magnitude estimation [Bart1979, Poin1980] (see Chapter 2 for details).

### 4.5.1 Averaging the Observer Responses

#### 4.5.1.1. Lightness

For lightness scaling, all observers applied the same numerical scale with the same fixed end points, i.e. between 0 (imaginary black) and 100 (reference white). Applying minimum and maximum values to judge the lightness attribute makes the observers use a partition technique rather than pure magnitude estimation. Therefore the arithmetic mean values of lightness were calculated and the standard deviation was also calculated to represent the scattering of the data. According to Stevens

[Stev1971], the proper averaging method for magnitude estimation is the geometric mean but the arithmetic mean is adequate for a partition experiment.

#### 4.5.1.2. Hue

The experimental procedure for hue scaling was also a partition method. In this case, the fixed points were the unique hues decided by each observer's own perception. Therefore the arithmetic mean was used to average observers' hue responses.

The experimental result, the hue composition of the test colour, was transformed onto a 0-400 scale. That is, 0-100 for Red-Yellow, 100-200 for Yellow-Green, 200-300 for Green-Blue and 300-400 for Blue-Red. This 0-400 hue scale was used to calculate the arithmetic mean and standard deviation.

If an observer's responses were a mixture of R-Y and B-R, one of the responses was moved to the other end of the scale between 0 and 400. For example the average of 20 (20% Yellow and 80% Red) and 390 (10% Blue and 90% Red) was 5 since 390 was converted to -10 (=390-400).

#### 4.5.1.3. Colourfulness

Stevens found that the appropriate central tendency measure for magnitude estimation experiments is the geometric mean [Stev1971, Section 2.3.2.3] and Bartleson demonstrated that the observers' colourfulness responses are related to each other as a power transformation [Bart1979]. Based on this evidence, the geometric mean has been used as an averaging method of colourfulness in many colour appearance experiments using magnitude estimation [Poin1980, Luo1991a,1993a,1993b,1997, Kuo1995, Juan2000], and hence it was also used in the present study. Colourfulness of any neutral colour was set to 1 rather than 0 when calculating the geometric mean.

Computation of the geometric mean automatically establishes a basis for normalising the results of an individual's data. If $S_i$ is an individual's rating of a test colour $i$, and $\overline{S}_i$ is the geometric mean of all observers' ratings of the same test colour, then $\log\overline{S}_i$ can be plotted against $\log S_i$ for all the test colours. A regression line can then be established to determine the $a$ and $b$ coefficients of each observer in the equation $\log\overline{S}_i = b\cdot\log S_i + a$, where $a$ is a scaling factor and $b$ is a compression (or expansion)

factor. The constants *a* and *b* for each observer enable the individual's data to be adjusted to a common scale [Bart1979, Luo1991a]. Therefore theoretically all observers' responses should be linearly related after a power transformation. In other words, the geometric mean must be same as the arithmetic mean of the observer's responses after applying a power transformation.

Figure 4–16 shows the direct comparison between geometric and arithmetic mean calculated after power transformation of each observer's data for the Filter0-02 phase. Contrary to the theoretical prediction, it shows a non-linear relationship. Other experimental phases also showed similar characteristics. This non-linearity arises from the noisy distribution of the raw data. In many cases, each observer's responses did not show a clear power relationship to the geometric means, making a power transformation meaningless. Note that a regression line for power transformation of each observer's data was obtained by minimising the errors between the geometric means and the observer's responses. This procedure changed the ranges of each observer's responses distorting the general tendency. This analysis result suggests that the conventional normalisation procedure will distort the data.

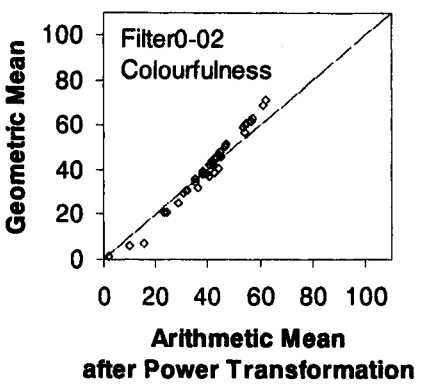


*Figure 4–16 Geometric mean vs. Arithmetic mean after power transformation (Filter0-02)*

The geometric mean has to be used to represent the central value of colourfulness responses because observers used different scales to each other, suggesting that assuming log-normal distribution of colourfulness responses is still reasonable. However unlike previous studies, transforming the observer's data to a common scale by power transformation is not the proper way to calculate the deviation of the data. Instead it is more reasonable to use a log scale to calculate the deviation of observers' responses and convert to the normal scale. Therefore the arithmetic mean ($\psi$) and

standard deviation ($\pm\sigma$) of log values of the observers' responses were calculated then converted to a normal scale. Averaged colourfulness data was represented as geometric mean ($10^{\psi}$), minimum ($10^{\psi-\sigma}$) and maximum ($10^{\psi+\sigma}$) limits.

When the colourfulness results of two independent data sets were compared, they was assumed to be a linear relationship between them. Note that each data set is supposed to represent the average responses of the whole population.

### 4.5.2 Comparing two data sets

It is necessary to determine the relationship between two data sets to quantify colour appearance phenomena and to derive a colour appearance model. In this thesis, the scatter diagram is employed to see the qualitative relationship between two data sets. The coefficient of variation (CV) is used as a statistical measure to investigate the agreement between any two sets of data, say $x$ and $y$. The equation to calculate the coefficient of variation is introduced in Eq. ( 4-2 ). Note that the equation is normalised by the average of the numerical values used. Therefore this CV formula will give the scale-independent value of each data set.

$$CV = 100 \cdot \frac{\sqrt{\sum (x_i - y_i)^2 / n}}{\bar{y}}, \qquad \begin{array}{l} n: \text{sample number in } x \text{ and } y \text{ sets} \\ \bar{y}: \text{the mean value of the } y \text{ set} \end{array} \qquad (4\text{-}2)$$

The main application of the equation was to calculate CV values between two sets of lightness, colourfulness or hue. For lightness and colourfulness data, Eq. ( 4-2 ) was directly used since the numbers correspond to the perceptual attributes. However the hue scale 0 to 400 (H) shows which hue is perceived, not the amount of hue. The meaning of hue difference ($\Delta$H) 10 for yellow (H=100) should be the same as that for blue (H=300). Therefore using the mean value to calculate CV value for hue scale is misleading. It matters little if the hues of test colours are equally distributed, since the average hue would be near 200 all the time. However if the distribution is unbalanced or the number of colours is not large enough to cover the whole hue area, the mean value of hue values may vary a lot affecting CV values seriously. To avoid this problem, in this thesis, the mean value of the $y$ set is put to 200 whenever hue data are compared.

## 4.6 Summary of Psychophysical Experiments

In this chapter, the experimental set-ups and procedures were introduced for the new colour appearance data set, CII-Kwak, which follow the LUTCHI experiments. The CII-Kwak data sets comprise five experimental groups with a total of 20 phases covering various display media, luminance levels, background luminance factors, surround conditions and stimulus sizes. On the average, 11 observers participated for each phase and estimated lightness, colourfulness and hue of each test colour.

# Chapter 5
# Observer Performances

## 5.1 Introduction

In Chapter 4, a series of experiments was introduced. The visual results were analysed and the typical performance of observers are reported in this chapter. Intrinsically, psychophysical experimental data has larger variations than physical measurements such as length, weight, etc. Therefore understanding the characteristics of the data gathered in the experiments is very important. In this chapter uncertainties within and between observer responses are discussed first, followed by the factors affecting the mean of and variations in colour appearance data. These factors include the effect of training, the correlation between colour attributes (lightness, colourfulness and hue) and the number of observers in a group. Finally the observer performances are summarised.

## 5.2 Repeatability of the Observers

Firstly, analysis was conducted to examine the stability of each observer's judgement. Conventionally, stability is represented by repeatability. To test repeatability, observers repeat the same colours twice in a session and a statistical measure is calculated between two answers. The coefficient of variation (CV) is used as the statistical measure to represent the observer repeatability in this study.

$$CV = 100 \cdot \frac{\sqrt{\sum (x_i - y_i)^2 / n}}{\bar{y}}, \qquad (5\text{-}1)$$

$n$ : Number of repeated test colours
$x_i$ : Second estimation, $y_i$ : First estimation
$\bar{y}$ : The mean value of the first estimations
($\bar{y} = 200$ for hue comparison)

### 5.2.1 Short Term Repeatability

During each session 10 test colours were repeated and the CV value was calculated between the repeated colours. Raw data was used to calculate CVs of all three attributes. Table 5-1 shows the average CV values of each group with the average and standard deviation of all 20 phases. Colourfulness showed the largest errors followed by lightness and hue. This indicates that hue is the easiest attribute to judge while judging colourfulness is most difficult for the observers. Repeatability values were similar between groups in general.

| Group | Lightness | Colourfulness | Hue |
|---|---|---|---|
| P (Presentation) | 19.0 | 26.5 | 8.8 |
| M (Monitor) | 15.7 | 27.6 | 9.1 |
| C (Cinema) | 17.5 | 24.5 | 6.3 |
| A (Ambient) | 15.0 | 22.5 | 7.3 |
| F (Filters) | 15.6 | 26.8 | 8.0 |
| Average of 20 phases ± Standard Deviation | 16.4 ± 2.4 | 26.0 ± 4.9 | 7.8 ± 1.4 |

***Table 5-1 Short term repeatability of the observers (Average CV ± Standard Deviation)***

Another factor considered is the luminance level of the image. Figure 5-1 shows the relationship between the luminance of the reference white of an experimental phase and the average observer repeatability. There was no clear luminance dependency of the repeatability of colour appearance attribute judgements except for a slightly poorer repeatability for the colourfulness results at a low luminance level (Filter3-02 and Filter3-10 phases).

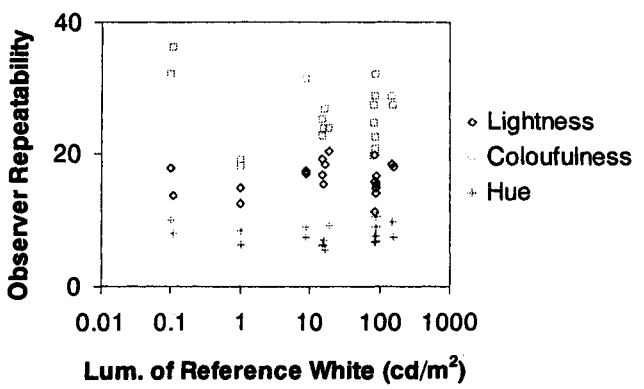


***Figure 5-1 Effect of luminance on observer repeatability***

### 5.2.2 Long Term Repeatability

A-Dark and Filter0-02 phases had the same experimental conditions with a time interval of three and half months between them. Both experiments were done in a dark room with the CRT monitor and had the same luminance of their reference white. Five observers attended both experiments and 27 colours were repeated.

| Attribute | Repeatability (CV) | O1 | O2 | O3 | O4 | O5 | Average |
|---|---|---|---|---|---|---|---|
| Lightness | A-Dark | 6.8 | 27.2 | 10.5 | 17.1 | 20.1 | 16.3 |
| | Filter0-02 | 10.7 | 27.3 | 9.0 | 23.2 | 17.2 | 17.5 |
| | A-Dark vs. F0-02 | 6.5 | 17.9 | 13.6 | 15.3 | 12.8 | 13.2 |
| Colourfulness | A-Dark | 14.0 | 23.4 | 20.0 | 24.1 | 18.3 | 20.0 |
| | Filter0-02 | 18.1 | 11.9 | 29.9 | 14.4 | 16.2 | 18.1 |
| | A-Dark vs. F0-02 | 13.0 | 16.6 | 20.8 | 44.4 | 39.6 | 26.9 |
| Hue | A-Dark | 3.2 | 9.2 | 5.6 | 4.7 | 4.0 | 5.3 |
| | Filter0-02 | 13.0 | 4.2 | 8.6 | 3.5 | 4.2 | 6.7 |
| | A-Dark vs. F0-02 | 8.3 | 4.9 | 6.3 | 3.7 | 7.3 | 6.1 |

***Table 5-2 Long term repeatability test results***

Table 5-2 compares the short- and long-term repeatability of each observer. The first and second rows of each attribute are CV values for 10 repeated colours and the third row is the CV value calculated using 27 repeated colours between the A-Dark and Filter0-02 phases. For lightness and hue, long term repeatability was similar to short term repeatability in general. Colourfulness was also similar between the short and long term tests except for two observers (O4 and O5) who showed very poor long term repeatability. In the case of these two observers, they attended the A-Dark experiment as their first experience of a magnitude estimation experiment. The other three observers had participated in most of the experiments, although they did not have any experience before the author's experiments. This result suggests that training (experience) might play an important role in improving the performance of observers in colour appearance scaling, especially for colourfulness.

### 5.2.3 Repeatability Comparison with Other Data Sets

The author's repeatability results were compared with those of other experiments. Table 5-3 shows the repeatability of the LUTCHI data. For the R-VL experiments [Luo1993a, Wang1994], colourfulness and hue were repeated for 6 phases. One phase of each of the LT and 35mm [Luo1993b, Wang1994] experiments were repeated and

used to calculate observer repeatability. Repeatability CV values of the LUTCHI data were nearly half those obtained in the present study.

| LUTCHI | Lightness | Colourfulness | Hue |
|---|---|---|---|
| R-VL | N/A | 12 | 3 |
| LT | 11 | 11 | 3 |
| 35mm | 7 | 11 | 3 |

*Table 5-3 Short term repeatability of LUTCHI data*

## 5.3 Accuracy of the Observers

Another measure to evaluate the performance of observers is the closeness of each individual result to the mean. The CV value between each observer's data and the average value is calculated. It is called the 'accuracy' of the observer. Good accuracy means that the specific observer's data is close to the mean data. Raw data was used for lightness and hue calculation, however the logarithmic value of raw colourfulness data was used based on the assumption that an individual's colourfulness scales are related to each other as a power transform (see Section 4.5.1.3 for more details).

| Group | Lightness | Colourfulness | Hue |
|---|---|---|---|
| P (Presentation) | 17.7 | 13.3 | 7.9 |
| M (Monitor) | 17.4 | 15.1 | 11.2 |
| C (Cinema) | 15.4 | 11.9 | 9.0 |
| A (Ambient) | 15.8 | 10.2 | 8.4 |
| F (Filters) | 19.7 | 19.4 | 10.7 |
| Average of 20 phases ± Standard Deviation | 17.8 ± 2.6 | 15.4 ± 5.2 | 9.8 ± 1.8 |

*Table 5-4 Accuracy of the observers*

Average accuracy values are summarised in Table 5-4. Accuracy of lightness and hue had values similar to their repeatability. It is not possible directly to compare with the colourfulness results since repeatability and accuracy were measured using different scales.

Figure 5-2 shows the results of the change in average accuracy according to luminance level. All attributes showed poorer accuracy under lower luminance levels. Note that the effect of luminance level on the observer's repeatability was not obvious. These results indicate that each observer's way of dealing with colour appearance

scaling under low luminance levels became more and more different to each other while they were using internally consistent scales. More analysis of the effect of luminance level will be given in Section 5.6.

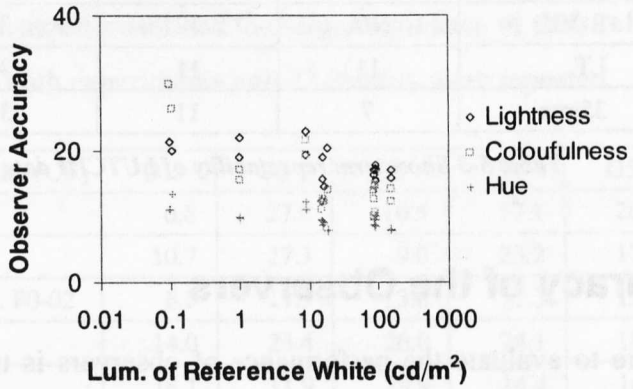


*Figure 5-2 Effect of luminance on observer accuracy*

### 5.3.1 Accuracy Comparison with Other Data Sets

The overall mean accuracy values of the LUTCHI and Juan&Luo data sets [Juan2000] are given in Table 5-5. Both data sets showed similar results with better performances than in the present study.

| | Phase | Lightness | Colourfulness | Hue |
|---|---|---|---|---|
| LUTCHI | R-HL,LL/CRT | 13 | 18 | 9 |
| | R-VL | 10 | 16 | 6 |
| | LT | 15 | 17 | 6 |
| | 35mm | 16 | 16 | 7 |
| Juan &Luo | Random Method | 13 | 18 | 7 |
| | Sorting Method | 11 | 16 | 6 |

*Table 5-5 Accuracy of the LUTCHI and Juan&Luo data sets*

One possible reason for the better repeatability and accuracy performances of the LUTCHI and Juan&Luo data sets are their training sessions. For those experiments, the training sessions were closer to educational sessions. The observers were taught the concepts of colour appearance attributes using Munsell and NCS systems before starting the experiments and also participated in a session of arranging colour chips in a two-dimensional space. This might have helped observers to have more consistent responses and also worked as a normalisation process between observers to give similar scale. Note that an educational session using colour order systems, e.g. Munsell or NCS, was not tried for the CII-Kwak data set since this process can bias

observers' responses to follow the Munsell or NCS scales rather than to repeat their own perceptions.

## 5.4 Effect of Experience on the Repeatability and Accuracy of Observers

In Section 5.2.2 it was suggested that having greater experience of colour appearance experiments might affect the repeatability performance. To find out the effect of experience, further analysis was performed using the author's experimental data set except for the Filter2 and Filter3 experiments since low luminance phases deteriorate the performances of observers in general.

There were five observers who attended more than five experimental groups among the six groups, namely groups P, M, C, A, Filter0 and Filter1. They did not necessarily attend all phases in a group. Three of them were observers O1, O2 and O3 in Table 5-2. The other two observers were designated as Oa and Ob. For those five observers, conducting the author's experiments was their first experience of colour appearance estimation. Each observer's repeatability and accuracy for each group in CV units were averaged and then inter-compared.

Figures 5-3, 5-4 and 5-5 show the change in repeatability and accuracy for lightness, colourfulness and hue respectively. The experimental groups on the $x$-axis are arranged according to the time sequence.

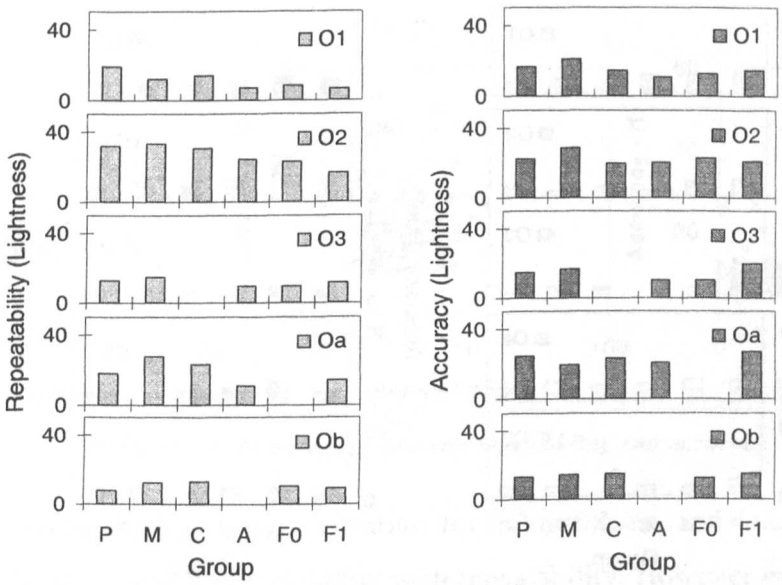


*Figure 5-3 Effect of experience on observer repeatability and accuracy for lightness*

In the case of lightness, most of the observers showed improvement of repeatability as time progressed, except for observers O3 and Ob, who showed constantly good performance throughout all the experiments. However this repeatability improvement did not directly affect their accuracy. A similar trend was found in the colourfulness result as shown in Figure 5-4. All of the observers showed improvement of repeatability but no change in accuracy except for observer Oa who did not show any improvement in repeatability or accuracy. Every observer showed slight improvements in repeatability for hue but no systematic change for accuracy.

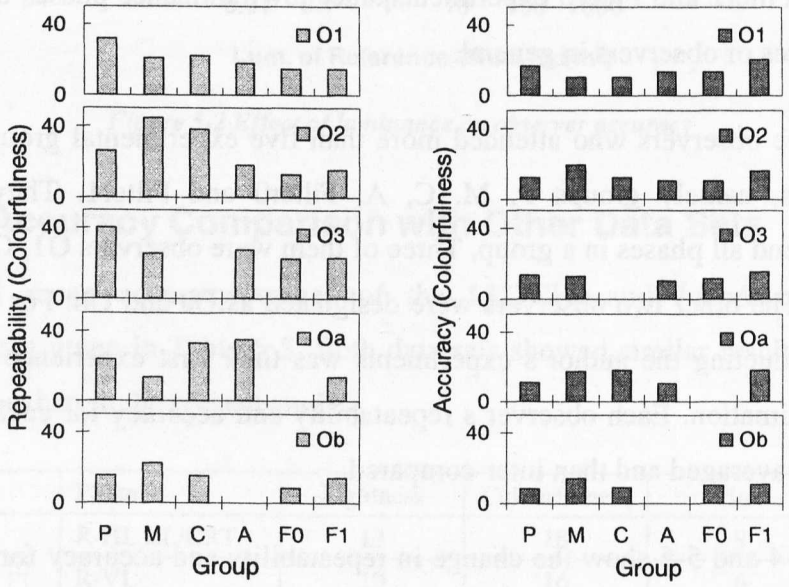


*Figure 5-4 Effect of experience on observer repeatability and accuracy for colourfulness*

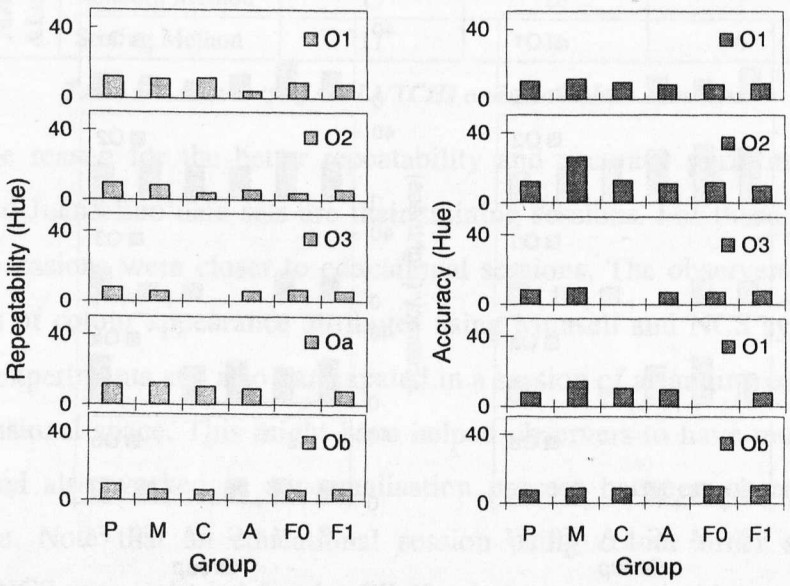


*Figure 5-5 Effect of experience on observer repeatability and accuracy for hue*

This analysis suggests that observers' repeatability might be improved by training to gain more experience. Attending more colour appearance experiments might help observers to make judgements more consistently, however the improvement in repeatability did not mean higher accuracy for the observers considered here. This also suggests that repeatability and accuracy are independent of each other.

## 5.5 Repeatability vs. Accuracy

It is not easy to define a reliable observer because there is no right or wrong answer for the observer responses (subject to them having a full understanding of experimental tasks). However repeatability and accuracy of the observers are good indices to represent their performances. An observer having a high repeatability and accuracy could be described as a reliable observer. This section investigates the relationship between repeatability and accuracy. We assume that an observer having a high repeatability will be more likely to represent the average responses of the group (high accuracy).

Each observer's repeatability and accuracy results are directly compared in Figure 5-6. In total, there are 251 data points for each attribute and the points are divided into two groups based on the luminance of the reference white of the phase. Twenty cd/m$^2$ is used as a dividing line between groups. Phase P-Filter, Group C, Filter1, Filter2 and Filter3 belong to the 'Low luminance' group and the others to the 'High luminance' group.

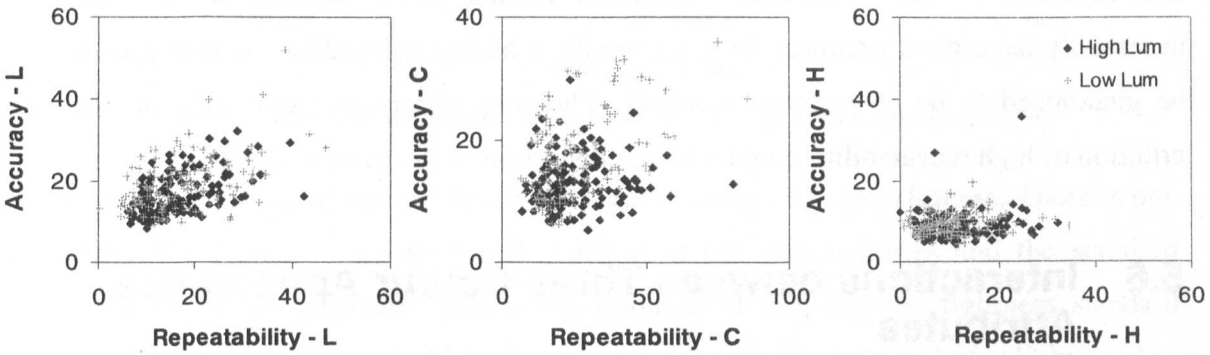


*Figure 5-6 Relationship between repeatability and accuracy*

In these figures, there is little correlation for colourfulness and hue while lightness shows a very weak positive correlation with repeatability. However even for lightness

the correlation does not seem obvious. The most significant effect of luminance level was on colourfulness. Lower luminance induced poorer colourfulness accuracy. Note that Figure 5-6 shows the same luminance effect described in Figure 5-2, in which the luminance level does affect the observer accuracy performance.

For numerical comparison, correlation coefficients between the CV values of accuracy and repeatability were calculated using Eq. ( 5-2 ) and the results are given in Table 5-6. The value of this coefficient ranges from 0, when there is no correlation, to ±1, when there is complete correlation.

$$r = \frac{N \cdot \Sigma x_i \cdot y_i - \Sigma x_i \cdot \Sigma y_i}{\left[N \cdot \Sigma x_i^2 - (\Sigma x_i)^2\right]^{1/2} \cdot \left[N \cdot \Sigma y_i^2 - (\Sigma y_i)^2\right]^{1/2}} \qquad (5\text{-}2)$$

where $N$ : Number of data points

$x_i$ : Accuracy

$y_i$ : Repeatability

| Accuracy / Repeatability | Lightness | | | Colourfulness | | | Hue | | |
|---|---|---|---|---|---|---|---|---|---|
| | All | High | Low | All | High | Low | All | High | Low |
| All | 0.487 | | | 0.299 | | | 0.262 | | |
| High Lum. | | 0.526 | | | 0.176 | | | 0.318 | |
| Low Lum. | | | 0.466 | | | 0.240 | | | 0.213 |

***Table 5-6 Correlation between repeatability and accuracy***

The numbers in Table 5-6 are close to 0 for colourfulness and hue and even for lightness they are only near 0.5, which implies that correlation between repeatability and accuracy is not significant. Observers having good repeatability do not necessarily have good accuracy. In other words, a highly repeatable observer cannot be guaranteed to be an accurate observer. Choosing observers based only on the criterion of high repeatability might result in distortion of the average data.

## 5.6 Interactions between Three Colour Appearance Attributes

Lightness, colourfulness and hue represent three dimensions of human colour vision. In this section, it is investigated whether there are any interactions between these three colour appearance attributes, i.e. whether observer judgements of one attribute are affected by the other two. Correlation of colour appearance attributes is tested by

plotting the relationship between the average and the standard deviation for each colour. There are a total of 775 data points per attribute. These points are again divided into two groups according to the luminance level: high and low. P-Filter, Group C, Filter1, 2 and 3 phases are in the 'Low Lum' category and the others are in 'High Lum'.

Figure 5-7 shows the relationship of the standard deviation of lightness with mean lightness, colourfulness and hue of each colour. The standard deviation of lightness is randomly distributed in all three diagrams showing the independence of the lightness judgement except at the two ends of lightness scale in the left diagram. Note that the ideal black and reference white were the anchor points of lightness judgement. Therefore nearly black or white colours were more easily estimated with smaller deviations. Another notable aspect is the luminance level dependency, which is also shown in the accuracy analysis. In general the low luminance group has a larger range of lightness deviation than that of high luminance group except for near yellow colours. This suggests that judging the lightness of a yellowish colour is easier than estimating the lightness of other hues under a low luminance level.

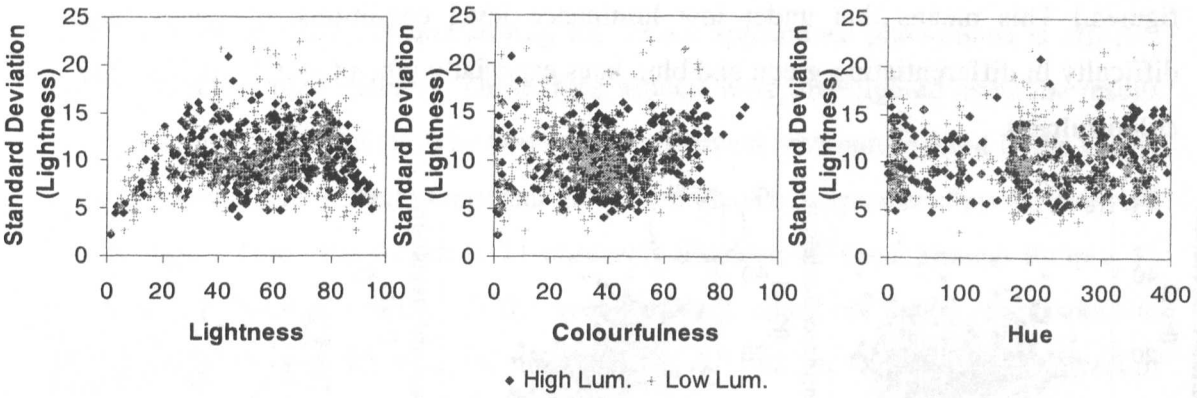


*Figure 5-7 Standard deviation of lightness vs. average colour appearance data*

Figure 5-8 shows the results for the standard deviation of colourfulness. There is one distinctive feature – the V-shaped distribution between lightness and the standard deviation of colourfulness. This is the opposite of lightness vs. lightness standard deviation. Near black and white colours are judged more consistently for lightness but with more variation for colourfulness. In other words the concept of colourfulness apparently became more controversial for observers in these areas. However colours with lightness less than 10 have smaller deviation since these colours were perceived

as nearly black. Colourfulness and hue do not affect the standard deviation of colourfulness in general except for low colourfulness colours, which show smaller deviations. Note that neutral grey was an anchor point for colourfulness judgement.

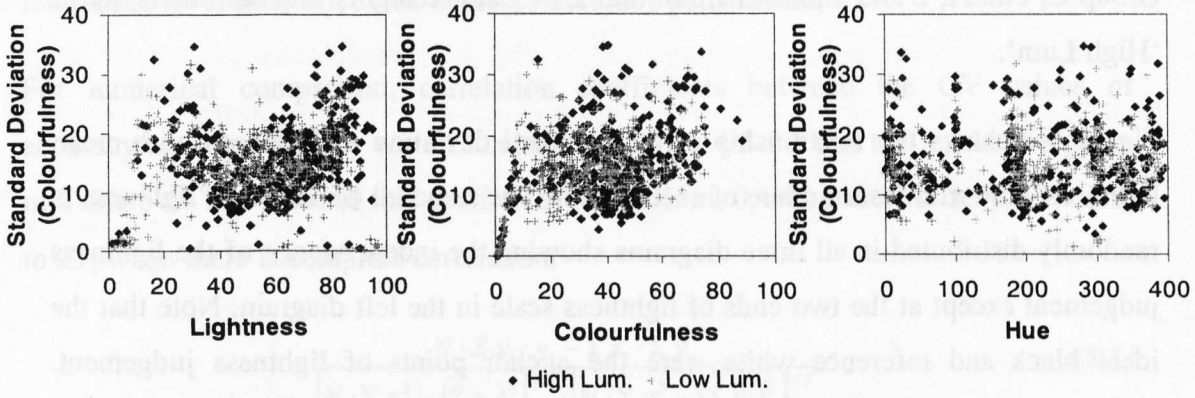


*Figure 5-8 Standard deviation of colourfulness vs. average colour appearance data*

Figure 5-9 illustrates for the standard deviation of hue. The first notable trend is a higher hue deviation for low colourfulness colours, which corresponds well to general experience. Also some colours show a larger variation under a low luminance level than at high luminance. These colours are very dark or very light with low colourfulness and belong to the green-blue hue area. (See circled points in the figures.) This means that under low luminance level conditions, observers have difficulty in differentiating green and blue hues especially when the colours have low colourfulness.

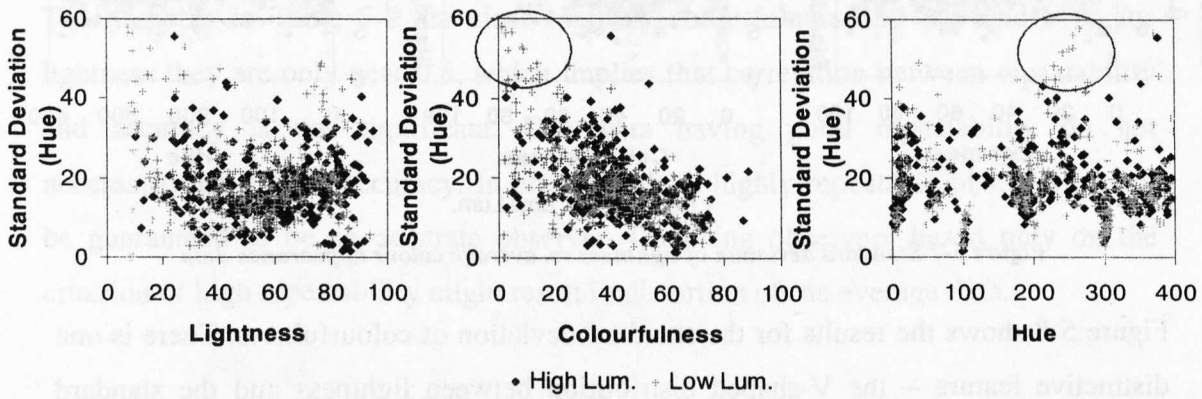


*Figure 5-9 Standard deviation of hue vs. average colour appearance data*

## 5.7 Effect of the Number of Observers

In psychophysical experiments, choosing observers means random sampling from the full human population who have normal colour vision. The average results ($\mu'$) of the

panel of observers should be distributed according to a Gaussian distribution with the mean ($\mu$) and standard deviation of those of the parent distribution and with the uncertainty ($\sigma_\mu$) of the estimated average as represented in Eq. ( 5-3 ):

$$\sigma_\mu \approx \frac{s}{\sqrt{N}} \qquad \begin{array}{l} s : \text{sample standard deviation} \\ N : \text{number of observation} \end{array} \qquad (5\text{-}3)$$

The equation shows that more observers would give more accurate mean results. Conventionally colour appearance experiments in the past have used 6 to 9 observers. An average of 11 observers participated in the author's study except in Group P experiments, which had 21 observers. It is always difficult to recruit a large number of observers who understand the concepts of colour appearance attributes, even though experimental experience is not needed.

Therefore it is important to understand how changing the number of observers will affect the final data. More specifically, three aspects of the effect of the number of observers are considered here. First is the variation of mean values for different subgroups with a certain number of observers against that of the parent group. Second is whether there is a systematic shift in the average data against the parent average. Third is how significantly quantifying the colour appearance phenomena is affected by the choice of the observers. These three aspects were investigated using the results of the Group P experiments. The twenty-one observers who participated in the Group P experiments were treated as a parent group and the subgroups were formed from the parent group. Note that the same 21 observers attended all three phases: P-Grey, P-Black and P-Filter. Even though the average of 21 observers cannot be assured to represent the true parent group, this analysis can still indicate the trend of the effect of number of observers.

For the analysis the average data of the subgroups were calculated and compared with that of the parent group. Linear scale data were used for all three attributes including colourfulness. Note that average colourfulness data of the groups are assumed to be linearly related to each other. Instead of examining all possible combinations, the subgroups with a specific number of observers were randomly chosen 30,000 times. Note that testing all combinations would involve too much work, i.e. 352,716 for 10 and 11 observers. The 30,000 groups randomly selected are considered to be a good

representation for the sampling strategy. Also these groups are large enough that each observer has a similar frequency of occurrence within the selected groups.

In the following sections, the results of the subgroups with 10 observers are shown because this has been the number of observers commonly used for other colour appearance studies.

### 5.7.1 Accuracy of Subgroups

Firstly, as a method of testing the deviation of the average of the subgroup from the parent group, CV values were calculated as in Eq. ( 5-4 ).

$$CV = 100\frac{\sqrt{\sum (x_i - y_i)^2 / n}}{\bar{y}}, \qquad (5\text{-}4)$$

$n$ : Number of test colours

$x_i$ : Average estimation of group of $i^{th}$ colour

$y_i$ : Average estimation of parent group of $i^{th}$ colour

$\bar{y}$ : The mean value of the estimations of parent group

Note that this calculation becomes the accuracy of the individual observers when the subgroups have 1 observer. Therefore this test was named as the accuracy of the subgroups.

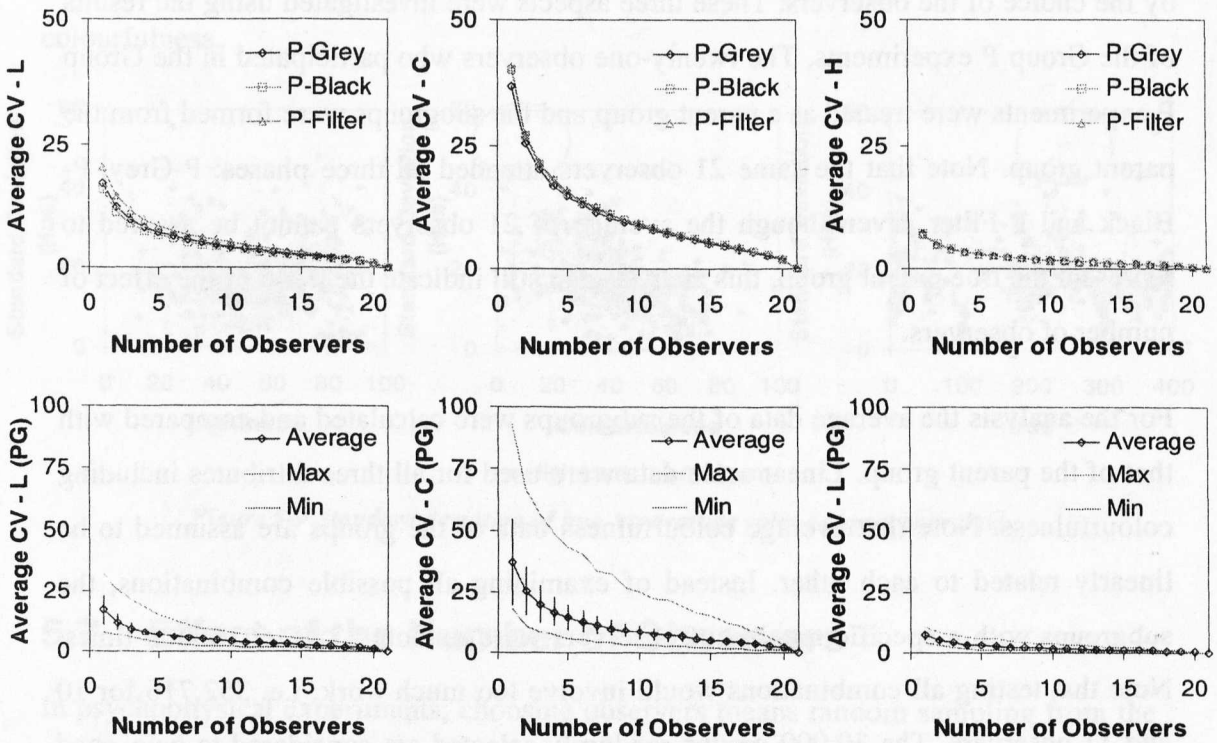


*Figure 5-10 Accuracy change of the subgroups by the number of observers*

The top three diagrams in Figure 5-10 show the changes of the average CV values by the number of observers. Colourfulness shows the largest change as the number of observers in a group is reduced, followed by lightness and hue. All three attributes show the same trend as described in Eq. ( 5-3 ) but with a rapid reduction towards the 21 observers since this test assumes those 21 observers as a parent group. The three diagrams in the second row of Figure 5-10 represent the average CV values of the phase P-Grey with the standard deviations shown with error bars. Also the maximum and minimum CVs of 30,000 trials are shown by the top and bottom thin lines respectively. These diagrams indicate that the subgroups cover the broad bands of CV values. However in the case of the subgroups with more than 10 observers, even the worst group had similar accuracy as the best performance of the individual observer for all three attributes. Numerical values of the CVs of the P-Grey phase shown in Figure 5-10 are summarised in Table 5-7.

| P-Grey | Lightness | | | Colourfulness | | | Hue | | |
|---|---|---|---|---|---|---|---|---|---|
| CV | Min | Avg | Max | Min | Avg | Max | Min | Avg | Max |
| 1 | 8.30 | 17.06 | 32.05 | 18.14 | 36.96 | 93.07 | 4.26 | 7.06 | 10.96 |
| 5 | 3.66 | 7.08 | 15.12 | 5.53 | 14.61 | 42.92 | 1.22 | 2.86 | 5.80 |
| 10 | 1.80 | 4.15 | 7.88 | 3.29 | 8.53 | 24.76 | 0.67 | 1.68 | 3.45 |
| 15 | 1.31 | 2.50 | 5.13 | 1.94 | 5.14 | 15.88 | 0.45 | 1.01 | 2.05 |
| 20 | 0.41 | 0.85 | 1.60 | 0.94 | 1.78 | 3.16 | 0.21 | 0.35 | 0.55 |

*Table 5-7 Accuracy of the subgroups (P-Grey)*

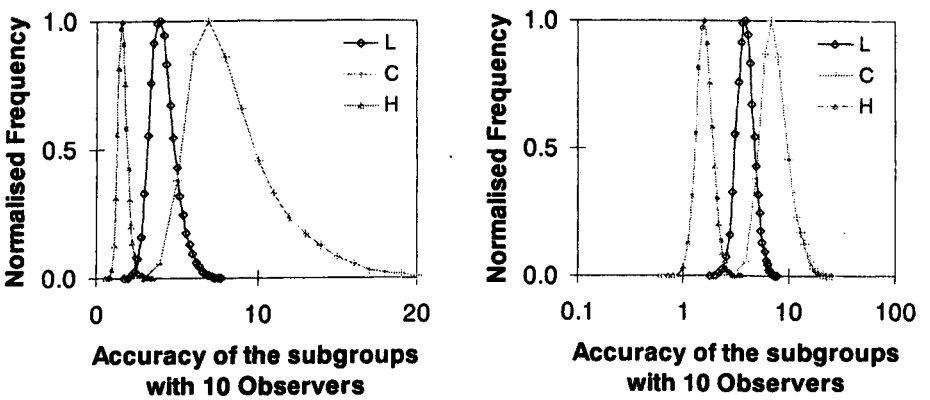


*Figure 5-11 Distribution of subgroup accuracy for the group with 10 observers*

Note that there is a larger difference between average and maximum values than between average and minimum in the diagrams in the second row of Figure 5-10, implying a skewed distribution of CV values with a long tail towards the maximum value. Figure 5-11 shows the distribution of normalised frequency against the

accuracy of a subgroup with 10 observers. The left diagram is the distribution in a linear scale for the $x$-axis whilst the right diagram has a log scale. These diagrams clearly show that all three attributes have log-normal distributions of subgroup accuracy.

### 5.7.2 Affecting Average Results by Observer Sampling

CV values are used as a standard measure to show how different two data sets are, however they cannot show whether large values are caused by the scattering of data or by some systematic change. Note that a systematic change of data is a more significant problem than a large variation for quantifying colour appearance.

It was therefore investigated as to whether there is any systematic drift of the average by the observer sampling. The least squares fitting to the straight line passing through the origin was performed between the average of the parent group and that of a subgroup for the lightness and colourfulness data. The results should show a linear relationship between two data sets. No fitting was done for hue data; the hue scale (0-400) has a circular characteristic therefore linear fitting cannot be used to predict hue shift.

The gradient between the average of the subgroup and that of the parent group was calculated for each phase. If there is no shift of the data, the gradient will be near 1. For lightness fitting, the linear equation is constrained to pass through (100,100) because the reference white is fixed at 100 for both data sets. In the case of colourfulness the straight line was adjusted to pass through the origin of the graph since neutral grey was the anchor point for colourfulness assessment. Equations of the straight line used for the least squares fitting are given in Eq. ( 5-5 ):

$$\text{Lightness} \quad y = b_L \cdot x + 100 \cdot (1 - b) \quad \text{where} \quad b_L = \frac{\Sigma x_i y_i - 100 \cdot \Sigma x_i - 100 \cdot \Sigma y_i + \Sigma 100^2}{\Sigma x_i^2 - 200 \cdot \Sigma x_i + \Sigma 100^2}$$

$$\text{Colourfulness} \quad y = b_C \cdot x \quad \text{where} \quad b_C = \frac{\Sigma x_i y_i}{\Sigma x_i^2} \qquad (5\text{-}5)$$

Table 5-8 summarises the gradient $b_L$ and $b_C$ of subgroups of Phase P-Grey. These data are plotted in Figure 5-12, which shows the average gradients of the subgroups with their standard deviations against the number of observers. Maximum and minimum values are also plotted.

| P-Grey | Lightness ($b_L$) | | | Colourfulness ($b_C$) | | |
|---|---|---|---|---|---|---|
| No. of Obs. | Min | Average | Max | Min | Average | Max |
| 1 | 0.771 | 0.954 | 1.117 | 0.548 | 0.942 | 1.476 |
| 5 | 0.893 | 0.993 | 1.131 | 0.733 | 0.989 | 1.332 |
| 10 | 0.922 | 0.998 | 1.079 | 0.822 | 0.997 | 1.195 |
| 15 | 0.952 | 0.999 | 1.042 | 0.888 | 0.999 | 1.108 |
| 20 | 0.992 | 1.000 | 1.012 | 0.976 | 1.000 | 1.023 |

*Table 5-8 Gradient of the subgroups compared to the parent group (P-Grey)*

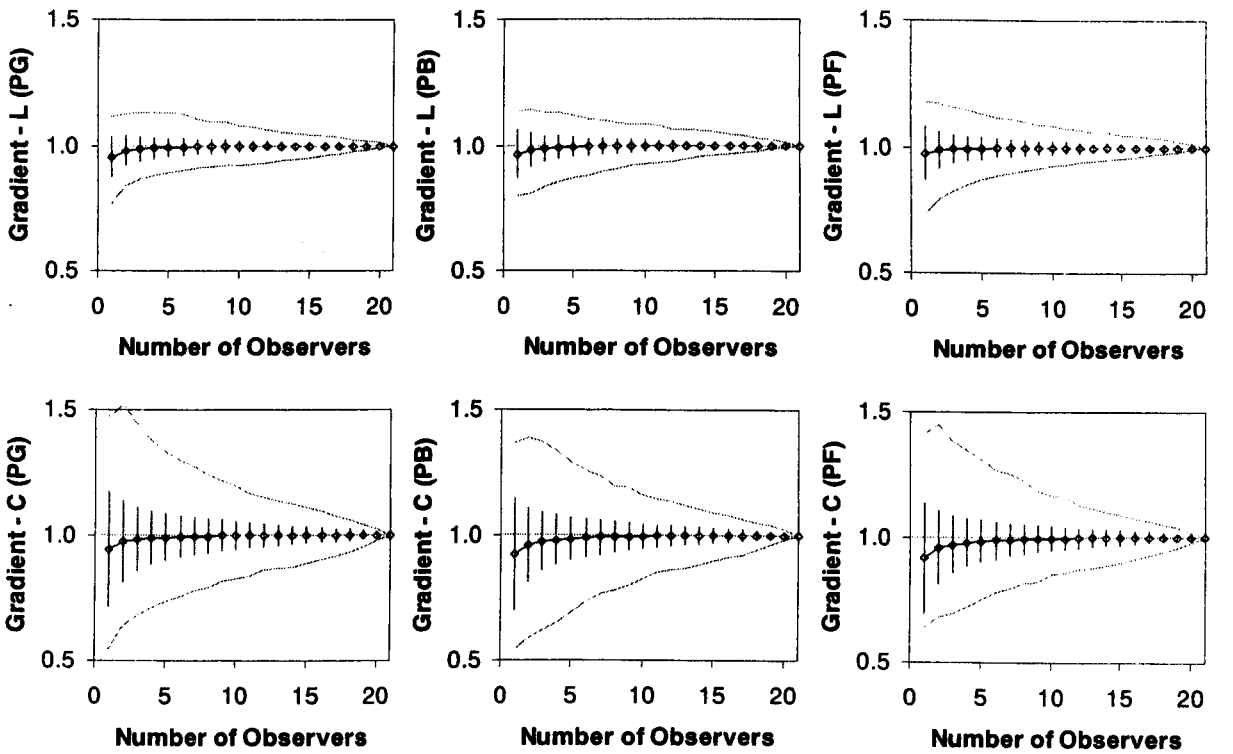


*Figure 5-12 Gradient of the subgroups compared to the parent group*

The average gradients of the subgroups show that there is little average shift for those subgroups having more than 10 observers for both lightness and colourfulness. However colourfulness shows a large standard deviation, implying that the colourfulness result would be more likely to be affected by the number of observers. For groups of fewer than 5 observers, the gradients are less than 1, i.e. the mean would be less than that for the large population.

The difference between the effects of the number of observers on lightness and colourfulness is shown as a frequency distribution of the gradients in Figure 5-13. This graph is for Phase P-Grey and the numbers of the subgroups within 0.01 gradient range were counted. Both lightness and colourfulness had Gaussian-like distributions

but the bandwidth of the colourfulness distribution was more than double that of lightness.

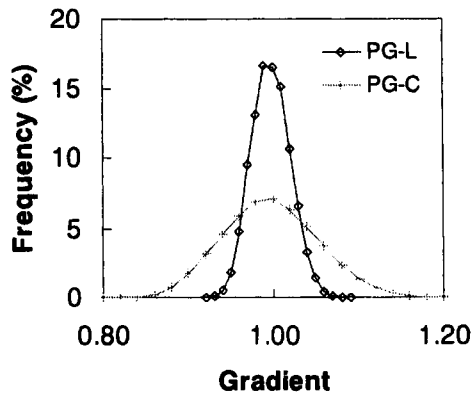


*Figure 5-13 Distribution of gradients of the subgroups with 10 observers (P-Grey)*

### 5.7.3 Affecting Colour Appearance Phenomena by Observer Sampling

Comparing the data between the P-Grey and P-Filter phases will show the effect of the luminance level on colour appearance, whereas comparing the P-Grey and P-Black phases will investigate the effect of the background luminance factor. More details will be discussed in Chapter 6. In this section, the gradients between the data of two phases, P-Grey vs. P-Filter and P-Grey vs. P-Black are calculated for each subgroup and compared with those of the parent group. The changes of gradients show whether the degree of colour appearance changes could vary according to the subgroups chosen. Eq. ( 5-5 ) was used for the calculations of gradients of lightness and colourfulness.

The effect of luminance level is summarised in Table 5-9 and the effect of background luminance factor is given in Table 5-10. The numbers show the quantity of the colour appearance phenomena in terms of gradients as depicted in Figure 5-14. The results show that the average gradients for the subgroups with more than 10 observers are not affected in either case but the distribution is broader than those in Figure 5-12, which shows the shift of the average data of a subgroup. This suggests that quantifying colour appearance phenomena will be more greatly affected by observer numbers. Also, these figures warn that if the effect is minor, it is possible to show the opposite phenomenon depending on the observer group. For example the gradients of lightness change between P-Grey and P-Black for the groups with 10

observers range from 0.86 (min) to 1.13 (max). Some subgroups of observers will see colours on the grey background as lighter (gradient > 1) while other subgroups see the opposite (gradient <1).

| PG/PF | Lightness ($b_L$) | | | Colourfulness ($b_C$) | | |
|---|---|---|---|---|---|---|
| No. of Obs. | Min | Average | Max | Min | Average | Max |
| 1 | 0.596 | 0.848 | 1.044 | 0.809 | 1.097 | 2.268 |
| 5 | 0.711 | 0.856 | 1.002 | 0.895 | 1.117 | 1.448 |
| 10 | 0.765 | 0.858 | 0.954 | 0.954 | 1.121 | 1.308 |
| 15 | 0.809 | 0.858 | 0.918 | 1.023 | 1.123 | 1.219 |
| 20 | 0.850 | 0.858 | 0.873 | 1.084 | 1.123 | 1.137 |

***Table 5-9 Impact of number of observers on the effect of luminance level***

| PG/PB | Lightness ($b_L$) | | | Colourfulness ($b_C$) | | |
|---|---|---|---|---|---|---|
| No. of Obs. | Min | Average | Max | Min | Average | Max |
| 1 | 0.491 | 0.946 | 1.205 | 0.650 | 1.090 | 2.445 |
| 5 | 0.745 | 0.997 | 1.196 | 0.854 | 1.100 | 1.506 |
| 10 | 0.859 | 1.005 | 1.132 | 0.935 | 1.103 | 1.301 |
| 15 | 0.924 | 1.008 | 1.082 | 0.984 | 1.104 | 1.210 |
| 20 | 0.990 | 1.009 | 1.027 | 1.061 | 1.105 | 1.128 |

***Table 5-10 Impact of number of observers on the effect of background luminance factor***

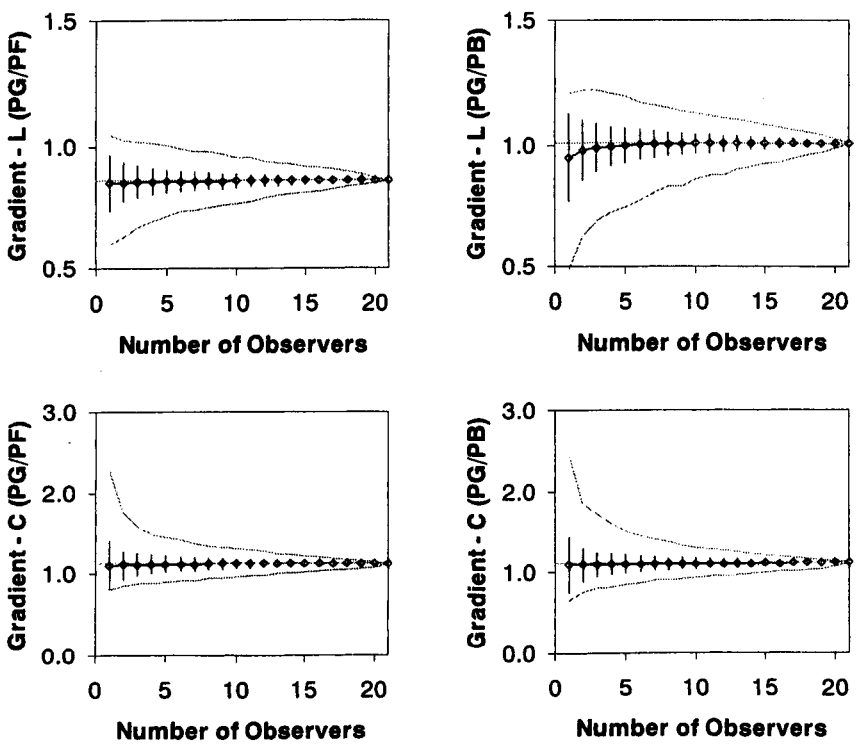


***Figure 5-14 Effect of number of observers on the colour appearance phenomena***

## 5.8 Comparison of the Observer Responses between Independent Experiments

In Section 5.7 the change of colour appearance results caused by the observer sampling among a confined observer population was investigated. In this section the observer response differences are investigated between independent experiments using the same test colours.

### 5.8.1 Repetition of the Same Experiment (A-Dark vs. F0-02)

Firstly, the colour appearance data of Phase A-Dark and Filter0-02 were directly compared, since both phases had the same experimental conditions with 27 common test colours. Eleven observers took part in the A-Dark experiment and 12 participated in Filter0-02. Five of them took part in both experiments. Note that the data of these five observers were also used to test long term repeatability in Section 5.2.2.

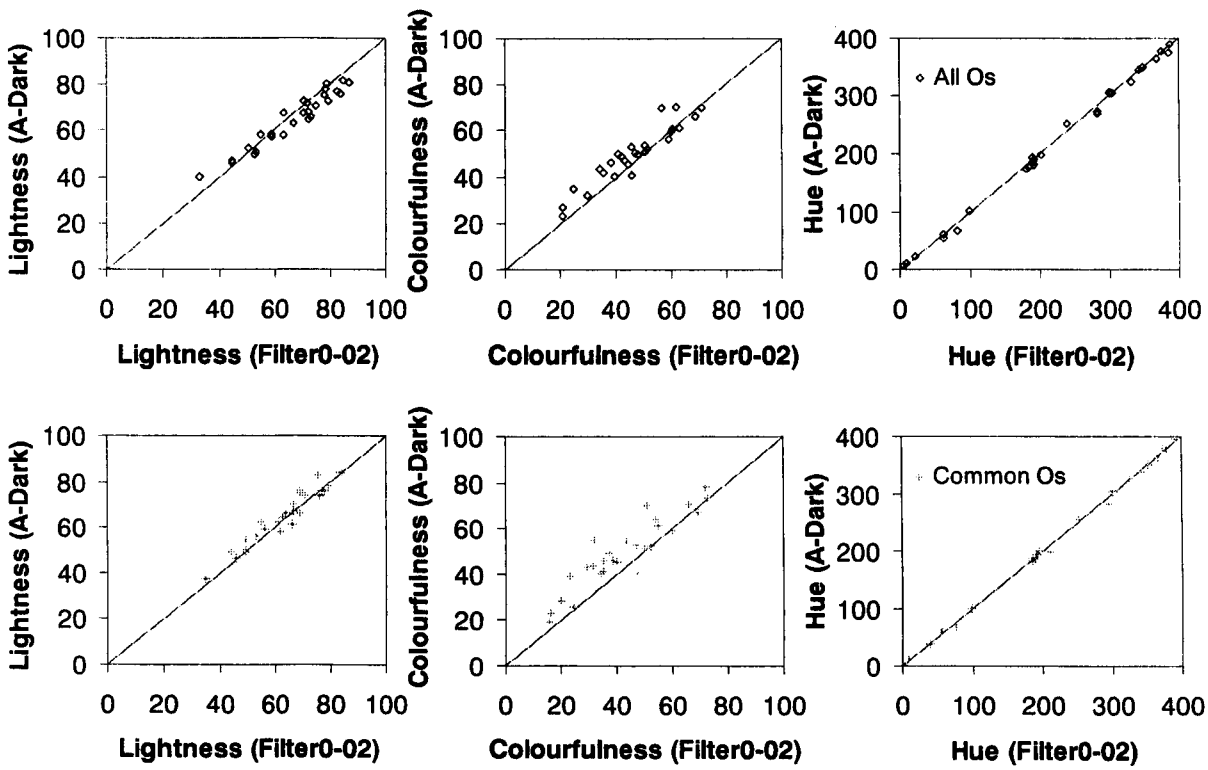


*Figure 5-15 Colour Appearance Comparison between A-Dark and Filter0-02 phases*

Figure 5-15 shows the comparison between the two experiments. The three diagrams in the top row are the results of all the observers and three diagrams in the bottom row are from the five common observers who did both experiments. The hue results (the two right diagrams) show no differences between the two experiments nor between

the two observer groups. For lightness (left diagrams), there is a slight shift for both diagrams but the difference is smaller for the common observers. The most significant difference is found in the colourfulness result (middle diagrams). The A-Dark experiment has higher colourfulness regardless of observer group. Lightness and colourfulness shifts between the two experimental phases, especially for the common observers, indicate how much colour appearance data can be changed by repetition.

Table 5-11 summarises the CV values and gradients of the diagrams shown in Figure 5-15. Both the CVs and gradients in the table are within the boundaries of the CV values and gradients between subgroups with around 10 observers and the parent group for the P-Grey experiment shown in Table 5-7 and Table 5-8.

| A-Dark vs. F0-02 | | Lightness | Colourfulness | Hue |
|---|---|---|---|---|
| All Observers | CV | 7.0 | 11.7 | 3.2 |
| | Gradient | 1.03 | 1.06 | N/A |
| Common Observers | CV | 5.5 | 19.2 | 2.5 |
| | Gradient | 0.96 | 1.12 | N/A |

***Table 5-11 Colour Appearance Comparison between A-Dark and Filter0-02***

## 5.8.2 Repetition of the LUTCHI 35mm Experiment

As mentioned in Section 4.3.3, Phase C-35mm in the Group C experiment used the same slides as the original LUTCHI 35mm experiments. Table 5-12 compares the experimental conditions between the LUTCHI and C-35mm experiments. They had same conditions except for luminance levels. It was found that the CIELAB colour differences between the new measurement data and the LUTCHI 35-mm data were quite small, with an average of 3.5 $\Delta E^*_{ab}$ in spite of 10 years' interval between these two experiments and using different slide projectors and screens. Note also that different colour measurement instruments were used.

| | Name | Mode | Device | CCT | Ref. White $L_w$ (cd/m$^2$) | Background $Y_b$ (%) | No. of Observers | No. of Samples |
|---|---|---|---|---|---|---|---|---|
| C | C-35mm | Dark | 35mm slide Projector | 3900 K | 15.42 | 20.38 | 11 | 40+10 |
| LUTCHI | Phase 1,4 | Dark | 35mm slide Projector | 4000 K | 113 | 19 | 6 | 40 |
| | Phase 3 | Dark | 35mm slide Projector | 4000 K | 45 | 19 | 6 | 40 |

***Table 5-12 Experimental Phases Comparison between LUTCHI 35mm and C-35mm***

To relate colour appearance results between the two experiments, lightness and hue results were directly compared. However direct comparison of visual colourfulness data was impossible between C-35mm and LUTCHI data because they had different luminance levels for the reference white and did not have the same reference colourfulness values. Therefore only the linearity of the two colourfulness data sets could be tested by scaling the colourfulness results of LUTCHI data using a single factor to have the same scale as the C-35mm data. Scaling factors were 1.006 for Phase 1, 1.047 for Phase 4 and 1.076 for Phase 3. Ideally, Phase 1 and Phase 4 would have the same scaling values since these two experiments had exactly the same experimental conditions. Different scaling values for Phase 1 and Phase 4 indicate the errors caused by repetition, as shown by the analysis in the previous section.

Figure 5-16 and Table 5-13 show that the two sets of experimental results agree with each other well. It is quite remarkable since these two experiments were conducted independently by different experimenters and by different groups of observers. This result strongly implies the stability of the psychophysical experiment using the magnitude estimation technique.

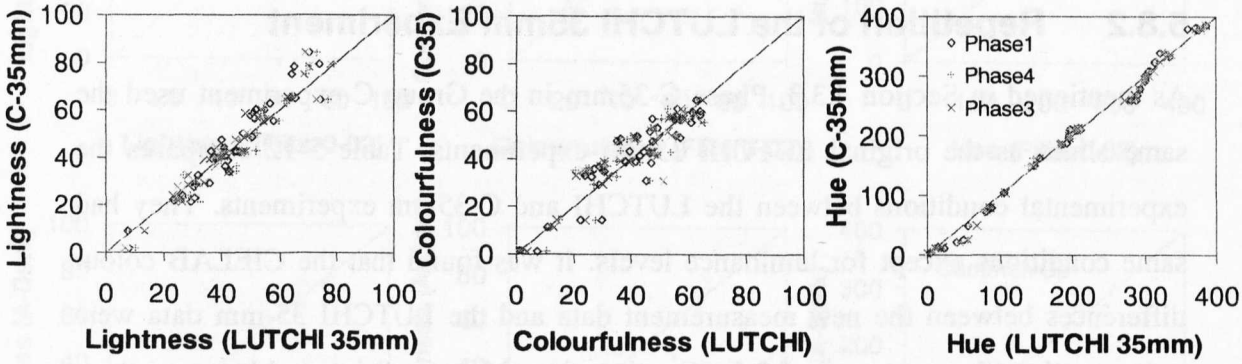


*Figure 5-16 LUTCHI 35mm vs. C-35mm phases*

| LUTCHI vs. C-35mm CV (Gradient) | Lightness | Colourfulness | Hue |
|---|---|---|---|
| Phase1 vs. C-35mm | 13.0 (0.997) | 15.9 | 5.2 |
| Phase4 vs. C-35mm | 12.3 (1.026) | 17.3 | 5.3 |
| Phase3 vs. C-35mm | 11.6 (0.986) | 16.0 | 5.0 |

*Table 5-13 CV values between LUTCHI 35mm and C-35mm experiments*

## 5.9 Conclusions on Observer Performance

A reliable colour appearance data set is essential for the development of a colour appearance model. Like any other area of science, proper sampling is needed to achieve more accurate results. In particular, colour appearance data obtained using psychophysical techniques are much noisier than other physical measurements. Therefore understanding the characteristics of the observers' responses is necessary before applying these data to develop colour appearance models. In this chapter the performances of observers were investigated from different aspects.

Firstly the stability of the observer responses (repeatability) and the diversity between observers (accuracy) were investigated. No strong correlation between the observer repeatability and accuracy was found implying that selecting only 'reliable' observers to improve repeatability or accuracy would distort the average data and shift the results.

Comparing the two independent studies showed quite good agreement especially for lightness and hue. Good long term repeatability of the observers supports the reliability of the magnitude estimation data, however analysis of the effects of the number of observers showed high probability of disagreement between subgroups. Poor agreements for colourfulness judgements between independent groups should not be ignored.

The best way to overcome the large variations between data sets is to collect as much colour appearance data as possible by independent research groups and to investigate whether a particular colour appearance phenomenon found in one research study is repeatedly observed in other studies. This process is especially important to quantify colour appearance phenomena. In this present study, therefore, more focus is given to determining the trend of colour appearance change than best fitting the results to minimise errors.

# Chapter 6
# Colour Appearance Phenomena

## 6.1 Introduction

In this chapter, the colour appearance data sets accumulated by the author (CII-Kwak) and the LUTCHI data are analysed to reveal colour appearance phenomena. Data analysis results of the LUTCHI data have already been published in several papers (see Section 2.6.1) but some results are shown here again to compare with those of the CII-Kwak data. Table 6-1 shows a summary of the experimental phases used in this chapter.

| | Group | Device | No. of Phases | Light Source (CCT) | Ref. White ($cd/m^2$) | Back-ground | No. of Observers | No. of Colours | No. of Estimations |
|---|---|---|---|---|---|---|---|---|---|
| CII-Kwak | P (Presentation) | Projector | 3 | 7200 K | 19, 154 | Grey Black | 21 | 32 | 6,048 |
| | M (Monitor) | LCD Monitor | 3 | 7200 K | ~ 90 | White Grey Black | 11 or 12 | 40 | 4,200 |
| | C (Cinema) | Projector | 4 | 7200 3900 K | ~ 16 | | 9 or 11 | 40 | 4,800 |
| | A (Ambient) | CRT Monitor | 2 | 7200 K | ~ 86 | Grey | 11 | 40 | 2,640 |
| | F (Filters) | CRT Monitor | 8 | 7200 K | 0.1 ~ 88 | Grey | 10 ~ 12 | 40 | 10,920 |
| LUTCHI | R-HL | Viewing Booth | 6 | D50, D65, WF, A | ~ 250 | White Grey Black | 6 or 7 | ~100 | 11,970 |
| | R-LL | Viewing Booth | 6 | | ~ 40 | | | | 11,970 |
| | CRT | CRT Monitor | 11 | | ~ 40,20 | | | | 19,390 |
| | 35mm | Projector | 6 | 4000 K | 47~113 | Grey | 5 or 6 | ~ 99 | 9,093 |
| | R-VL | Viewing Booth | 6 | 5000 K | 0.4~843 | Grey | 4 | 40 | 5,760 |

*Table 6-1 Summary of experimental phases used to analyse colour appearance phenomena*

Details of the CII-Kwak data sets were introduced in Chapter 4 and a full list containing details of the phases in Table 6-1 is given in Appendix 1. The LUTCHI data can be accessed from the web site http://colour.derby.ac.uk/colour/info/lutchi/ and the CII-Kwak data are shown in Appendix 4.

This chapter investigates the change of colour appearance (lightness, colourfulness and hue) caused by different (1) media, (2) luminance levels, (3) luminance factors of the backgrounds, (4) surround conditions, and (5) sizes of colour stimulus. Finally colour appearance change under (6) mesopic vision is also investigated. Mainly qualitative comparisons have been performed by providing various diagrams. Colour appearance phenomena found in this chapter will be modelled in Chapter 8.

## 6.2 Media Dependency of Colour Appearances

The first analysis was to test whether colour appearance has an objective characteristic purely depending on the spectral distribution of a test colour or whether it changes according to which imaging device is used to display the colour. To test this so called media dependency of colour appearance, several colour appearance data sets accumulated using different devices but with the same viewing conditions were compared. Table 6-2 shows the experimental phases used in this analysis. The P-Grey, M-Grey and Filter0-02 experiments were performed using an LCD projector, an LCD monitor and a CRT monitor respectively to display colours but the displayed patterns were all the same with similar luminances for their reference white. All experiments were conducted in a dark room.

| | Name | Mode | Device | CCT | Ref. White $L_w$ (cd/m$^2$) | Background $Y_b$ (%) | Ref. C (40) CIELAB $C^*$ |
|---|---|---|---|---|---|---|---|
| P | P-Grey | Dark Room | LCD Projector | 7200 K | 154.0 | 18.34 | 54.2 |
| M | M-Grey | Dark Room | LCD monitor | 7200 K | 90.33 | 20.65 | 54.7 |
| F | Filter0-02 | Dark Room | CRT Monitor | 6800 K | 87.37 | 19.76 | 33.5 |

***Table 6-2 Experimental phases used to test media dependency of colour appearance***

As described in Section 4.3.2, the M-Grey experiment was designed to compare the colour appearance of LCD monitor colours with projected colours collected in the P-Grey experiment. The reference white and reference colourfulness patches of Phase

M-Grey were adjusted to have same chromaticities as those of Phase P-Grey. Note that this was a metameric match between the two experiments for the 2° CIE standard observer. Filter0-02 was also chosen for this analysis since it has similar setting to M-Grey but uses a different device, i.e. a CRT monitor, to display test colours.

Since each experimental phase employed an independent set of test colours, an indirect comparison method was developed to compare the colour appearances of P-Grey, M-Grey and Filter0-02, i.e. comparing the predictions of the CIELAB model with visual data. CIELAB $L^*$, $C^*$ and $h$ were used to compare with visual lightness, colourfulness and hue respectively.

Lightness comparison results are shown in Figure 6–1. The visual lightness of the test colours of the three phases are plotted on the same diagram against the CIELAB $L^*$ values. For a good agreement, data points should show similar trends. The left diagram in Figure 6–1 shows the lightness comparison between the LCD projector and LCD monitor colours. The middle and right diagrams are for LCD projector vs. CRT monitor and LCD monitor vs. CRT monitor respectively. The diagrams do not show any distinctive difference between them, although the P-Grey phase had slightly higher luminance level. The results show that similar visual lightness perceptions will be evoked as long as the same stimuli are shown to the observers regardless of which display is used to make test colours.

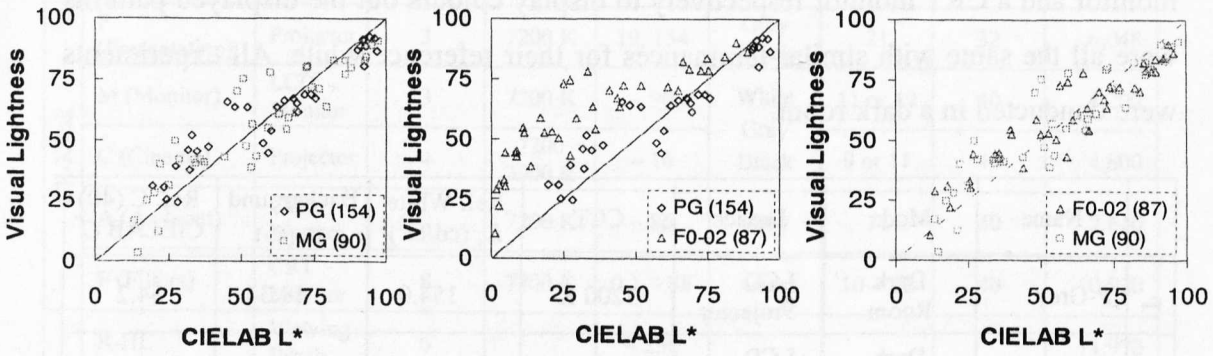


***Figure 6–1 Media dependency of lightness***

P-Grey and M-Grey did not have the same reference white luminances but used reference colourfulness patches with similar CIELAB $C^*$ values. Therefore their visual colourfulness should be similar to each other if there is no media dependency. Also their visual hue should be similar since the same chromaticity of white was set for both cases. The media independence of visual colourfulness and hue is confirmed

in Figure 6–2 by comparing the relationship of CIELAB $C^*$ vs. visual colourfulness and CIELAB hue angle vs. visual hue between P-Grey and M-Grey. F0-02 phase was not used in the colourfulness and hue analysis because of a different reference colourfulness and different chromaticity of the reference white from P-Grey and M-Grey phases.

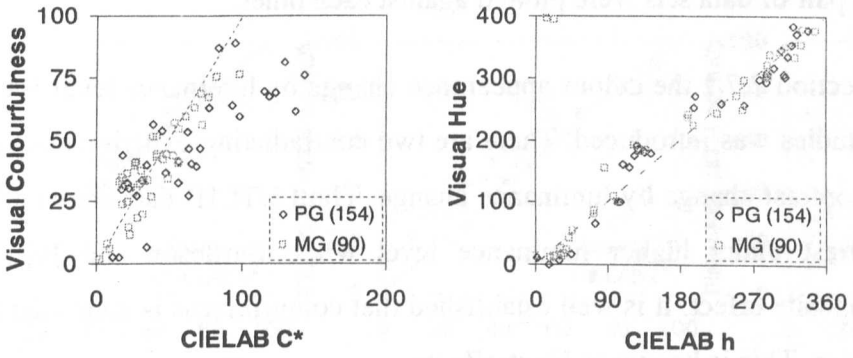


*Figure 6–2 Media dependency of colourfulness and hue*

## 6.3 Effect of Luminance Level

The luminance level of an image is one of the important factors affecting its colour appearance. Two colour appearance data sets having the same test colours and reference white (in terms of chromaticity) at different luminance levels were directly compared. Table 6-3 shows the pairs of data sets used for direct comparison. Visual results of each pair of data sets were plotted against each other.

Note that in Section 2.7.1 the colour appearance change by luminance level found in the previous studies was introduced. There are two contradicting experimental results for lightness contrast change by luminance change. The LUTCHI data showed lower lightness contrast under higher luminance level while Bartleson and Breneman showed the opposite effect. It is well established that colourfulness is increased under higher luminance. This is known as Hunt effect.

| | | | High Luminance | | Low Luminance | |
|---|---|---|---|---|---|---|
| | | | Name | $Y_L$ (cd/m$^2$) | Name | $Y_L$ (cd/m$^2$) |
| Dark Surround | CII-Kwak | 1 | P-Grey | 154.0 | P-Filter | 18.77 |
| | | 2 | Filter0-02 | 87.37 | Filter1-02 | 8.856 |
| | | 3 | Filter0-02 | 87.37 | Filter2-02 | 1.007 |
| | | 4 | Filter0-02 | 87.37 | Filter3-02 | 0.097 |
| | | 5 | Filter0-10 | 87.37 | Filter1-10 | 8.856 |
| | | 6 | Filter0-10 | 87.37 | Filter2-10 | 1.007 |
| | | 7 | Filter0-10 | 87.37 | Filter3-10 | 0.097 |
| | LUTCHI | 8 | 35mm Phase 1 | 113 | 35mm Phase 3 | 47 |
| | | 9 | 35mm Phase 4 | 113 | 35mm Phase 3 | 47 |
| Average Surround | | 10 | R-HL 1 | 264 | R-LL 1 | 44 |
| | | 11 | R-HL 2 | 252 | R-LL 2 | 42 |
| | | 12 | R-HL 3 | 252 | R-LL 3 | 42 |
| | | 13 | R-HL 4 | 243 | R-LL 4 | 40.5 |
| | | 14 | R-HL 5 | 252 | R-LL 5 | 42 |
| | | 15 | R-HL 6 | 232 | R-LL 6 | 42 |
| | | 16 | R-VL 1 | 843 | R-VL 2 | 200 |
| | | 17 | R-VL 1 | 843 | R-VL 3 | 62 |
| | | 18 | R-VL 1 | 843 | R-VL 4 | 17 |
| | | 19 | R-VL 1 | 843 | R-VL 5 | 6 |
| | | 20 | R-VL 1 | 843 | R-VL 6 | 0.4 |

*Table 6-3 Comparison pairs for the effect of luminance level*

### 6.3.1 Lightness Change by Luminance Level

Figure 6–3 shows the comparison of lightness for dark surround and Figure 6–4 for average surround. CIELAB $L^*$ is also included for reference. In all diagrams, CIELAB $L^*$ values are mostly located on the 45° lines showing that lightness change is not caused by the measurement differences. Note that CIELAB does not compensate for colour appearance change by luminance level.

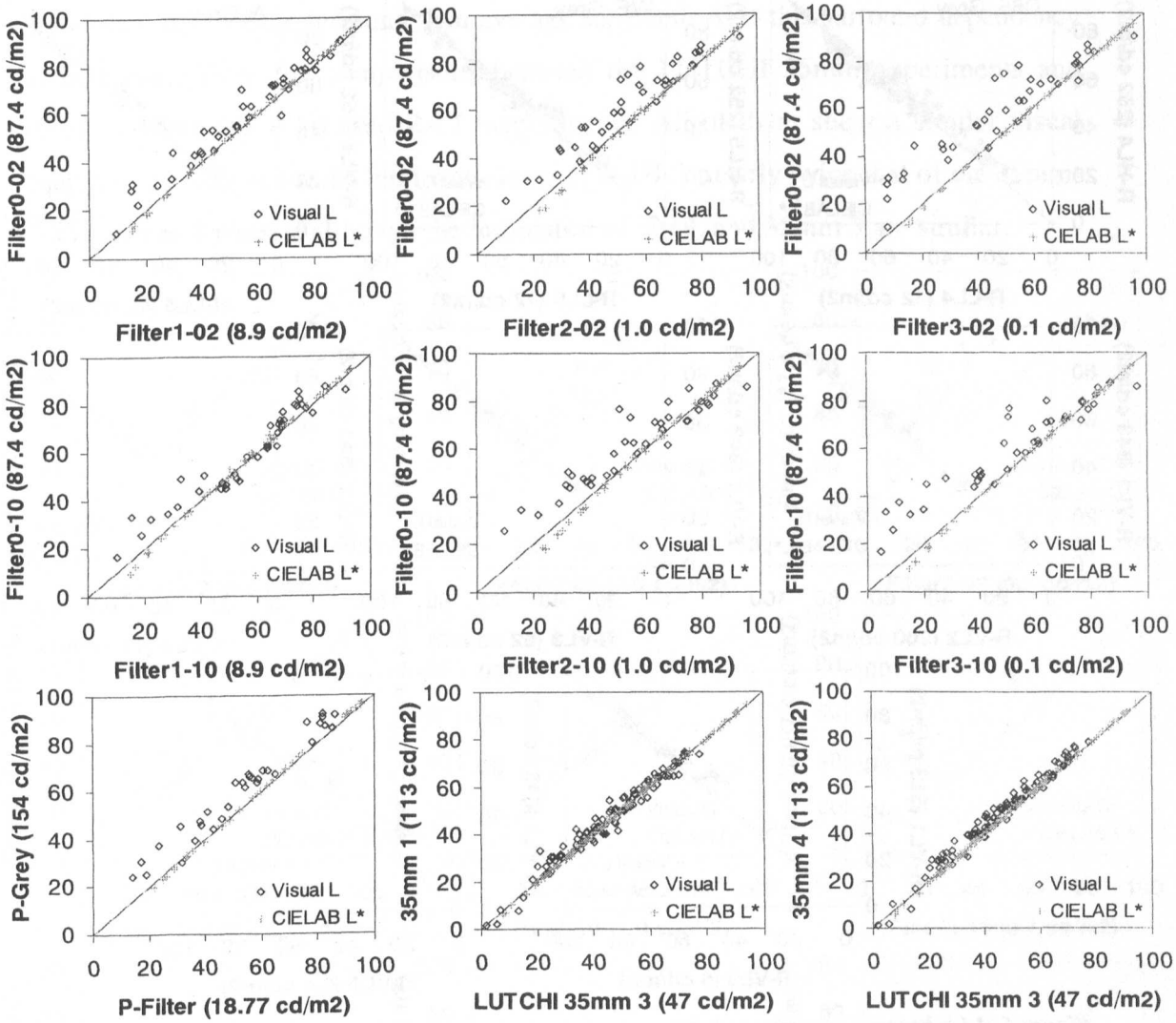


*Figure 6–3 Lightness comparisons between the two phases with the same viewing condition except the luminance levels under dark surround*

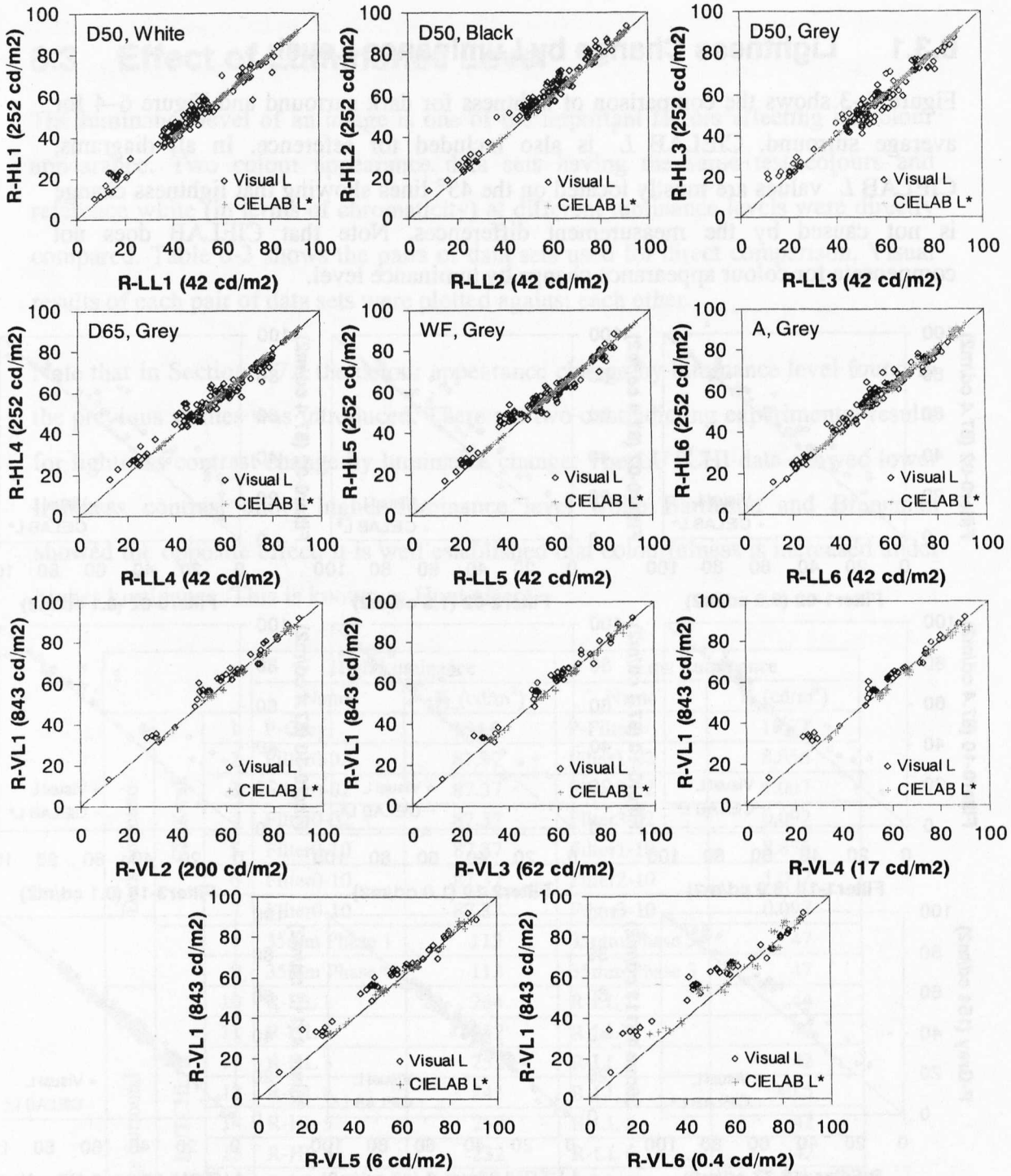


***Figure 6–4 Lightness comparisons between the two phases with the same viewing conditions except the luminance levels under average surround***

These diagrams clearly show that colours appear lighter at higher luminance levels, under both dark and average surround conditions. In other words higher luminance induced lower lightness contrast. Note that the lightness of the reference white is always fixed at 100 regardless of luminance level. The results for dark surround are mainly from the author's study confirming the results found in the LUTCHI data and defying the experimental results of Bartleson and Breneman.

It was also found that the degree of lightness contrast change depends on the difference of luminance levels between phases. Lightness data from the Filter0 experiment showed continuous increments compared to those from Filter1, 2 and 3 respectively as shown in first and second rows in Figure 6–3. Similar features are shown for the R-VL series (see the third and fourth rows in Figure 6–4) but with a smaller change compared to the Filter series, although the R-VL experiments had larger luminance changes. This indicates that lightness contrast change is more significant under dark surround than average surround. Also this surround dependency is noticeable from the comparisons between the LUTCHI 35mm experiments and those between the R-HL and R-LL experiments. All of them show a similar visual lightness increment but the luminance level of R-HL is nearly twice that of the 35mm-1 and 35mm-4 phases, although the luminance of R-LL and 35mm 3 are similar.

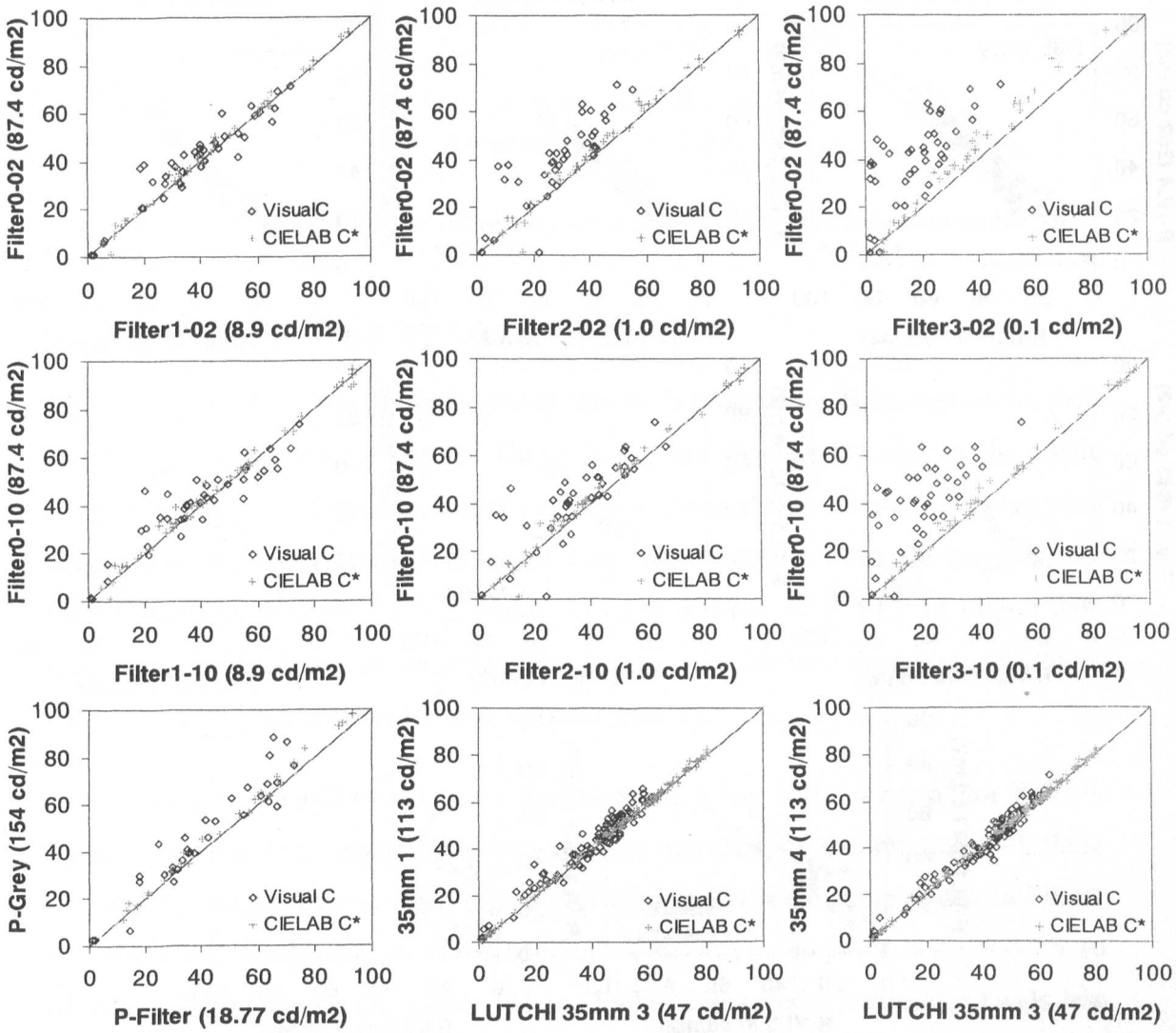


*Figure 6–5 Colourfulness comparisons between the two phases with the same viewing conditions except the luminance levels under dark surround*

### 6.3.2 Colourfulness Change by Luminance Level

Colourfulness changes between experimental phases are shown in Figures 6-5 and 6-6 for dark and average surround respectively. All diagrams in these two figures confirm the Hunt effect, i.e. a colourfulness increment under higher luminance levels. However the surround effect is not so obvious as the lightness contrast changes.

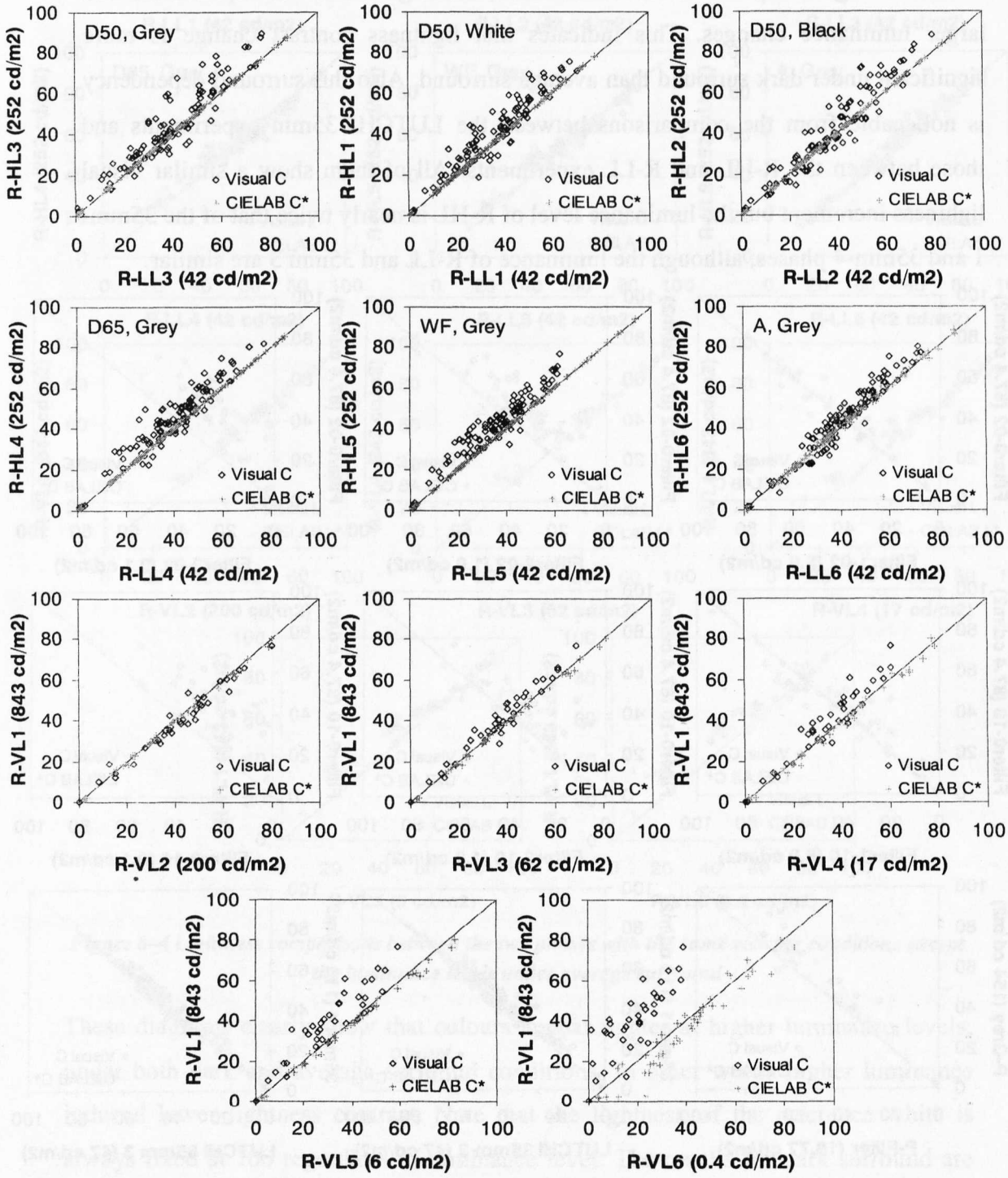


*Figure 6–6 Colourfulness comparisons between the two phases with the same viewing conditions except the luminance levels under average surround*

Two phases were chosen for further investigation of the surround condition dependency of the Hunt effect. The selected phases were R-VL6 (63 cd/m$^2$) and R-VL3 (6 cd/m$^2$) for average surround condition and Filter0-02 (87.4 cd/m$^2$) and Filter1-02 (8.9 cd/m$^2$) for dark surround. They have similar high and low luminances. Figure 6–7 shows the comparison result. Both surround conditions had a difference of 1 log-unit between the low and high luminance phases and showed a similar degree of colourfulness increments.

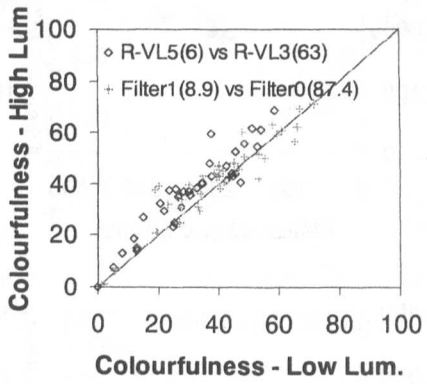


*Figure 6–7 Colourfulness increment comparison between dark and average surrounds*

### 6.3.3 Hue Change by Luminance Level

Figures 6-8 and 6-9 show the hue change due to luminance level change under dark and average surround respectively. There are no hue changes throughout the whole comparison except when colours under photopic luminance level are compared with those having reference white luminance of less than 1 cd/m$^2$. Note the diagrams for Filter3-02/10 vs. Filter0-02/10 in Figure 6–8 and R-VL6 vs. R-VL1 in Figure 6–9. Hue shifts can be found in the green-blue hue area in all three diagrams, indicating that colours look bluer under lower luminance level.

Filter3 had a luminance of 0.1 cd/m$^2$ for reference white and 0.4 cd/m$^2$ for R-VL6. These hue shifts were apparent only when other hue data were compared with these two phases. They appeared when Filter3 (0.1 cd/m$^2$) data were compared with Filter2 (1 cd/m$^2$) and also when R-VL6 (0.4cd/m$^2$) data were compared with R-VL5 (6 cd/m$^2$). It is evident that green-blue colours looked bluer under luminance levels less than 1 cd/m$^2$ in the range of mesopic vision.

In Section 5.6, observer performance analysis showed that this green-blue area had the largest observer variation under low luminance level. Here the hue comparison results show that, although there are somewhat large observer errors under lower luminance level, it is true that green-blue colours appear bluer under luminance less than 1 cd/m$^2$.

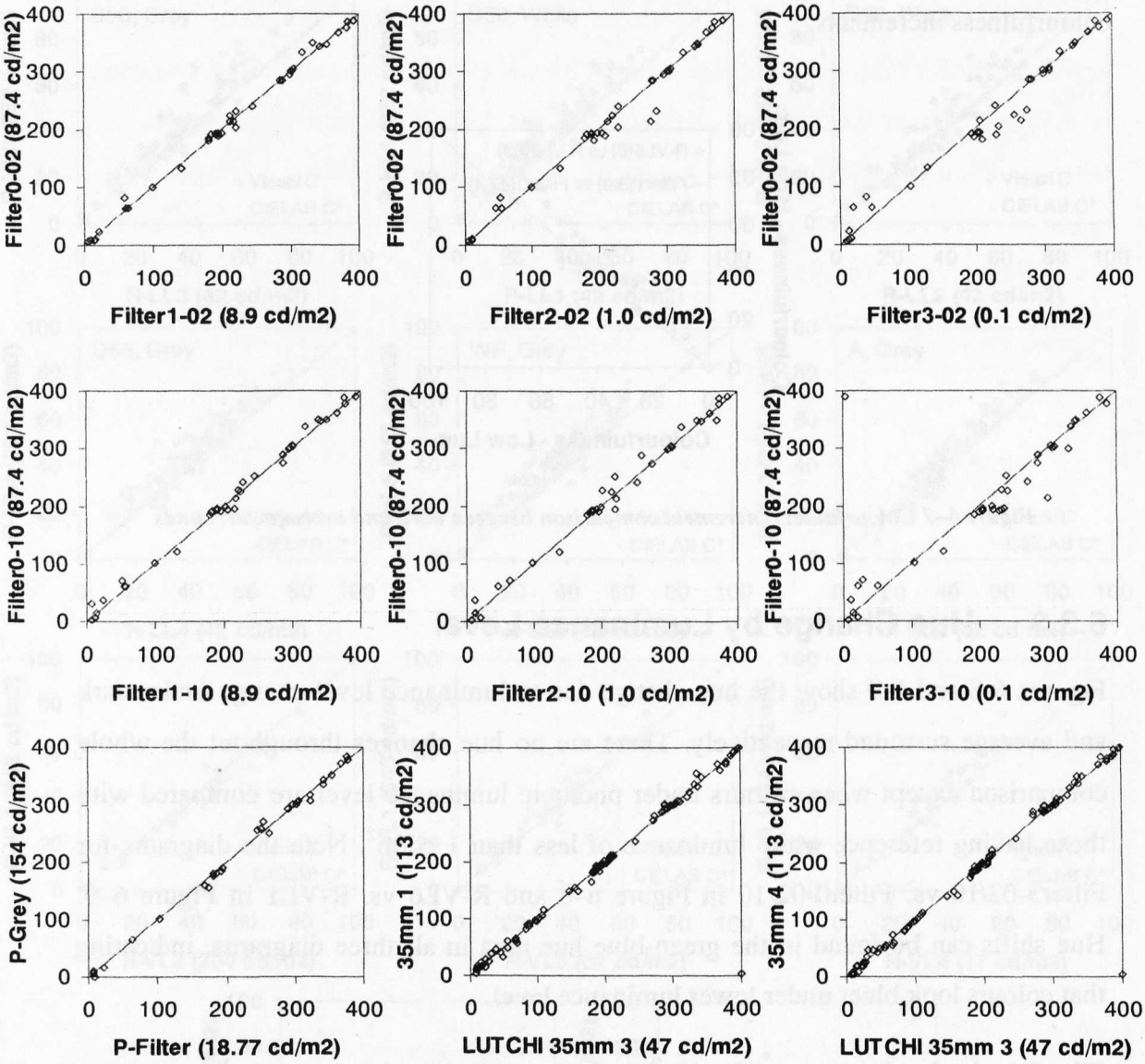


***Figure 6–8 Hue comparisons between the two phases with the same viewing conditions except the luminance levels under dark surround***

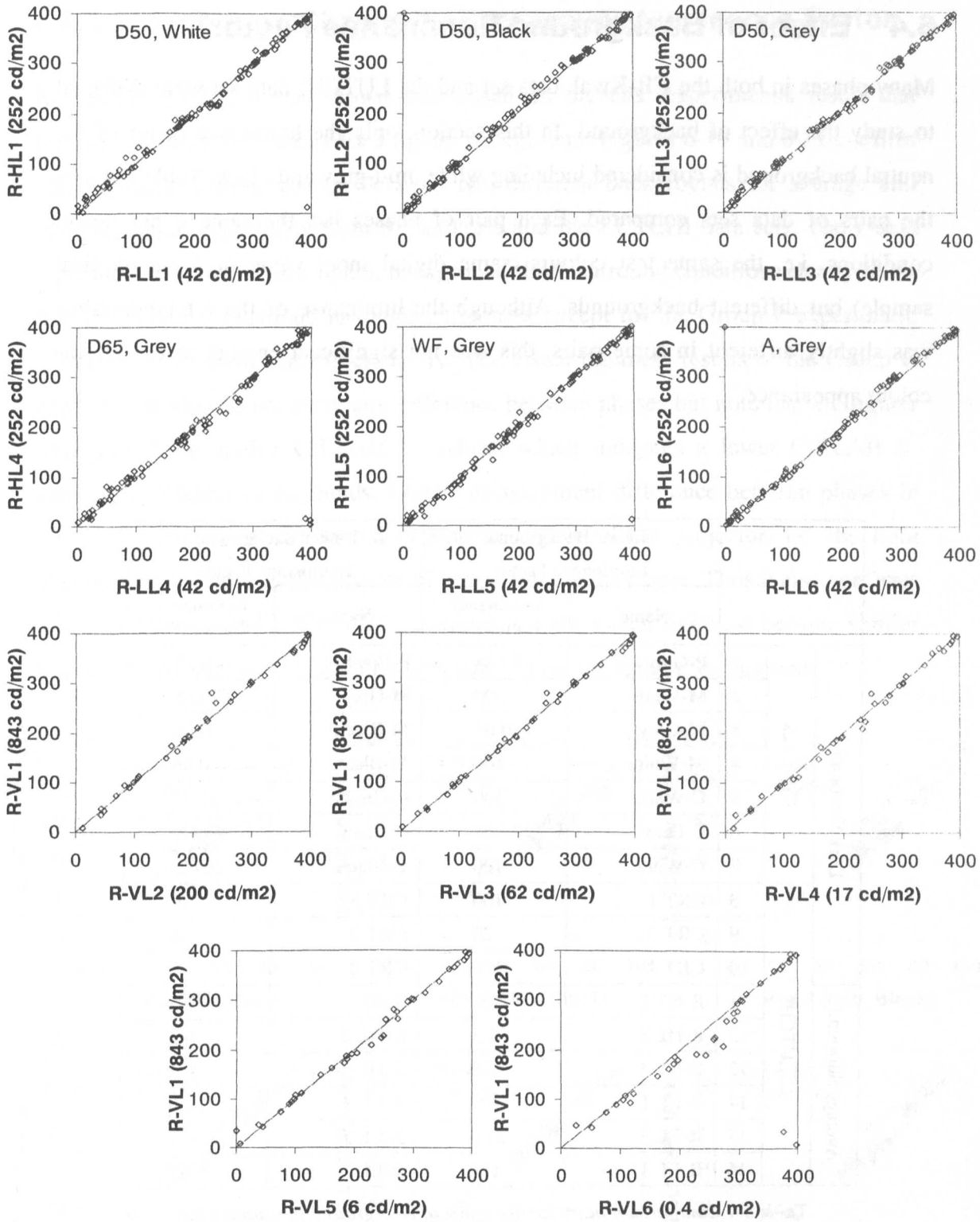


*Figure 6–9 Hue comparisons between the two phases with the same viewing conditions except the luminance levels under average surround*

## 6.4 Effect of Background Luminance Factor

Many phases in both the CII-Kwak data set and the LUTCHI data set were designed to study the effect of background. In this section, only the luminance factor of the neutral background is considered including white, mid-grey and black. Table 6-4 lists the pairs of data sets compared. Each pair of phases has the same experimental conditions, i.e. the same test colours (same digital input value or same physical sample) but different backgrounds. Although the luminance of the reference white was slightly different in some pairs, this was not significant enough to change the colour appearance.

| | | | Higher Background Luminance Factor | | Lower Background Luminance Factor | |
|---|---|---|---|---|---|---|
| | | | Name | Luminance Factor (%) | Name | Luminance Factor (%) |
| Dark Surround | CII-Kwak | 1 | P-Grey | 18.34 | P-Black | 0.42 |
| | | 2 | M-White | 100 | M-Grey | 20.65 |
| | | 3 | M-Grey | 20.65 | M-Black | 0.36 |
| | | 4 | M-White | 100 | M-Black | 0.36 |
| | | 5 | C-White | 100 | C-Grey | 17.37 |
| | | 6 | C-Grey | 17.37 | C-Black | (0.42) |
| | | 7 | C-White | 100 | C-Black | (0.42) |
| | LUTCHI | 8 | CRT 1 | 100 | CRT 3 | 20 |
| | | 9 | CRT 3 | 20 | CRT 2 | 5 |
| | | 10 | CRT 1 | 100 | CRT 2 | 5 |
| Average Surround | | 11 | R-HL 1 | 100 | R-HL 3 | 21.5 |
| | | 12 | R-HL 3 | 21.5 | R-HL 2 | 6.2 |
| | | 13 | R-HL 1 | 100 | R-HL 2 | 6.2 |
| | | 14 | R-LL 1 | 100 | R-LL 3 | 21.5 |
| | | 15 | R-LL 3 | 21.5 | R-LL 2 | 6.2 |
| | | 16 | R-LL 1 | 100 | R-LL 2 | 6.2 |

***Table 6-4 Comparison pairs for the effect of background luminance factor***

### 6.4.1 Lightness Change by Background Luminance Factor

In Section 2.7.2.1, it was shown that, based on Stevens' experimental result that lightness contrast increases with a lighter background. Figures 6-10 and 6-11 confirm this lightness contrast change between two different backgrounds for average and dark surround respectively from the author's and the LUTCHI data sets. The $y$-axis represents the phase with a lighter background. Both surround conditions clearly show that the darker background has higher lightness except for the Group P experiment, which does not show this effect clearly. The visual lightness results of the Group C experiments also do not show any difference between phases but note that the lighter background has higher CIELAB $L^*$ values, which indicates a lower CIELAB $L^*$ contrast for lighter backgrounds. Colour measurement difference between phases in Group C arises from the spatial dependency of the LCD projector, i.e. the light background increases the luminance of test colours in the centre. Thus it also confirms the same effect found in the other experiments since visual lightness became similar because of the increased visual lightness contrast for the lighter background.

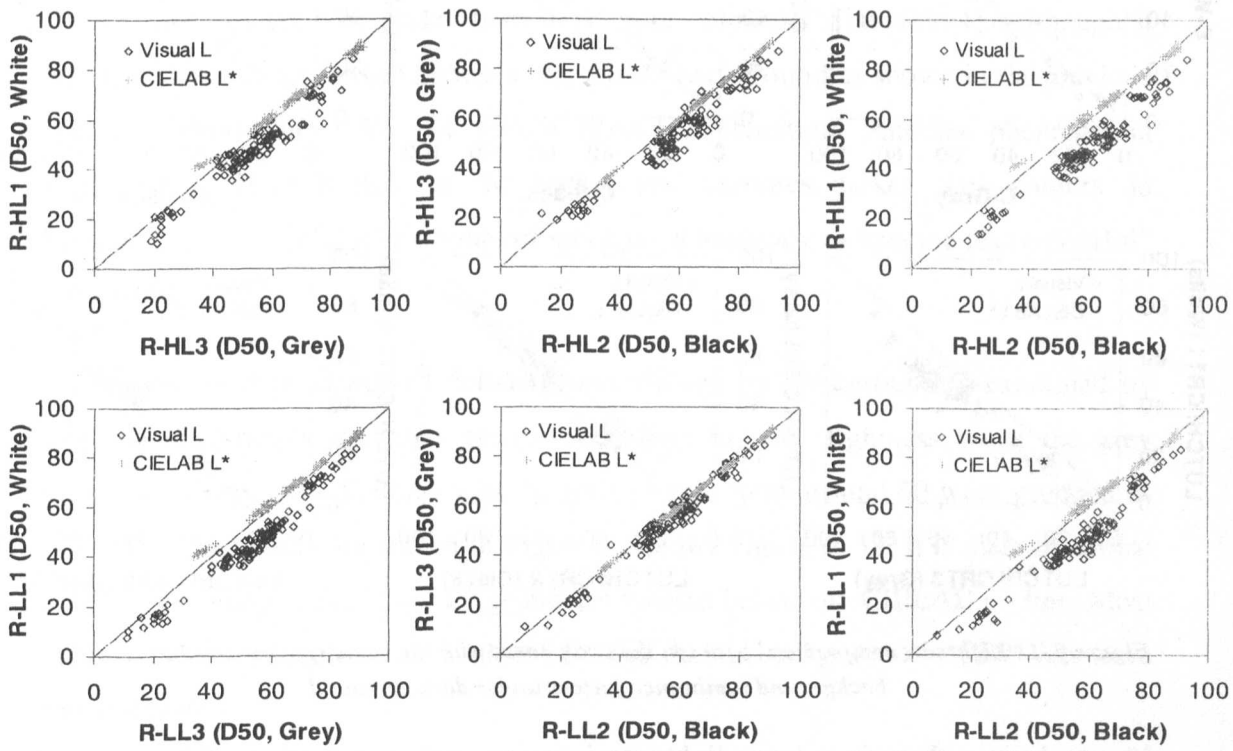


*Figure 6–10 Lightness comparisons between the two phases with the same viewing conditions except background luminance factors under average surround*

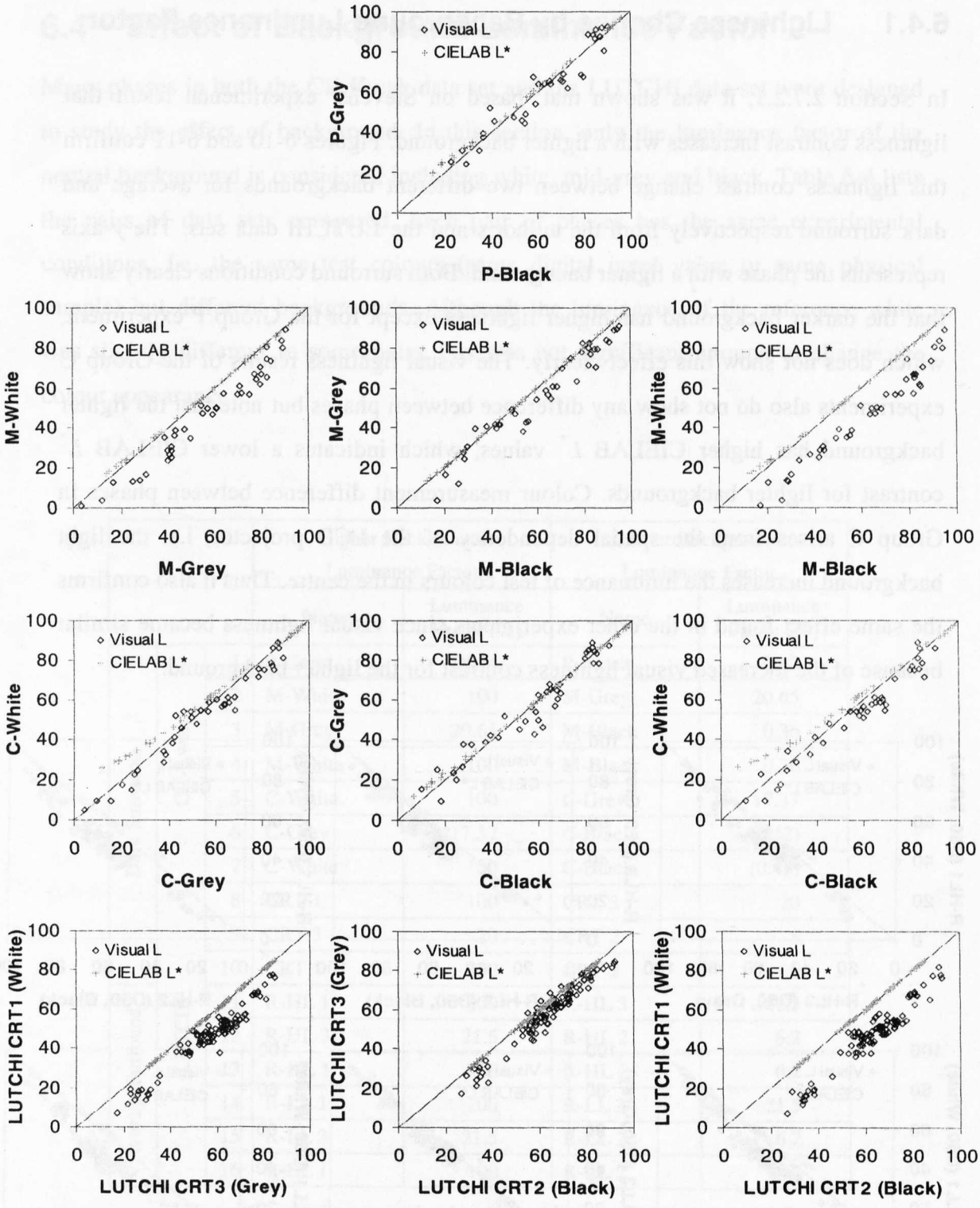


***Figure 6–11 Lightness comparisons between the two phases with the same viewing conditions except background luminance factors under dark surround***

In conclusion, there is a large lightness increase with a reduction of background luminance factor. This change is clearer between mid-grey and white backgrounds than between mid-grey and black backgrounds.

### 6.4.2 Colourfulness Change by Background Luminance Factor

The colourfulness comparison results between two different background luminance factors are shown in Figure 6–12 for dark surround and in Figure 6–13 for average surround. CIELAB $C^*$ values are depicted together with visual colourfulness to show whether there is any measurement difference between the two phases. Note that CIELAB $C^*$ is purely based on chromaticity and does not compensate for any background effect, therefore comparing the relationship between visual data with that between CIELAB $C^*$ data will show any colourfulness change due to background luminance factor.

The diagrams show that most colours look more colourful with a lighter background except for the CRT data, which show larger scatter rather than a systematic shift. Most data points are located above the line formed by the CIELAB $C^*$ comparisons. This phenomenon confirms Pitt and Winter's experimental results introduced in Section 2.7.2.2 but contradicts previous understanding adopted by most colour appearance models that "as the background becomes darker, most colours appear lighter, and this tends to make them look more colourful" [Hunt1994]. Although it was true that colours looked lighter under darker background as shown in the previous section, colourfulness did not follow Hunt's explanation. Another phenomenon explained by Hunt is that "as the background becomes darker, dark colours do become more colourful while light colours have a tendency to become less colourful" [Hunt1994].

This lightness dependency of colourfulness change by background is examined by dividing data points into two groups according to their lightness when the grey background was used. Colours with lightness lower than around 50 were grouped as "Low L". The results are shown in Figure 6–13 and Figure 6–12. It is clear that most colours belonging to the "Low L" group are located below the CIELAB $C^*$ line. Most colours that show higher colourfulness for the darker background in CRT data have low lightness.

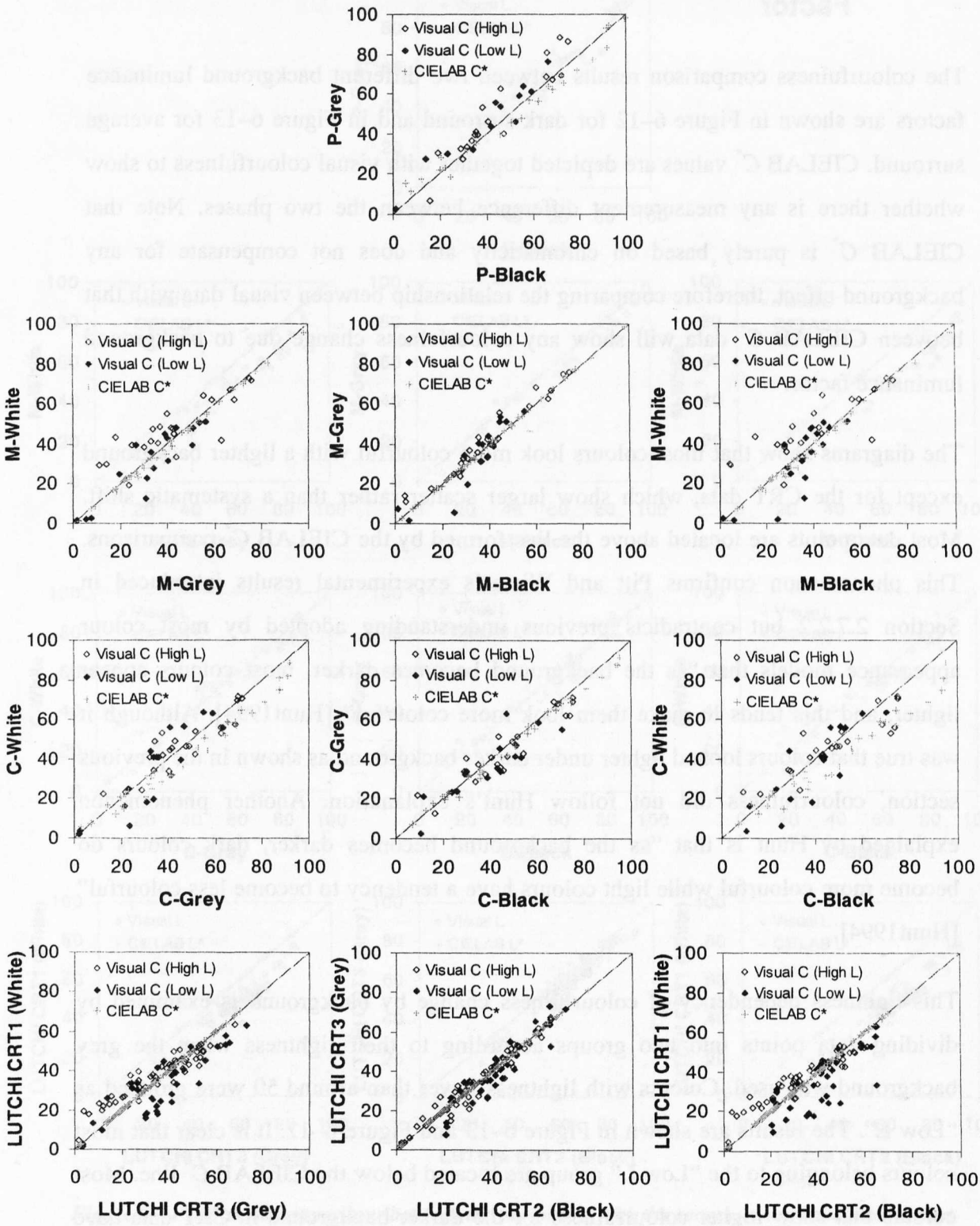


*Figure 6–12 Colourfulness comparison between two phases with the same viewing conditions except background luminance factors under dark surround*

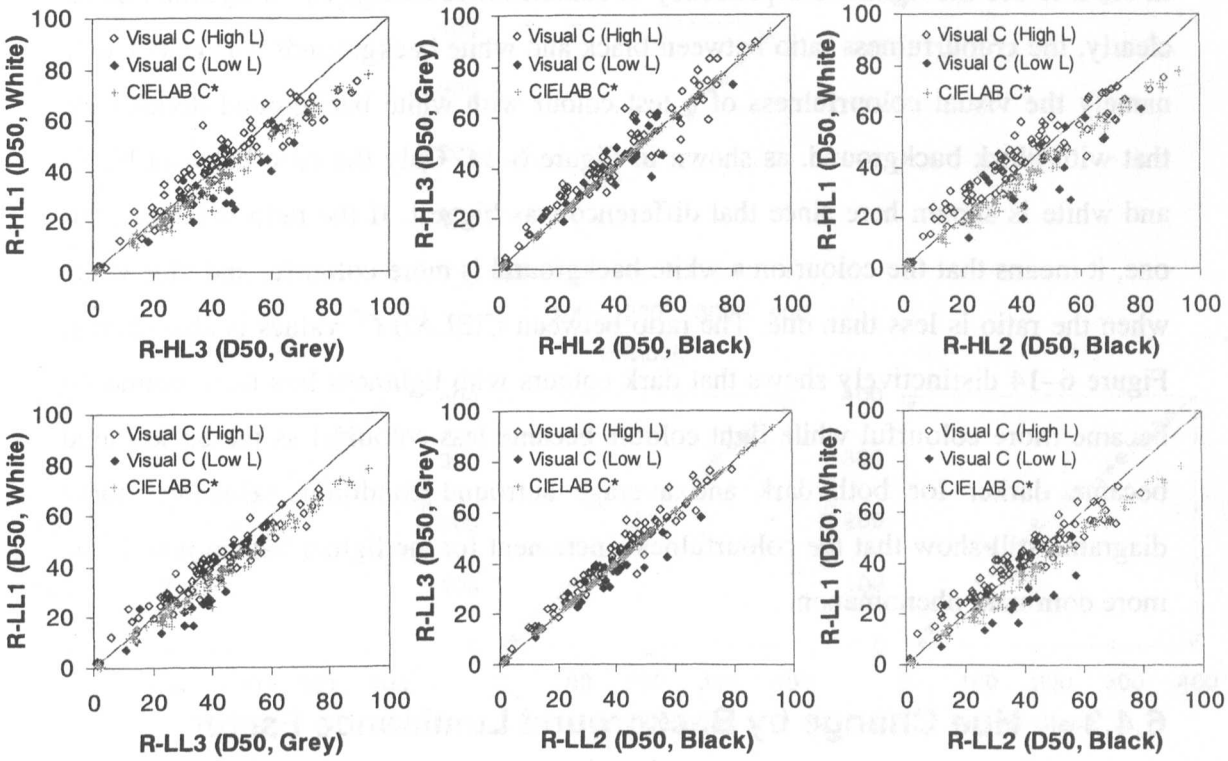


*Figure 6–13 Colourfulness comparisons between the two phases with the same viewing conditions except background luminance factors under average surround*

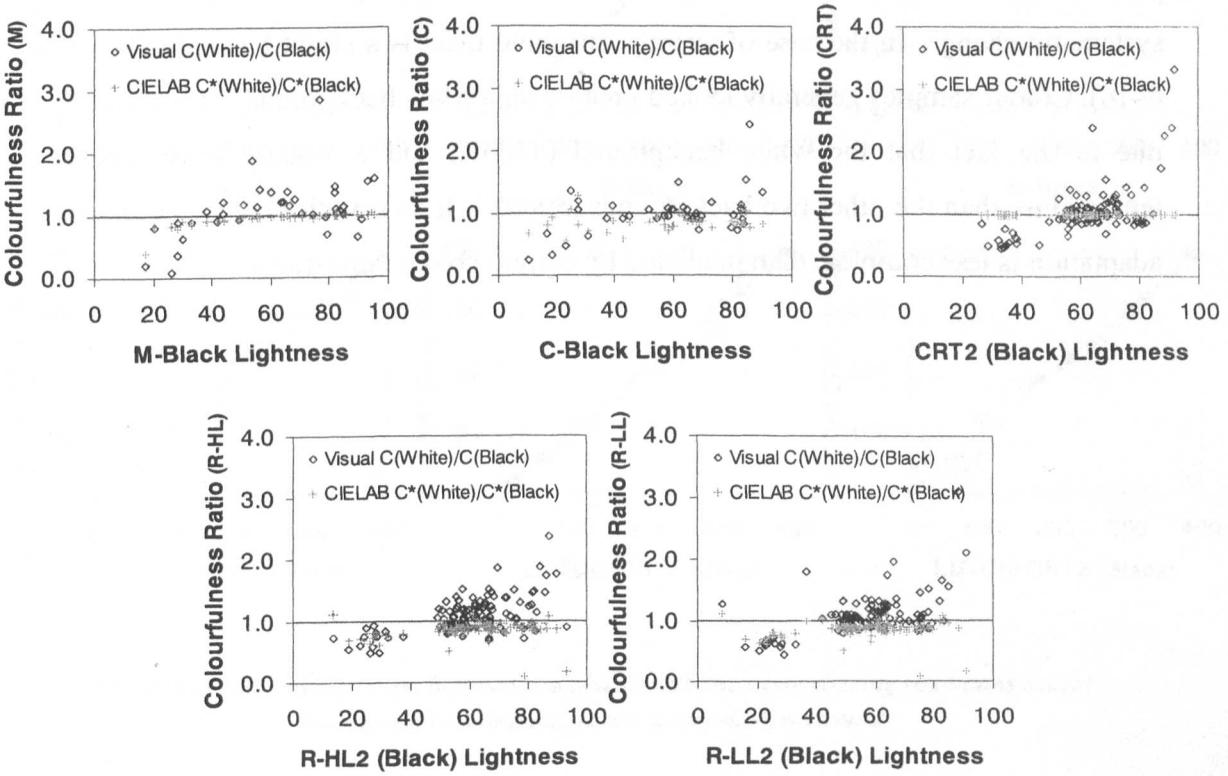


*Figure 6–14 Lightness dependency of colourfulness change by background level*

In order to see the lightness dependency of colourfulness change by background more clearly, the colourfulness ratio between black and white backgrounds was calculated, namely the visual colourfulness of a test colour with white background divided by that with black background, as shown in Figure 6–14. Only the ratio between black and white is shown here since that difference was biggest. If the ratio is larger than one, it means that the colour on a white background is more colourful and vice versa when the ratio is less than one. The ratio between CIELAB $C^*$ values is also shown. Figure 6–14 distinctively shows that dark colours with lightness less than around 40 became more colourful while light colours became less colourful as the background became darker for both dark and average surround conditions. However these diagrams still show that the colourfulness increment for the lighter background is the more dominant phenomenon.

### 6.4.3 Hue Change by Background Luminance Factor

Hue change by background luminance factor is shown in Figures 6-15 and 6-16. There is little hue change except scattering for dark surround (see Figure 6–15). In particular, CRT hue data shows larger differences between phases but without any systematic change. In the case of average surround there is a slight hue shift (Figure 6–16). Colour samples generally looked greener on a white background. This could be due to the fact that the white background (4700K) had a slightly lower colour temperature than the other two backgrounds (5000K). If so it indicates that chromatic adaptation is less complete than predicted by current colour appearance models.

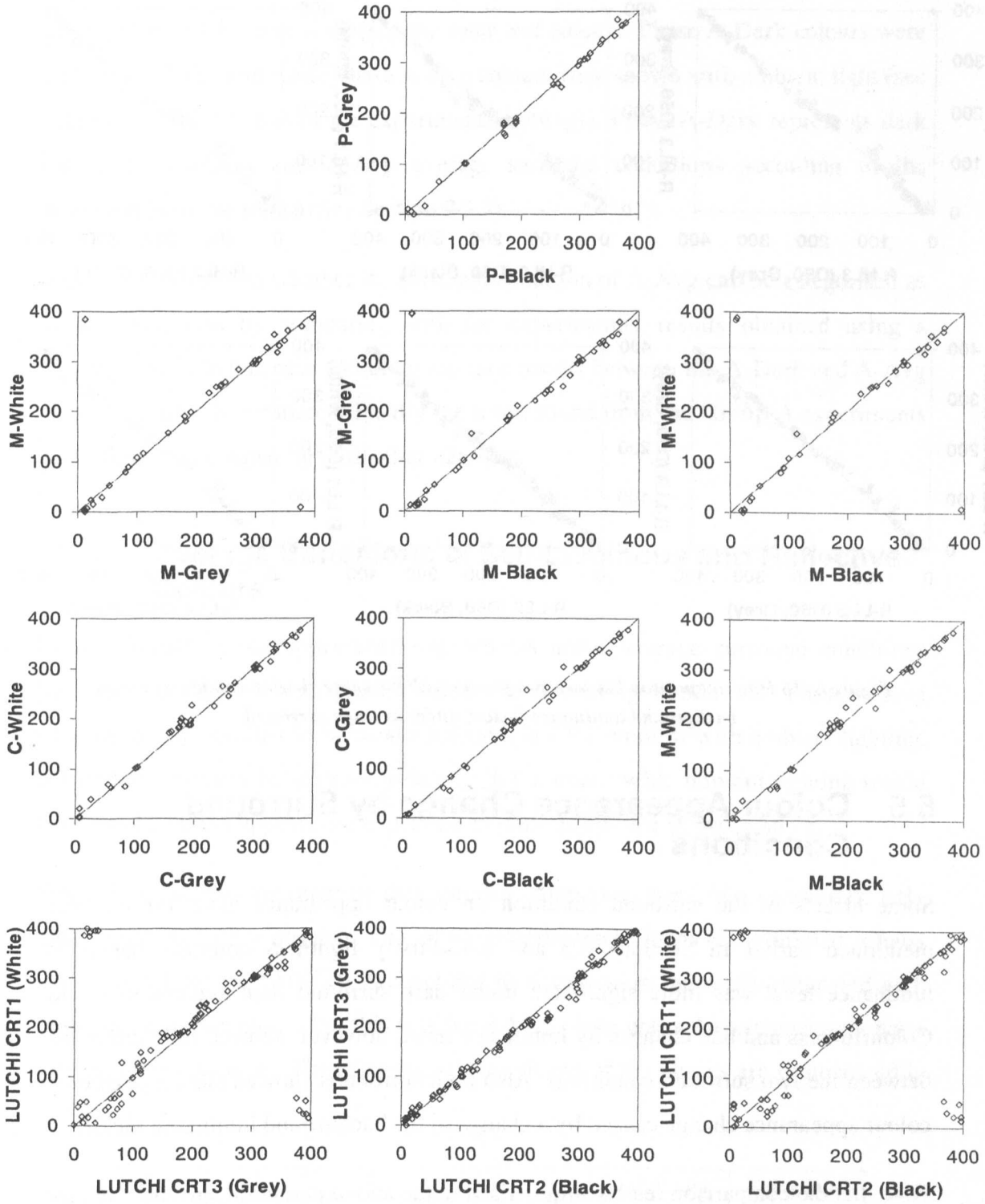


*Figure 6–15 Hue comparison between two phases with the same viewing conditions except background luminance factors under dark surround*

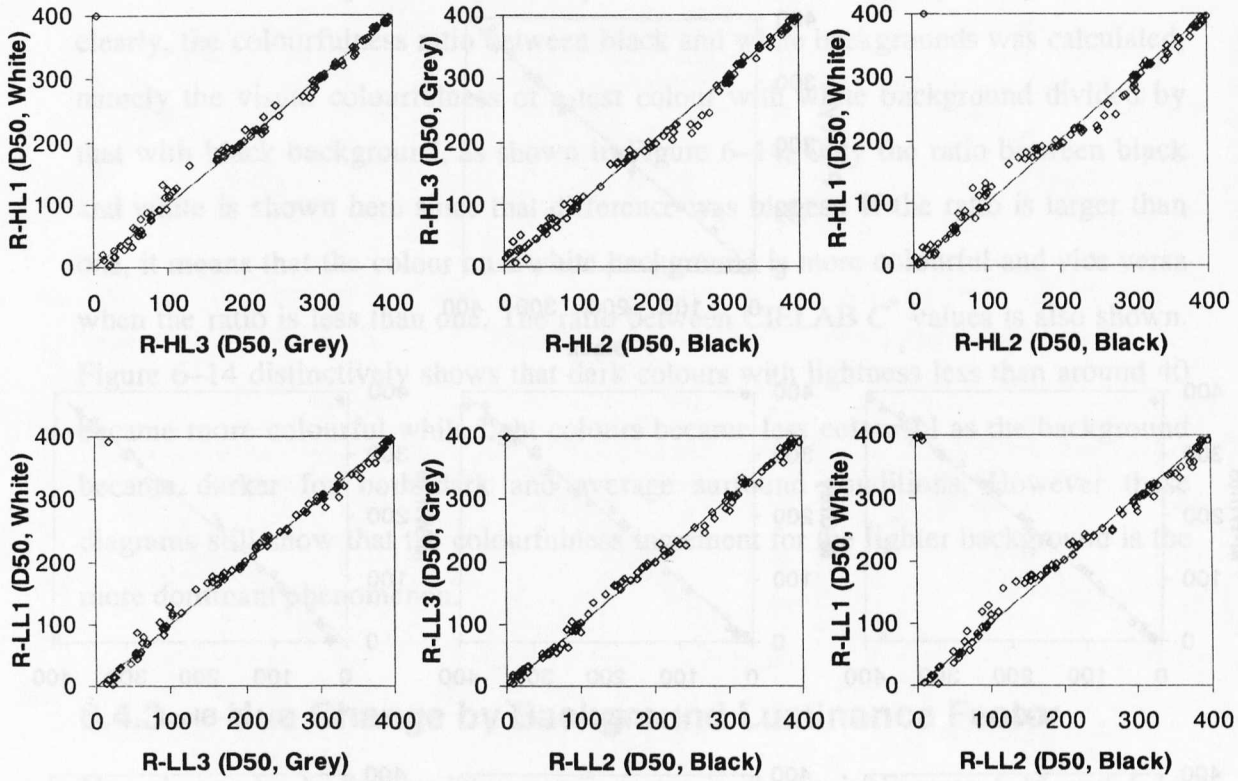


*Figure 6–16 Hue comparison between two phases with the same viewing conditions except background luminance factors under average surround*

## 6.5 Colour Appearance Change by Surround Conditions

Some effects of the surround condition on colour appearance have already been mentioned earlier in Sections 6.3 and 6.4. Firstly lightness contrast change by luminance level was more significant under dark surround than average surround. Colourfulness and hue changes by luminance level, however, showed little difference between the two surround conditions. Also both surrounds showed similar degrees of colour appearance change caused by a change in the background luminance factor.

Note that the comparison results summarised in the above paragraph are about relative colour appearance changes within dark or average surround, not direct colour appearance comparison between dark and average surround. These results cannot answer which surround condition would induce higher lightness or colourfulness contrast. The Group A experiment was especially designed to investigate the effect of surround condition directly and the experimental results are summarised here. Group

A experiments consisted of two phases. Both phases used self-luminous colours displayed on a CRT monitor using the same test colours. Phase A-Dark colours were shown in a dark room while Phase A-Avg colours were shown with ambient light (see Section 4.3.4 for details of the experimental settings). Phase A-Dark represents dark surround conditions and A-Avg average surround conditions according to the definition of the surround (See Section 2.5.2).

It is investigated as to whether the surround condition of A-Avg can be categorised as average surround by comparing with the experimental results obtained using a viewing booth. In this case colour appearance results between the A-Dark and A-Avg phases are directly compared. Finally the result found from the Group A experiments is confirmed by comparing with other data sets.

### 6.5.1 Average Conditions of Self-Luminous and Reflective Colours

Conventionally colour appearance experiments under average surround conditions have been performed with printed colours in a viewing booth. The Phase A-Avg experiment was the first to be conducted using a CRT monitor with ambient lighting. It therefore needs to be tested whether a CRT monitor with ambient lighting would have similar colour appearance to printed colours shown in a viewing booth.

Since there are no experimental data directly comparing these two conditions, only indirect comparison is possible. One of the experimental phases using printed colours was chosen from the LUTCHI data set and its results were indirectly compared with those of the A-Avg phase. For this task the R-VL3 phase was selected because it has a similar luminance level. The experimental conditions of the phases are summarised in Table 6-5.

| | Name | Mode | Media | CCT (K) | Ref. White $L_w$ (cd/m$^2$) | Background $Y_b$ (%) |
|---|---|---|---|---|---|---|
| A | A-Avg | Ambient Lighting | CRT Monitor | 6800 | 89.13 | 24.0 |
| R-VL | R-VL3 | Viewing Booth | Printed Colours | 5000 | 62 | 21.5 |

*Table 6-5 Viewing conditions of A-Avg and R-VL3*

These two data sets had independent colourfulness estimations and also had different colour temperature therefore it was not possible to have any meaningful comparison results for colourfulness and hue. Only lightness results were compared using the same strategy used for the device dependency test. Normalised luminances and CIELAB $L^*$ of test colours were plotted against visual lightness results as shown in Figure 6–17. It can be seen that there is little difference between the two surround conditions.

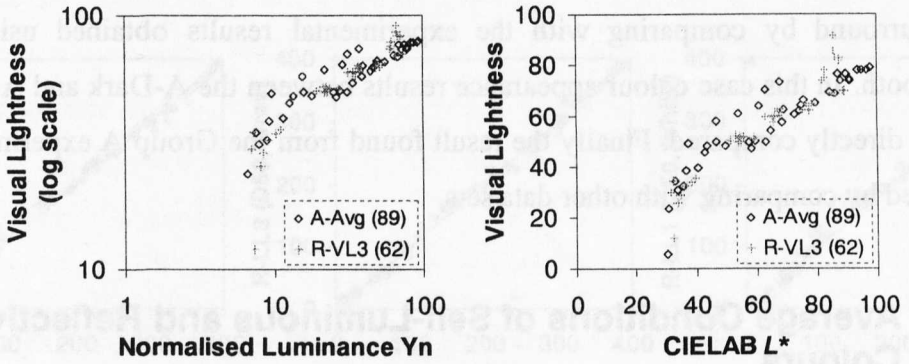


*Figure 6–17 Lightness contrast comparisons between A-Avg and R-VL3*

It may be debatable whether showing similar lightness contrast is sufficient to conclude that both experiments have the same surround conditions without any comparison results for colourfulness and hue, however colour appearance changes by luminance level and background showed that both lightness and colourfulness were changed while hue showed little difference. It is very unlikely that colourfulness and hue would show different characteristics between them.

This result suggests that CRT monitor colours with ambient lighting have colour appearances in terms of estimated lightness, colourfulness and hue similar to colour samples shown in a viewing booth. It also suggests the media independence of the average condition, which needs more investigation.

### 6.5.2 Direct Colour Appearance Comparison between Dark and Average Surround Conditions

Figure 6–18 shows the direct comparison of colour appearance data between the A-Dark and A-Avg phases. CIELAB $L^*$, $C^*$ and hue angle are plotted together to show the colour change of the stimulus. For hue angles, 0 to 360 degrees are re-scaled to 0 to 400 by multiplying a factor 400/360.

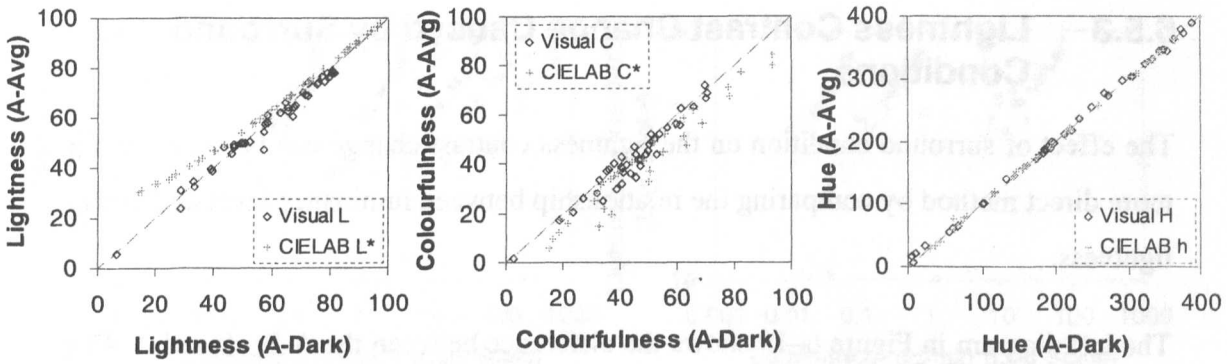


*Figure 6–18 Colour appearance comparisons between dark (A-Dark) and average (A-Avg) surround conditions*

In the case of visual lightness data (left diagram in Figure 6–18), there is little difference between the two phases but measurement data shows a large CIELAB $L^*$ increment when the ambient light is on caused by reflected ambient light from the monitor. (Refer to Section 3.5.1 for the characteristics of monitor colours with and without ambient light.) This means that visual lightness of a dark colour in a dark room looked similar to the corresponding colour with the same digital input values in an average surround in spite of its lower luminance because of a tendency for dark colours to look lighter in the dark surround than in the average surround. In other words, average surround induces higher lightness contrast, which agrees well with the previous studies (see Section 2.7.3.1).

The result of colourfulness comparison (middle diagram in Figure 6–18) is less obvious than lightness because of the large scattering of CIELAB $C^*$ data. It is still recognisable, however, that the visual colourfulness data points are located above the CIELAB $C^*$ data indicating that the average surround condition induces higher colourfulness. This result also confirms the previous studies. See Section 2.7.3.2 for details.

In the case of hue comparison (right diagram in Figure 6–18), there was no difference between visual and measurement data.

### 6.5.3 Lightness Contrast Change Caused by Surround Conditions

The effect of surround condition on the lightness contrast change can be shown via a more direct method by comparing the relationship between luminance level and visual lightness.

The left diagram in Figure 6–19 shows the difference between the A-Dark and A-Avg phases. It clearly shows a contrast reduction, i.e. a lower slope in the log-log diagram, due to dark surround. Also the lightness results between P-Grey (projected colours in a dark room) and R-VL2 (printed colours in a viewing booth) shown in the right diagram have a similar trend. Note that both of them have similar reference white luminances and that the dark surround (P-Grey) shows lower lightness contrast.

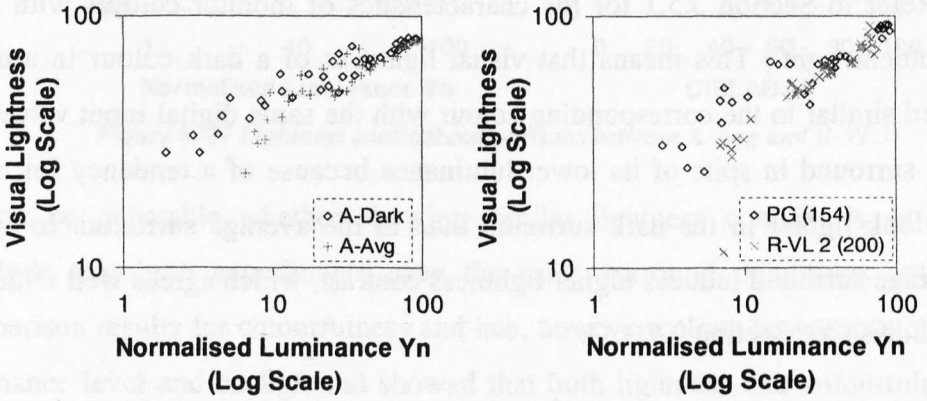


*Figure 6–19 Lightness contrast comparison between dark and average surrounds (1)*

Figure 6–20 shows two sets of experimental series. The left graph is for the Filter-02 series and the right diagram represents the visual lightness of the R-VL series as a function of the luminance of test colours. The R-VL series consisted of six experiments carried out using a viewing booth and the Filter-02 series had four phases that used a CRT monitor in a dark room. Both experiments had the same background level: mid-grey. Examining these diagrams confirms that lightness contrast changes by both luminance level and surround condition. Firstly each diagram shows that higher luminance levels had lower contrast (a lower slope in the graph). Secondly when the two diagrams are compared, the left diagram (which is for dark surround) had a lower slope, which means lower contrast. Lightness contrast change by luminance level and surround change is modelled in Section 8.7.2.1.

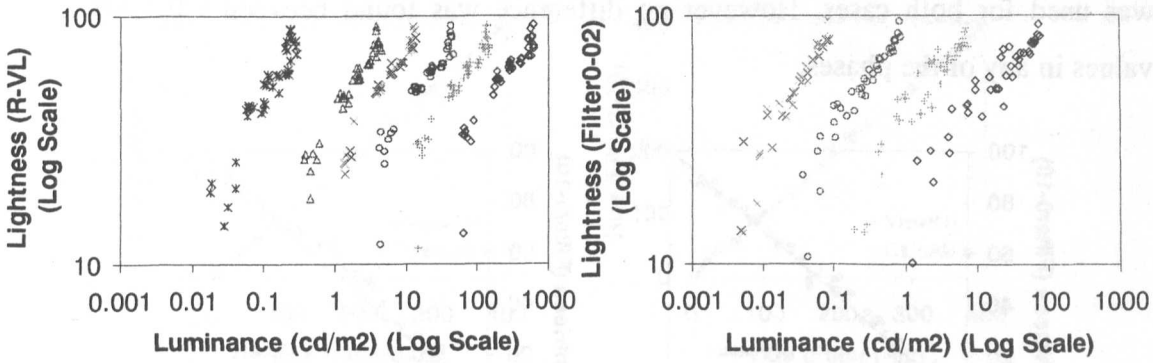


*Figure 6–20 Lightness contrast comparison between dark and average surrounds (2)*

## 6.6 Colour Appearance Difference between 2° and 10° Visual Field Size

It is well known that there is a non-uniform distribution of photoreceptors in the retina therefore colour appearance can be expected to change when the visual field size is changed. This is why there are two standard colour matching functions (corresponding to 2° and 10° visual angles). The difference between colour matching functions or tristimulus values calculated from them cannot, however, provide information about colour appearance differences between 2° and 10° stimuli.

The Group F experiment was designed to investigate colour appearance change due to the size of viewing angle of a test colour. During the experiment the same test colours with different viewing angles (2° and 10°) were assessed under four different luminance levels with a reference white ranging from 87 to 0.1 cd/m$^2$. Refer to Section 4.3.5 for details of the experimental settings.

Figures 6-21, 6-22 and 6-23 show the lightness, colourfulness and hue comparison results respectively between two patch sizes. Together with visual data, CIELAB $L^*$, $C^*$ and hue angle (rescaled to 0-400) are plotted to show the measurement differences between the colour stimuli assessed in two phases. CIELAB values were calculated using $XYZ$ for the 2° patch and $X_{10}Y_{10}Z_{10}$ for the 10° patch.

Figure 6–21 shows that most data points are located slightly above the 45° lines indicating that the 10° stimulus appears relatively brighter than the 2° stimulus. Note that the word 'brighter' is used here instead of 'lighter' since the same reference white

was used for both cases. However no difference was found between CIELAB $L^*$ values in any of the phases.

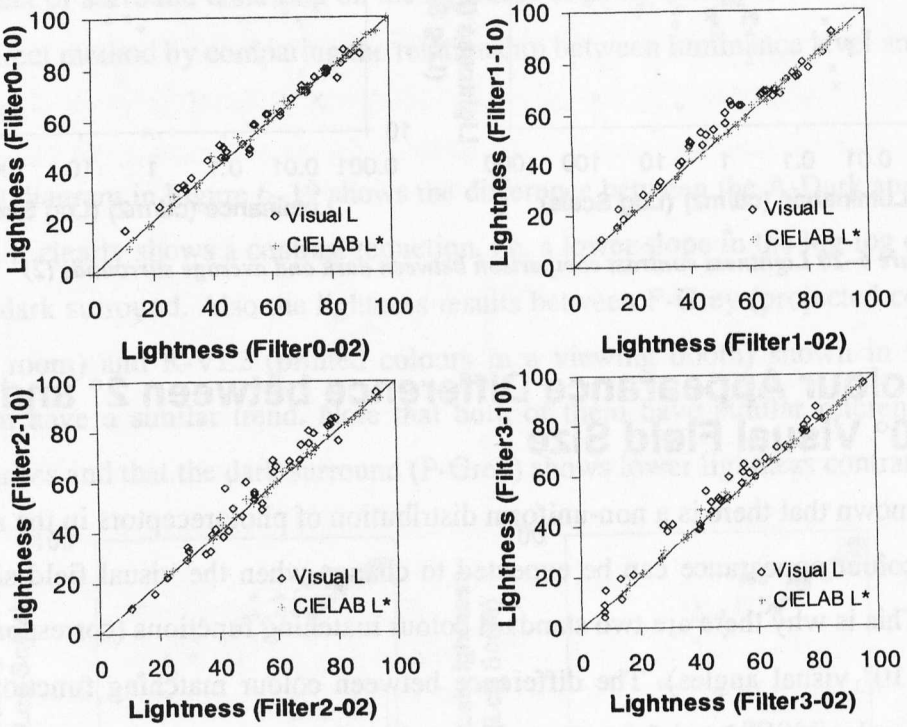


*Figure 6–21 Lightness comparison between 2° and 10° colour patches*

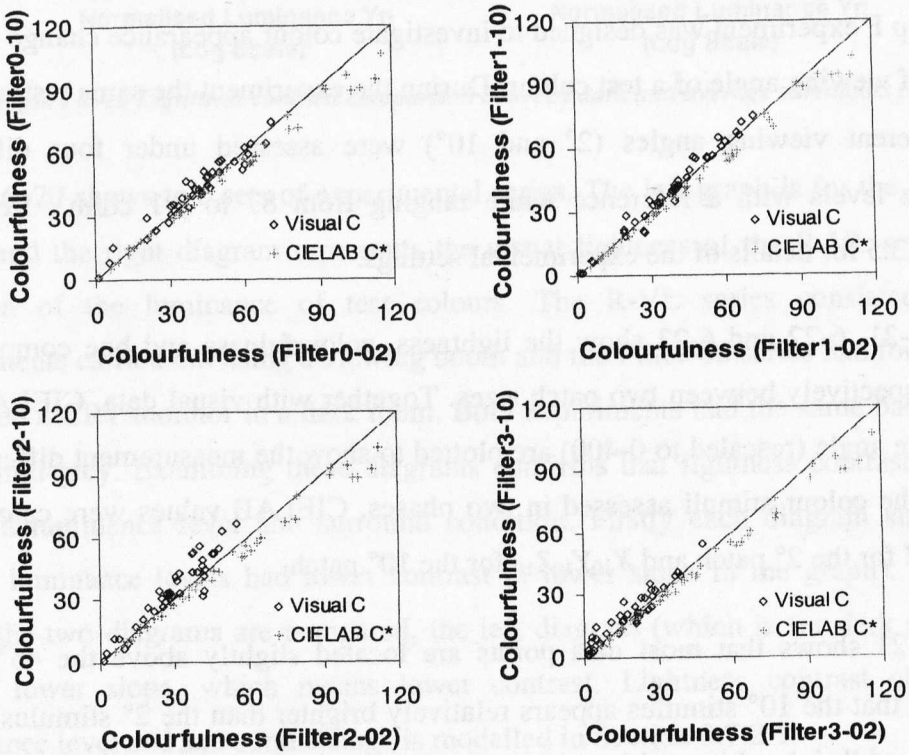


*Figure 6–22 Colourfulness comparison between 2° and 10° colour patches*

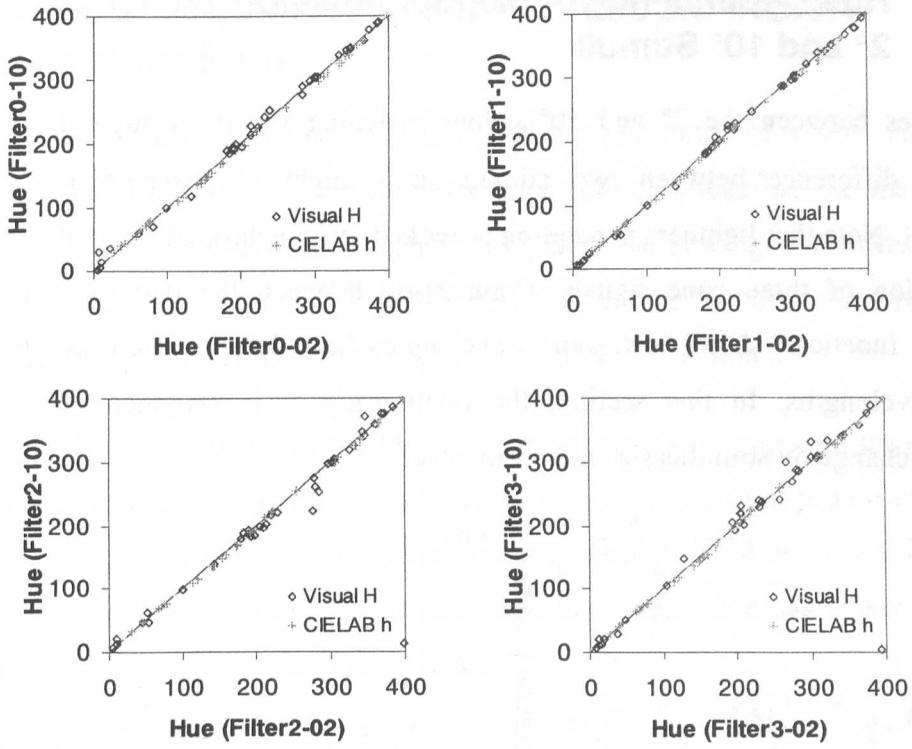


*Figure 6–23 Hue comparison between 2° and 10° colour patches*

Increased brightness must induce higher colourfulness for the 10° patch as shown in Figure 6–22. There is little colourfulness difference in the Filter0 experiment but the difference increases when the luminance level decreases however CIELAB $C^*$ shows the opposite effect meaning that applying different colour matching functions is not enough to predict the colourfulness change by stimulus size change.

There is almost no hue change due to the size change of the stimulus except for a slight perturbation in the hue range green-blue (between 200-300) at the lower luminance levels (Filter2 and Filter3), as shown in Figure 6–23. The CIELAB hue angle also showed no difference between the two stimuli sizes.

These results show that using different colour matching functions to calculate tristimulus value is insufficient to predict colour appearance changes caused by viewing angle change. The stimulus size effect must therefore be luminance level dependent, i.e. larger luminance difference evokes a larger effect.

### 6.6.1 Hue Dependency of the Lightness Difference between 2° and 10° Stimuli

Differences between the 2° and 10° colour matching functions suggests that the lightness difference between two stimuli sizes might be wavelength (or hue) dependent. Note that lightness perception is evoked by an achromatic signal that is the combination of three cone signals. Comparison between the two sets of colour matching functions shows that short wavelengths have larger differences than the other wavelengths. In this section, the relationship is investigated between the lightness change by stimulus size and visual hue.

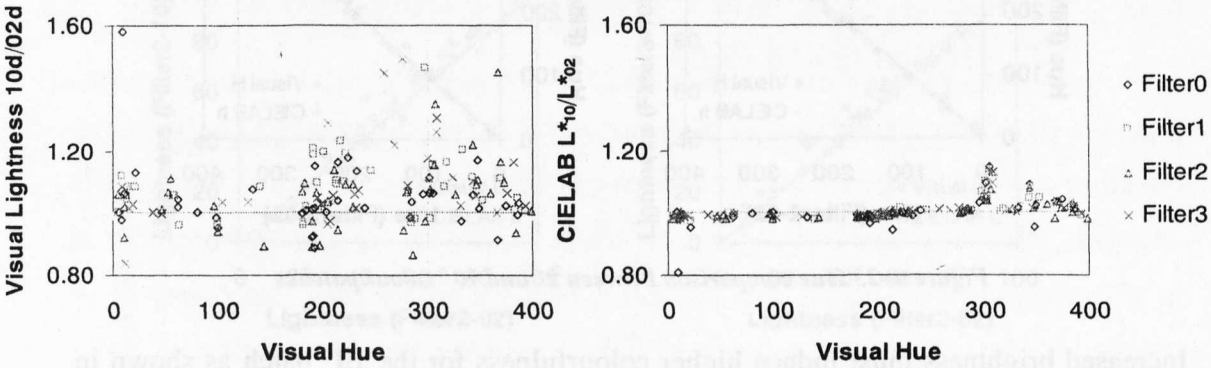


*Figure 6–24 Hue dependency of lightness change by stimulus size*

The left diagram in Figure 6–24 represents the visual lightness of the 10° patch divided by that of the 2° patch and this lightness ratio is plotted against the visual hue. The majority of points are located above 1.0 confirming a generally higher lightness for the 10° stimulus as shown in Figure 6–21. This effect became larger at lower luminance levels.

Another distinctive feature is the much higher lightness increment for green-blue colours (hue range 200-300) than in other hue regions, especially for the Filter3 experiment. The right diagram in Figure 6–24 shows the predictions of CIELAB $L^*$, which also exhibits higher lightness for 10° patches than 2° patches for blue colours due to the difference in colour matching functions. The predicted hue dependency is, however, far smaller than observed and there is no difference by luminance change.

This analysis result suggests that another mechanism apart from colour matching functions is working for colour appearance change by stimulus size. In Section 8.7.3, modelling of colour appearance change by stimulus size is tried.

## 6.7 Colour Appearance under Mesopic Vision: Purkinje Shift

Group F experiments cover both photopic and mesopic range of vision. Note that under mesopic vision, both cones and rods are functioning together. In this section some evidence of rod contribution under mesopic vision is sought by investigating whether the Purkinje shift is seen in the visual data. The Purkinje shift is a well known phenomenon under low luminance levels. (Refer to Section 2.7.1.2.)

In Section 6.3.1 it was seen that the visual lightness of a colour becomes lower as the luminance level of the image decreases however if the Purkinje shift is active then the reduction of lightness will depend on the colour's spectral distribution. For example blue colours that look darker than red colours in the highest luminance level appear relatively lighter at very low luminance levels.

Since the Purkinje shift has a wavelength-dependent characteristic, spectrally pure red and blue colours would show the Purkinje shift most effectively therefore the most spectrally pure red and blue test colours were chosen from the Group F experiments. Their digital input values were (255,51,51) and (51,51,255) for the Filter0 phase and the average visual hues of four phases were 6 and 304 for both 2° and 10° patches. The results are shown in Figure 6–25. The left and middle diagrams show the visual lightness changes of the red and blue colours for 2° and 10° patches respectively. Both graphs strongly suggest the Purkinje shift. There is a greater degree of lightness reduction for the red colour at low luminance levels than for the blue colour.

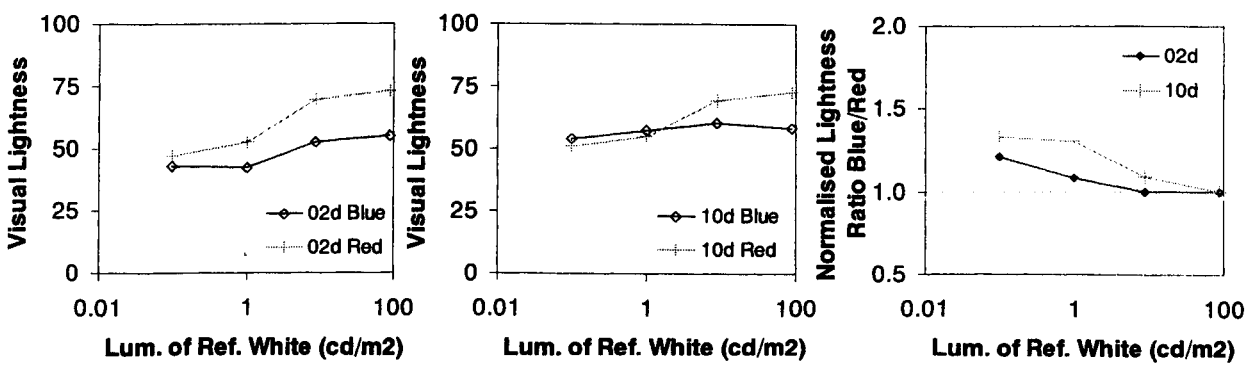


*Figure 6–25 Purkinje shift shown by spectrally pure red and blue colours (Group F experiment)*

A further means of comparison was employed to demonstrate the Purkinje shift more effectively. The mean visual lightness of the blue colour was divided by that of the red colour to calculate the lightness ratio between two colours, then the ratio at each luminance level was normalised to that of highest luminance level. The right diagram in Figure 6–25 shows the result. It is clear that blue colours look relatively lighter than red colours (higher ratio in the diagram) as the luminance decreases. This effect is more significant for the larger colour patches.

## 6.8 Summary of Colour Appearance Phenomena

In this chapter, an investigation was carried out into the colour appearance changes by the luminance levels of a reference white, background luminance factors, the surround conditions and the stimulus sizes from the CII-Kwak and LUTCHI data sets. These two independent colour appearance data sets showed the same effects due to these factors.

It was found that a higher luminance level of the reference white in an image makes colours look lighter (i.e. lower lightness contrast) and more colourful. Colours look darker but more colourful with a lighter background. Average surround also induces lower lightness (i.e. higher lightness contrast) and colourfulness compared to dark surround conditions.

A stimulus having a 10 viewing angle looks slightly lighter and more colourful than that one with a 2 viewing angle. Also 10 stimuli show stronger Purkinje shift than 2 stimuli under mesopic vision.

# Chapter 7
# Testing the Colour Appearance Models

## 7.1 Introduction

In this chapter, the performances of eight colour appearance models were tested using the LUTCHI data and the new colour appearance data CII-Kwak collected by the author. The eight models were CIELAB, LLAB, RLAB, Hunt94, CIECAM97s, FC, Fairchild and CIECAM02. The equations of each model were introduced in Section 2.8. The performances of the models were tested in two ways. Firstly the ability of each model to predict the mean visual data was described using coefficient variation (CV) values. Secondly the ability to predict colour appearance phenomena was revealed using scatter diagrams.

All models tested in this study need the relative tristimulus values of the test colours and the reference white as input data. Table 7-1 summarises the input information of each model needed apart from tristimulus values. These input parameters decide which colour appearance phenomena each model is able to predict. For example RLAB considers both the surround condition and luminance level of an image to predict colour appearances however appearance change due to background is not considered.

| | Surround | Luminance Level | Background | Rod Contribution |
|---|---|---|---|---|
| CIELAB | | | | |
| LLAB | × | × | × | |
| RLAB | × | × | | |
| Hunt94 | × | × | × | × |
| CIECAM97s, FC, Fairchild, CIECAM02 | × | × | × | |

***Table 7-1 Summary of input information to colour appearance models***

The same colour appearance data sets used for colour phenomena analysis in Chapter 6 were also used for this task as summarised in Table 7-2. Details of each of the 61 phases are given in Appendix 1. Twenty-four of them were conducted under average surround and 36 under dark surround. (The definition of surround was introduced in Section 2.5.2.) Reflective colours shown in a viewing booth or self-luminous colours with ambient light belong to the average surround. Self-luminous colours shown in a dark room belong to the dark surround. Fifty of them were conducted under a grey background. There were also six black and five white background phases respectively.

| | Group | Surround | No. of Phases | Light Source | Ref. White | Back-ground | No. of Observers | No. of Colours | No. of Estimations |
|---|---|---|---|---|---|---|---|---|---|
| CII-Kwak | P (Presentation) | Dark | 3 | 7200 K | 19, 154 | Grey Black | 21 | 32 | 6,048 |
| | M (Monitor) | Dark | 3 | 7200 K | ~ 90 | White Grey Black | 11 or 12 | 40 | 4,200 |
| | C (Cinema) | Dark | 4 | 7200 3900 K | ~ 16 | | 9 or 11 | 40 | 4,800 |
| | A (Ambient) | Dark Average | 2 | 7200 K | ~ 86 | Grey | 11 | 40 | 2,640 |
| | F (Filters) | Dark | 8 | 7200 K | 0.1 ~ 88 | Grey | 10 ~ 12 | 40 | 10,920 |
| LUTCHI | R-HL | Average | 6 | D50, D65, WF, A | ~ 250 | White Grey Black | 6 or 7 | ~100 | 11,970 |
| | R-LL | Average | 6 | | ~ 40 | | | | 11,970 |
| | CRT | Dark | 11 | | ~ 40,20 | | | | 19,390 |
| | 35mm | Dark | 6 | 4000 K | 47~113 | Grey | 5 or 6 | ~ 99 | 9,093 |
| | R-VL | Average | 6 | 5000 K | 0.4~843 | Grey | 4 | 40 | 5,760 |

***Table 7-2 Summary of the experimental phases used to test colour appearance models***

## 7.2 Testing Method

### 7.2.1 Parameters of the Models to be Tested

Testing a colour appearance model using experimental data is quite straightforward after the surround condition has been decided, except that CIELAB does not make use of this information. Another factor which must be determined is the degree of chromatic adaptation, *D*. CIECAM97s recommends that "if the colour of the illuminant is completely discounted (complete chromatic adaptation) *D* is set equal to 1.0" [Luo1998]. In the author's experiments, a reference white was shown to the observers all the time and it was assumed that they were fully adapted to the

chromaticity of the reference white. This assumption was indirectly tested by comparing the performances of each colour appearance model with complete ($D$=1) and partial (using the model's equation to predict $D$) chromatic adaptation.

Hunt94 is the most comprehensive model among the eight models tested here. It considers a unique colour appearance phenomenon, the Helson-Judd effect, which is not considered by other models. In short, the Helson-Judd effect is where a sample exhibits a hue change according to the colour of illuminant as described in Section 2.7.4. Also Hunt94 provides two lightness predictors, $J$ and $J_p$, the latter of which was specifically developed to improve the lightness prediction for projected colours. Another distinctive feature of Hunt94 is that it includes rod contribution in the achromatic signal. These features were tested and results will be given in Section 7.3.

### 7.2.2 Comparison between Visual Data and Model Predictions

Colour appearance predictions by each model were compared with the mean visual data using scatter diagrams and coefficients of variation (CV) which were calculated to show the performance of the model in a quantitative way. The equation to calculate CV values is introduced in Eq. ( 7-1 ). For colourfulness or brightness comparison, a scaling factor ($k$) is also needed since the visual data and model predictions may have different scales. The scaling factor is the gradient calculated by linear fitting between the predicted and visual data with the constraint of passing through the origin. In other words, the constant $k$ in Eq. ( 7-1 ) is obtained by minimising CV values. Each model requires a different colourfulness or brightness scaling factor to scale the predicted colourfulness or brightness.

$$CV = 100\frac{\sqrt{\sum (k \cdot x_i - y_i)^2 / n}}{\bar{y}} \qquad (7\text{-}1)$$

$n$ : Total number of samples
$x_i$ : Predicted data of $i^{th}$ sample
$y_i$ : Visual data of $i^{th}$ sample
$\bar{y}$ : The mean value of the visual data
$k$ : Scaling Factor, $k = 1$ for lightness and hue

Colour appearance data sets were categorised according to the colourfulness scales used during the experiments when calculating the colourfulness scaling factor. Phases belonging to the same category need to use only one unique scaling factor. The CII-Kwak data set consists of five groups (P, M, C, A and F), which are divided into four

categories. Note that Group A and Group F belong to the same category since they used the same reference colourfulness. Each category in the CII-Kwak data set requires a different scaling factor. The LUTCHI data was supposed to have the same colourfulness scale over the whole set of experiments. In the case of brightness there is only one experimental group, R-VL, in the LUTCHI data having the same scale throughout the whole set of experiments.

Conventionally two methods have been used to calculate scaling factor. The first method uses the average value after calculating scaling factors of individual phases in a category. The second method combines all data points of the phases in a category and then calculates the scaling factor. The main difference between the two methods depends on which is more important – the experimental phase as a whole or an individual data point. If each phase has a similar number of data points the results will be weighted equally. However if one phase has a much larger number of data points the scaling factor of this phase would have a more significant weight using the second method. Note that both methods would distribute the errors (the difference between predicted and visual data) to all phases and the results would be affected by the composition of the experimental phases in a group.

In this study, a new method was adapted for calculating the scaling factor to avoid the problems that might arise when conventional methods are used. A standard phase was chosen per category and the scaling factor of that phase was applied to all other phases in the category. This method is simpler and gives additional information about which phases agree or disagree with the standard phase. The phase showing poorer performance indicates that a specific model has poorer performance for that particular viewing condition.

Table 7-3 shows the list of standard phases used to calculate the colourfulness scaling factor for each category. In the case of the CII-Kwak data set, phases shown in the table were the standard phases used for colourfulness scaling during the experiment. Note that during the experiment, observers were asked to memorise the reference colourfulness patch in the standard phase before starting a new phase and they estimated the new reference colourfulness compared to the standard reference colourfulness. (Refer to Section 4.4.6 for the details of colourfulness scaling for the author's experiment. Table 4-7 in Section 4.4.6 listed the standard phase of each

experimental group for colourfulness scaling.) For the LUTCHI data, the R-HL3 phase was chosen since the R-HL experiments were the first experiment group conducted in the LUTCHI experiments and R-HL3 used a grey background like the other standard phases in the CII-Kwak experiments. In the case of brightness, R-VL1 was used as a standard phase.

| | Group | Surround | Standard Phase | Surround | Lum.of Ref. White ($cd/m^2$) | Background (%) |
|---|---|---|---|---|---|---|
| CII-Kwak | P (Projector) | Dark | P-Grey | Dark | 154.0 | 18.34 |
| | M (Monitor) | Dark | M-Grey | Dark | 90.33 | 20.65 |
| | C (Cinema) | Dark | C-Grey | Dark | 15.68 | 17.37 |
| | A (Ambient) | Dark/Avg | A-Dark | Dark | 85.77 | 19.82 |
| | F (Filters) | Dark | | | | |
| LUTCHI | R-HL | Average | R-HL3 | Average | 252 | 21.5 |
| | R-LL | Average | | | | |
| | CRT | Dark | | | | |
| | 35mm | Dark | | | | |
| | R-VL | Average | | | | |

***Table 7-3 Standard experimental phases used to calculate the colourfulness scaling factor***

Chroma predictors were also tested even though the observer did not evaluate this attribute. Testing the performance of chroma is based on the idea that there is no perceptual difference between colourfulness and chroma for an isolated experimental phase i.e. colourfulness and chroma differ from each other by the brightness of the reference white. A scaling factor was calculated per experimental phase to compare predicted chroma and visual colourfulness data. In a strict sense, this test is equivalent to a linearity test of the chromatic predictor for each model rather than a real perceptual chroma comparison. The brightness, colourfulness and chroma scaling factors used for each model are listed in Appendix 3.

## 7.3 Test Results for the Hunt94 Model

Applying the Hunt94 model requires input of the surround condition, the inclusion or exclusion of the Helson-Judd effect and the specification of which lightness predictor, $J$ or $J_p$, to be used. Hunt suggested several viewing conditions where the Helson-Judd effect does not occur [Hunt1995 p716] such as projected colours in dark rooms. The lightness predictor $J_p$ is for projected colours in a dark room. In this study all possible combinations of model parameters were examined under all viewing conditions to test

the performance of the guideline itself and also to determine the best setting for using the Hunt94 model. Results with the best setting were used to compare the performance with other models in the next section.

The model parameters studied here include chromatic adaptation factor ($F_\rho$ $F_\gamma$ $F_\beta$), Helson-Judd effect factor ($\rho_D$ $\gamma_D$ $\beta_D$), two lightness predictors ($J$, $J_p$) and rod contribution (with and without scotopic component, $A_s$, in the achromatic signal, $A$). This makes six combinations with two lightness predictions. Combinations of the factors are summarised in Table 7-4. Note that the Helson-Judd effect does not occur under complete chromatic adaptation.

| | Chromatic Adaptation | Helson-Judd Effect | Achromatic Signal |
|---|---|---|---|
| Case 1 | $F_\rho$, $F_\gamma$, $F_\beta$ | On $\rho_D$ $\gamma_D$ $\beta_D$ | Photopic + Scotopic |
| Case 2 | | | Photopic only |
| Case 3 | | Off $\rho_D = \gamma_D = \beta_D = 0$ | Photopic + Scotopic |
| Case 4 | | | Photopic only |
| Case 5 | Complete Adaptation $F_\rho = F_\gamma = F_\beta = 1$ | No Effect | Photopic + Scotopic |
| Case 6 | | | Photopic only |

Achromatic Signal Photopic + Scotopic $A = N_{bb}[A_a\text{-}1+A_s\text{-}0.3+(1^2+0.3^2)^{1/2}]$

Achromatic Signal Photopic only $A = N_{bb} A_a$

***Table 7-4 Combinations of factors for the Hunt94 model test***

## 7.3.1 Performance of Lightness Predictors *J* and $J_p$ of the Hunt94 Model

Performances of lightness predictors are reported using the average CV values of 61 phases in Table 7-5. Averaged CVs of each surround condition are also given. The purpose of this is to investigate whether there is any surround condition dependency of the performance of the lightness predictor due to model parameters.

| CV | *J* | | | | | | *Jp* | | | | | |
|---|---|---|---|---|---|---|---|---|---|---|---|---|
| | *A = Ap + As* | | | *A = Ap* | | | *A = Ap + As* | | | *A = Ap* | | |
| | +HJ | -HJ | D=1 | +HJ | -HJ | D=1 | +HJ | -HJ | D=1 | +HJ | -HJ | D=1 |
| Dark | 16.0 | 16.1 | 16.0 | 16.6 | 16.8 | 16.7 | 13.5 | 13.7 | 13.6 | 14.5 | 14.7 | 14.5 |
| Average | 13.2 | 13.3 | 13.2 | 13.4 | 13.5 | 13.4 | 10.9 | 10.9 | 10.9 | 11.2 | 11.3 | 11.2 |
| All | 15.0 | 15.1 | 15.1 | 15.5 | 15.7 | 15.5 | 12.6 | 12.7 | 12.6 | 13.4 | 13.5 | 13.4 |

Note : +HJ : Include Helson-Judd Effect

-HJ : Exclude Helson-Judd Effect

D=1 : Perfect chromatic adaptation

*A* : Achromatic Signal, *Ap* : Photopic component, *As* : Scotopic (Rod) Component

***Table 7-5 CV values of lightness predictors J and Jp for Hunt94***

In Table 7-5, the CV values clearly show that the lightness predictor $J_p$, which is derived for projected colours, also works well for reflective colours. There was little change produced by Helson-Judd effect factors. Also a change in chromatic adaptation factor did not affect the performance of the lightness predictor. Both surround conditions had similar trends. Using the achromatic signal combining photopic and scotopic signals gave slightly better performance than just using photopic signals but this effect was minor (less than 1 CV unit) in most cases. Only Phases Filter3-02 and Filter3-10 showed a significant improvement in performance by including rod contribution in the achromatic signal. These two phases had the lowest luminance of reference white, 0.1 cd/m$^2$, among the experimental phases used in this study. Table 7-6 summarises the performance of the lightness predictor for those two phases. This result agrees with the fact that the rod contribution is most active under the lowest luminance level.

| CV | *J* | | | | | | *Jp* | | | | | |
|---|---|---|---|---|---|---|---|---|---|---|---|---|
| | *A = Ap + As* | | | *A = Ap* | | | *A = Ap + As* | | | *A = Ap* | | |
| | +HJ | -HJ | D=1 | +HJ | -HJ | D=1 | +HJ | -HJ | D=1 | +HJ | -HJ | D=1 |
| Filter3-02 | 12.5 | 12.5 | 12.5 | 22.8 | 22.4 | 22.0 | 12.3 | 12.2 | 12.2 | 24.0 | 23.7 | 23.2 |
| Filter3-10 | 12.7 | 12.7 | 12.8 | 17.4 | 17.1 | 16.8 | 13.6 | 13.7 | 13.7 | 20.0 | 19.7 | 19.4 |

***Table 7-6 Effect of rod contribution for the Filter3 experiment***

## 7.3.2 Performance of Chroma Predictor $C_{94}$ and Colourfulness Predictor $M_{94}$ for the Hunt94 Model

The performances of the chroma and colourfulness predictors are summarised in Table 7-7. Like the lightness predictor test, six possible model parameter combinations were tested. The relation between chroma and colourfulness results is not discussed here, only which model parameter combination gives the best performance for chroma and colourfulness.

| CV | $C_{94}$ | | | | | | $M_{94}$ | | | | | |
|---|---|---|---|---|---|---|---|---|---|---|---|---|
| | *A = Ap + As* | | | *A = Ap* | | | *A = Ap + As* | | | *A = Ap* | | |
| | +HJ | -HJ | D=1 | +HJ | -HJ | D=1 | +HJ | -HJ | D=1 | +HJ | -HJ | D=1 |
| Dark | 22.8 | 22.6 | 21.7 | 22.7 | 22.6 | 21.7 | 26.2 | 25.7 | 25.6 | 26.1 | 25.7 | 25.6 |
| Average | **19.0** | **21.3** | 18.1 | 19.0 | 21.3 | 18.1 | **21.3** | **23.4** | 20.6 | 21.3 | 23.4 | 20.6 |
| All | 21.2 | 22.1 | *20.3* | 21.2 | 22.1 | *20.3* | 24.2 | 24.8 | *23.6* | 24.1 | 24.7 | *23.5* |

***Table 7-7 CV values of chroma predictor $C_{94}$ and colourfulness predictor $M_{94}$ for Hunt94***

The most distinctive feature seen in Table 7-7 is that the performance of the chromatic predictors is affected by the Helson-Judd factor. Including the Helson-Judd factor gave slightly better performance for average surround but little difference for dark surround in terms of average CV value. Figure 7–1 shows the impact of the Helson-Judd factor more clearly. CV values calculated with and without Helson-Judd effect were directly compared to each other in a diagram. Except for the 35mm experiments in the LUTCHI data, all other experiments – even in a dark surround – had slightly better or at least similar performance when the Helson-Judd effect factor was included.

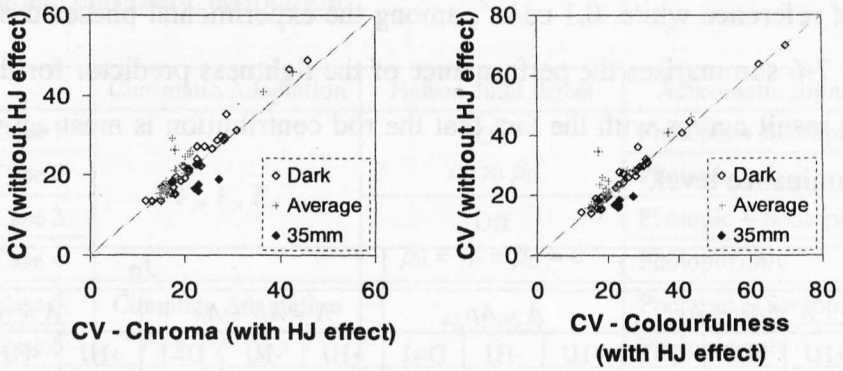


*Figure 7–1 Results of the Helson-Judd effect factor on chroma and colourfulness predictors for Hunt94*

Although there were some changes in performance according to the Helson-Judd factor, using complete chromatic adaptation gave slightly better performance through out all experimental phases. There was little impact on chroma and colourfulness performance from rod contribution, even for the Filter3 experiments.

### 7.3.3 Performance of the Hue Predictor $H_{94}$ for the Hunt94 Model

Hue is the attribute that should be affected most by the Helson-Judd factor since this effect concerns the change of hue according to the chromaticity of the illuminant. The achromatic signal is not involved in hue prediction and therefore only three combinations were tested for the hue predictor without considering rod contribution. Performance test results for hue predictor of the Hunt94 model are shown in Table 7-8.

As expected, the performances of the various combinations were quite different. The best performance was shown when complete chromatic adaptation was assumed. The

CV values in Table 7-8 are also represented as diagrams in Figure 7–2. The left diagram shows a clear distinction between the two surround conditions except four data points under dark surround. These were Phases CRT8, 9, 10 and 11. The correlated colour temperatures were 3500 K (White Fluorescent) for CRT8 and CRT9 and 2500 K (A) for CRT10 and CRT11. Also for reflective colours under the average condition, Phase R-HL5,6 and R-LL5,6 had very poor performance without the Helson-Judd factor. R-HL5 and R-LL5 used illuminant WF (3500 K) and illuminant A (3500 K) was used for R-HL6 and R-LL6. Note that, except for these eight phases, most experimental phases used correlated colour temperatures higher than 5000 K. WF and A are the most different illuminants from the equi-energy stimulus used in the colour appearance experiment. Data points for these two illuminants are shown in the right diagram in Figure 7–2. Experimental phases under illuminant A showed poorer performance without Helson-Judd effect than illuminant WF. This implies that the Helson-Judd factor should be included regardless of surround condition for low colour temperature illuminants.

| CV | Hue Quadrature H | | |
|---|---|---|---|
| | +HJ | -HJ | D=1 |
| Dark | 10.9 | 10.1 | 9.6 |
| Average | 7.5 | 10.3 | 6.5 |
| All | 9.5 | 10.2 | 8.3 |

***Table 7-8 CV values of hue predictor H***

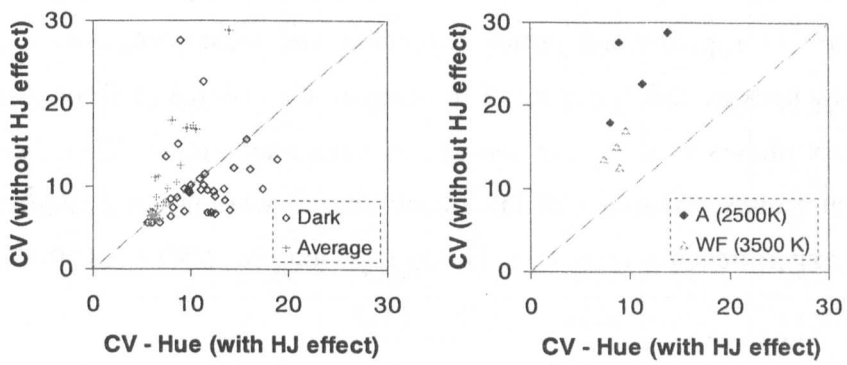


***Figure 7–2 Effect of the Helson-Judd effect factor on hue predictors for Hunt94***

### 7.3.4 Summary of optimum model parameter setting for Hunt94

Based on the performance test of Hunt94 using several parameter combinations, the following four points are concluded.

(1) Lightness predictor $J_p$ works better than $J$ in any surround condition.
(2) Complete chromatic adaptation works better than using the partial chromatic adaptation function.
(3) When partial chromatic adaptation is used the Helson-Judd factor should be included for average surround but not for dark surround. Excluding the Helson-Judd factor in dark surround conditions might slightly deteriorate the performance of colourfulness but improve the performance of hue.
(4) Even under dark surround, the Helson-Judd effect should be included when the chromaticity of the reference white is that of illuminant WF (3500K) or A (2500K).

## 7.4 Quantitative Performance Test Results of Colour Appearance Models

In this section, the performances of lightness, chroma, colourfulness and hue predictors of eight colour appearance models are represented using CV values between predicted and visual data. The average CV of each surround condition is given together with those of all the phases. Performance change by background luminance factor (black, grey, white) was also tested. Model performance represented by CV values is experimental group dependent and most phases were conducted against a grey background. It is not fair to compare the average of 50 phases with that of five or six phases to show the average of each background. Therefore only the experimental groups containing all three backgrounds were used to calculate average CV. These experimental groups were Group C, Group M, CRT1,2,3, R-HL1,2,3 and R-LL1,2,3.

Each model was tested twice, for partial and complete chromatic adaptation. For the latter, parameter $p$ (the proportion of complete von Kries adaptation) was set to one for RLAB while parameter $D$ (cognitive discounting-the-illuminant) was not changed. $D$ was set to one for average surround and 0.5 for dark surround. For other models,

parameter or function $D$ was set to one for complete chromatic adaptation. For the Hunt94 model, the Helson-Judd factor was included for average surround and excluded for dark surround. Lightness predictor $J_p$ was used for all phases for the Hunt94 model.

### 7.4.1 Performance of Lightness Predictors

Table 7-9 summarises the performance of lightness predictors in terms of CV values. The effect is minor but the dark surround condition shows a slightly better performance when chromatic adaptation is complete and the opposite for average surround. Every model tested except Hunt94 shows this effect. Hunt94 shows better performance under complete adaptation for both dark and average surround conditions. Another feature shown by all models is that the performance became poorer for a lighter background. Black background shows the best performance and white background is worst. In particular this effect is most significant for CIELAB and RLAB, in which lightness predictors do not have background dependency. In general, Hunt94 shows the best performance for lightness prediction followed by the CIECAM97s-based models, which are CIECAM97s, FC, Fairchild and CIECAM02.

| Lightness | | | CIELAB | LLAB | RLAB | Hunt94 | CIECAM 97s | FC | Fairchild | CIECAM 02 |
|---|---|---|---|---|---|---|---|---|---|---|
| Surround | Dark | $D$ | 18.12 | 15.88 | 29.91 | 13.67 | 15.96 | 15.31 | 14.79 | 16.02 |
| | | $D$=1 | | 15.78 | 29.57 | 13.58 | 15.85 | 15.27 | 14.70 | 15.96 |
| | Average | $D$ | 21.29 | 13.15 | 18.60 | 10.94 | 11.49 | 11.73 | 12.28 | 11.66 |
| | | $D$=1 | | 13.15 | 20.26 | 10.85 | 12.07 | 12.37 | 13.11 | 11.69 |
| Background | Black | $D$ | 13.90 | 10.54 | 15.05 | 10.76 | 10.36 | 10.85 | 9.73 | 10.64 |
| | | $D$=1 | | 10.49 | 15.87 | 10.67 | 11.57 | 10.68 | 9.60 | 10.47 |
| | Grey | $D$ | 19.15 | 13.29 | 23.42 | 12.61 | 12.67 | 13.54 | 12.94 | 13.38 |
| | | $D$=1 | | 13.18 | 24.31 | 12.52 | 12.58 | 13.50 | 12.83 | 13.32 |
| | White | $D$ | 35.26 | 16.74 | 44.13 | 13.67 | 15.81 | 16.80 | 15.50 | 17.40 |
| | | $D$=1 | | 16.61 | 43.92 | 13.57 | 15.75 | 16.78 | 15.42 | 17.35 |
| | All | $D$ | 19.22 | 14.94 | 26.00 | 12.73 | 14.62 | 14.31 | 14.22 | 14.54 |
| | | $D$=1 | | 14.87 | 26.35 | 12.63 | 14.54 | 14.27 | 14.15 | 14.49 |

***Table 7-9 CV Performance test results for lightness predictors***

### 7.4.2 Performance of Brightness Predictors

There is only one data set having visual brightness assessment results: R-VL in the LUTCHI data, which has 12 phases. The first six phases were used to estimate

lightness and the other six phases were used to estimate brightness using exactly the same experimental conditions as the first six phases. Table 7-10 shows the CV values for each model. CIECAM02 shows the worst performance and the other models have similar performances to each other.

| Brightness | | | CIELAB | LLAB | RLAB | Hunt94 | CIECAM 97s | FC | Fairchild | CIECAM 02 |
|---|---|---|---|---|---|---|---|---|---|---|
| R-VL | Average Surround | *D* | N/A | N/A | N/A | 11.99 | 13.61 | 13.02 | 12.14 | 22.29 |
| | | *D*=1 | N/A | N/A | N/A | 11.54 | 13.63 | 14.92 | 12.10 | 22.28 |

***Table 7-10 CV Performance test results for brightness predictors***

The performances of brightness predictors were further analysed by comparing them with those of lightness. Note that brightness and lightness predictors are positively correlated to each other in all models. Table 7-11 gives the CVs for brightness and lightness predictors in the R-VL experiments. Performances between the two attributes are similar for CIECAM97s and FC while Fairchild shows better performance for predicting brightness than lightness. CIECAM02 shows the best performance for lightness and the worst for brightness. CIECAM02 has a different function for brightness prediction compared to other CIECAM97s-based models and this new function has deteriorated performance especially under low luminance levels. The discrepancy between lightness and brightness performance suggests that each model can be improved by correcting one of the attributes since these two attributes are closely associated with each other. This is illustrated by the fact that poor performance of lightness in the Fairchild model was improved by modifying the power function in the FC model to produce good performances for the lightness and brightness predictors at the same time [Hunt2002, Section 2.8.7].

| CV | Brightness | | | | | Lightness | | | | |
|---|---|---|---|---|---|---|---|---|---|---|
| | Hunt 94 | CIE-CAM97s | FC | Fair-child | CIE-CAM02 | Hunt 94 | CIE-CAM97s | FC | Fair-child | CIE-CAM02 |
| R-VL1, 7 | 7.72 | 7.84 | 7.75 | 7.86 | 10.26 | 14.22 | 14.18 | 12.29 | 15.63 | 13.92 |
| R-VL2, 8 | 9.13 | 10.70 | 10.65 | 9.40 | 15.20 | 13.02 | 12.52 | 11.30 | 14.31 | 10.88 |
| R-VL3, 9 | 17.58 | 20.90 | 19.23 | 18.05 | 16.73 | 14.45 | 13.78 | 12.83 | 16.08 | 11.60 |
| R-VL4,10 | 7.68 | 9.17 | 9.16 | 7.77 | 23.80 | 12.18 | 11.55 | 10.91 | 14.57 | 9.40 |
| R-VL5,11 | 10.59 | 12.97 | 11.93 | 10.83 | 26.94 | 13.99 | 12.70 | 12.64 | 16.87 | 10.21 |
| R-VL6,12 | 16.52 | 20.10 | 19.39 | 18.94 | 40.80 | 18.34 | 16.72 | 17.71 | 21.46 | 15.35 |
| Average | 11.54 | 13.61 | 13.02 | 12.14 | 22.29 | 14.37 | 13.57 | 12.95 | 16.49 | 11.89 |

***Table 7-11 Performance comparison between brightness and lightness predictors***

### 7.4.3 Performance of Chroma Predictors

The performance of chroma predictors are summarised in Table 7-12. Note that the performance test of the chroma predictor was done by applying a different scaling factor for each phase. As mentioned earlier, the CIELAB chroma predictions do not consider the colour appearance change caused by surround or background conditions. There is little performance difference between dark and average surround but CIELAB $C^*$ performed less well under the white background than the other backgrounds, implying that chroma change by background luminance factor needs to be considered in colour appearance models.

| Chroma | | | CIELAB | LLAB | RLAB | Hunt94 | CIECAM 97s | FC | Fairchild | CIECAM 02 |
|---|---|---|---|---|---|---|---|---|---|---|
| Surround | Dark | $D$ | 26.26 | 20.74 | 26.35 | 22.32 | 20.18 | 20.52 | 24.78 | 20.55 |
| | | $D$=1 | | 21.26 | 27.49 | 21.73 | 20.83 | 21.18 | 25.90 | 22.31 |
| | Average | $D$ | 26.44 | 22.12 | 29.33 | 19.03 | 18.60 | 18.83 | 21.76 | 19.13 |
| | | $D$=1 | | 22.12 | 29.32 | 18.14 | 18.46 | 18.67 | 21.32 | 18.84 |
| Background | Black | $D$ | 25.69 | 21.13 | 25.71 | 21.55 | 21.18 | 21.40 | 24.87 | 18.32 |
| | | $D$=1 | | 21.60 | 26.50 | 19.64 | 19.33 | 19.46 | 22.98 | 19.22 |
| | Grey | $D$ | 25.11 | 20.57 | 25.53 | 17.63 | 17.39 | 17.56 | 20.78 | 18.83 |
| | | $D$=1 | | 20.94 | 26.17 | 17.80 | 17.86 | 17.93 | 21.72 | 19.40 |
| | White | $D$ | 29.29 | 22.59 | 29.68 | 21.75 | 24.17 | 23.70 | 34.36 | 23.16 |
| | | $D$=1 | | 23.15 | 30.38 | 21.34 | 23.80 | 23.39 | 33.81 | 23.51 |
| | All | $D$ | 26.33 | 21.30 | 27.57 | 20.97 | 19.53 | 19.82 | 23.54 | 19.97 |
| | | $D$=1 | | 21.61 | 28.24 | 20.26 | 19.86 | 20.16 | 24.03 | 20.89 |

***Table 7-12 Performance test results for chroma predictors***

Chroma predictors in LLAB and RLAB do not consider chroma change due to background but include those parameters determined by surround conditions, which cannot be cancelled out by using different scaling factors. Both models show slightly worse performance under average surround than dark surround, implying that modifying the parameter for surround conditions would improve the model performance for average surround. In the case of background change, the white background shows the worst performance. Both models show slightly better performance when partial chromatic adaptation is used for dark surround and little difference for average surround.

For Hunt94 and CIECAM97s based models, the chroma predictor includes a constant called the chromatic surround induction factor ($N_c$) but the effect of this factor is cancelled out by applying different scaling factors in each phase. The chroma

predictor, however, is calculated using the lightness (or brightness in the case of Hunt94) predictor, which already takes into account the surround effect. Since CIELAB shows little difference between dark and average surround, performance differences by surround condition for Hunt94 and CIECAM97s based models are caused by the lightness performance difference. Note that average surround shows better lightness performance for these models and likewise for the chroma predictor.

Hunt94 and the other CIECAM97s-based models also consider background change to predict chroma, however, as with surround condition, most parts compensating for the effect of background change on chroma are cancelled out except for that from the lightness predictor. Most of the tested models show their best performance when the grey background was used followed by black background, however CIECAM02 shows a similar performance for both grey and black backgrounds. The white background exhibits the poorest performance for all models.

Hunt94 has better performance for complete rather than incomplete chromatic adaptation. In the case of CIECAM97s-based models, however, dark surround has better performance when the chromatic adaptation function is used and assuming complete chromatic adaptation works better under the average surround conditions, which is the opposite effect compared to the lightness results. As with the lightness case, the performance difference due to the chromatic adaptation function was minor. In general CIECAM97s-based models performed well except for the Fairchild model.

### 7.4.4 Performance of Colourfulness Predictors

Test results for the colourfulness predictors are shown in Table 7-13. General performances in terms of CV values are similar between all models except for the Fairchild model, which showed a much poorer performance.

CIECAM97s-based models calculate colourfulness by multiplying an adaptation luminance dependency function such as $F_L^{0.25}$ in CIECAM02 to the chroma predictor. Therefore examining the performance change by luminance level is important when comparing the colourfulness performance of the models. This cannot easily be shown using the averaged CV values in Table 7-13 since CV values cannot indicate if a large CV value is caused by data scattering or by some systematic change. More detailed

colourfulness performance change by luminance level will be discussed in Section 7.5.1.

Colourfulness performance change by background luminance factor was similar to that of the chroma predictor. All models showed their best performance for grey background and were poorer for black and white backgrounds. However black and white backgrounds show poorer performance compared to chroma predictors. The colourfulness or chroma performance changes by background luminance factor which occur in CIECAM97s, FC, Fairchild and CIECAM02 result from the function $N_{cb}$, whose effect is cancelled out for the chroma performance test by the scaling factor. The effect of background on colourfulness in Hunt94 is more complicated but mostly from $N_{cb}$, which has exactly the same form for all these models as given in Eq. ( 7-2 ). Performance difference between chroma and colourfulness strongly suggests that the function $N_{cb}$ needs to be modified to improve the models' performances.

$$N_{cb} = 0.725 \cdot \left(\frac{Y_w}{Y_b}\right)^{0.2} \qquad (7\text{-}2)$$

Like chroma predictors, colourfulness predictors also showed the same change by chromatic adaptation factors. Hunt94 showed better performance for complete chromatic adaptation under both surround conditions while only under average surround for other models.

| Colourfulness | | | CIELAB | LLAB | RLAB | Hunt94 | CIECAM 97s | FC | Fairchild | CIECAM 02 |
|---|---|---|---|---|---|---|---|---|---|---|
| Surround | Dark | *D* | | 23.96 | | 25.72 | 22.79 | 23.15 | 28.84 | 24.60 |
| | | *D*=1 | | 24.50 | | 25.65 | 23.33 | 23.72 | 29.92 | 25.49 |
| | Average | *D* | | 20.97 | | 21.26 | 20.53 | 20.79 | 24.50 | 21.56 |
| | | *D*=1 | | 20.98 | | 20.59 | 20.42 | 20.70 | 24.37 | 21.47 |
| Background | Black | *D* | | 20.68 | | 25.26 | 21.02 | 20.94 | 23.58 | 23.09 |
| | | *D*=1 | | 21.51 | | 25.36 | 21.47 | 21.61 | 24.58 | 23.91 |
| | Grey | *D* | | 20.40 | | 17.64 | 17.40 | 17.57 | 20.81 | 18.95 |
| | | *D*=1 | | 21.16 | | 17.81 | 17.87 | 17.95 | 21.76 | 19.54 |
| | White | *D* | | 21.48 | | 22.36 | 26.79 | 26.09 | 38.89 | 24.33 |
| | | *D*=1 | | 22.09 | | 21.89 | 26.58 | 25.92 | 38.72 | 24.65 |
| | All | *D* | | 22.74 | | 23.89 | 21.86 | 22.18 | 27.06 | 23.35 |
| | | *D*=1 | | 23.05 | | 23.57 | 22.14 | 22.48 | 27.65 | 23.84 |

***Table 7-13 CV Performance test results for colourfulness predictors***

### 7.4.5 Performance of Hue Predictors

The CV values of hue predictors are summarised in Table 7-14. CIECAM97s-based models show similarly good performances for hue prediction. The effect of chromatic adaptation factor on hue performance was also similar to that of chroma and colourfulness. Complete chromatic adaptation showed better performance for average surround conditions and the opposite for dark surround. Hue predictors in CIECAM97s-based models do not contain surround or background factors. It is believed that performance differences by these two factors indicate a difference in visual data due to scattering rather than a general systematic change.

| Hue | | | CIELAB | LLAB | RLAB | Hunt94 | CIECAM 97s | FC | Fairchild | CIECAM 02 |
|---|---|---|---|---|---|---|---|---|---|---|
| Surround | Dark | *D* | | 9.78 | 12.02 | 8.97 | 8.45 | 8.60 | 8.46 | 8.30 |
| | | *D*=1 | | 10.72 | 13.36 | 9.58 | 9.34 | 9.35 | 9.40 | 9.23 |
| | Average | *D* | | 7.66 | 10.09 | 7.47 | 7.08 | 7.04 | 7.12 | 6.55 |
| | | *D*=1 | | 7.66 | 10.08 | 6.47 | 6.42 | 6.41 | 6.46 | 6.26 |
| Background | Black | *D* | | 8.67 | 10.00 | 9.36 | 7.66 | 7.45 | 7.67 | 7.18 |
| | | *D*=1 | | 8.99 | 10.46 | 7.33 | 7.41 | 7.38 | 7.47 | 7.22 |
| | Grey | *D* | | 8.88 | 11.39 | 8.22 | 7.84 | 7.95 | 7.87 | 7.53 |
| | | *D*=1 | | 9.50 | 12.27 | 8.40 | 8.17 | 8.19 | 8.23 | 8.05 |
| | White | *D* | | 9.58 | 11.04 | 8.58 | 8.58 | 8.67 | 8.61 | 8.53 |
| | | *D*=1 | | 9.67 | 11.40 | 8.47 | 8.68 | 8.63 | 8.72 | 8.57 |
| | All | *D* | | 8.92 | 11.23 | 8.36 | 7.88 | 7.96 | 7.91 | 7.58 |
| | | *D*=1 | | 9.47 | 12.02 | 8.30 | 8.14 | 8.15 | 8.20 | 8.01 |

***Table 7-14 CV Performance test results for hue predictors***

## 7.5 Qualitative Performance Test Results

In Section 7.4, the performances of eight colour appearance models were reported using CV values. In this section scatter diagrams are used to compare the models' prediction of colour appearance phenomena with those found in the visual data. The predicted colour appearance changes by luminance level, background luminance factor and surround condition are compared. Visual colour appearance changes by these viewing condition changes have already been shown in Chapter 6. Predicted lightness and colourfulness are shown and discussed in this section but hue is not considered since hue did not show any significant change due to the viewing parameters studied here. The models in this section used chromatic adaptation functions except for Hunt94, which assumed complete chromatic adaptation.

### 7.5.1 Model Predictions of the Effect of Luminance Levels

The experimental phases used to test the model prediction of colour appearance change by luminance level are listed in Table 7-15. These are part of the Group P, Group F and R-VL experiments. The R-VL experiment has six luminance levels. Only three of them – the highest, middle and lowest luminance phases were chosen and shown here.

| Surround | Name | Device | Lum. of Ref. White ($cd/m^2$) | Background (%) |
|---|---|---|---|---|
| Dark | P-Grey | LCD Projector | 154.0 | 18.34 |
| | P-Filter | | 18.77 | 18.68 |
| | Filter0-02 | CRT Monitor | 87.37 | 19.76 |
| | Filter1-02 | | 8.856 | 20.86 |
| | Filter2-02 | | 1.007 | 19.49 |
| | Filter3-02 | | 0.097 | 19.82 |
| Average | R-VL1 | Viewing Booth | 843 | 21.5 |
| | R-VL3 | | 62 | 21.5 |
| | R-VL6 | | 0.4 | 21.5 |

***Table 7-15 List of experimental phases for the model prediction test on the effect of luminance level***

#### 7.5.1.1. Predictions of Lightness Change by Luminance Level

In Section 6.3.1 it was found that colours appeared lighter under high luminance level. In other words lightness contrast was decreased as luminance level increased and this effect was more significant in dark surround conditions.

Model predictions of the lightness contrast change under dark surround are shown in Figure 7–3. These diagrams show that all models failed to predict lightness change. CIELAB does not consider luminance effect. LLAB and RLAB require the input of luminance of a reference white but their lightness predictors do not have luminance level dependent functions. These three models are, therefore, expected to fail to predict lightness change by luminance levels. However even the models compensating luminance level for lightness prediction resulted in lightness changes far smaller than the visual data. In the case of CIECAM97s, an opposite effect was shown in Figure 7–3 when lowest luminance level was compared. The odd performance of the CIECAM97s lightness predictor under low luminance level is already a well-known problem. The constant added to the achromatic signal as a noise

component prevents the lightness predictor from being zero when the input tristimulus values are zero and this effect becomes more serious under low luminance levels. Refer to Section 2.8.5.4 for the details.

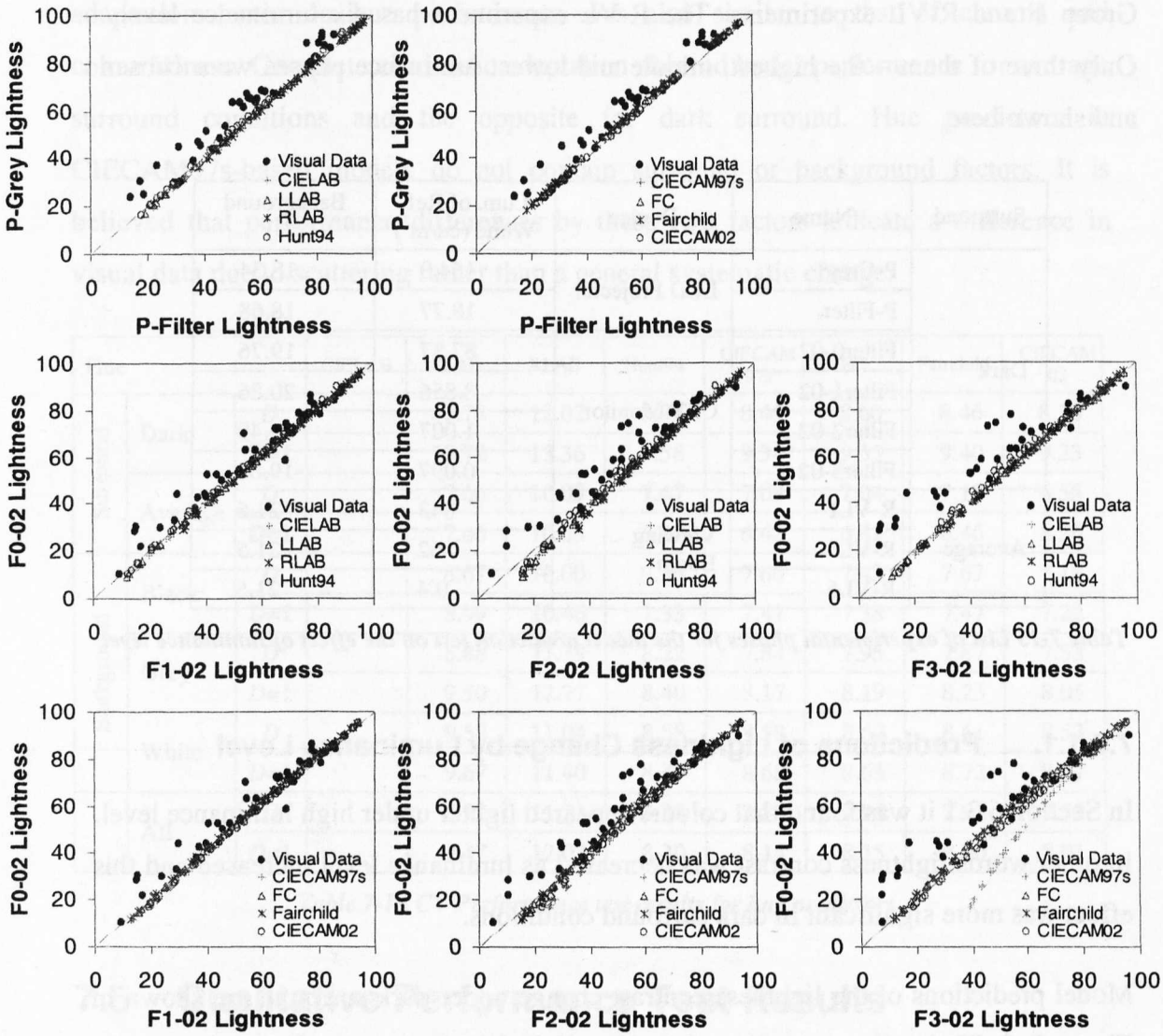


*Figure 7–3 Prediction of lightness contrast change by luminance level under dark surround*

Model predictions under average surround conditions were examined using the R-VL experiments from the LUTCHI data set. Figure 7–4 shows the comparison between R-VL1 and R-VL3 and between R-VL1 and R-VL6. Unlike for the dark surround conditions, several models performed quite well. Hunt94, FC and Fairchild give good results across these three luminance levels. CIECAM97s works well between R-VL1 and R-VL3 but the mathematical problem in the definition of the achromatic signal starts to affect the comparison with phase R-VL6. CIELAB, LLAB and RLAB did not

show any change as expected and CIECAM02 also failed to predict the effect as in dark surround.

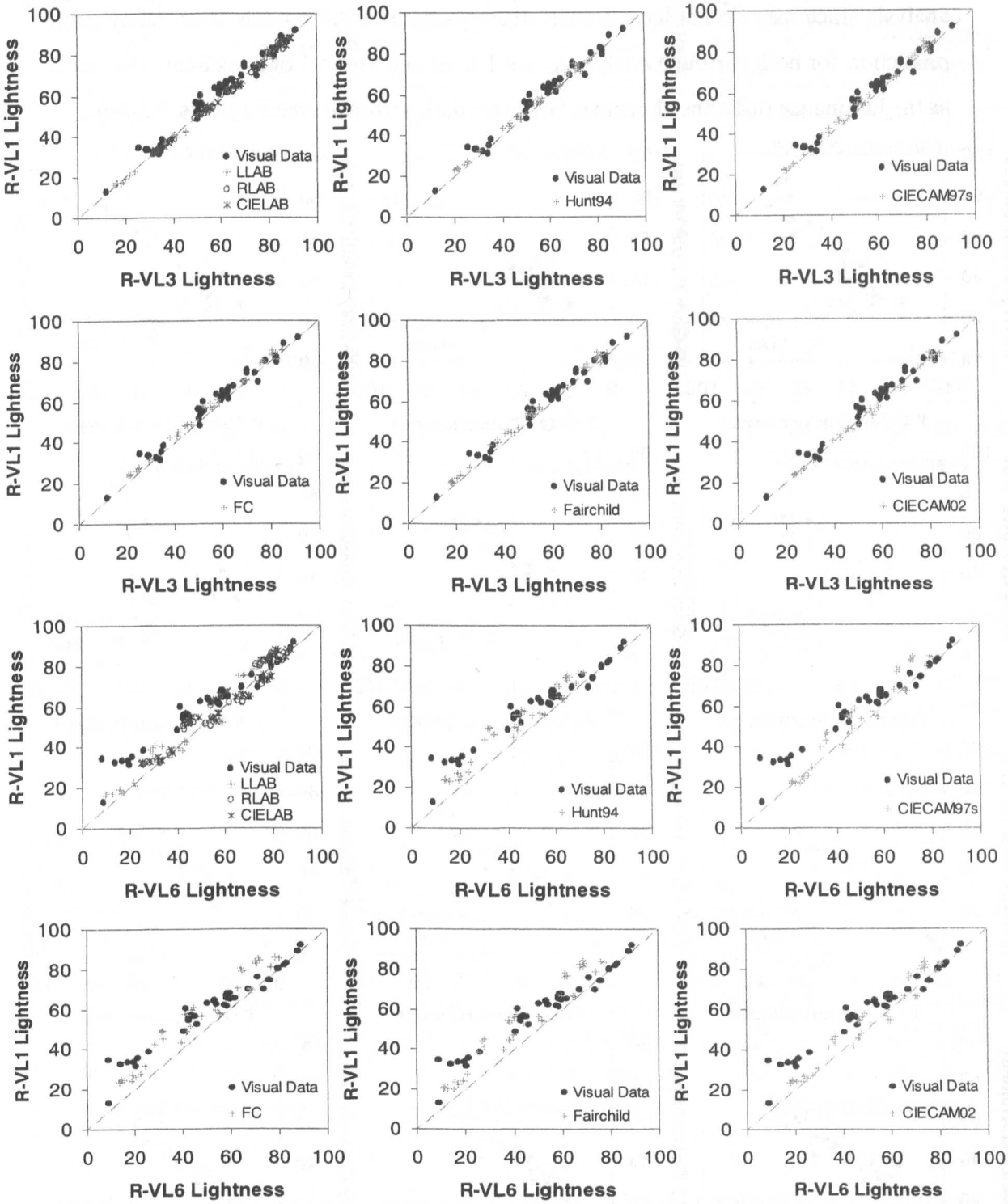


*Figure 7–4 Prediction of lightness contrast change by luminance level under average surround*

### 7.5.1.2. Predictions of Colourfulness Change by Luminance Level

Figure 7–5 shows colourfulness contrast change by luminance level for dark surround and Figure 7–6 for average surround. CIELAB and RLAB were not considered in this analysis since they do not have colourfulness predictors. All models show fairly good prediction for both surround conditions but LLAB and Hunt94 over-estimate the effect as the luminance difference becomes larger for dark surround (see F3-02 vs. F3-10).

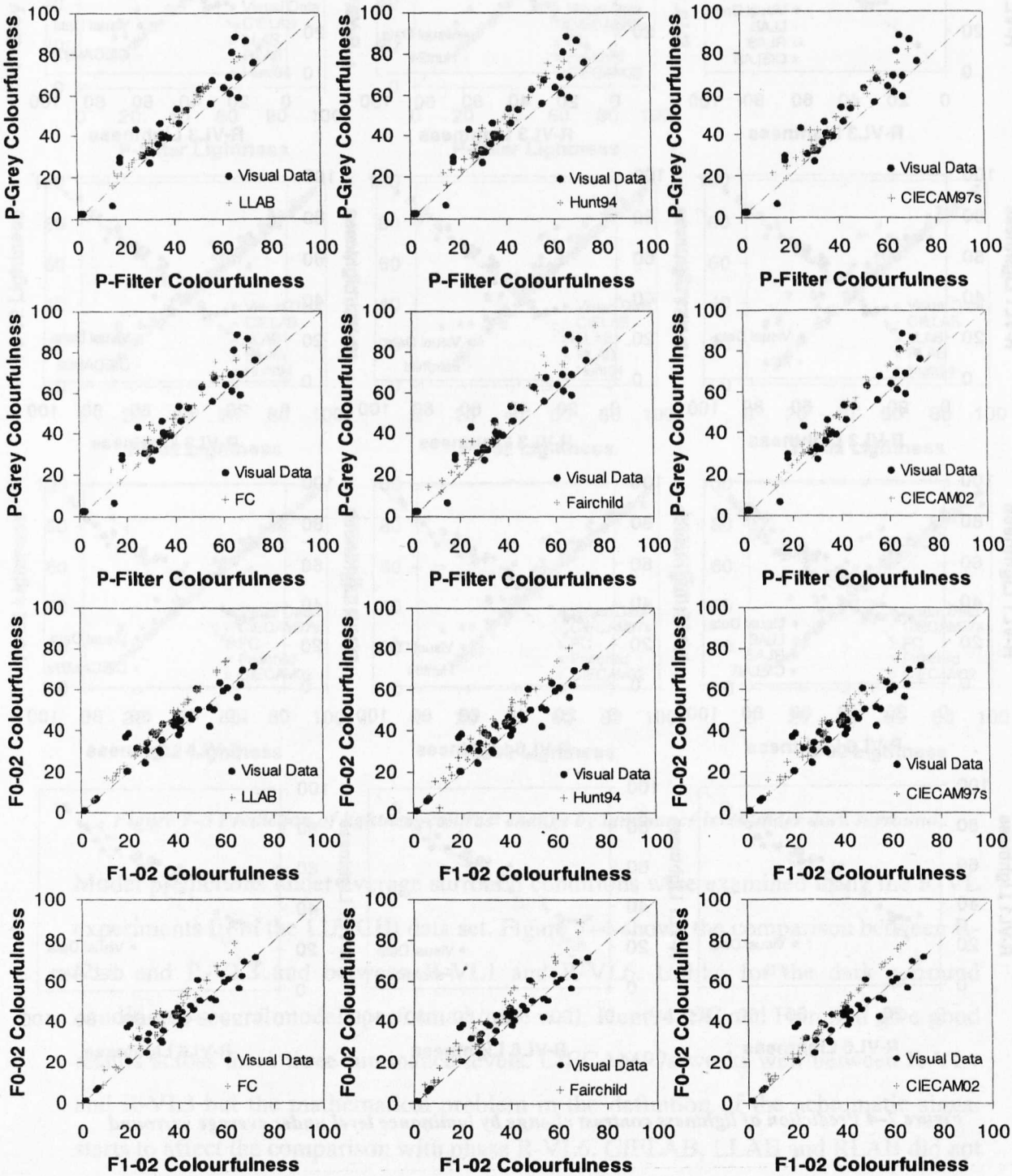


*Figure 7–5 Prediction of colourfulness contrast change by luminance level under dark surround*

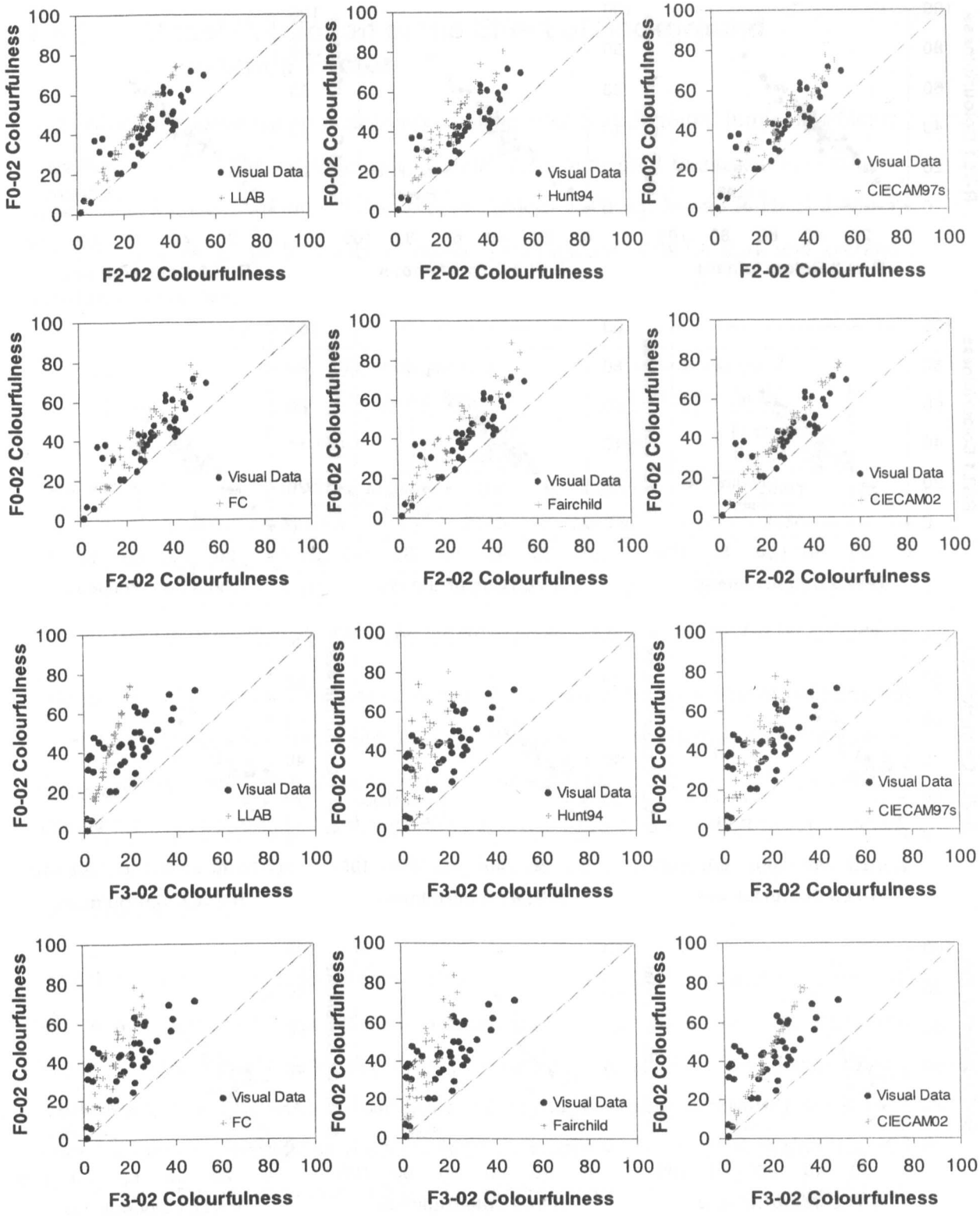


*(Continued) Figure 7–5 Prediction of colourfulness contrast change by luminance level under dark surround*

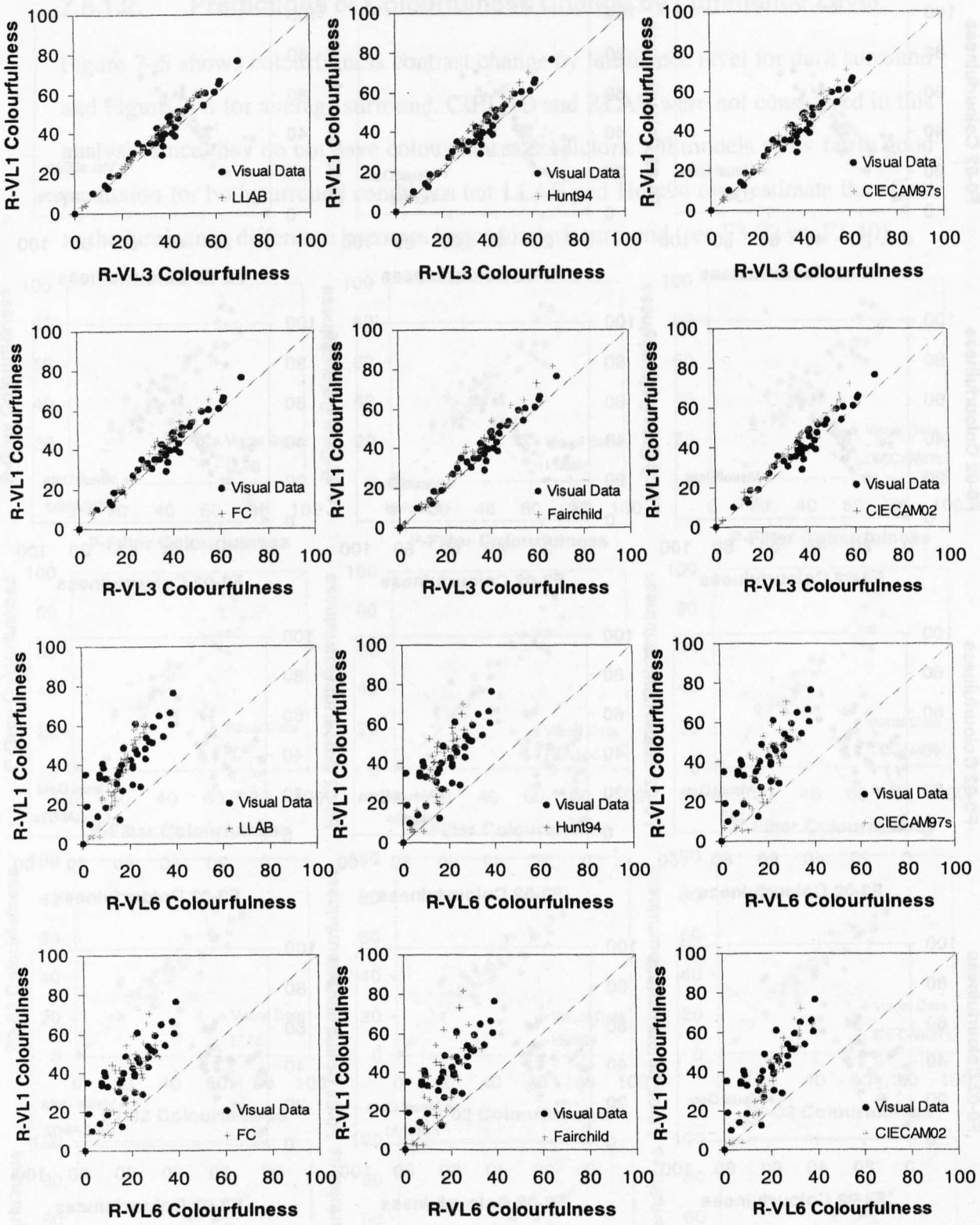


*Figure 7–6 Prediction of colourfulness contrast change by luminance level under average surround*

### 7.5.2 Model Prediction of the Effect of Background Luminance Factor

In Section 6.4, visual colour appearance changes due to background luminance factor were investigated. The relevant experimental data were used to test various colour appearance models. Among the data sets in Table 6-4, Group M and R-HL1, 2 and 3 are used to show the performance of colour appearance models for dark and average surround conditions.

| | | Higher Background Luminance Factor | | Lower Background Luminance Factor | |
|---|---|---|---|---|---|
| | | Name | Luminance Factor (%) | Name | Luminance Factor (%) |
| Dark | CII-Kwak | M-White | 100 | M-Grey | 20.65 |
| | | M-Grey | 20.65 | M-Black | 0.36 |
| Avg | LUTCHI | R-HL 1 | 100 | R-HL 3 | 21.5 |
| | | R-HL 3 | 21.5 | R-HL 2 | 6.2 |

***Table 7-16 List of experimental phases for the model prediction test on the effect of background***

Figures 7-7 and 7-8 show the predicted lightness change due to different background luminance factors with visual lightness for dark and average surround respectively. These diagrams indicate that all models are successfully predicting lightness contrast change for both surround conditions. Although there are differences between models, especially between M-Grey and M-Black, it is not clear from these diagrams which model performs best.

Model predictions of colourfulness change by background luminance factor are shown in Figure 7–9 for dark surround and in Figure 7–10 for average surround. These diagrams clearly show that most models fail to predict the visual data except for the comparison between R-HL2 (black background, average surround) and R-HL3 (grey background, average surround), where all models show good prediction. Hunt94 shows the best performance while the others predict an overall colourfulness increment for the darker background, which is not found in the visual data.

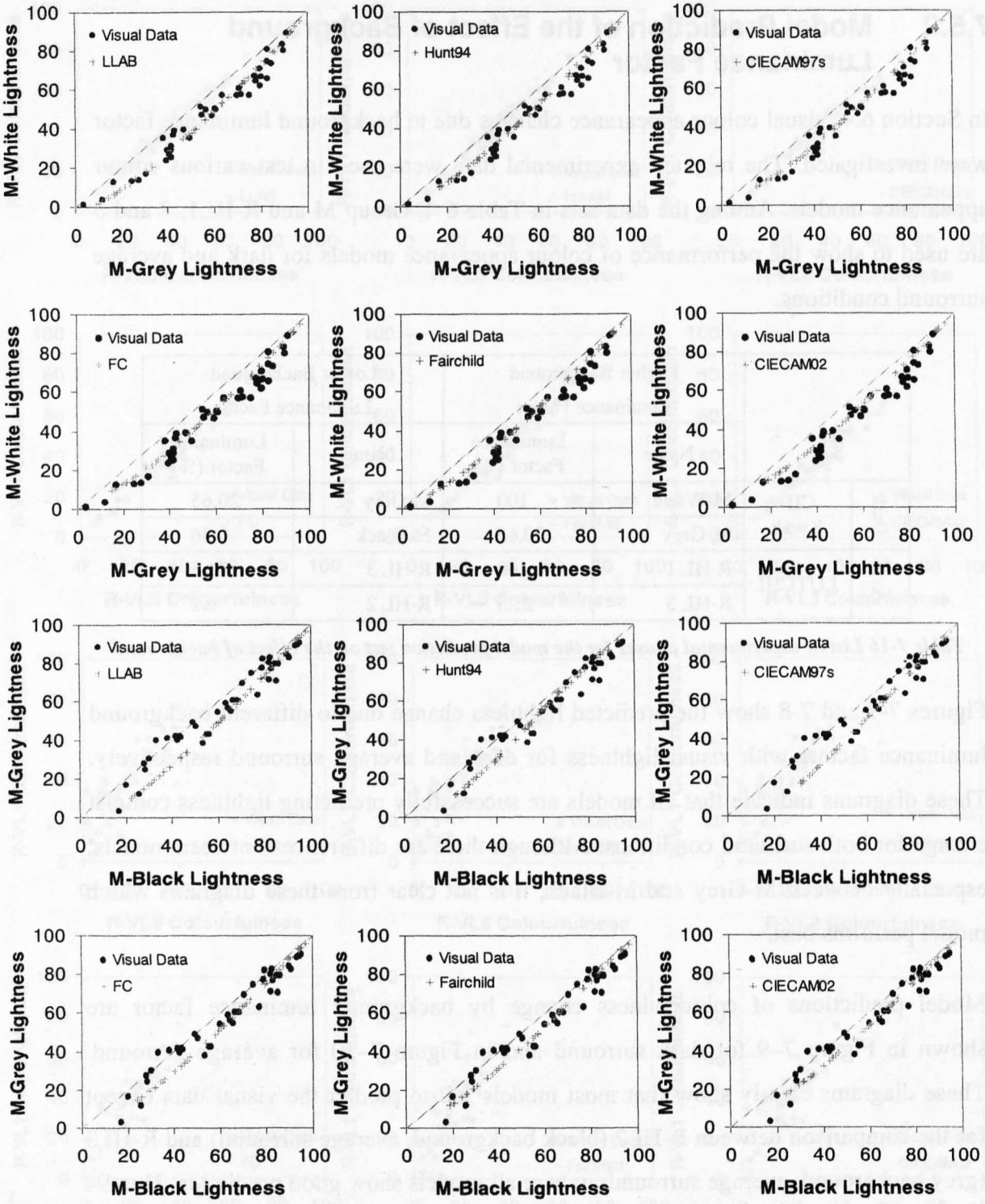


*Figure 7–7 Model predictions of lightness contrast change by background luminance factor under dark surround (Group M)*

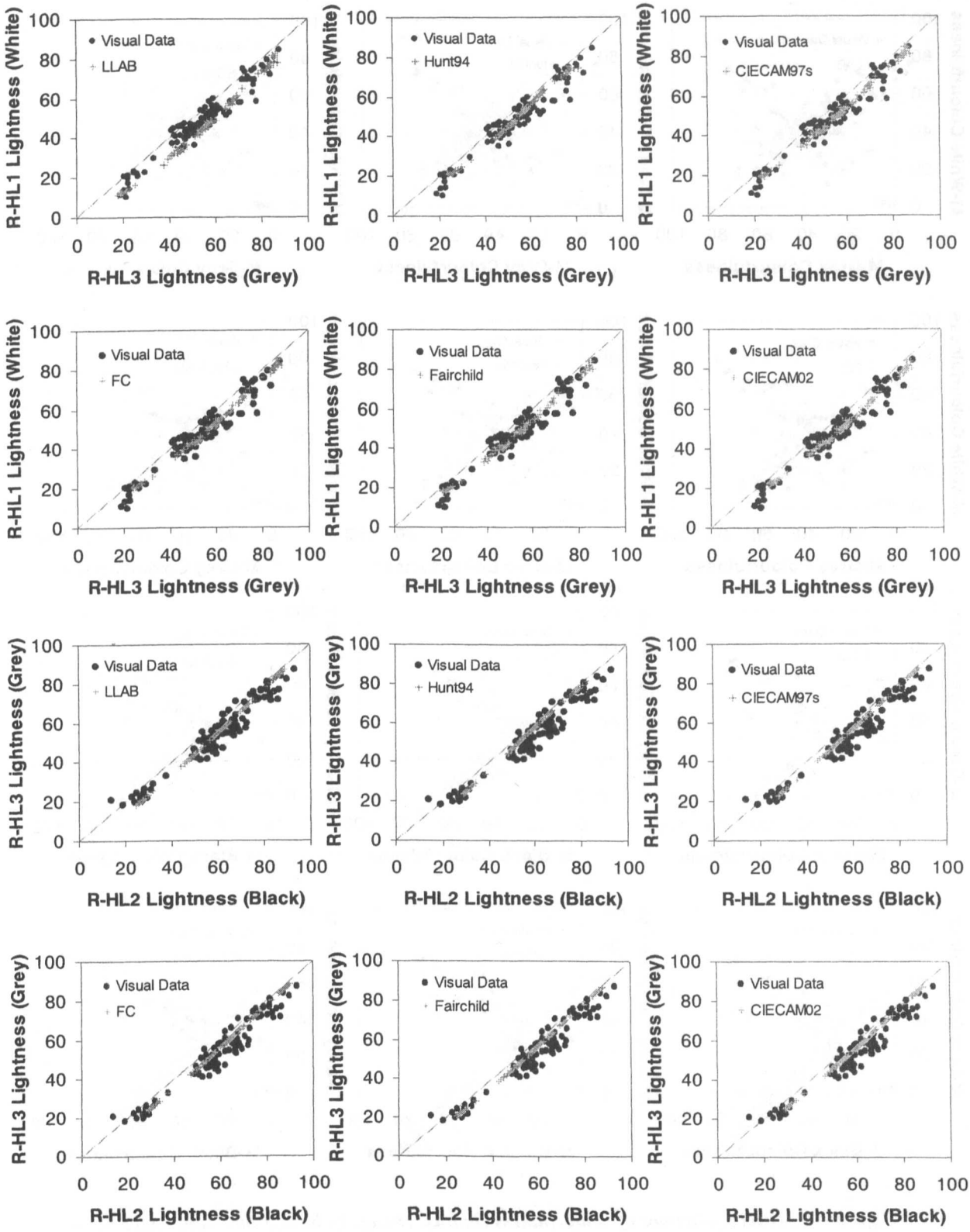


*Figure 7–8 Model predictions of lightness contrast change by background luminance factor under average surround (R-HL1,2,3)*

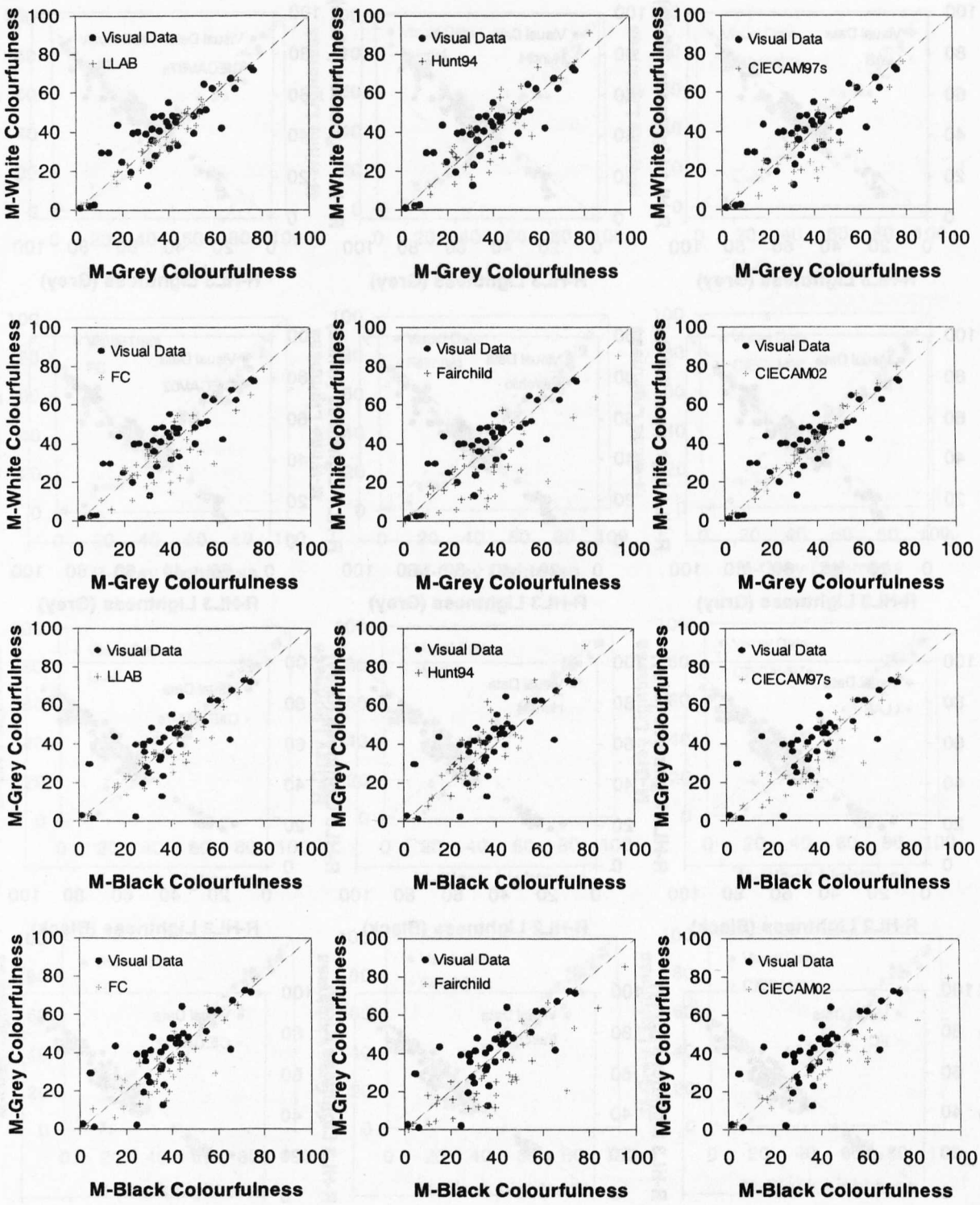


*Figure 7–9 Model predictions of colourfulness contrast change by background luminance factor under dark surround (Group M)*

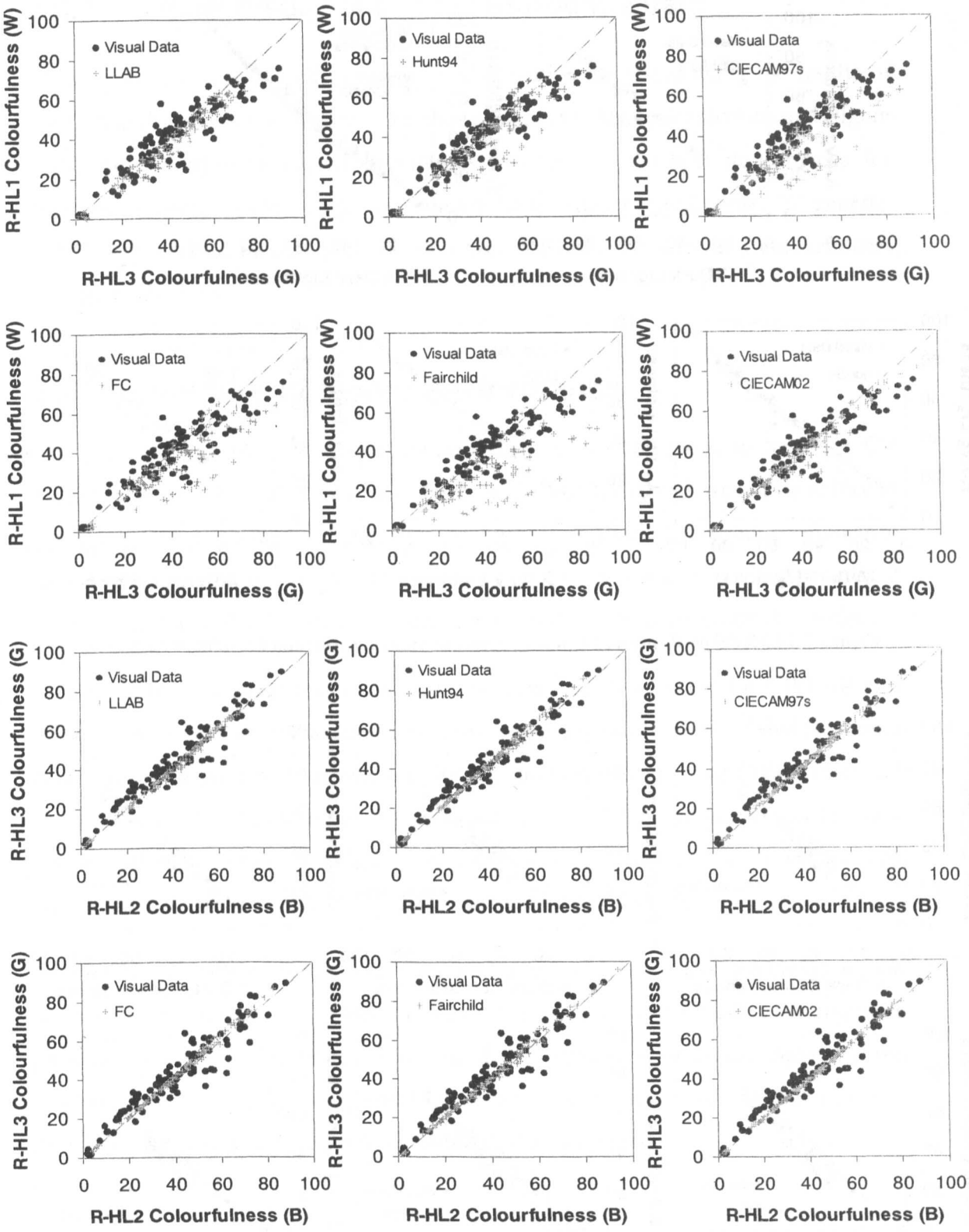


*Figure 7–10 Model predictions of colourfulness contrast change by background luminance factor under average surround (R-HL1,2,3)*

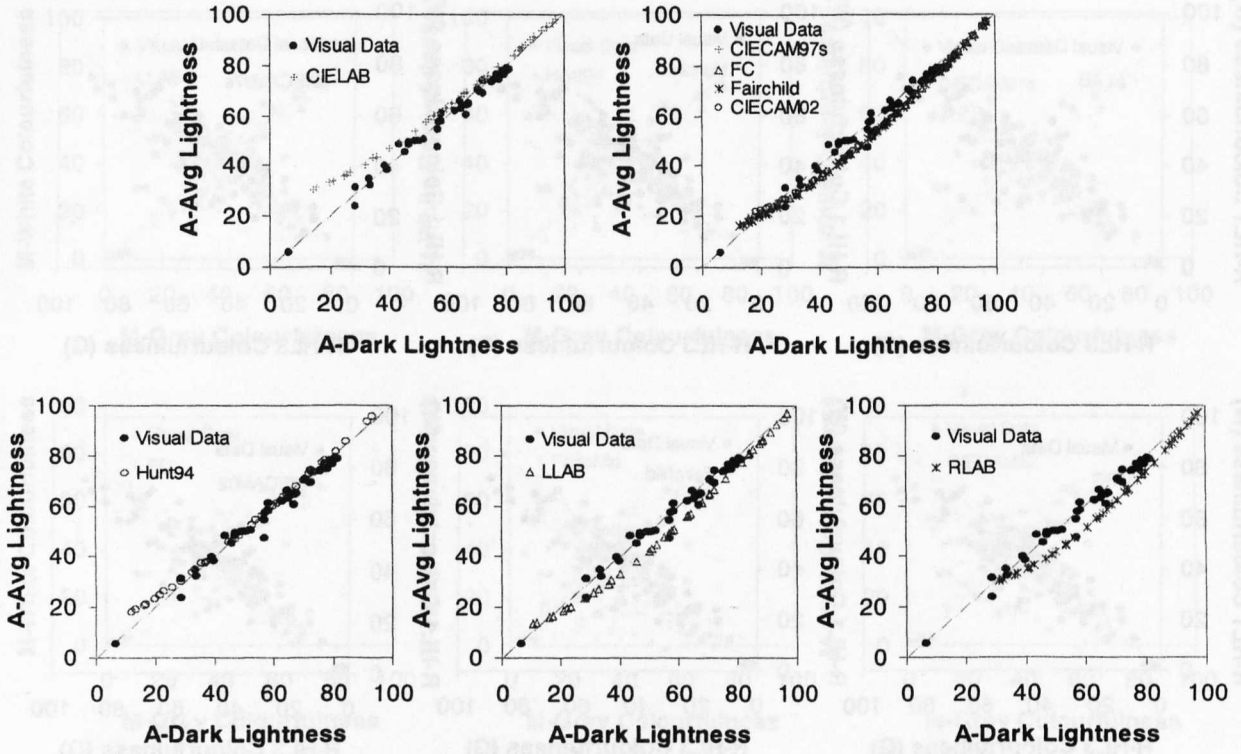


*Figure 7–11 Model predictions of lightness contrast change by surround condition (Group A)*

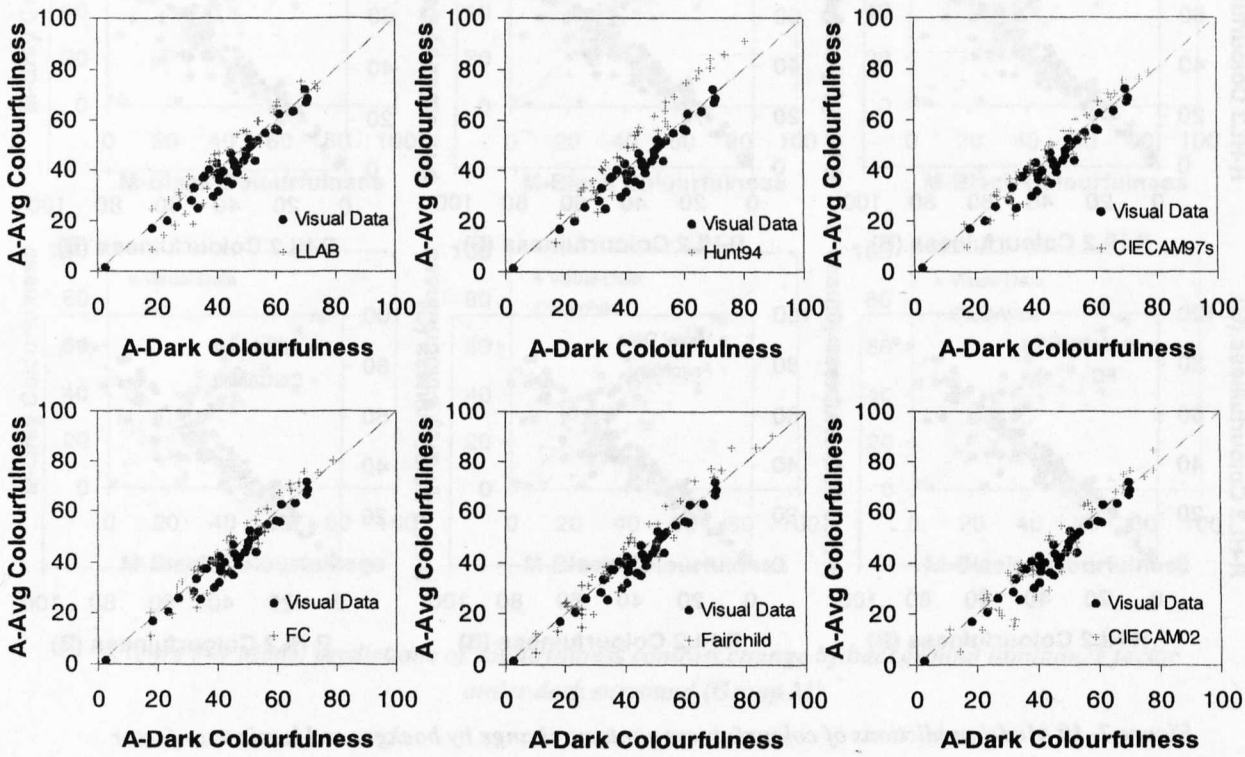


*Figure 7–12 Model predictions of colourfulness contrast change by surround condition*

### 7.5.3 Model Predictions of the Surround Effect

Model predictions of the effect of surround condition are tested using the results of the Group A experiment. Figure 7–11 shows lightness change predictions and Figure 7–12 the colourfulness change predictions. Hunt94 has the best performance for lightness change while worst for colourfulness change prediction. In general, CIECAM97s-based models perform well both for both lightness and colourfulness change predictions.

## 7.6 Summary of Model Performance

The performances of eight colour appearance models were tested in terms of CV values together with scatter diagrams. Each model was tested in terms of its ability to predict colour appearance change due to luminance level, background luminance factor and surround conditions. The CV values of each phase listed in Appendix 2 were calculated under the chromatic adaptation condition determined by the model.

In general the performances of colour appearance models – except for CIELAB and RLAB – were both good and similar in terms of their CV values. The Fairchild model had a relatively poor performance for chroma and colourfulness and CIECAM02 had the worst brightness prediction. It was found that the chromatic adaptation function did not affect the results significantly. There was little change in CV values between the calculated chromatic adaptation factor and complete adaptation.

Predictions of colour appearance phenomena showed two main problems in the current colour appearance models. Firstly all models failed to predict the lightness contrast change by luminance level in dark surround conditions. Secondly the colourfulness change by background factor was not predicted well, which was also found by comparing CV values of chroma and colourfulness.

# Chapter 8
# New Colour Appearance Model Kwak03

## 8.1 Introduction

In Chapter 7, it was shown that existing colour appearance models fail to predict several colour appearance changes especially under dark surround condition. These results strongly support the development of a new colour appearance model, Kwak03, to improve the predictions based on the analysis of the previous chapter.

Hunt said in the introduction to his latest model, Hunt94, that 'in our present state of knowledge, it is not possible to construct a model of colour vision that is supported at each stage by physiological data. In particular, quantitative modelling of the effects of adaptation and induction has to be approached at present largely empirically' [Hunt1995 p706]. Things have not changed much since Hunt's introduction was written. Most of the physiological processes of colour vision are still not well known and even the latest colour appearance models take a largely empirical approach. Note however that colour appearance models are generally developed for practical applications in the colour imaging industry. Empirically derived models may be not good enough to be used as a model of human vision but are still good enough for practical applications.

The new colour appearance model, Kwak03, has also been empirically derived using two colour appearance data sets: CII-Kwak and part of the LUTCHI data. They are the same sets used for analysing colour appearance phenomena (Chapter 6) and testing colour appearance models (Chapter 7) in this thesis.

Kwak03 follows the structure of CIECAM02, the latest colour appearance model, since it has been modified to correct several problems found in previous models. Kwak03 can be divided into three stages. Firstly, the input tristimulus values under the test conditions are transformed to compressed cone signals under the reference conditions after a chromatic adaptation process. Secondly, opponent colour signals are calculated using the compressed cone signals. Thirdly, colour appearance predictors are calculated from the three opponent colour signals.

In this chapter Kwak03 is introduced step by step and compared with CIECAM02. Note that the colour appearance data used in this study do not include dim surround conditions. Parameters for dim surround were arbitrarily taken to lie in between values for the dark and average surrounds.

## 8.2 Visual Areas Used in the Model Kwak03

The visual areas used in Kwak03 were adapted from the definitions proposed by Hunt [Hunt1995, Section 2.5.2] since they are the most widely agreed upon [Fair1995].

*Stimulus*: Typically a uniform patch of about 2° angular subtense.

*Background*: The environment of the colour element considered extending typically for about 10° from the edge of the stimulus in all, or most, directions.

*Surround*: The field outside the background.

Table 8-1 summarises the viewing angle of the displayed screen width of the CII-Kwak data sets. In most cases the viewing angles of the image correspond closely to the definition of background, subtending around 20°, except for the Group F experiments.

| | Experimental Group | Colour Patch (Stimulus) | Background | Viewing Distance |
|---|---|---|---|---|
| CII-Kwak | P | 1° | 22.1° | 300 cm |
| | M | 1° | 22.6° | 70 cm |
| | C | ~ 1° | 20° ~ 30° | 620 ~ 890 cm |
| | A | 1.4° | 30.4° | 70 cm |
| | F | 2°/10° | 40.1° | 52 cm |

***Table 8-1 Viewing angle of displayed images in the CII-Kwak data set***

Surround is defined by the relative ratio between the luminance of the reference white in the image and the luminance of surround. It is the peripheral area outside the background and it used as a categorical term in colour appearance models (refer to Section 2.5.2). In Kwak03, surround conditions are categorised as Average, Dim and Dark following the approach of CIECAM02. The Average condition covers reflective colours and self-luminous or projected images with ambient lighting only if the luminance level of ambient light was similar to that of the image. The Dark condition is for self-luminous or projected colours in a darkened room. The Dim condition is possible only for self-luminous or projected colours with significantly dim ambient lighting compared to the luminance of the displayed image. Note that reflective colours always belong to the average surround and display colours shown in a dark room always have dark surround regardless of the luminance level of the image, since surround condition is determined by 'relative luminance ratio' and this ratio is not affected by absolute luminance level.

## 8.3 Input Parameters

Table 8-2 shows the input parameters required in Kwak03. Like other CIECAM97s-based colour appearance models, Kwak03 only considers neutral backgrounds and so only the $Y$ value of background is needed. Also the equi-energy illuminant, $S_E$, is used as the reference illuminant.

| | |
|---|---|
| Samples in test condition | Relative tristimulus values $X\ Y\ Z$ |
| Reference white in test condition | Relative tristimulus values $X_w\ Y_w\ Z_w$ |
| Background in test condition | Relative tristimulus value $Y_b$ |
| Luminance of reference white in test condition | $L_w$ (cd/m$^2$) |
| Surround condition | Average, Dim or Dark |
| Reference white in reference condition | Equi-energy illuminant $S_E$<br>$X_{wr} = Y_{wr} = Z_{wr} = 100$ |

***Table 8-2 Input parameters for Kwak03***

Kwak03 needs the luminance of the reference white instead of the luminance of the adapting field that is used in CIECAM97s based models. Using the luminance of reference white is mathematically convenient and it is an attempt to distinguish between the effect of the luminance of reference white and that of background luminance factor. The luminance of the adapting field used in the other models is a

multiplication of the luminance of the reference white with the background luminance factor divided by 100. Therefore it includes two parameters. These two parameters, luminance of reference white and background luminance factor, were treated as independent variables when deriving Kwak03.

## 8.4 Chromatic Adaptation

The first step of Kwak03 is to transform the tristimulus values of the test colour under a given test condition to cone signals in a reference condition using chromatic adaptation. The chromatic adaptation equation has been taken from CIECAM02 [Moro2002], which is the latest revision of CIECAM97s.

Firstly, tristimulus values $X$, $Y$, $Z$ measured in the test viewing condition are transformed to $R$, $G$, $B$ space by a 3x3 matrix – the modified Li et al. [Li2002] matrix $M_{CAT02}$– followed by incomplete chromatic adaptation based on the simple von Kries type model. The chromatic adaptation model changes the $R$, $G$, $B$ values under the test viewing condition to $R_C$, $G_C$, $B_C$ values under the reference viewing condition under an equal-energy illuminant. Finally, $R_C$, $G_C$, $B_C$ are transformed to the Hunt-Pointer-Estevez cone space. Parameter $F$ equals one for average surround and 0.9 and 0.8 for dim and dark surrounds respectively.

$$\begin{vmatrix} R \\ G \\ B \end{vmatrix} = M_{CAT02} \cdot \begin{vmatrix} X \\ Y \\ Z \end{vmatrix} = \begin{vmatrix} 0.7328 & 0.4296 & -0.1624 \\ -0.7036 & 1.6975 & 0.0061 \\ 0.0030 & 0.0136 & 0.9834 \end{vmatrix} \cdot \begin{vmatrix} X \\ Y \\ Z \end{vmatrix}$$

$$R_C = \left[ D \cdot \left( \frac{Y_W}{R_W} \right) + 1 - D \right] \cdot R \ , \ G_C = \left[ D \cdot \left( \frac{Y_W}{G_W} \right) + 1 - D \right] \cdot G \ , \ B_C = \left[ D \cdot \left( \frac{Y_W}{B_W} \right) + 1 - D \right] \cdot B$$

where $R_W$, $G_W$, $B_W$ : $R$, $G$ and $B$ of the refrence white respectively

$$D = F \cdot \left[ 1 - \frac{1}{3.6} \cdot e^{\frac{-L_W - Y_b/100 - 42}{92}} \right]$$

$$\begin{vmatrix} R' \\ G' \\ B' \end{vmatrix} = M_H \cdot M_{CAT02}^{-1} \begin{vmatrix} R_C \\ G_C \\ B_C \end{vmatrix} = \begin{vmatrix} 0.7410 & 0.2180 & 0.0410 \\ 0.2854 & 0.6242 & 0.0904 \\ -0.0096 & -0.0057 & 1.0153 \end{vmatrix} \cdot \begin{vmatrix} R_C \\ G_C \\ B_C \end{vmatrix} \qquad (8\text{-}1)$$

## 8.5 Dynamic Adaptation Function

The next step after chromatic adaptation in CIECAM97s-based models is to apply a dynamic adaptation function to changes in the three cone signals $R'$, $G'$, $B'$. Dynamic

adaptation means adaptation of cone signals to luminance level. Note that $R'$, $G'$ and $B'$ are normalised cone signals. The role of the dynamic adaptation function is to convert these normalised values to absolute cone signals using the luminance-level adaptation factor, $F_L$, shown in Eq. ( 8-2 ) and a non-linear function. CIECAM97s, FC and Fairchild all use the same function but the latest model, CIECAM02, has a modified form. Eq. ( 8-3 ) shows the equation for CIECAM97s. This function is based on physiological measurement of primate vision [Hunt1995 p714]. Several shortcomings were found in this function [Hunt2003] leading to a revised dynamic adaptation function in CIECAM02, given in Eq. ( 8-4 ). Only the equation for the $R$ cone is shown here since other the cone signals, $G$ and $B$, have the same form.

$$F_L = 0.2 \cdot k^4 \cdot (5 \cdot L_A) + 0.1 \cdot (1 - k^4)^2 \cdot (5 \cdot L_A)^{1/3} \qquad (8\text{-}2)$$

where $L_A = L_W \cdot Y_b/100$, $k = 1/(5 \cdot L_A + 1)$

CIECAM97s/FC/Fairchild $$R_a' = 40 \frac{(F_L R'/100)^{0.73}}{(F_L R'/100)^{0.73} + 2} + 1 \qquad (8\text{-}3)$$

CIECAM02 $$R_a' = 400 \frac{(F_L R'/100)^{0.42}}{(F_L R'/100)^{0.42} + 27.3} + 0.1 \qquad (8\text{-}4)$$

In Section 6.3.1 it was shown that lightness contrast is changed by luminance level. The lightness predictor, $J$, in CIECAM97s-based models does not need information about luminance. Lightness contrast change is compensated for by the dynamic function at an earlier stage. The effectiveness of the new dynamic function in CIECAM02 in compensating for the lightness contrast change was examined by comparing two functions, $F1$ and $F2$.

$$F1 = 100 \cdot \frac{(F_L R'/100)^{0.73}}{(F_L R'/100)^{0.73} + 2} \cdot \frac{F_L^{0.73} + 2}{F_L^{0.73}} \qquad (8\text{-}5)$$

$$F2 = 100 \cdot \frac{(F_L R'/100)^{0.42}}{(F_L R'/100)^{0.42} + 27.3} \cdot \frac{F_L^{0.42} + 27.3}{F_L^{0.42}} \qquad (8\text{-}6)$$

$F1$ is from CIECAM97s and $F2$ from CIECAM02. The final term in each equation was normalised to 100 since the lightness predictor always uses a normalised achromatic signal. Also a noise factor was not considered in this comparison. Note that the noise from the three cone signals are cancelled out in lightness prediction because the sum of the noise is subtracted in the equation used to calculate the achromatic signal. Four levels of luminance of the adapting field $L_A$ (=$L_W Y_b/100$), 0.1,

10, 100 and 1000 cd/m$^2$ were input corresponding to 0.071, 0.368, 0.794 and 1.710 of the $F_L$ function and the outputs of functions $F1$ and $F2$ were compared. Figure 8–1 shows the results by plotting $F1$ and $F2$ against $R'$. The left diagram is for function $F1$ and the right is for $F2$.

The right diagram clearly shows that the $F2$ function, which is used for CIECAM02, is not changed by luminance level at all. That means that the lightness output by $F2$ cannot be changed by luminance level thus failing to compensate for lightness contrast change. Note that in Section 7.5.1.1 the model testing results using colour appearance data also showed that CIECAM02 had poorer performance at predicting lightness change by luminance level, i.e. CIECAM02 did not show any lightness change due to luminance level. The right diagram in Figure 8–1 confirms the behaviour of the lightness predictor of CIECAM02 (also see Eq. ( 8-7 )). The left diagram in Figure 8–1, which represents the dynamic function for CIECAM97s, shows some contrast change due to luminance level but this function still does not perform well because it fails to predict the visual data as shown in Section 7.5.1.1 especially for the dark surround condition.

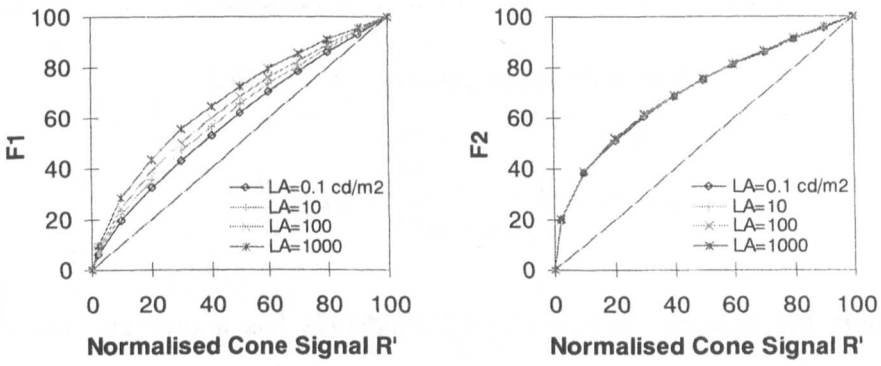


***Figure 8–1 Performance of the dynamic adaptation functions for CIECAM97s, FC, Fairchild and CIECAM02***

As mentioned earlier, the dynamic function in CIECAM02 was developed to fix the problem of CIECAM97s. The hue and saturation of CIECAM97s vary if the luminance factor changes for a colour of a given chromaticity. This is undesirable in practical applications. Firstly, a power function was tried as a solution but the current dynamic function in CIECAM02 was finally chosen so as to have a physiologically plausible form [Hunt2003].

Figure 8–2 shows the difference between the power function and the dynamic function in CIECAM02. There is little difference between the two functions when $F_L R'$ is smaller than around $10^4$, which requires $F_L$ to be larger than 100. Note that $10^8$ cd/m$^2$ of reference white, approximated by $5 \cdot L_A$, is needed to make an $F_L$ equal to 100 as shown in the right diagram. This means that the viewing conditions with a reference white of less than $10^8$ cd/m$^2$ the dynamic function in CIECAM02 behaves as a power function. Note that if a power function is used for the dynamic function, the luminance-level adaptation factor, $F_L$, is cancelled out for the lightness calculation causing no lightness contrast change due to luminance level change as shown in Eq. ( 8-7 ). This explains why CIECAM02 failed to predict visual lightness change.

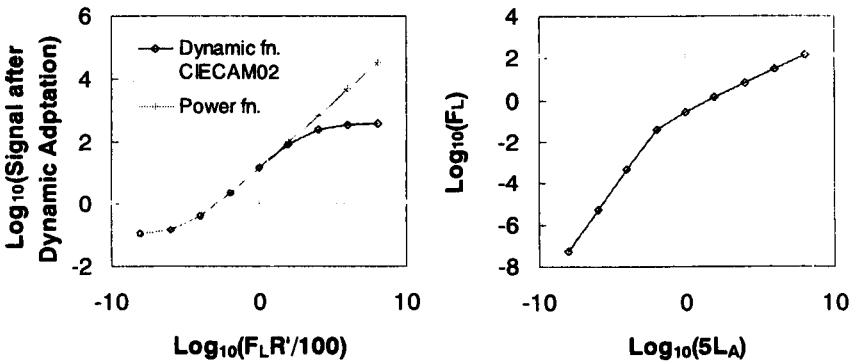


*Figure 8–2 Dynamic function of CIECAM02*

$$F3 = 100 \cdot \frac{(F_L R'/100)^{0.42}}{(F_L 100/100)^{0.42}} = 100 \cdot \left(\frac{R'}{100}\right)^{0.42} \qquad (8\text{-}7)$$

In conclusion, the dynamic function in CIECAM97s has a problem with hue and saturation change by luminance factor change and also is not effective enough to compensate for lightness contrast change. A power function for dynamic adaptation can solve the first problem in CIECAM97s but there is no lightness contrast change. Therefore in Kwak03 it was decided not to use a dynamic function to compensate for the effect of luminance level. Modifying the dynamic function for CIECAM97s or CIECAM02 was not effective enough. Instead the effect of luminance level adaptation is compensated for at later stages in the model. (Refer to Section 8.8.1.)

## 8.6 Compression of Cone Signals

It is well known that the three colour signals generated by the cone photoreceptors are transformed to one achromatic and two opponent colour difference signals. Colour appearance predictors in CIECAM97s-based models also use the latter three signals – one achromatic and two colour difference signals – rather than using the cone signals directly.

Hunt found that if the cone responses are taken as being proportional to the square-root of the stimulus intensity, the curvatures of the lines of constant hue represented by the four unique NCS hues in chromaticity diagrams can be predicted well using a simple criterion for constant hue [Hunt1998 P.212, Hunt1982]. Note that the cone signals $R'$, $G'$, $B'$ calculated from Eq. ( 8-1 ) have a linear relationship with normalised tristimulus values $X$, $Y$, $Z$ which themselves are linearly related to stimulus intensity. Hunt's finding suggests that compressed cone signals need to be used to calculate achromatic and colour difference signals. Therefore although a dynamic adaptation function was not introduced in Kwak03, the cone signals $R'$, $G'$, $B'$ still need to be compressed as $R_k'$, $G_k'$, $B_k'$ to improve the performance. Compression is done using the power function given in Eq. ( 8-8 ).

$$R_k' = \left(\frac{R'}{100}\right)^{0.42}, \quad G_k' = \left(\frac{G'}{100}\right)^{0.42}, \quad B_k' = \left(\frac{B'}{100}\right)^{0.42} \qquad (8\text{-}8)$$

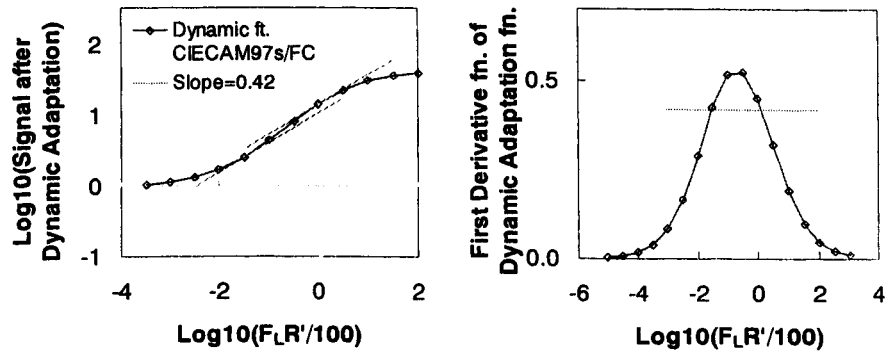


*Figure 8–3 Dynamic function of CIECAM97s and FC and its first derivative function*

The exponent in each of the power functions follows that of the dynamic adaptation function in CIECAM02, which is in turn based on the dynamic function of CIECAM97s [Hunt2003]. Figure 8–3 shows the dynamic function of CIECAM97s

with its first derivative function (right diagram). The approximate central value of the exponent, 0.42 makes the power function close to the dynamic function used for CIECAM97s.

Note that using the newly-derived cone signals $R_k'$, $G_k'$, $B_k'$, compressed using the power function solves the problem of hue and saturation differences of colours with the same chromaticity but different luminance factors in CIECAM97s. In the CIECAM97s-based models, the hue and saturation of two colours would be same if the ratios between their compressed cone signals, $R_k':G_k':B_k'$ were the same regardless of their luminance factors. (See Eq. ( 8-18 ) for the hue predictor and Eq. ( 8-32 ) for the saturation predictor.) Cone signals $R'$, $G'$, $B'$ are linearly related to the change in luminance factor and linear changes to cone signals do not affect the ratios of cone signals compressed by the power function. In contrast, cone signals compressed by the dynamic function in CIECAM97s have non-linear relationships between them.

Table 8-3 shows an example of cone signal ratio changes due to luminance factor with the same chromaticity for CIECAM97s and Kwak03. The ratios between the three cones are normalised for the green cone.

| Test Colours ($x$, y, $Y$) | CIECAM97s ( $R_a' : G_a' : B_a'$ ) | Kwak03 ( $R_k' : G_k' : B_k'$ ) |
|---|---|---|
| (0.35, 0.55, 15) | 0.939: 1.000 : 0.471 | 0.949: 1.000 : 0.480 |
| (0.35, 0.55, 60) | 0.936 : 1.000 : 0.403 | 0.949: 1.000 : 0.480 |

***Table 8-3 Example of compressed cone signal ratio changes for CIECAM97s and Kwak03***

## 8.7 Opponent Colour Signals

As mentioned earlier, Kwak03 also follows the zone theory in that compressed cone signals are changed to opponent colour signals, which should be used for colour appearance predictors. Opponent colour signals consist of an achromatic signal, $A$, and two colour difference signals, $a$ and $b$, like CIELAB or other CIECAM97s-based models.

### 8.7.1 Achromatic Signal A

An achromatic signal in photopic vision is a function of the signals from the three different types of cones. Since the numbers of the three types of cone are not equal, the contribution of each type to the achromatic signal is also not equal. The ratios of

$R_k'$ to $G_k'$ to $B_k'$ are assumed to be 40 to 20 to 1 in the Hunt94 model [Hunt1995 p720, Walr1966] and all other CIECAM97s-based models follow this assumption.

During the optimisation process to derive the new colour appearance model, it was found that changing the ratios between the three types of cone signals could dramatically improve the performance of lightness predictor. For CIECAM97s-based models, the optimised ratio was 2:1:0.5 instead of 2:1:0.05 for $R_k':G_k':B_k'$ indicating that the role of the blue cone needs more emphasis. Table 8-4 shows the performance test results of the lightness predictor in CIECAM02. The first column is from the original achromatic signal and the second column is the result when the new achromatic signal is used. This table clearly shows that there is a significant performance improvement by changing the equation of the achromatic signal. Figure 8–4 shows an example of improvement in lightness prediction.

| Average CV for Lightness Predictor $J$ | Original CIECAM02 $A = 2R'_a+G'_a+0.05B'_a$ | CIECAM02 with Modified $A$ $= 2R'_a+G'_a+0.5B'_a$ |
|---|---|---|
| CII-Kwak | 16.06 | 15.16 |
| LUTCHI | 13.72 | 11.94 |
| All | 14.46 | 12.95 |

***Table 8-4 Performance change of lightness predictor J by changing the ratios of cone signals for CIECAM02***

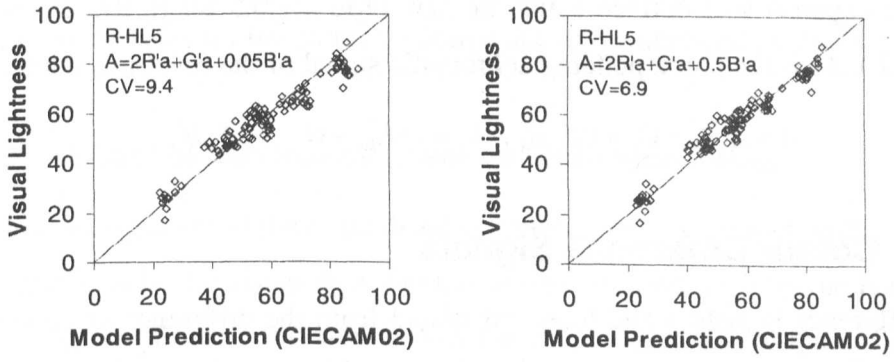


***Figure 8–4 Effect of achromatic signal change (Phase R-HL5)***

The effect of changing the cone signal ratios was examined using the spectral sensitivity curves of cones and achromatic signal in CIECAM02. Spectral sensitivity curves were calculated using the 2° CIE colour matching functions and are shown in Figure 8–5. The left figure shows the spectral sensitivity of the compressed cone signals and the right figure compares the three achromatic sensitivity curves. These

consist of two achromatic curves, $A$ (= $2R'_a+G'_a+0.05B'_a$) and modified $A$ (= $2R'_a+G'_a+0.5B'_a$), compared with the standard luminosity sensitivity curve $V(\lambda)$. Both achromatic signals have a broader bandwidth than the $V(\lambda)$ function but include a larger hump in the short wavelength area for the modified achromatic signal.

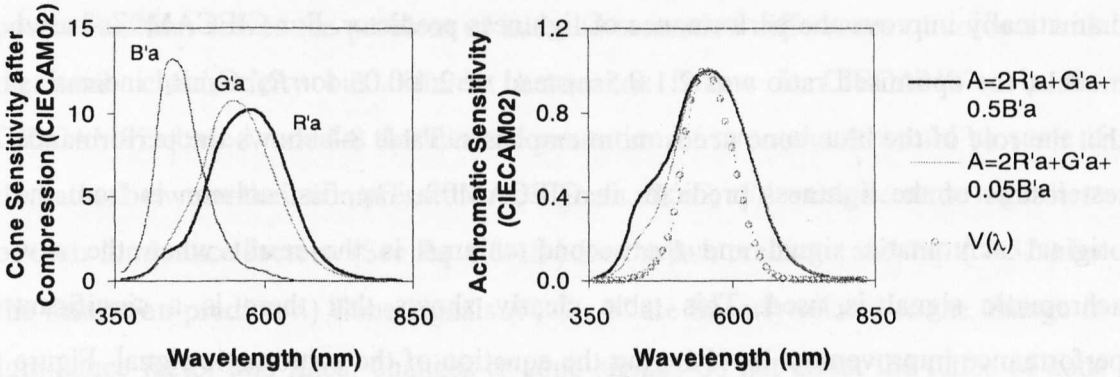


*Figure 8–5 Achromatic sensitivities of CIECAM02*

The new ratio 2:1:0.5 for $R_a':G_a':B_a'$ was obtained purely by numerical fitting to colour appearance data without any physiological evidence to support it. This simple change, however, showed a significant improvement in the performance of the colour appearance model. This is contrary to the conventional view of the role of the blue cone. The ratio 2:1:0.5 may not be exactly correct but it is clear that previously the contribution of the blue cone was significantly underestimated. In Kwak03 the achromatic signal $A$ was defined using the new ratio 2:1:0.5 for $R_k':G_k':B_k'$ as shown in Eq. ( 8-9 ). $A_w$ is the corresponding achromatic signal of the reference white.

$$A = 2\cdot R_k^{'} + G_k^{'} + 0.5\cdot B_k^{'},\ A_w = 2\cdot R_{kw}^{'} + G_{kw}^{'} + 0.5\cdot B_{kw}^{'} \qquad (8\text{-}9)$$

## 8.7.2 Colour Difference Signals

Colour difference signals $a$ and $b$ are calculated from the difference of cone signals. Equations of redness-greenness $a$ and yellowness-blueness $b$ used in CIECAM97s-based models are introduced below in Eq. ( 8-10 ) and the same equations are used in Kwak03.

$$\text{Redness - Greenness} \quad a = R_k^{'} - \frac{12}{11}\cdot G_k^{'} + \frac{1}{11}\cdot B_k^{'}$$

$$\text{Yellowness - Blueness} \quad b = \frac{1}{9}\left(R_k^{'} + G_k^{'} - 2\cdot B_k^{'}\right) \qquad (8\text{-}10)$$

## 8.8 Achromatic Predictors

Achromatic predictors include both lightness and brightness predictors. These two predictors follow the same structure as CIECAM97s-based models. Firstly the lightness predictor was established using the achromatic signal, which is a function of $R_k'$, $G_k'$, $B_k'$. The brightness predictor is based on the lightness predictor.

### 8.8.1 Lightness Predictor J

The lightness predictor in Kwak03 also has the same form as other CIECAM97s-based models. The achromatic signal normalised by that of the reference white is compressed using the power function shown in Eq. ( 8-11 ).

$$J = 100 \cdot \left( \frac{A}{A_w} \right)^{c(L_w)z(Y_b)} \qquad (8\text{-}11)$$

The exponent in the equation controls the degree of lightness contrast. Since lightness contrast varies according to both the luminance of the reference white and background luminance factor, the exponent should be a function of these two parameters. Note that the achromatic signal in Kwak03 is independent of luminance and background luminance factor. It is assumed that these two parameters are independent of each other. Function $c(L_w)$ controls the lightness contrast change due to luminance level and $z(Y_b)$ compensates for the contrast change due to background luminance factor.

#### 8.8.1.1. Effect of Luminance Level on Lightness: $c(L_W)$

The optimised exponent of the normalised achromatic signal for each individual phase was calculated to fit the visual data. Optimisation was conducted by the least squares method using the 'Solver' function in MS Excel. The aim was to quantify lightness contrast change due to luminance level, i.e. to model the function $c(L_w)$. Only the experimental data with a mid-grey background were used to eliminate the effect of background luminance factor.

Figure 8–6 shows the relationship between optimised powers and luminances of reference white. The left diagram is for average surround and the right is for dark surround. There are some discrepancies in the optimised exponents between the different data groups. Optimised exponents of the R-HL and R-LL experiments in the

LUTCHI data are larger than those of the other data sets and the CRT experiments also showed quite different features from other experiments. These diagrams clearly show two general trends. Firstly, the exponents decrease with increasing luminance level for both surround conditions. Exponent reduction means lowered lightness contrast. Secondly, the rate of change in exponent due to luminance is steeper under the dark surround condition. Current colour appearance models do not consider the latter characteristic. CIECAM97s-based models also predict increasing lightness contrast in dark surround rather than average surround however they also assume that the contrast differences between two surrounds are always the same.

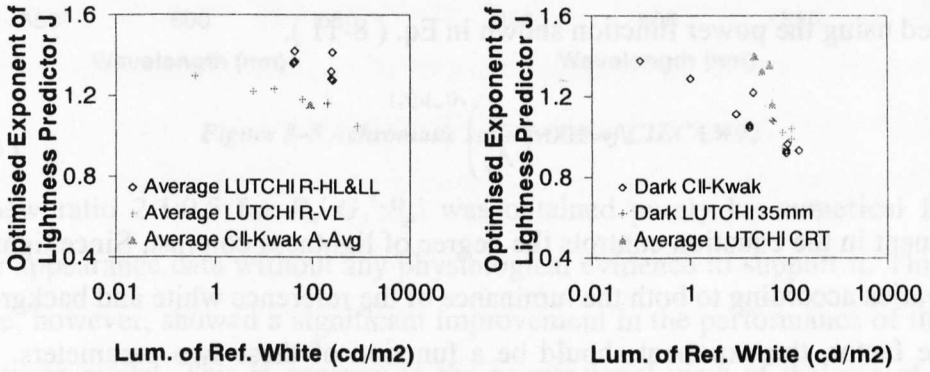


***Figure 8–6 Changes of optimised exponents for lightness predictor J with a luminance of reference white (mid-grey background only)***

The equations for dark and average surrounds shown below were used to try to fit the experimental data in Figure 8–6. Figure 8–7 shows the predictions of the Kwak03 model. The equation for dim surround was arbitrarily chosen to be in the middle of dark and average surround.

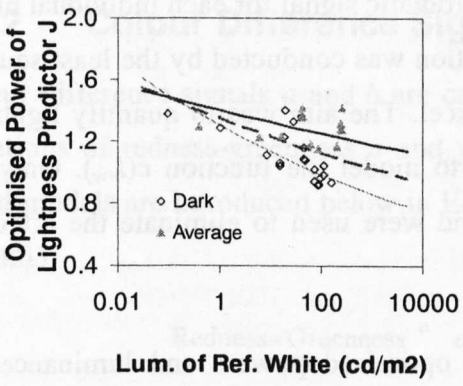


$$c(L_w) = 1.3 \cdot L_w^{-0.060} \quad \text{for Dark Surround}$$

$$c(L_w) = 1.35 \cdot L_w^{-0.040} \quad \text{for Dim Surround}$$

$$c(L_w) = 1.4 \cdot L_w^{-0.025} \quad \text{for Average Surround}$$

***Figure 8–7 Optimised exponents for lightness predictor J with the prediction by Kwak03***

### 8.8.1.2. Effect of Background Luminance Factor on Lightness: $z(Y_b)$

A similar strategy used for modelling $c(L_w)$ was applied to model the $z(Y_b)$ function. In this analysis only the data sets having all three backgrounds were used. They are the same data sets used in Section 6.4, which looked at the effect of background luminance factor i.e. Group P, Group M, Group C in the CII-Kwak data set and each three phases from CRT, R-HL and R-LL sets in the LUTCHI data. The details of each phase were given in Table 6-4.

First of all, optimised exponents were calculated to fit the visual lightness data then were optimised values were divided by the predictions from the $c(L_w)$ function. The output value from this procedure should be a function only of background luminance level, thus eliminating the effect of luminance level of the reference white.

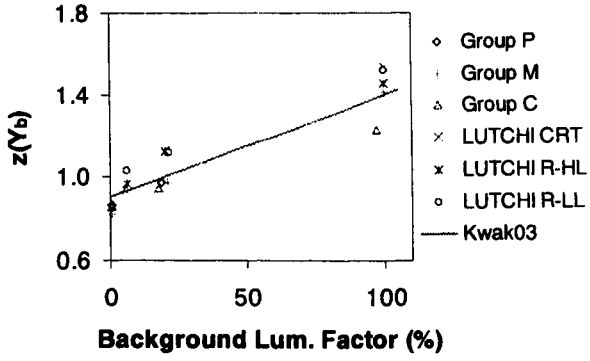


***Figure 8–8 Changes of optimised exponents for lightness predictor J by background luminance factor***

Figure 8–8 shows the change in optimised exponents by background luminance factor. In the Kwak03 model, a linear function was tried to predict the experimental data as shown below in Eq. ( 8-12 ) and the resulting predictions are shown in Figure 8–8 with the experimental data. Note that in this equation $z$ becomes one for a mid-grey background when $Y_b$ is 20 since the $c(L_w)$ function is calculated using the data for mid-grey background.

$$z(Y_b) = 0.9 + 0.5 \cdot \left(\frac{Y_b}{100}\right) \qquad (8\text{-}12)$$

CIECAM97s-based models use a square root function for $z(Y_b)$. Predicted $z(Y_b)$ functions for CIECAM97s, FC and CIECAM02 are shown in Figure 8–9 together with the experimental data. Eq. ( 8-13 ) summarises the model equations used in

Figure 8–9, which are normalised to pass through the point ($Y_b$, $z$) = (20, 1). It shows that the square root function for $z(Y_b)$ is less effective than a linear function.

$$\text{CIECAM97s/Fairchild} \quad z(Y_b) = \left(1.0 + \sqrt{Y_b/100}\right) \Big/ \left(1.0 + \sqrt{0.2}\right) \qquad (8\text{-}13)$$

$$\text{FC} \quad z(Y_b) = \left(0.85 + \sqrt{Y_b/100}\right) \Big/ \left(0.85 + \sqrt{0.2}\right)$$

$$\text{CIECAM02} \quad z(Y_b) = \left(1.48 + \sqrt{Y_b/100}\right) \Big/ \left(1.48 + \sqrt{0.2}\right)$$

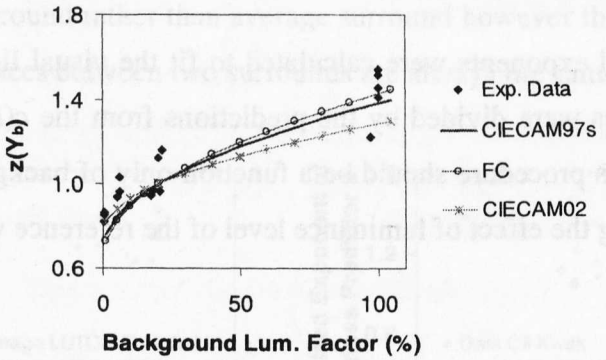


*Figure 8–9 Comparison of $z(Y_b)$ functions of CIECAM97s-based models*

## 8.8.2 Lightness Predictor $J_{10}$ for 10-degree stimuli

In Section 6.6, it was shown that there is a lightness change by stimulus size. The 10° stimuli showed a higher lightness than 2-degree stimuli. The left diagram in Figure 8–10 shows the visual data together with the predictions of the lightness predictor $J$. $X_{10}$, $Y_{10}$, $Z_{10}$ were used to calculate $J$ for 10° stimuli. Using a different colour matching function, however, does not make any difference to lightness, suggesting that a new lightness predictor $J_{10}$ needs to be derived for 10° colour patches.

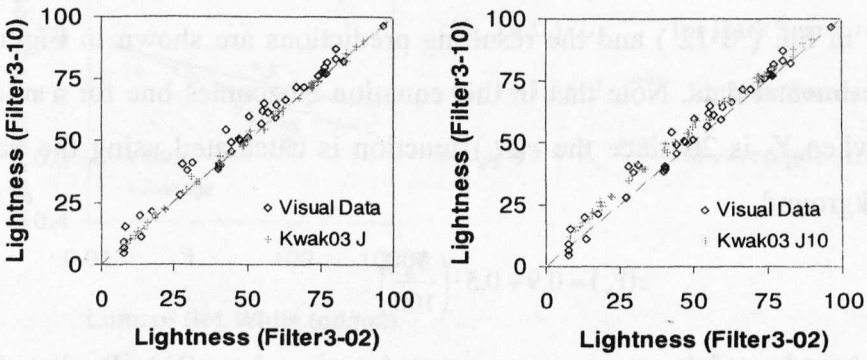


*Figure 8–10 Predictions of lightness change due to stimulus size by Kwak03 J and $J_{10}$*

Figure 8–11 shows the difference by optimised exponents for the lightness predictor between 2° and 10° stimuli. The results show that the 10° stimulus clearly shows a lower contrast. The experimental data used is from Group F experiments. In Eq. ( 8-14 ), the term $c_{10}(L_w)$ was used to predict experimental data for 10° patches.

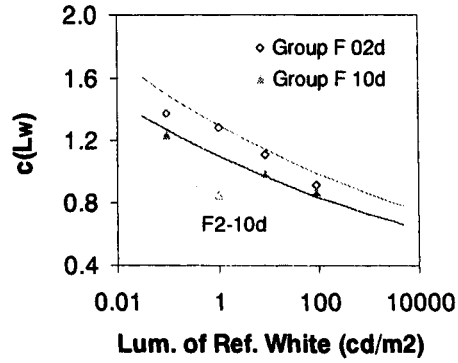


*Figure 8–11 Optimised exponents for lightness predictor $J_{10}$ with the prediction of Kwak03*

$$c(L_w) = 1.3 \cdot L_w^{-0.060} \quad \text{for 2° Stimulus (Dark Surround)}$$
$$c_{10}(L_w) = 1.1 \cdot L_w^{-0.060} \quad \text{for 10° Stimulus (Dark Surround)} \qquad (8\text{-}14)$$
$$= 0.85 \cdot c(L_w)$$

Lightness prediction using $J_{10}$ for 10° patch size and $J$ for 2° patch size is shown in the right diagram of Figure 8–10, indicating good agreement with the visual data. Also, the performance improvements are summarised as CV values in Table 8-5. All phases with a 10° patch size show better performance overall when $J_{10}$ is used, except for the Filter2-10d experiment. Note that the Filter2-10d phase shows abnormal behaviour in Figure 8–11 resulting in deteriorated CV values for $J_{10}$ although the difference is minor in terms of CV units.

| CV | Ref. White ($cd/m^2$) | -2d | -10d | |
|---|---|---|---|---|
| | | $J$ | $J$ | $J_{10}$ |
| Filter0 | 87.37 | 12.50 | 13.44 | 12.38 |
| Filter1 | 8.856 | 15.10 | 15.12 | 13.42 |
| Filter2 | 1.007 | 10.95 | 12.11 | 12.35 |
| Filter3 | 0.097 | 10.99 | 14.59 | 10.18 |

*Table 8-5 Performance improvements using lightness predictor $J_{10}$ for the 10° patch*

In Section 6.6, it was shown that the 10° patch not only appears lighter than the 2° patch but also there is hue dependency as shown in Figure 8–12 (a), in which the

visual lightness of the 10° patch divided by that of the 2° patch is plotted against the visual hue. This hue dependency also can be predicted by applying $c_{10}(L_w)$ for the experiments with 10° patches.

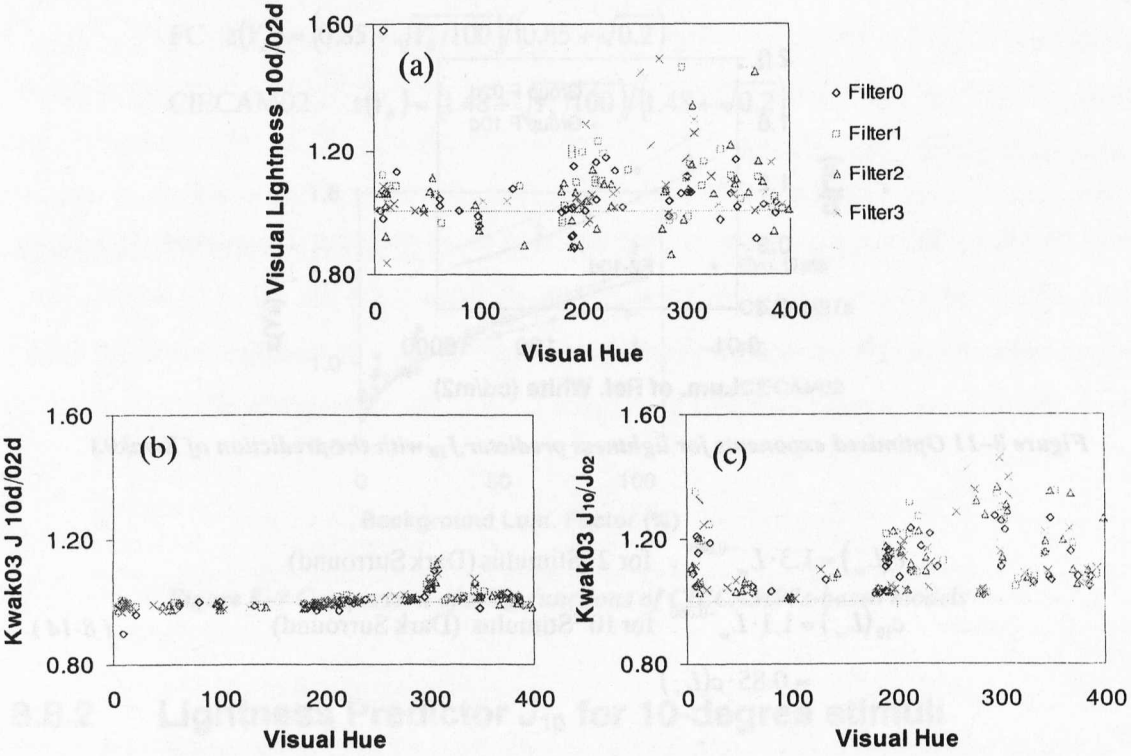


***Figure 8–12 Optimised exponents for lightness predictor $J_{10}$ with prediction by Kwak03***

Figure 8–12 (b) illustrates the prediction when the lightness predictor $J$ is used for both 2° and 10° stimuli that were calculated from the measured spectral power distribution using different colour matching functions. This diagram shows a similar trend to that found using CIELAB $L^*$ values in the right diagram of Figure 6–24. There is slight increase in the ratio near blue but very little change is found for the other hue areas. This change in blue colour is caused by the difference between the 2° and 10° colour matching functions. Note that the 10° colour matching function has a larger value for the $\bar{z}(\lambda)$ function, however when $J_{10}$ is used for the 10° patch, a similar trend for the visual data is found in the predicted data (Figure 8–12 (c)). Note that applying different $c(L_w)$ functions in the lightness predictor amplifies the difference shown in diagram (b) and this difference will be larger for lower luminance levels since the difference between the $c(L_w)$ and $c_{10}(L_w)$ functions becomes larger at lower luminance levels as shown in Figure 8–11.

### 8.8.3 Lightness Predictor $J_{p+s}$ and $J_{10p+s}$ including Rod Contribution

Lightness predictors $J$ and $J_{10}$ in Kwak03 consider only cone signals like other CIECAM97s-based colour appearance models. Several phases in the CII-Kwak data set however had very low luminance levels where rods are definitely contributing. Therefore, in the Kwak03 model another lightness predictor $J_{p+s}$ ($J_{10p+s}$ for 10° stimuli) combining both rod and cone signals has been tried. Note that the Group F experiments were specifically designed to investigate the effect of rods on colour appearances.

Modelling rod contribution follows the assumption of Hunt94, which was the only model containing rod contribution among those tested in this study. In Hunt94 it is assumed that the compressed rod signal is combined with compressed cone signals in the achromatic channel by simple addition. The rod signal, however, is not involved in the colour difference signals and therefore rod contribution should affect visual lightness the most and lightness change due to the rod signal will have a secondary effect on the chromatic components.

$$A_{Total} = A + \alpha \cdot A_s \qquad (8\text{-}15)$$

$$A = 2 \cdot R_k' + G_k' + 0.5 \cdot B_k', \quad A_s = \left(\frac{Y'}{100}\right)^{0.42}$$

where Scotopic Luminance $Y' = 1700 \int V'(\lambda) \cdot P(\lambda) \cdot d\lambda$

$P(\lambda)$: Power spectrum of test colour

$$J_{p+s} = 100 \cdot \left(\frac{A_{Total}}{A_{Total,w}}\right)^{c(l_w) \cdot z(Y_b)}, \quad J_{10p+s} = 100 \cdot \left(\frac{A_{Total}}{A_{Total,w}}\right)^{c_{10}(l_w) \cdot z(Y_b)} \qquad (8\text{-}16)$$

Eq. ( 8-15 ) was derived to represent a total achromatic signal, $A_{Total}$, containing both rod and cone signals. In this equation, $A$ is the cone contribution to the achromatic signal and $A_s$ means the rod contribution. $A_s$ was developed in the same way as for the cone contribution. Firstly, the rod signal was calculated using normalised scotopic luminance and compressed by a power function as for the cone signal. Scotopic luminance was calculated using the CIE standard scotopic luminosity function, $V'(\lambda)$. $\alpha$ is a constant determining the ratio between cone and rod contributions, which needs

to be determined empirically. Using the new total achromatic signal, lightness predictors $J_{p+s}$ and $J_{10p+s}$ are expressed in Eq. (8-16).

The constant $\alpha$ was calculated by the least squares method using the visual data of the Group F experiment. The 'Solver' function in MS Excel was used for the calculation. Table 8-6 shows the calculated $\alpha$ and the ratio of rod contribution in the total achromatic signal of each phase. Also the performances of lightness predictors $J$ and $J_{p+s}$ ($J_{10}$ and $J_{10p+s}$ for 10° stimuli) are represented using CV values. The ratio of the rod contribution is also shown graphically as a function of luminance of the reference white in Figure 8–13.

| Stimulus Size | | Ref. White ($cd/m^2$) | $\alpha$ | $A_s/A_{Total}$ | $J / J_{10}$ (CV) | $J_{p+s} / J_{10p+s}$ (CV) |
|---|---|---|---|---|---|---|
| 2° | Filter0-02 | 87.37 | 0.000 | 0.000 | 12.50 | 12.50 |
| | Filter1-02 | 8.856 | 0.000 | 0.000 | 15.10 | 15.10 |
| | Filter2-02 | 1.007 | 0.000 | 0.000 | 10.95 | 10.95 |
| | Filter3-02 | 0.097 | 0.207 | 0.056 | 10.99 | 10.94 |
| 10° | Filter0-10 | 87.37 | 0.000 | 0.000 | 12.38 | 12.38 |
| | Filter1-10 | 8.856 | 0.000 | 0.000 | 13.42 | 13.42 |
| | Filter2-10 | 1.007 | 0.251 | 0.067 | 12.35 | 12.31 |
| | Filter3-10 | 0.097 | 0.495 | 0.124 | 10.18 | 9.96 |

***Table 8-6 Ratio of rod contribution and performance comparison between lightness predictors J and $J_{p+s}$***

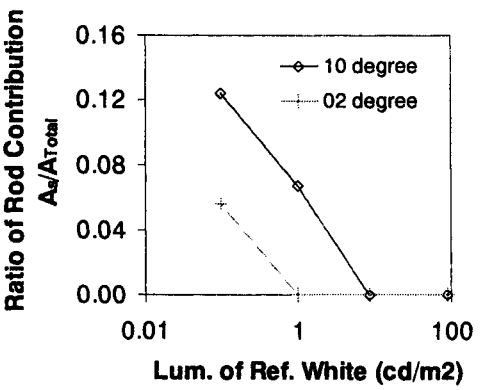


***Figure 8–13 Ratio of rod contribution in the achromatic signal***

Figure 8–13 shows that in the case of the 2° stimulus rod contribution is not needed at all except for the phase having lowest luminance level. The 10° stimulus also shows the effect for both the second lowest and lowest phases. Two conclusions are that the rod contribution is increased under lower luminance levels and that the 10° stimulus

shows a larger proportion of rod contribution than the 2° stimulus. Both phenomena confirm the general idea of the role of rods, which function under mesopic vision with more rods working outside the foveal area.

The Purkinje shift is one particular colour appearance phenomenon expected when rod vision is active. In Section 6.7, the visual data in the Group F experiments showed this effect clearly. Note that lightness predictors $J$ and $J_{10}$ cannot predict Purkinje shift since they do not have a component that can be changed between red and blue colours according to luminance level. However $J_{p+s}$ and $J_{10p+s}$ include scotopic luminances, which would make a difference between red and blue, together with a weighting factor for scotopic luminance, which changes with luminance level. Therefore it is expected that lightness predictors $J_{p+s}$ and $J_{10p+s}$ could predict the Purkinje shift.

The diagrams in Figure 8–14 show the Purkinje shift introduced in Figure 6–25 of Section 6.7 with predictions by lightness predictors $J$, $J_{10}$ and $J_{p+s}$, $J_{10p+s}$. The left diagrams in the first and second rows show the visual lightness change of selected red and blue colours against luminance levels. The middle and right diagrams illustrate predictions by $J$ and $J_{p+s}$ respectively ($J_{10}$ and $J_{10p+s}$ for the second row). The third row shows the ratios between blue and red colours calculated by dividing the lightness of each blue colour by that of red then normalising the ratio of highest luminance level to be one. The lightness ratio change of the visual data is shown together with the predicted ratio changes of $J$ and $J_{p+s}$. The left diagram in the third row is for the 2° stimulus and the right for the 10° stimulus.

Figure 8–14 clearly shows that $J_{p+s}$ and $J_{10p+s}$ do predict Purkinje shift but the predicted effects are smaller than those observed. The predicted lightness by $J$ and $J_{10}$ shows no effect as expected. Note that optimised parameters were directly used for the model predictions. No attempt was made to derive equations to fit the optimised values since the visual data were insufficient to generalise the function.

In conclusion, including a rod contribution in the achromatic signal did not affect the performance of the lightness predictor significantly. The improvement in performance was minor in terms of CV values, however it was found that adding rod contribution is critical to predicting the colour appearance phenomena observed in mesopic vision.

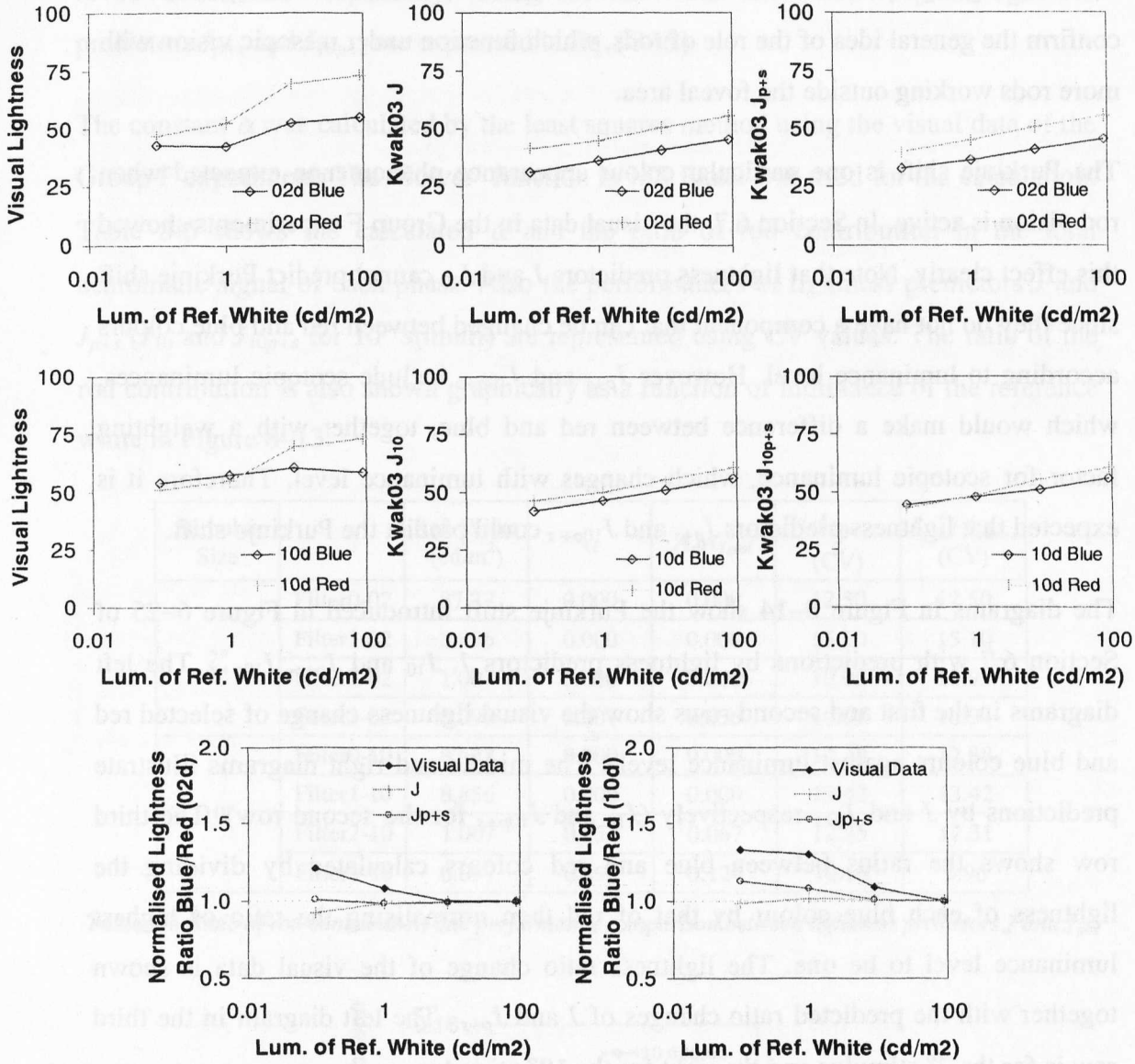


*Figure 8–14 Prediction of Purkinje shift by lightness predictor $J/J_{10}$ and $J_{p+s}/J_{10p+s}$*

## 8.8.4 Brightness Predictor *Q*

The CII-Kwak data sets do not include brightness visual data. Currently the only available colour appearance data set for brightness is from the Group R-VL experiments in the LUTCHI data. The R-VL experiments had 12 phases. Each phase had 40 reflective colours and the same test samples were shown throughout the whole experiments. The first six phases, from R-VL1 to R-VL6, estimated lightness, colourfulness and hue under changing luminance levels. The next six phases, from R-VL7 to R-VL12, repeated the previous six experiments but this time brightness, colourfulness and hue were estimated. Thus the R-VL data has visual lightness and

brightness for each test colour making it possible to compare visual brightness and lightness directly as shown in Figure 8–15.

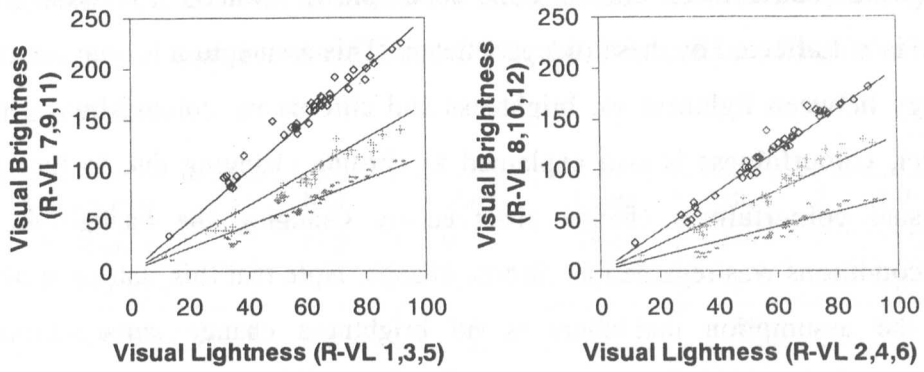


***Figure 8–15 Direct comparison between visual lightness and brightness (R-VL) (Straight lines represent the predictions of Kwak03)***

In CIECAM97s-based models, the brightness predictor is represented as a non-linear function of lightness (e.g. CIECAM02 uses a square root function) however Figure 8–15 does not show any clear evidence that brightness and lightness are non-linearly related. In fact all six data sets seem to be linearly related to each other therefore the brightness predictor in Kwak03 was derived by calculating the scaling factor between visual lightness and brightness.

Figure 8–16 shows the calculated scaling factor between visual brightness and visual lightness as a function of luminance of the reference white and it is found that Eq. ( 8-17 ) can predict this relationship quite well as shown by the straight line. The six straight lines in Figure 8–15 represent the model predictions using Eq. ( 8-17 ) and the dotted lines are predictions of CIECAM02 (refer to Section 2.8.8.3 for the equation). It is clear that Kwak03 outperforms CIECAM02.

$$Q = J \cdot (L_w)^{0.16} \qquad (8\text{-}17)$$

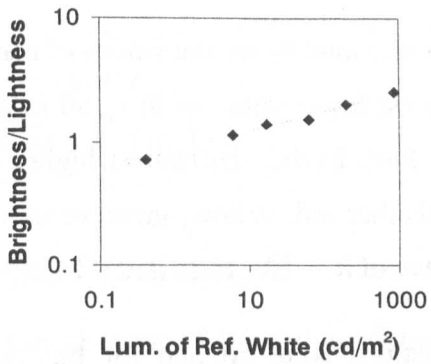


***Figure 8–16 Performance of brightness predictor Q***

The R-VL experiments only considered brightness change due to luminance level. There is no available visual brightness data to show brightness change due to background luminance factor and surround condition. In Kwak03 it is assumed that brightness is not affected by these two parameters. This assumption is connected with the analogy between lightness vs. brightness and chroma vs. colourfulness. In this new model, colourfulness is also explained as chroma changing due to luminance level. Visual colourfulness change observed by changing the background and surround conditions was regarded as chroma change. Note that this statement already contains the assumption that there is no brightness change since chroma is colourfulness judged relative to the brightness of the reference white. The mathematical meaning of this assumption is shown in Section 8.10.1.3.

## 8.9 Hue Predictors

In CIECAM97s-based models, hue predictors are represented in a two-dimensional space based upon redness-greenness, $a$, and yellowness-blueness, $b$, as its two axes. Hue can be represented as hue angle, $h$, or hue quadrature, $H$, in conventional colour appearance models. Hue angle is represented as degrees changing from 0° to 360° and hue quadrature ranges from 0 to 400. The equation used in CIECAM97s-based models is introduced in Eq. ( 8-18 ). The function for an eccentricity factor $e$ is from CIECAM02.

$$h = \tan^{-1}(b/a) \qquad (8\text{-}18)$$

$$H = H_1 + \frac{100 \cdot (h - h_1)/e_1}{(h - h_1)/e_1 + (h_2 - h)/e_2}$$

$$e = \frac{1}{4} \cdot \left[ \cos\left( h \frac{\pi}{180} + 2 \right) + 3.8 \right]$$

In the hue quadrature equation, $e_1$and $h_1$ are the values of $e$ and $h$, respectively, for the unique hues having the nearest lower value of $h$; $e_2$ ad $h_2$ are the values of $e$ and $h$, respectively, for the unique hues having the nearest higher value of $h$. $H_1$ is 0, 100, 200, or 300 according to whether red, yellow, green or blue, respectively, is the hue having the nearest lower value of $h$.

In Kwak03, the same equations were applied for hue angle and hue quadrature predictors but the hue angles corresponding to the unique hues were changed since a

different compression method was applied to the cone signals. Table 8-7 shows the hue angles of the unique hues used in Kwak03. Note that changing hue angles for the unique hues affects the relationship between hue angle and the eccentricity factor however the same equation for $e$ from CIECAM02 is used in Kwak03 since the difference is minor.

| Unique Hue | Red | Yellow | Green | Blue | Red |
|---|---|---|---|---|---|
| Hue angle $h$ | 13.0 | 93.5 | 153.6 | 246.8 | 373.0 |
| Eccentricity $e$ | 0.8 | 0.7 | 1.0 | 1.2 | 0.8 |
| Hue quadrature H | 0 | 100 | 200 | 300 | 400 |

***Table 8-7 Hue angles of the unique hues in Kwak03***

## 8.10 Chromatic Predictors

CIECAM97s-based models predict saturation, chroma and colourfulness for chromatic attributes. (Refer Section 2.6.1 for the CIE definitions of these attributes.) Colourfulness is an absolute chromatic scale varied by the luminance level of the reference white, background luminance factor and surround condition. Chroma is colourfulness without the luminance level dependency since it is judged relative to the brightness of a reference white. As mentioned in Section 8.8.4 that discussed the brightness predictor, it is assumed that the brightness of the reference white is not changed by background luminance factor or surround condition, therefore there should be a chroma change produced by different background luminance factors or surround conditions. Saturation is chroma judged in proportion to its lightness. It has to be independent of lightness. The lightness dependent part has to be excluded from the chroma predictor to make a saturation predictor. The structures of chromatic predictors in Kwak03 are given in Eq. ( 8-19 ).

$$\begin{aligned} &\text{Saturation} && s = f\left(R_k', G_k', B_k'\right) \cdot f\left(Y_b\right) \cdot f(\text{Surround}) \\ &\text{Chroma} && C = s \cdot f(J) \\ &\text{Colourfulness} && M = C \cdot f\left(L_w\right) \end{aligned} \qquad (8\text{-}19)$$

### 8.10.1 Colourfulness Predictor, *M*

Eq. ( 8-20 ) shows the general form of the colourfulness predictor, $M$, which has various factors: an eccentricity factor, $e$, the combination of yellowness-blueness and

redness-greenness $a^2+b^2$, the summation of compressed cone signals $R_k'+G_k'+B_k'$, lightness $J$, background $Y_b$, surround condition and luminance of reference white $L_w$. Each component is taken from CIECAM97s-based models and it has been confirmed in this study that all of these components are important to improving the model performance. For comparison, the colourfulness predictor of CIECAM02 is given in Eq. ( 8-21 ), which is arranged to have the same format as Eq. ( 8-20 ). Note that function $e$ in Eq. ( 8-21 ) represents the one given in Eq. ( 8-18 ) not the one in Section 2.8.8.3.

$$M = 300 \cdot \frac{e^{\alpha} \cdot \left(a^2+b^2\right)^{\beta}}{\left(R_k'+G_k'+B_k'\right)^{2\cdot\beta}} \cdot \left(\frac{J}{100}\right)^{\gamma} \cdot f(Y_b) \cdot f(\text{Surround}) \cdot f(L_w) \qquad (8\text{-}20)$$

$$M_{\text{CIECAM02}} = \left(\frac{12500}{13\times 4}\right)^{0.9} \cdot \frac{e^{0.9} \cdot \left(a^2+b^2\right)^{0.45}}{\left(R_a'+G_a'+B_a'\right)^{0.9}} \cdot \left(\frac{J}{100}\right)^{0.5} \times \left[N_{cb}^{0.9} \cdot \left(1.64-0.29^{Y_b/Y_w}\right)^{0.73}\right] \cdot N_c^{0.9} \cdot F_L^{0.25} \qquad (8\text{-}21)$$

Firstly the exponents of four components, $e$, $a^2+b^2$, $R_k'+G_k'+B_k'$, and $J$, were calculated by optimising to minimise the prediction errors. Optimised exponents were calculated for each experimental phase and the average values of the whole experimental data sets were used in the Kwak03 model. The least squares method was employed and the 'Solver' function in MS Excel was used to minimise the errors. The results are shown in Eq. ( 8-22 ). Note that $f(Y_b)$, $f$(Surround) and $f(L_w)$ cannot be calculated with this method since the output values of these two functions are constants within an experimental phase cancelled out by a linear fitting process.

$$M = 300 \cdot \frac{e^{0.5} \cdot \left(a^2+b^2\right)^{0.4}}{\left(R_k'+G_k'+B_k'\right)^{0.8}} \cdot \sqrt{J/100} \cdot f(Y_b) \cdot f(\text{Surround}) \cdot f(L_w) \qquad (8\text{-}22)$$

#### 8.10.1.1. Effect of Background Luminance Factor on Colourfulness: $f(Y_b)$

The experimental groups containing all three background luminance factors were used to derive the $f(Y_b)$ function in the colourfulness predictor $M$. These were Group M and Group C in the CII-Kwak data set plus three phases from each of the CRT, R-HL and R-LL sets in the LUTCHI data. The function $f(Y_b)$ predicts the effect of background luminance factor on colourfulness.

Firstly, the scaling factor was calculated between the visual colourfulness of each phase and prediction by Eq. ( 8-23 ), which is the part of Eq. ( 8-22 ). Then scaling factors in a group were normalised with those of the experimental phase with a white background. Note that scaling factor calculated contains information not only of the background, $f(Y_b)$, but also of luminance level, $f(L_w)$, and surround, $f$(Surround). The normalisation process, however, eliminates other factors except for background since the experiments with all three backgrounds have the same luminance level and surround condition.

$$300 \cdot \frac{e^{0.5} \cdot \left(a^2 + b^2\right)^{0.4}}{\left(R_k' + G_k' + B_k'\right)^{0.8}} \cdot \sqrt{J/100} \qquad (8\text{-}23)$$

Figure 8–17 shows the normalised scaling factor as a function of background luminance factor. Except for the CRT experiments (LUTCHI-CRT), the other data points have similar trends and are fitted well by a linear function. The equation to fit the data is given in Eq. ( 8-24 ), which is derived excluding the LUTCHI-CRT data because of their abnormal behaviour.

$$f(Y_b) = 0.79 + 0.21 \cdot \frac{Y_b}{100} \qquad (8\text{-}24)$$

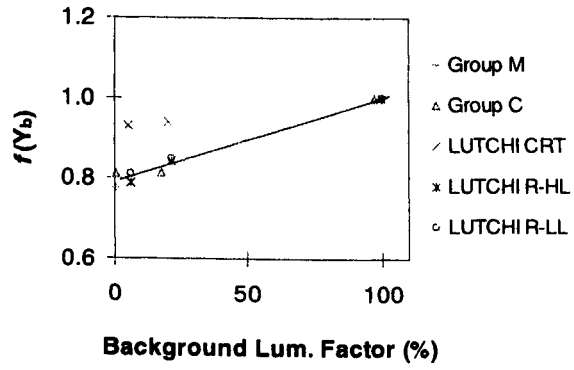


*Figure 8–17 Normalised colourfulness scaling factor change by background luminance factor*

In Section 6.4.2, it was previously shown that lighter backgrounds have higher colourfulness, which is also confirmed here. Also the visual data showed that colourfulness change by background factor has a lightness dependency. Dark colours showed the opposite colourfulness change however this effect is not considered in Kwak03 because it is less significant than the overall colourfulness shift.

### 8.10.1.2. Effect of Surround Condition on Colourfulness: *f* (Surround)

Figure 8–18 shows the colourfulness scaling factors of the LUTCHI data and Group A experiments against the luminance of reference white. All phases in the figure had grey backgrounds. The scaling factor is calculated to fit the result of Eq. ( 8-23 ) to visual colourfulness of each phase. This diagram shows the colourfulness change due to surround condition. The LUTCHI 35mm experiment, which used a dark surround, shows a lower scaling factor than the average surround (R-HL and R-LL). It is also shown in the Group A experiments that the average surround (phase A-Avg) has a larger scale than the dark surround (A-Dark).

These two independent studies clearly show that colours look more colourful under average surround but the information is rather limited since the current data do not indicate whether or not the size of the surround effect could change due to luminance level. In Kwak03 a chromatic surround induction factor, $N_c$, is considered to be a constant following other CIECAM97s-based models. $N_c$ is calculated by comparing the scaling factors between two surround conditions. The LUTCHI and Group A experiments have slightly different values so an average value was taken from the two studies. The surround colourfulness induction factor $N_c$ in Kwak03 is one for average surround and 0.85 for dark surround. For dim surround 0.92 was chosen. The performance of the LUTCHI CRT experiment was not considered when deriving a chromatic surround induction factor, because it has abnormal behaviour in other respects.

$$f(\text{Surround}) = N_c = 1 \text{ for Average}, 0.92 \text{ for Dim or } 0.85 \text{ for Dark Surround} \qquad (8\text{-}25)$$

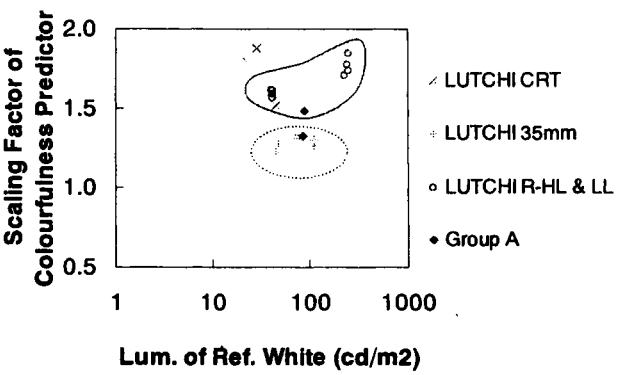


*Figure 8–18 Normalised colourfulness scaling factor change due to surround condition*

### 8.10.1.3. Effect of Luminance of Reference White on Colourfulness : $f(L_w)$

A similar strategy was applied to obtain the $f(L_w)$ function. Figure 8–19 shows the scaling factors of the LUTCHI data and groups A and F. The scaling factors for average surround were corrected using the surround colourfulness induction factor $N_c$ in order to have the same scale as that of the dark surround.

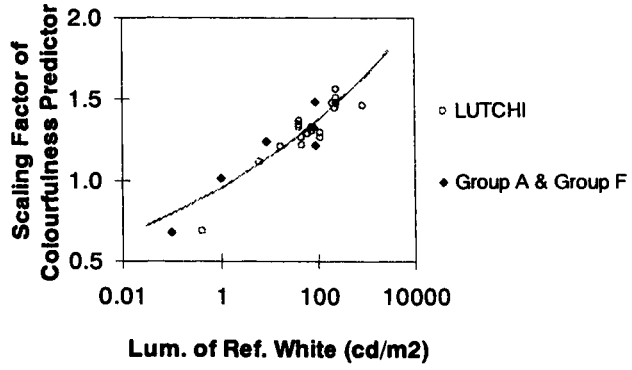


*Figure 8–19 Normalised colourfulness scaling factor change due to luminance of reference white*

$$f(L_w) = L_w^{0.08} \qquad (8\text{-}26)$$

The curve in Figure 8–19 represents the function given in Eq. ( 8-26 ). It is clear that this function fits the experimental data well. This equation is actually mathematically deduced based on the assumption that the brightness of the reference white is not changed by either background luminance factor or surround condition to make the brightness predictor. The procedure of deduction is introduced below.

Following the assumption, the brightness predictor was represented as a function of lightness multiplied by a function of luminance of reference white (see Eq. ( 8-17 )). The brightness predictor, $Q$, is given again in Eq. ( 8-27 ).

$$Q = J \cdot f_Q(L_w) = J \cdot (L_w)^{0.16} \qquad (8\text{-}27)$$

In Eq. ( 8-20 ), it was shown that the colourfulness predictor is proportional to the square root of the lightness predictor. Chroma also has to be proportional to the square root of the lightness predictor according to Eq. ( 8-19 ), which is also based on the assumption made for Eq. ( 8-27 ). By definition, chroma is colourfulness judged in proportion to the brightness of reference white. In an isolated experimental condition, chroma and colourfulness make no difference and the same applies for lightness and

brightness. Therefore the relationship between chroma and lightness should also apply between colourfulness and brightness as summarised in Eq. ( 8-28 ).

$$C \propto \sqrt{J} \quad \because C = \frac{M}{f_M(L_w)} \text{ and } M \propto \sqrt{J} \cdot f_M(L_w) \qquad (8\text{-}28)$$

$$\therefore M \propto \sqrt{Q} \quad \text{(by definition)}$$

Combining Eq. ( 8-27 ) and Eq. ( 8-28 ) leads to the next relationship, Eq. ( 8-29 );

$$M \propto \sqrt{J} \cdot f_M(L_w) = \sqrt{\frac{Q}{f_Q(L_w)}} \cdot f_M(L_w) \qquad (8\text{-}29)$$

$$\therefore \quad f_M(L_w) = \sqrt{f_Q(L_w)} = \sqrt{L_w^{0.16}} = L_w^{0.08}$$

It is encouraging that the function for the colourfulness predictor cannot only be mathematically deduced from the assumption made for the brightness predictor but also fits almost perfectly all the experimental data.

## 8.10.2 Chroma Predictor, *C* and Saturation Predictor, *s*

The final colourfulness predictor, *M*, is given in Eq. ( 8-30 ). Based on this equation, a chroma predictor, *C*, and saturation predictor, *s*, were derived by the relationship described in Eq. ( 8-19 ).

$$M = 300 \cdot \frac{e^{0.5} \cdot \left(a^2 + b^2\right)^{0.4}}{\left(R_k' + G_k' + B_k'\right)^{0.8}} \cdot \sqrt{J/100} \cdot \left(0.79 + 0.21 \cdot \frac{Y_b}{100}\right) \cdot N_c \cdot L_w^{0.08} \qquad (8\text{-}30)$$

$$C = 300 \cdot \frac{e^{0.5} \cdot \left(a^2 + b^2\right)^{0.4}}{\left(R_k' + G_k' + B_k'\right)^{0.8}} \cdot \sqrt{J/100} \cdot \left(0.79 + 0.21 \cdot \frac{Y_b}{100}\right) \cdot N_c \qquad (8\text{-}31)$$

$$s = 300 \cdot \frac{e^{0.5} \cdot \left(a^2 + b^2\right)^{0.4}}{\left(R_k' + G_k' + B_k'\right)^{0.8}} \cdot \left(0.79 + 0.21 \cdot \frac{Y_b}{100}\right) \cdot N_c \qquad (8\text{-}32)$$

## 8.11 Performance Test of Kwak03

The performance of Kwak03 is also examined using same method as for other colour appearance models in Chapter 7. Table 8-8 summarises the average CVs for each attribute of Kwak03 along with the other eight colour appearance models. Model predictions are calculated using the degree of chromatic adaptation function, $D$. The lightness predictor $J_{10}$ is used for 10° stimuli. Kwak03 shows significant improvement for lightness and brightness prediction and also the performance of other attributes is slightly better than for the other models. The CV value of each phase is shown in Appendix 2.

| Average CV | CIELAB | LLAB | RLAB | Hunt94 | CIECAM 97s | FC | Fairchild | CIECAM 02 | Kwak03 |
|---|---|---|---|---|---|---|---|---|---|
| Lightness | 19.2 | 14.9 | 26.0 | 12.6 | 14.6 | 14.3 | 14.2 | 14.5 | *11.8* |
| Brightness | | | | 11.5 | 13.6 | 13.0 | 12.1 | 22.3 | *11.4* |
| Chroma | 26.3 | 21.3 | 27.6 | 20.3 | 19.5 | 19.8 | 23.5 | 20.0 | *18.9* |
| Colourfulness | | 22.7 | | 23.6 | 21.9 | 22.2 | 27.1 | 23.4 | *21.4* |
| Hue | | 8.9 | 11.2 | 8.3 | 7.9 | 8.0 | 7.9 | 7.6 | *7.4* |

***Table 8-8 Average CVs for each attribute of Kwak03***

The next four figures show the colour appearance predictions of Kwak03 for the mean visual data. Figures 8-20 and 8-21 illustrate the predictions of lightness and colourfulness contrast change due to luminance level respectively. Figures 8-22 and 8-23 show lightness and colourfulness contrast change due to background luminance factor. Predictions of other colour appearance models were discussed in Section 7.5.1 for the effect of luminance level and in Section 7.5.2 for the effect of background luminance factor.

It is noticeable that Kwak03 shows better prediction than any other colour appearance model. In particular, Kwak03 compensates successfully for lightness contrast change due to luminance level and colourfulness change due to background, which could not be predicted by any other colour appearance model studied.

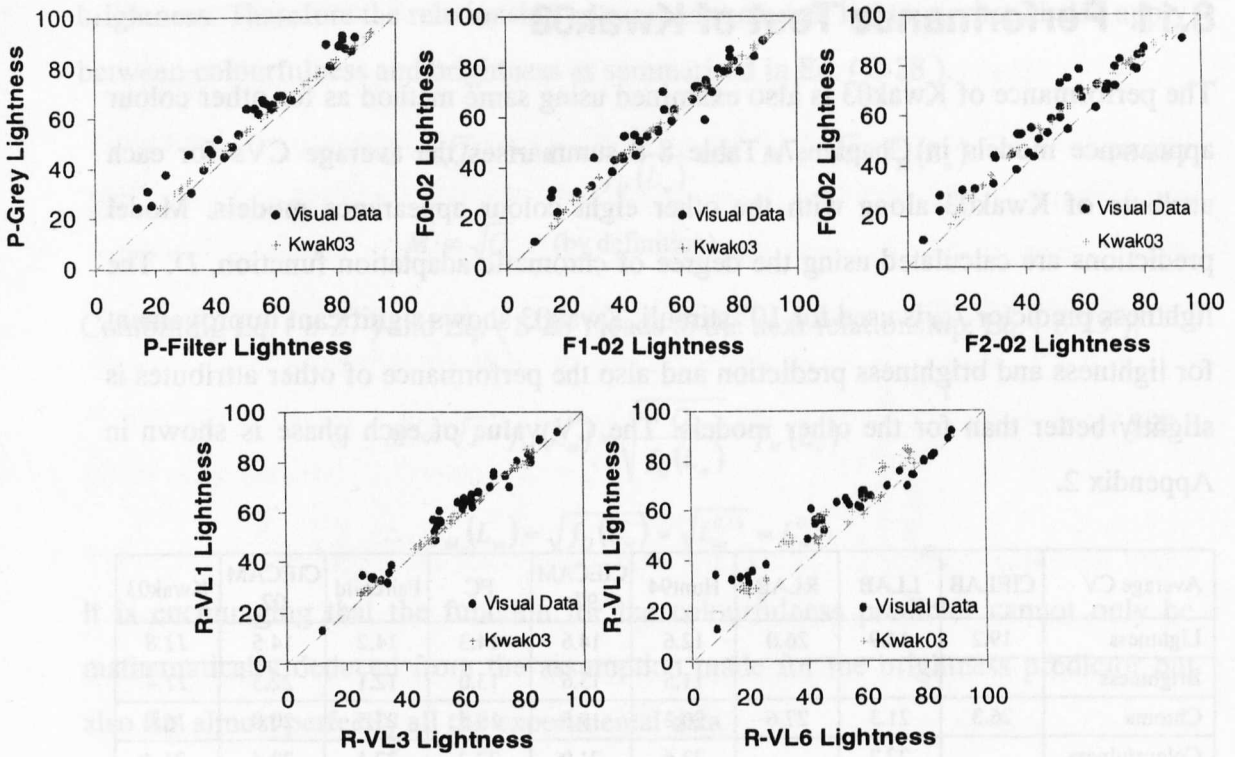


*Figure 8–20 Prediction of lightness contrast change due to luminance level (Kwak03)*

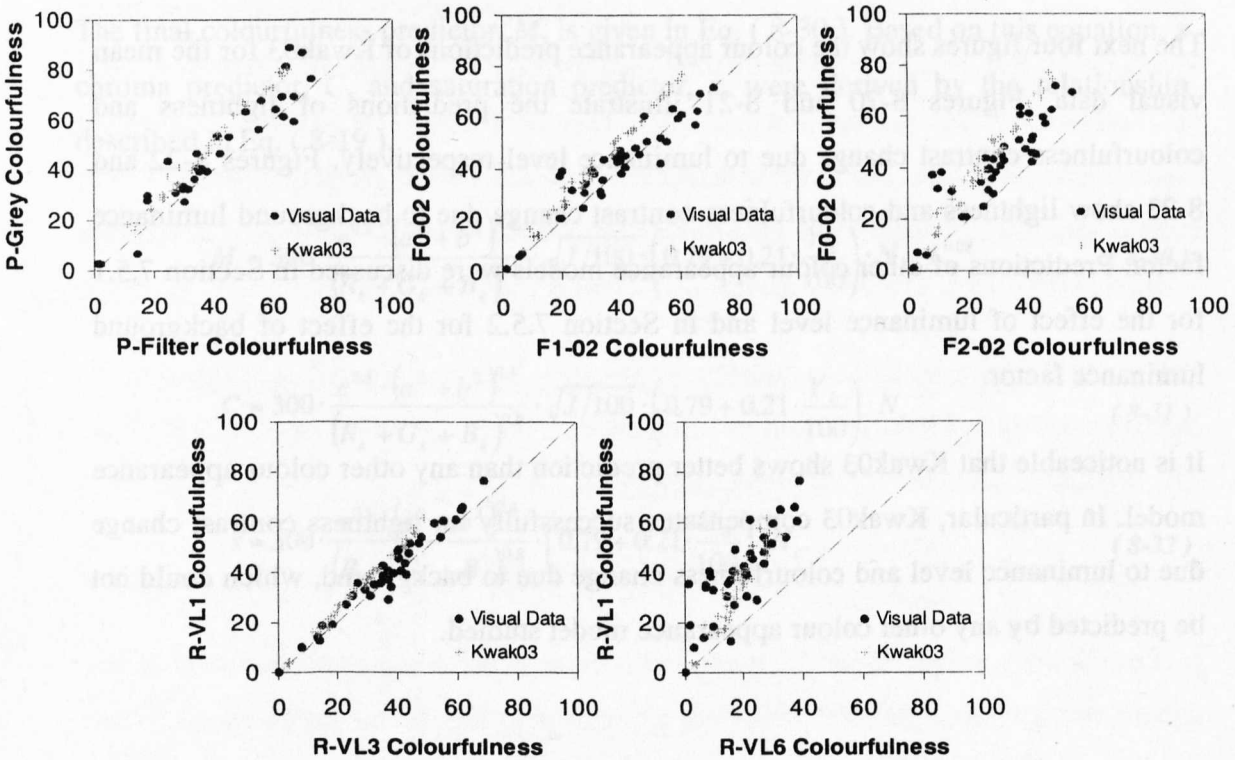


*Figure 8–21 Prediction of colourfulness contrast change due to luminance level (Kwak03)*

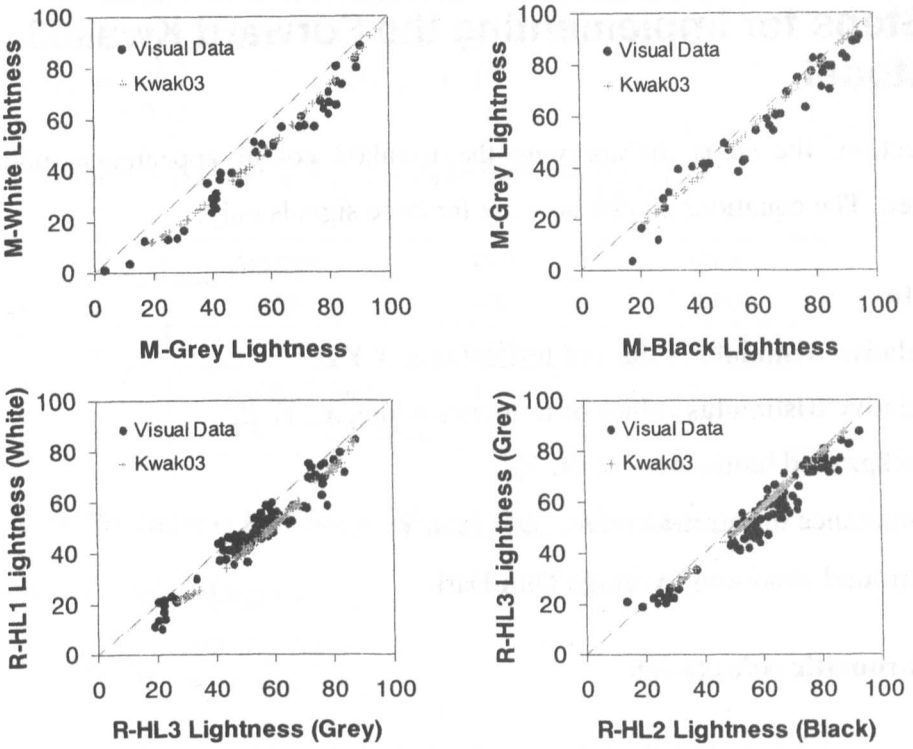


*Figure 8–22 Prediction of lightness contrast change due to background (Kwak03)*

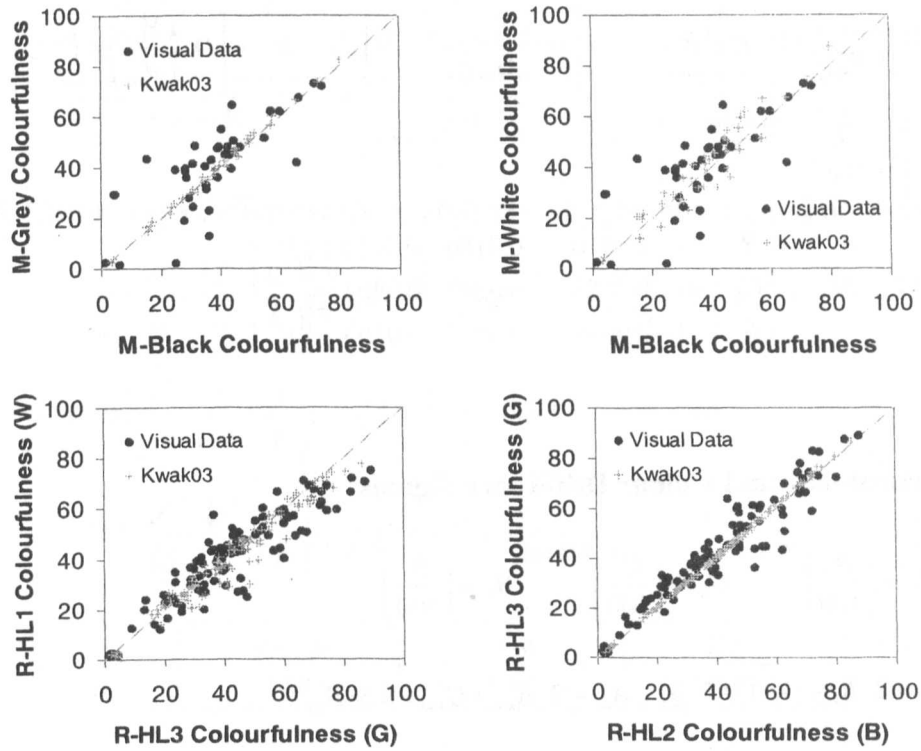


*Figure 8–23 Prediction of colourfulness contrast change due to background (Kwak03)*

## 8.12 Steps for Implementing the Forward Kwak03 Model

In this section, the steps for applying the Kwak03 colour appearance model are summarised. The equations shown here are for cone signals only.

### Input Data

- Relative tristimulus values of test colours, $X\,Y\,Z$
- Relative tristimulus values of reference white, $X_w\,Y_w\,Z_w$
- Background luminance factor, $Y_b$
- Luminance of reference white, $L_w$ (cd/m$^2$)
- Surround condition, Average/Dim/Dark

### Step 1. Chromatic Adaptation

$$\begin{vmatrix} R \\ G \\ B \end{vmatrix} = M_{CAT02} \cdot \begin{vmatrix} X \\ Y \\ Z \end{vmatrix} = \begin{vmatrix} 0.7328 & 0.4296 & -0.1624 \\ -0.7036 & 1.6975 & 0.0061 \\ 0.0030 & 0.0136 & 0.9834 \end{vmatrix} \cdot \begin{vmatrix} X \\ Y \\ Z \end{vmatrix}$$

$$R_C = \left[ D \cdot \left( \frac{Y_W}{R_W} \right) + 1 - D \right] \cdot R \;,\; G_C = \left[ D \cdot \left( \frac{Y_W}{G_W} \right) + 1 - D \right] \cdot G \;,\; B_C = \left[ D \cdot \left( \frac{Y_W}{B_W} \right) + 1 - D \right] \cdot B$$

$$D = F \cdot \left[ 1 - \frac{1}{3.6} \cdot e^{\frac{-L_W \cdot Y_b / 100 - 42}{92}} \right]$$

$$\begin{vmatrix} R' \\ G' \\ B' \end{vmatrix} = M_H \cdot M_{CAT02}^{-1} \begin{vmatrix} R_C \\ G_C \\ B_C \end{vmatrix} = \begin{vmatrix} 0.7410 & 0.2180 & 0.0410 \\ 0.2854 & 0.6242 & 0.0904 \\ -0.0096 & -0.0057 & 1.0153 \end{vmatrix} \cdot \begin{vmatrix} R_C \\ G_C \\ B_C \end{vmatrix}$$

### Step 2. Achromatic and Colour Difference Signals

$$R'_k = \left( \frac{R'}{100} \right)^{0.42} \;,\quad G'_k = \left( \frac{G'}{100} \right)^{0.42} \;,\quad B'_k = \left( \frac{B'}{100} \right)^{0.42}$$

$$A = 2 \cdot R'_k + G'_k + 0.5 \cdot B'_k \;,\; A_w = 2 \cdot R'_{kw} + G'_{kw} + 0.5 \cdot B'_{kw}$$

Redness - Greenness $\quad a = R'_k - \frac{12}{11} \cdot G'_k + \frac{1}{11} \cdot B'_k$

Yellowness - Blueness $\quad b = \frac{1}{9} \left( R'_k + G'_k - 2 \cdot B'_k \right)$

## Step 3. Achromatic Predictors: Lightness $J$ & Brightness $Q$

$$J = 100 \cdot \left( \frac{A}{A_w} \right)^{c(L_w) z(Y_b)} \qquad Q = J \cdot (L_w)^{0.16}$$

where $c(L_w) = p \cdot q \cdot L_w^{\ n}$ , $z(Y_b) = 0.9 + 0.5 \cdot \left( \frac{Y_b}{100} \right)$

| | Average | Dim | Dark |
|---|---|---|---|
| $q$ | 1.30 | 1.35 | 1.40 |
| $n$ | -0.060 | -0.040 | -0.025 |
| $p$ | $p = 0.85$ for stimuli > 4°<br>$p = 1$ otherwise | | |

## Step 4. Hue Predictors: Hue angle, $h$, and Hue quadrature, $H$

$$h = \tan^{-1}(b/a) \quad \text{[degrees]}$$

$$H = H_1 + \frac{100 \cdot (h - h_1)/e_1}{(h - h_1)/e_1 + (h_2 - h)/e_2}$$

$$e = \frac{1}{4} \left[ \cos\left( h \frac{\pi}{180} + 2 \right) + 3.8 \right]$$

| Unique Hue | Red | Yellow | Green | Blue | Red |
|---|---|---|---|---|---|
| Hue angle $h$ | 13.0 | 93.5 | 153.6 | 246.8 | 373.0 |
| Eccentricity $e$ | 0.8 | 0.7 | 1.0 | 1.2 | 0.8 |
| Hue quadrature H | 0 | 100 | 200 | 300 | 400 |

## Step 5. Chromatic Predictors: Colourfulness, $M$, Chroma, $C$, and Saturation, $s$

$$M = 300 \cdot \frac{e^{0.5} \cdot \left( a^2 + b^2 \right)^{0.4}}{\left( R' + G' + B' \right)^{0.8}} \cdot \sqrt{J/100} \cdot \left( 0.79 + 0.21 \cdot \frac{Y_b}{100} \right) \cdot N_c \cdot L_w^{0.08}$$

$$C = 300 \cdot \frac{e^{0.5} \cdot \left( a^2 + b^2 \right)^{0.4}}{\left( R' + G' + B' \right)^{0.8}} \cdot \sqrt{J/100} \cdot \left( 0.79 + 0.21 \cdot \frac{Y_b}{100} \right) \cdot N_c$$

$$s = 300 \cdot \frac{e^{0.5} \cdot \left( a^2 + b^2 \right)^{0.4}}{\left( R' + G' + B' \right)^{0.8}} \cdot \left( 0.79 + 0.21 \cdot \frac{Y_b}{100} \right) \cdot N_c$$

| | Average | Dim | Dark |
|---|---|---|---|
| $N_c$ | 1.00 | 0.92 | 0.85 |

## 8.13 Steps for Implementing the Reverse Kwak03 Model

This section summarises the steps to calculate tristimulus values from colour appearance attributes. Kwak03 is analytically reversible. The only errors occurring by the inverse procedure are numerical errors.

**Input Data**

- Colour appearance attributes: Lightness $J$, Colourfulness $M$, Hue quadrature $H$
- Relative tristimulus values of reference white, $X_w\ Y_w\ Z_w$
- Background luminance factor, $Y_b$
- Luminance of reference white, $L_w$ (cd/m$^2$)
- Surround condition, Average/Dim/Dark

**Step 1. Calculate Hue angle, $h$, from Hue quadrature, $H$**

$$h = \frac{(H - H_1)\cdot(e_2 h_1 - e_1 h_2) - 100\cdot e_2 h_1}{(e_2 - e_1)\cdot(H - H_1) - 100\cdot e_2} \quad \text{[degrees]}$$

**Step 2. Calculate Chroma, $C$, and Saturation, $s$, from Colourfulness, $M$**

$$C = M\cdot L_w^{-0.08}$$

$$s = C\cdot\sqrt{\frac{100}{J}}\cdot\left(0.79 + 0.21\cdot\frac{Y_b}{100}\right)^{-1}\cdot N_C^{-1}$$

**Step 3. Calculate achromatic signal, $A$, from Lightness, $J$**

$$A = \left(\frac{J}{100}\right)^{-c(L_w)z(Y_b)}\cdot A_w$$

**Step 5. Calculate compressed cone signals $R_k'$, $G_k'$, $B_k'$**

$$R_k' = \frac{2A}{7}\cdot\left(k + \frac{117}{23}\cdot\tan(h\cdot\pi/180) + \frac{231}{161}\right)\cdot\left(k + \frac{63}{23}\cdot\tan(h\cdot\pi/180) + \frac{66}{161}\right)^{-1}$$

$$G_k' = \frac{2A}{7}\cdot\left(k + \frac{90}{23}\cdot\tan(h\cdot\pi/180) - \frac{231}{161}\right)\cdot\left(k + \frac{63}{23}\cdot\tan(h\cdot\pi/180) + \frac{66}{161}\right)^{-1}$$

$$B_k' = \frac{2A}{7}\cdot\left(k - \frac{207}{23}\cdot\tan(h\cdot\pi/180)\right)\cdot\left(k + \frac{63}{23}\cdot\tan(h\cdot\pi/180) + \frac{66}{161}\right)^{-1}$$

where $k = e^{5/8} \cdot \cos^{-1}(h \cdot \pi/180) \cdot (s/300)^{-5/4}$

$$e = \frac{1}{4}\left[\cos\left(h\frac{\pi}{180} + 2\right) + 3.8\right]$$

**Step 6. Calculate tristimulus values, *X*, *Y*, *Z***

$$R' = 100 \cdot (R_k')^{1/0.42},\ G' = 100 \cdot (G_k')^{1/0.42},\ B' = 100 \cdot (B_k')^{1/0.42}$$

$$\begin{vmatrix} R_C \\ G_C \\ B_C \end{vmatrix} = M_{CAT02} \cdot M_H^{-1} \begin{vmatrix} R' \\ G' \\ B' \end{vmatrix} = \begin{vmatrix} 1.55915 & -0.54472 & -0.01445 \\ -0.71433 & 1.85031 & -0.13598 \\ 0.01078 & 0.00522 & 0.98401 \end{vmatrix} \cdot \begin{vmatrix} R' \\ G' \\ B' \end{vmatrix}$$

$$R = R_C \cdot \left[D \cdot \left(\frac{100}{R_W}\right) + 1 - D\right]^{-1},\ G = G_C \cdot \left[D \cdot \left(\frac{100}{G_W}\right) + 1 - D\right]^{-1},\ B = B_C \cdot \left[D \cdot \left(\frac{100}{B_W}\right) + 1 - D\right]^{-1}$$

where $D = F \cdot \left[1 - \frac{1}{3.6} \cdot e^{\frac{-L_W \cdot Y_b/100 - 42}{92}}\right]$

$$\begin{vmatrix} X \\ Y \\ Z \end{vmatrix} = M_{CAT02}^{-1} \cdot \begin{vmatrix} R \\ G \\ B \end{vmatrix} = \begin{vmatrix} 1.09612 & -0.27887 & 0.18275 \\ 0.45437 & 0.47353 & 0.07210 \\ -0.00963 & -0.00570 & 1.01533 \end{vmatrix} \cdot \begin{vmatrix} R \\ G \\ B \end{vmatrix}$$

## 8.14 Summary of the Kwak03 Model

In this chapter the Kwak03 model was introduced. This is a modification of the CIECAM02 model to improve performance particularly in predicting colour appearance phenomena, which were failed, by other colour appearance models.

Major features of the Kwak03 different from CIECAM97s-based models are (1) the omission of the dynamic function by compensating the effect of luminance of the reference white at the later stage, (2) the change of the ratios of three cone signals from 2:1:0.05 to 2:1:0.5, (3) the addition of the rod contribution to the achromatic signal function and (4) the prediction of the size effect. Also the prediction of the colourfulness changes due to background luminance factor is the opposite of other models following the findings from the LUTCHI and CII-Kwak data sets. It is shown that the Kwak03 performs better than the other models studied.

# Chapter 9
# Conclusions

## 9.1 Overview of the Findings

The major aims of this study were to accumulate a colour appearance data set especially for display colours and to improve a colour appearance model to have better performance for the LUTCHI and new colour appearance data. These aims were successfully accomplished with two major outcomes: the CII-Kwak data set and a new colour appearance model, Kwak03. This investigation has focused on the colour appearance of projected and self-luminous colours. The displays used in the study include an LCD projector, a 35-mm slide projector, an LCD monitor and a CRT monitor. Although the new data set covers only display colours, the Kwak03 model performed well not only for display colours but also for reflective colours because of the inclusion of the LUTCHI data in its development. In this section, the findings of the whole study are summarised.

### 9.1.1 Device Characterisation

Prior to the psychophysical experiments, the performance of the colour measurement instruments and devices were investigated, i.e. the spectroradiometers and various displays. Firstly three spectroradiometers – a Bentham, a Minolta CS-1000 and a PhotoResearch PR-650 – were compared. The results showed a non-linear relationship between the measurement data of these three instruments. This implies that it is important to specify which instrument is used for an experiment. Also, it is necessary to use one instrument for the whole set of data to have a consistent relationship between the measurement data. For example, if it is found that one

instrument gives higher luminance than others, comparing the measurement data from two different instruments measured under different conditions could cause confusion. All measurement data in this study were gathered using the PR-650.

Six displays, including a CRT monitor, two LCD projectors and three LCD monitors, were examined to compare their performances. Firstly, the colour characteristics were tested and compared in terms of their chromaticities and spectral power distributions of primary colours, colour gamut, additivity and colour tracking. Secondly, mathematical characterisation models were investigated. It was found that the GOG model performs well for CRT monitors even in the presence of ambient light. However LCD projectors and monitors in general had S-shaped tone curves and poor colour tracking characteristics, which made the GOG model perform very poorly. Therefore two mathematical characterisation models, S-Curve Model I and S-Curve Model II, were developed for LCD projectors and monitors. Both of them are based on the GOG model, but S-Curve Model I only models the S-shaped tone curve whereas the S-Curve Model II models both the S-shaped tone curve and also the colour tracking characteristics.

### 9.1.2 New Colour Appearance Data Set: CII-Kwak

All psychophysical experiments were conducted using the magnitude estimation technique. This resulted in the CII-Kwak data set, which comprises five groups, i.e. P (Presentation), M (Monitor), C (Cinema), A (Ambient), F (Filter), with a total of 20 phases. For each phase, 11 observers participated on average and each colour was assessed in terms of lightness, colourfulness and hue for 40 test colours except for Group P, which had 32 colours per phase. The CII-Kwak data set covers four different kinds of displays (LCD projector, LCD monitor, 35-mm slide projector and CRT monitor), three different backgrounds (white, mid-grey and black), two surround conditions (dark and average), two stimulus sizes (2° and 10°) and luminance levels of reference white ranging from 0.1 to 154 cd/m$^2$.

### 9.1.3 Analysis of Observer Performance

Observer performance was analysed and the results showed that a lengthy training programme or previous experience of colour appearance estimation can improve

observers' repeatabilities but there was no strong evidence that a highly repeatable observer would have good accuracy. Also it was shown that judgement of a particular colour appearance attribute may be affected by the other attributes. For example, it is difficult to judge the colourfulness of a colour with very low or high lightness and to judge the hue of a colour with low lightness and colourfulness.

The number of observers was also investigated to show how much the data accuracy could be affected by the sampling of observers by comparing the average data from different observer groups. The results indicated a larger variation between groups with smaller numbers of observers; in particular, quantifying colour appearance phenomena was more dependent on the observer group used. Ideally it is recommended that as many observers as possible be used however it would be more practical and convenient to repeat similar experiments several times to confirm any colour appearance change. The author's and LUTCHI data sets showed very good agreement. This confirms that colour appearance data collected using magnitude estimation are repeatable and effective for revealing visual phenomena. Also, in both studies the same colour appearance effects were found.

### 9.1.4 Colour Appearance Phenomena

As mentioned before, four different displays were used in this study but no strong evidence was found that the choice of display would affect colour appearance. Any type of display would give the same visual results as long as colours with the same tristimulus values with the same reference white are displayed. It was found that the luminance levels of the reference white, the background colour and surround conditions all had a larger impact on colour appearance than the type of display used. The effects of colour appearance changes due to these factors, which were revealed from the CII-Kwak and part of LUTCHI data sets, are summarised below.

(1) A colour with a higher luminance level for its reference white would induce lower lightness contrast and increase colourfulness compared with a lower luminance level. There was little effect on hue however there was a consistent small effect in that green-blue colours appeared bluer under mesopic vision.

(2) A higher background luminance factor induces a higher lightness contrast and increases colourfulness with no effect on hue. For an increment in

colourfulness, however, there is a subtle difference between dark and light colours. Colours having visual lightness less than 40 appear to be more colourful against a dark background. This effect is small relative to overall colourfulness increments.

(3) A colour appears more colourful and of higher lightness contrast under average surround than under dark surround. There is no hue change due to surround condition change.

(4) A colour with a 10° viewing field looks slightly lighter and more colourful than with a 2° viewing field. The lightness difference between a 2° stimulus and a 10° stimulus is larger for a colour with a green-blue hue than with other hues under mesopic vision.

(5) The Purkinje shift is confirmed under mesopic vision, i.e. blue colours appear relatively lighter than red colours as the lumnanace level decreases. This effect is larger for a 10° stimulus than a 2° stimulus.

### 9.1.5 Testing the Results of Colour Appearance Models

The CII-Kwak and LUTCHI data sets were used to test eight colour appearance models: CIELAB, LLAB, RLAB, Hunt94, CIECAM97s, FC, Fairchild and CIECAM02. For lightness and brightness predictions, Hunt94 gives the best performance followed by CIECAM97s-based models. Note that the lightness predictor specifically developed for projected colours in Hunt94 performs best even for reflective colours in the LUTCHI data. Comparing chroma and colourfulness results, all CIECAM97s-based models performed well except for the Fairchild model. All CIECAM97s-based models show good performance on hue prediction. This atypical behaviour of the Fairchild model is apparently because it was fitted to Munsell Chroma data.

It was found that the models tested gave poor prediction of some colour appearance phenomena. All models tested in the study failed to predict lightness contrast change by luminance level and colourfulness change by background luminance factor especially under dark surround conditions.

### 9.1.6 New Colour Appearance Model: Kwak03

A new colour appearance model, Kwak03, was developed specifically to perform better at predicting colour appearance phenomena under the dark surround condition. The Kwak03 model is based on the CIECAM02 model, which is the most up-to-date CIE colour appearance model intended to replace the CIECAM97s model. Most of the equations in the Kwak03 model, however, have been modified from CIECAM02 to give better performance in fitting the CII-Kwak and LUTCHI data sets.

The notable changes made in Kwak03 in comparison with the other CIECAM97s-based models are:

(1) The dynamic function is not used in the Kwak03 model. Instead, colour appearance change by luminance factor is compensated at a later stage. For example, lightness contrast change due to luminance of the reference white is taken into account by a new $c(L_w)$ function instead of the constant used in other CIECAM97s-based models.

(2) For the achromatic signal $A$, the ratios between three types of cone signals, $R_k'$:$G_k'$:$B_k'$, are modified from 2:1:0.05 to 2:1:0.5. This modification does not have any physiological evidence to support it but improves the performance of the lightness predictor significantly.

(3) The effect of colourfulness change caused due to background luminance factor is remodelled to fit the author's data set, which contradicts the predictions of other colour appearance models.

(4) The effects of rods and stimulus size are included in the Kwak03 model. The rod signals are included in the achromatic signal function, which is capable of predicting the Purkinje shift. The size effect is included in the lightness predictor, which subsequently affects chromatic predictors.

The Kwak03 model was also tested with the same data sets used to test other colour appearance models. It was shown that the model performed the best among all the colour appearance models studied. More importantly it also gave the best performance in predicting a range of colour appearance phenomena.

## 9.2 Future Work

Although the current results showed that the Kwak03 model performs best compared with the previous colour appearance models, there are still many things to be confirmed and improved upon.

Firstly, the modifications made to the Kwak03 model are purely based on empirical fitting to colour appearance data collected by the author and the LUTCHI data set. Independent research is required to confirm these modifications.

Secondly, most of the experimental phases used to derive the Kwak03 model have luminance levels between 0.1 and 250 cd/m$^2$, thus its performance may be inferior outside this luminance range. Further studies on colour appearance at very low luminances in the range of mesopic to scotopic vision and also at very high luminance levels are necessary to develop a more comprehensive model. In particular, recent state-of-art displays provide ever higher luminance levels for which no colour appearance data are available.

Thirdly, the Kwak03 model also has the same limitations as other CIECAM97s-based models. These models are based on experiments with simple colour patches shown against a neutral background. Although decoration colours were adopted to simulate a complex image during the experiment, the performance of the model still needs to be tested using real complex images.

Fourthly, the Kwak03 model requires the luminance of reference white, the background luminance factor and surround condition. Note that these factors are used to set the state of visual adaptation, although the term 'state of adaptation' is not explicitly used in the model. There is, however, no guideline as to how to apply these values for a complex image, which has no white colour in the scene. Also there is little research to date on how to determine the background luminance factor of a complex image or scene. The choice of a surround condition is still ambiguous based on the current definitions because there are no guidelines for measuring the surround luminance.

The Kwak03 model provides the numbers representing colour appearance attributes however there are no meaningful relationships between attributes to derive uniform

colour space or colour difference equations. Note that achieving a uniform colour space is very important for colour imaging applications such as colour gamut mapping. Further research is strongly required to expand the Kwak03 model to have a uniform colour space.

Fairchild [Fair2002] recently suggested a new paradigm for the colour appearance model. In short, his idea is to extend the colour appearance model from treating each pixel in an image as an independent stimulus to including spatial interactions between pixels by considering spatial appearance phenomena. Note that even in this paradigm, an accurate colour appearance model for predicting an individual colour stimulus is still essential. It will need thorough investigation to determine how best to include the spatial properties of an image in a comprehensive model of colour appearance.

# References


ANSI ANSI/SMPTE 196M-1986, Screen luminance and viewing conditions – Indoor theater projection

Bart1967 C.J. Bartleson & E.J. Breneman, Brightness perception in complex fields, *J. Opt. Soc. Am.* **57**, 953-957 (1967)

Bart1979 C.J. Bartleson, Changes in color appearance with variations in chromatic adaptation, *Color Res. Appl.* **4**, 119-138 (1979)

Bern1985 R.S. Berns & F.W. Millmeyer, Jr., Development of the 1929 Munsell book of color: A historical review, *Col. Res. Appl.* **10**, 246-250, (1985)

Bern1993 R.S. Berns, R. J. Motta & M. E. Gorzynski, CRT colorimetry, part I: theory and practice, *Col. Res. Appl.* **18**, 299-314, (1993)

Bern1995 R.S. Berns, Methods for characterizing CRT displays, *Displays*, **16**, 173-182, (1995)

Bern2000 R.S. Berns, *Billmeyer and Saltzman Principles of color technology 3rd Ed.*, John Wiley & Sons (2000)

Boyn1970 R.M. Boynton & D.N. Whitten, Visual adaptation in monkey cones: recordings of late receptor potentials, *Science*, **170**, 1423-1426 (1970)

Bren1962 E.J. Breneman, The effect of level of illuminance and relative surround luminance on the appearance of black-and-white photographs, *Phot. Sci. Eng.*, **6**, 172 (1962)

Bren1977 E.J. Breneman, Perceived saturation in complex stimuli viewed in light and dark surrounds, *J. Opt. Soc. Am.* **67**, 657-662 (1977)

Bren1987 E.J. Breneman, Corresponding chromaticities for different states of adaptation to complex visual fields, *J. Opt. Soc. Am. A.* **4**, 1115-1129 (1987)

CIE1924 *CIE Proceedings 1924*, p.67 (also p.232), Cambridge University Press, Cambridge, 1926

CIE1951 *CIE Proceedings 1951*, Vol. 1, Sec. 4; Vol. 3, p.37, Bureau Central de la CIE, Paris, 1951

CIE1971 CIE, *Colorimetry*, CIE Publ. No. 15, Vienna (1971)

CIE1986 CIE, *Colorimetry*, CIE Publ. No. 15.2, Vienna (1986)

CIE1987 CIE, *International Lighting Vocabulary*, CIE Publ. No. 17.4, Vienna (1987)

CIE1998 CIE, *The CIE 1997 interim colour appearance model (simple version), CIECAM97s*, CIE Publication 131-1998, Vienna (1996)

Enge2000 P.G. Engeldrum, *Psychometric scaling: A toolkit for imaging systems development*, Incotek press, Massachusetts (2000)

Fair1993 M.D. Fairchild & R.S. Berns, Image color appearance specification through extension of CIELAB, *Color Res. Appl.* **18**, 178-190 (1993)

Fair1994 M.D. Fairchild, visual evaluation and evolution of the RLAB color space, *Proc. IS&T.SID 2nd Color Imaging Conference*, Scottsdale, Ariz. 9-13 (1994)

Fair1995 M.D. Fairchild, Considering the surround in device-independent color imaging, *Color Res. Appl.* **20**, 352-363 (1995)

Fair1996 M.D. Fairchild, Refinement of the RLAB color space, *Color Res. Appl.* **21**, 338-346 (1996)

Fair1998a M.D. Fairchild, *Color appearance models*, Addison-Wesley, Massachusetts (1998)

Fair1998b M.D. Fairchild & D. R. Wyble, Colorimetric characterization of the apple studio display (Flat panel LCD), *Munsell Color Science Laboratory Technical Report*, July, (1998)

Fair2001 M.D. Fairchild, A revision of CIECAM97s for practical applications, *Color Res. Appl.* **26**, 418-427 (2001)

Fair2002 M.D. Fairchild and G.M. Johnson, Meet iCAM: A next-generation color appearance model, *Proc. The 10th Color Imaging Conference*, Scottsdale, USA, Nov. (2002)

Fech1860 G.T. Fechner, *Element der psychophysik*, Breikopf & Harterl, Leipzig (1860)

Fech1966 G.T. Fechner, *Elements of psychophysics Vol. I* (trans. by H.E. Adler), Holt, Rinehart and Wintston, New York, N.Y. (1966)

Finl1999 G.D. Finlayson, M.S. Drew, Positive Bradford curves through sharpening, *Proc. IS&T/SID 7th Color Imaging Conference*, Scottsdale, p.227-232 (1999)

Finl2000 G.D. Finlayson, S. Susstrunk, Performance of a chromatic adaptation transform based on spectral sharpening, *Proc. IS&T/SID 8th Color Imaging Conference*, Scottsdale, p.56-60 (2000)

Gesc1997 G. A. Gescheider, *Psychophysics: The fundamentals, 3rd Edition*, Lawrence Erlbaum Associates, (1997)

Hans1997 A.R. Hanson, *Measurement and standardisation in the colorimetry of CRT displays*, In L. MacDonald & A. Lowe (Eds.), Display systems: Technology and applications, Wiley, (1997)

Hels1938 H. Helson, Fundamental problems in color vision. I. The principle governing changes in hue, saturation, and lightness of non-selective samples in chromatic illumination, *J. Exp. Psych.* **23**, 439-477 (1938)

Heri1964 E. Hering, *Outlines of a theory of the light sense*, Translation by L.M. Hurvich and D. Jameson, Harvard University Press, Cambridge, MA, (1964)

Hunt1952 R.W.G. Hunt, Light and dark adaptation and the perception of color, *J. Opt. Soc. Am.* **42**, 190-199 (1952)

Hunt1977a R.W.G. Hunt, The specification of colour appearance. I. Concepts and terms, *Color Res. Appl.* **2**, 55-68 (1977)

Hunt1977b R.W.G. Hunt, The specification of colour appearance. II. Effects of changes in viewing conditions, *Color Res. Appl.* **2**, 109-120 (1977)

Hunt1982 R.W.G. Hunt, A model of colour vision for predicting colour appearance, *Color Res. Appl.* **7**, 95-112 (1982)

Hunt1985 R.W.G. Hunt and M. R. Pointer, A colour-appearance transform for the 1931 standard colorimetric observer, *Color Res. Appl.* **10**, 165-179 (1985)

Hunt1987 R.W.G. Hunt, A model of colour vision for predicting colour appearance in various viewing condition, *Color Res. Appl.* **12**, 297-314 (1987)

Hunt1991 R.W.G. Hunt, Revised colour-appearance model for related and unrelated colours, *Color Res. Appl.*, **16**, 146-165 (1991)

Hunt1994 R.W.G. Hunt, An improved predictor of colourfulness in a model of colour vision, *Color Res. Appl.* **19**, 23-26 (1994)

Hunt1995 R.W.G. Hunt, *The reproduction of colour, 5th Edition*, Fountain Press, (1995)

Hunt1998 R.W.G. Hunt, *Measuring colour*, 3rd Edition, Fountain Press, (1998)

Hunt2002 R.W.G. Hunt, C.J. Li, L.Y. Juan and M.R. Luo, Further improvements to CIECAM97s, *Color Res. Appl.* **27**, 164-170 (2002)

Hunt2003 R.W.G. Hunt, C.J. Li and M.R. Luo, Dynamic cone response functions for models of color appearance, *Color Res. Appl.* (submitted)

Hurv1985 .L.M. Hurvich, *Color Vision*, Sinauer Associates, Sunderland, Mass., U.S.A. (1981)

Isha1970 I.G.H. Ishak, H. Bouma. And H.J.J. Van Bussel, Subjective estimates of colour attributes for surface colours, *Vision Res.*, **10**, 489-500 (1970)

John1996 T. Johnson, Methods for characterising colour scanners and digital cameras, *Displays*, **16**, 183-191 (1996)

Juan2000 L.G. Juan, Verification of colour appearance models using magnitude estimation data, *PhD Thesis*, University of Derby, U.K. (2000)

Judd1949 D.B. Judd, Response functions for types of vision according to the Muller theory, *J. Res. Nat. Bur. Standards* (*Washington, DC*) **42**, 1 (1949)

Judd1950 D.B. Judd, Basic correlates of the visual stimulus, in: *Handbook of experimental psychology*, Chapter 22 (S.S. Stevens, Ed.), pp.811-867, Wiley, New York, (1951)

Kais1996 P.K. Kaiser and P.M. Boynton, *Human color vision*, Optical Society of America (1996)

Kolb2003 H. Kolb, E. Fernandez and R. Nelson, Webvision: the organization of the retina and visual system, http://webvision.med.utah.edu/index.html, Last updated: March 24, 2003

Kuo1995 W.G. Kuo, M.R. Luo and H.E. Bez, Various chromatic-adaptation transforms tested using new colour appearance data in textile, *Color Res. Appl.*, **20**, 313-327 (1995)

Kwak2000 Y. Kwak and L. MacDonald, Characterisation of a desktop LCD projector, *Displays*, **21**, 179-194, (2000)

Kwak2003 Y. Kwak, C. Li and L. MacDonald, Controling color of liquid-crystal displays, *Journal of the SID*, **11/2**, (2003)

Lam1985 K.M. Lam, *Metamerism and colour constancy*, Ph.D. thesis, University of Bradford, (1985)

Li2000 C.J. Li, M.R. Luo and R.W.G. Hunt, A revision of the CIECAM97s model, *Color Res. Appl.* **25**, 260-266 (2000)

Li2002 C.J. Li, M.R. Luo, B. Rigg and R.W.G. Hunt, CMC2000 chromatic adaptation transform: CMCCAT2000, *Color Res. Appl.* **27**, 49-58 (2002)

Luo1991a M.R. Luo, A.A. Clarke, P.A. Rhodes, A. Schappo, S.A.R. Scrivener and C.J. Tait, Quantifying colour appearance. Part I. LUTCHI colour appearance data, *Color Res. Appl.* **16**, 166-180 (1991)

Luo1991b M.R. Luo, A.A. Clarke, P.A. Rhodes, A. Schappo, S.A.R. Scrivener and C.J. Tait, Quantifying colour appearance. Part II. Testing colour models

performance using LUTCHI colour appearance data, *Color Res. Appl.* **16**, 181-197 (1991)

Luo1993a M.R. Luo, X.W. Gao, P.A. Rhodes, H.J. Xin, A.A. Clarke and S.A.R. Scrivener, Quantifying colour appearance. Part III. Supplementary LUTCHI colour appearance data, *Color Res. Appl.* **18**, 98-113 (1993)

Luo1993b M.R. Luo, X.W. Gao, P.A. Rhodes, H.J. Xin, A.A Clarke and S.A.R. Scrivener, Quantifying colour appearance. Part IV. Transmissive media, *Color Res. Appl.* **18**, 191-209 (1993)

Luo1996 M.R. Luo, M.C. Lo and W.G. Kuo, The LLAB(l:c) colour model, *Color Res. Appl.*, **21**, 412-429 (1996)

Luo1997 M.R. Luo, H. Xu, S. Tang and F. Zhou, Testing colour models performance using unrelated colour appearance data, *Proc. the AIC '97 Kyoto*, 175-178 (1997)

Luo1998 M.R. Luo, R.W.G. Hunt, The structure of the CIE 1997 colour appearance model (CIECAM97s), *Color Res. Appl.* **23**, 138-146 (1998)

Luo1999 M.R. Luo, *Colour science: past, present and future*, In L.W. MacDonald & M.R. Luo (Eds.), Colour imaging: Vision and technology, John Wiley & Sons, (1999)

Luo2000 M.R. Luo, A review of chromatic adaptation transform, *Rev. Prog. Coloration*, **30**, 77-91 (2000)

LUTCHI Official web site for the LUTCHI data set: http://colour.derby.ac.uk/colour/info/lutchi/

MacD1995 L.W. MacDonald, Developments in colour management systems, *Displays*, **16**, 203-211 (1995)

McCa1976 C.S. McCamy, H. Marcus and J.G. Davidson, A color-rendering chart, *Journal of Applied Photographic Engineering*, **2**(3), 95-99 (1976)

Moro1998 N. Moroney, A comparison of CIELAB and CIECAM97s, *Proc. The 6th Color Imaging Conference*, Scottsdale, p.17-21 (1998)

Moro2000 N. Moroney, Usage guidelines for CIECAM97s, *Proc. PICS Conference*, p.164-168 (2000)

Moro2002 N. Moroney, M.D. Fairchild, R.W.G. Hunt, C. Li, M.R. Luo, T. Newman, The CIECAM02 colour appearance model, *Proc. The 10th color imaging conference*, Scottsdale, USA, Nov. (2002)

Morov1996 J. Morovic and M.R. Luo, Two unsolved issues in colour management - colour appearance and gamut mapping, *The 5th international conference on high technology on imaging science and technology - evolution and promise*, Chiba, Japan, 11-14 September, (1996)

Mull1930 G. E. Muller, Uber die farbenempfindungen, *Z.Psychol., Erganzungsb.* **17** and **18** (1930)

Naya1972 Y. Nayatani, T. Yamanaka, and H. Sobagaki, Subjective estimation of color attributes for surface colors (Part1: Reproducibility of estimations) *Acta Chromatica*, **2**, 129-138 (1972)

Newh1940 S.M. Newhall, Preliminary report on the OSA subcommittee on the spacing of the Munsell colors, *J. Opt. Soc. Am.* **30**, 617-645 (1940)

Newh1943 S.M. Newhall, D. Nickerson & D.B. Judd, Final report of the OSA subcommittee on the spacing of the Munsell colors, *J. Opt. Soc. Am.* **33**, 385-418 (1943)

Newm2000 T. Newman, E. Pirrotta, The darker side of colour appearance models and gamut mapping, *Proc. Colour imaging science conference*, Derby, p.215-223 (2000)

Norm1979 R.A. Normann & I. Perlman, The effects of background illumination on the photoresponses of red and green cones, *J. Physiol*, **286**, 491-507, (1979)

Oste1935 G.A. Osterberg, Topography of the layer of rods and cones in the human retina, *Acta Ophthal.* **13** (Supplement **6**) 1-97 (1935)

Pitt1974 I.T. Pitt & L.M. Winter, Effect of surround on perceived saturation, *J. Opt. Soc. Am.* **64**, 1328-1331 (1974)

Poin1977 M.R. Pointer, J.S. Ensell, & L.M. Bullock, Grids for assessing colour appearance, *Color Res. Appl.* **2**, 131-136 (1977)

Point1978 M.R. Pointer, Colourfulness: A new concept, in Fred W. Billmeyer, Jr., and Gunter Wyszecki, Ed., *Color77*, Adam Hilger, Bristol, England, p.327-330 (1978)

Poin1980 M.R. Pointer, The concept of colourfulness and its use for deriving grids for assessing colour appearance, *Color Res. Appl.* **5**, 99-107 (1980)

Rhod1996 P.A. Rhodes and M.R. Luo, A system for WYSIWYG colour communication, *Displays*, **16**, 213-221 (1996)

Rowe1972 S.C.H. Rowe, The subjective scaling of colours, Ph.D. Thesis, The city university, London (1972)

Steve1963 J.C. Stevens and S.S. Stevens, Brightness function: Effects of adaptation, *J. Opt. Soc. Am.* **53**, 375-385 (1963)

Stev1957a S.S. Stevens, On the psychophysical law, *Psychological Review*, **64**, 153-181 (1957)

Stev1957b S.S. Stevens, E.H. Galanter, Ratio scales and category scales for a dozen perceptual continua, *Journal of experimental psychology*, **54**, 377-411 (1957)

Stev1960 S.S. Stevens, *Ratio scales, partition scales and confusion scales*, In H. Gulliksen & S. Messick (Eds.), Psychological scaling: Theory and application. Wiley, New York (1960)

Stev1961 S.S. Stevens, To honour Fechner and repeal his law: A power function, not a log function describes the operating characteristic of a sensory system, *Science*, **133**, p.80-86 (1961)

Stev1971 S.S. Stevens, Issues in psychophysical measurement, *Psychological review*, **78**, 426-450 (1971)

Stil1959 W. S. Stiles & J. M. Burch, NPL colour-matching investigation: Final report. *Optica Acta*, **6**, 1-26 (1959)

Stoc2000 A. Stockman & L. T. Sharpe, Spectral sensitivities of the middle- and long-wavelength sensitive cones derived from measurements in observers of known genotype, *Vision research*, **40**, 1711-1737 (2000)

Thur1959 L.L. Thurstone, *The measurement of values*, University of Chicago press, Chicago (1959)

Vale1983 J.M. Valeton & D. Van Noreen, Light adaptation of primate cones: An analysis based on extracellular data, *Vision Res.* **23**. 1539-1547 (1983)

VonK1902 J. von Kries, *Chromatic adaptation*, Festschrift der Albrecht-Ludwig-Universitat (Fribourg) (1902) [Translation: D.L. MacAdam, *Sources of color science*, MIT Press, Cambridge, Mass. (1970)]

VonK1911 J. von Kries, In Handbuch der physiologisches optik, Vol. II (W. Nagel, ed), pp.366-369, Leopold Voss, Hamburg (1911)

Wang1994 X. Wang, Modelling of colour appearance, *PhD Thesis*, the Loughborough university of technology, U.K. (1994)

Walr1966 P.L. Walraven and M.A. Bouman, *Vision Res.* **6**. 567 (1966)

Wybl2000 D.R. Wyble and M.D. Fairchild, Prediction of Munsell appearance scales using various color Appearance Models, *Color Res. Appl.* **25**, 132-144 (2000)

Wysz1973 G. Wyszecki, Current developments in colorimetry, *Proc. AIC Color 73*, 21-51 (1973)

Wysz1982 G. Wyszecki & W.S. Stiles, *Color science: Concepts and methods, quantitative data and formulae*, 2nd Edition, John Wiley & Sons, (1982)

Zwin1996 J.C. Zwinkels, Colour-measuring instruments and their calibration, *Displays,* **16**, 163-171 (1996)

# Appendix 1
# List of Experimental Phases

# A1.1 CII-Kwak Data Set

| | | Name | Surround | Device | CCT (K) | Lw*1 | Yb*2 | No. of Observers | No. of Samples |
|---|---|---|---|---|---|---|---|---|---|
| CII-Kwak | P | P-Grey | Dark | Projector | 7200 | 154.0 | 18.34 | 21 | 32+10 |
| | | P-Black | Dark | Projector | 7200 | 152.7 | 0.42 | 21 | 32+10 |
| | | P-Filter | Dark | Projector | 7200 | 18.77 | 18.68 | 21 | 32+10 |
| | M | M-Grey | Dark | LCD Monitor | 7200 | 90.33 | 20.65 | 12 | 40+10 |
| | | M-Black | Dark | LCD Monitor | 7200 | 89.81 | 0.36 | 11 | 40+10 |
| | | M-White | Dark | LCD Monitor | 7200 | 90.22 | 100.0 | 12 | 40+10 |
| | C | C-Grey | Dark | Projector | 7200 | 15.68 | 17.37 | 9 | 40+10 |
| | | C-White | Dark | Projector | 7200 | 16.28 | 97.42 | 9 | 40+10 |
| | | C-Black | Dark | Projector | 7200 | 15.00 | 0.4 | 11 | 40+10 |
| | | C-35mm | Dark | Projector | 3900 | 15.42 | 20.38 | 11 | 40+10 |
| | A&F | A-Dark | Dark | CRT Monitor | 6800 | 85.77 | 19.82 | 11 | 40+10 |
| | | A-Avg | Average | CRT Monitor | 6800 | 89.13 | 24.00 | 11 | 40+10 |
| | | Filter0-02 | Dark | CRT Monitor | 6800 | 87.37 | 19.76 | 12 | 40+10 |
| | | Filter0-10 | Dark | CRT Monitor | 6800 | 87.37 | 19.77 | 12 | 40+10 |
| | | Filter1-02 | Dark | CRT Monitor | 6700 | 8.856 | 20.86 | 13 | 40+10 |
| | | Filter1-10 | Dark | CRT Monitor | 6700 | 8.856 | 20.89 | 12 | 40+10 |
| | | Filter2-02 | Dark | CRT Monitor | 6700 | 1.007 | 19.49 | 10 | 40+10 |
| | | Filter2-10 | Dark | CRT Monitor | 6700 | 1.007 | 18.96 | 11 | 40+10 |
| | | Filter3-02 | Dark | CRT Monitor | 6700 | 0.097 | 19.82 | 11 | 40+10 |
| | | Filter3-10 | Dark | CRT Monitor | 6700 | 0.105 | 19.83 | 10 | 40+10 |

*1 Lw : Luminance of reference white (cd/m2)

*2 Yb : Background luminance factor (%)

# A1.2 LUTCHI Data Set

| | | Name | Surround | Device | CCT (K) | Lw*1 | Yb*2 | No. of Observers | No. of Samples |
|---|---|---|---|---|---|---|---|---|---|
| LUTCHI** | 35 | 35mm 1 | Dark | Projector | 4000 | 113.0 | 18.90 | 6 | 99 |
| | | 35mm 2 | Dark | Projector | 5600 | 45.00 | 18.90 | 6 | 99 |
| | | 35mm 3 | Dark | Projector | 4000 | 47.00 | 19.20 | 6 | 99 |
| | | 35mm 4 | Dark | Projector | 4000 | 113.0 | 18.90 | 6 | 99 |
| | | 35mm 5 | Dark | Projector | 4000 | 75.00 | 14.70 | 5 | 95 |
| | | 35mm 6 | Dark | Projector | 4000 | 75.00 | 15.60 | 5 | 36 |
| | CRT | CRT 01 | Dark | CRT Monitor | 5000 (D50) | 40.0 | 100.0 | 6 | 94 |
| | | CRT 02 | Dark | CRT Monitor | 5000 (D50) | 44.5 | 5.00 | 6 | 100 |
| | | CRT 03 | Dark | CRT Monitor | 5000 (D50) | 44.5 | 20.00 | 6 | 100 |
| | | CRT 04 | Dark | CRT Monitor | 5000 (D50) | 44.5 | 20.00 | 6 | 100 |
| | | CRT 05 | Dark | CRT Monitor | 5000 (D50) | 44.5 | 20.00 | 6 | 100 |
| | | CRT 06 | Dark | CRT Monitor | 7000 (D65) | 40.5 | 21.50 | 7 | 103 |
| | | CRT 07 | Dark | CRT Monitor | 7000 (D65) | 40.5 | 21.50 | 7 | 103 |
| | | CRT 08 | Dark | CRT Monitor | 3500 (WF) | 28.4 | 21.50 | 7 | 86 |
| | | CRT 09 | Dark | CRT Monitor | 3500 (WF) | 28.4 | 21.50 | 7 | 86 |
| | | CRT 10 | Dark | CRT Monitor | 2500 (A) | 20.3 | 21.50 | 7 | 61 |
| | | CRT 11 | Dark | CRT Monitor | 2500 (A) | 20.3 | 21.50 | 7 | 61 |
| | R-VL | R-VL1 | Average | Reflective | 5000 | 843 | 21.50 | 4 | 40 |
| | | R-VL2 | Average | Reflective | 5000 | 200 | 21.50 | 4 | 40 |
| | | R-VL3 | Average | Reflective | 5000 | 62 | 21.50 | 4 | 40 |
| | | R-VL4 | Average | Reflective | 5000 | 17 | 21.50 | 4 | 40 |
| | | R-VL5 | Average | Reflective | 5000 | 6 | 21.50 | 4 | 40 |
| | | R-VL6 | Average | Reflective | 5000 | 0.4 | 21.50 | 4 | 40 |
| | | R-VL7 | Average | Reflective | 5000 | 843 | 21.50 | 4 | 40 |
| | | R-VL8 | Average | Reflective | 5000 | 200 | 21.50 | 4 | 40 |
| | | R-VL9 | Average | Reflective | 5000 | 62 | 21.50 | 4 | 40 |
| | | R-VL10 | Average | Reflective | 5000 | 17 | 21.50 | 4 | 40 |
| | | R-VL11 | Average | Reflective | 5000 | 6 | 21.50 | 4 | 40 |
| | | R-VL12 | Average | Reflective | 5000 | 0.4 | 21.50 | 4 | 40 |
| | R-H&LL | R-HL1 | Average | Reflective | 4700 (D50) | 264.0 | 100.0 | 6 | 105 |
| | | R-HL2 | Average | Reflective | 5000 (D50) | 252.0 | 6.20 | 6 | 105 |
| | | R-HL3 | Average | Reflective | 5000 (D50) | 252.0 | 21.50 | 6 | 105 |
| | | R-HL4 | Average | Reflective | 7000 (D65) | 243.0 | 21.50 | 7 | 105 |
| | | R-HL5 | Average | Reflective | 3500 (WF) | 252.0 | 21.50 | 6 | 105 |
| | | R-HL6 | Average | Reflective | 2500 (A) | 232.0 | 21.50 | 7 | 105 |
| | | R-LL1 | Average | Reflective | 4700 (D50) | 44.0 | 100.0 | 6 | 105 |
| | | R-LL2 | Average | Reflective | 5000 (D50) | 42.0 | 6.20 | 6 | 105 |
| | | R-LL3 | Average | Reflective | 5000 (D50) | 42.0 | 21.50 | 6 | 105 |
| | | R-LL4 | Average | Reflective | 7000 (D65) | 40.5 | 21.50 | 7 | 105 |
| | | R-LL5 | Average | Reflective | 3500 (WF) | 42.0 | 21.50 | 6 | 105 |
| | | R-LL6 | Average | Reflective | 2500 (A) | 42.0 | 21.40 | 7 | 105 |

*1 Lw : Luminance of reference white (cd/m2)

*2 Yb : Background luminance factor (%)

** Note that only the phases used in this study are listed here.

# Appendix 2

# Performance of Colour Appearance Models (CV)

# A2.1 Performance of Brightness Predictors

| | | Name | CIE LAB | LLAB | RLAB | Hunt 94 | CIE CAM 97s | FC | Fair-child | CIE CAM 02 | Kwak 03 |
|---|---|---|---|---|---|---|---|---|---|---|---|
| LUTCHI | R-VL | R-VL7 | N/A | N/A | N/A | 7.72 | 7.84 | 7.75 | 7.86 | 10.26 | 10.02 |
| | | R-VL8 | N/A | N/A | N/A | 9.13 | 10.70 | 10.65 | 9.40 | 15.20 | 8.19 |
| | | R-VL9 | N/A | N/A | N/A | 17.58 | 20.90 | 19.23 | 18.05 | 16.73 | 14.80 |
| | | R-VL10 | N/A | N/A | N/A | 7.68 | 9.17 | 9.16 | 7.77 | 23.80 | 9.15 |
| | | R-VL11 | N/A | N/A | N/A | 10.59 | 12.97 | 11.93 | 10.83 | 26.94 | 10.59 |
| | | R-VL12 | N/A | N/A | N/A | 16.52 | 20.10 | 19.39 | 18.94 | 40.80 | 15.83 |

# A2.2 Performance of Lightness Predictors

| | | Name | CLAB | LLAB | RLAB | H94 | 97s | FC | Fd | 02s | K03 |
|---|---|---|---|---|---|---|---|---|---|---|---|
| CII-Kwak | P | P-Grey | 15.14 | 16.15 | 17.57 | 16.77 | 13.85 | 13.66 | 15.99 | 12.87 | 12.18 |
| | | P-Black | 16.18 | 11.30 | 13.12 | 12.03 | 10.24 | 10.40 | 11.58 | 10.13 | 9.41 |
| | | P-Filter | 18.58 | 16.85 | 31.55 | 11.12 | 15.03 | 15.83 | 14.64 | 17.03 | 14.76 |
| | M | M-Grey | 18.28 | 19.20 | 23.48 | 20.13 | 16.96 | 16.93 | 18.69 | 16.33 | 17.29 |
| | | M-Black | 15.17 | 10.17 | 12.84 | 14.74 | 10.98 | 9.57 | 10.69 | 9.55 | 11.33 |
| | | M-White | 27.77 | 22.34 | 46.06 | 16.93 | 18.98 | 19.44 | 19.54 | 19.13 | 18.05 |
| | C | C-Grey | 17.29 | 17.23 | 25.33 | 15.60 | 15.21 | 15.79 | 17.22 | 15.45 | 12.75 |
| | | C-White | 24.17 | 21.35 | 39.05 | 18.12 | 18.80 | 18.96 | 20.44 | 17.80 | 16.65 |
| | | C-Black | 15.58 | 16.65 | 19.12 | 10.44 | 13.89 | 14.91 | 12.98 | 14.86 | 10.72 |
| | | C-35mm | 16.26 | 16.55 | 36.04 | 17.39 | 16.26 | 16.35 | 18.84 | 15.59 | 15.02 |
| | A&F | A-Dark | 18.38 | 19.97 | 20.80 | 18.38 | 17.86 | 18.03 | 20.29 | 16.80 | 14.52 |
| | | A-Max | 20.24 | 24.51 | 18.64 | 17.46 | 21.42 | 20.67 | 23.64 | 19.54 | 16.51 |
| | | Filter0-02 | 15.72 | 17.46 | 18.47 | 17.91 | 15.16 | 15.11 | 17.74 | 14.03 | 12.49 |
| | | Filter0-10 | 16.64 | 18.65 | 16.97 | 19.20 | 16.09 | 16.12 | 18.89 | 14.74 | 12.38 |
| | | Filter1-02 | 18.76 | 18.15 | 29.10 | 16.01 | 16.63 | 16.90 | 17.65 | 17.41 | 15.10 |
| | | Filter1-10 | 15.75 | 16.61 | 22.24 | 18.04 | 15.50 | 15.79 | 18.37 | 14.77 | 13.42 |
| | | Filter2-02 | 19.98 | 16.82 | 35.49 | 9.71 | 17.00 | 14.82 | 12.93 | 18.69 | 10.96 |
| | | Filter2-10 | 16.85 | 14.34 | 31.26 | 14.33 | 15.32 | 13.52 | 13.32 | 16.30 | 12.35 |
| | | Filter3-02 | 22.35 | 18.62 | 39.64 | 12.23 | 36.43 | 15.46 | 12.57 | 21.70 | 10.99 |
| | | Filter3-10 | 16.65 | 13.93 | 32.18 | 13.66 | 28.81 | 12.55 | 12.46 | 16.64 | 10.18 |
| LUTCHI | 35 | 35mm 1 | 19.58 | 19.46 | 34.23 | 16.09 | 18.64 | 19.17 | 19.45 | 18.11 | 15.54 |
| | | 35mm 2 | 19.66 | 18.78 | 36.94 | 14.05 | 18.11 | 18.75 | 18.81 | 18.71 | 14.11 |
| | | 35mm 3 | 18.93 | 18.03 | 36.65 | 14.47 | 17.65 | 18.23 | 18.20 | 17.88 | 14.14 |
| | | 35mm 4 | 16.96 | 17.85 | 29.27 | 16.62 | 16.88 | 16.87 | 18.52 | 15.45 | 12.80 |
| | | 35mm 5 | 19.67 | 19.50 | 33.37 | 16.72 | 18.67 | 19.12 | 19.86 | 18.28 | 15.32 |
| | | 35mm 6 | 12.74 | 13.92 | 22.17 | 16.49 | 13.27 | 12.36 | 15.99 | 10.96 | 9.84 |
| | CRT | CRT 01 | 36.15 | 14.23 | 55.57 | 9.44 | 15.56 | 16.93 | 13.80 | 20.69 | 12.17 |
| | | CRT 02 | 6.79 | 7.83 | 16.53 | 11.05 | 8.03 | 8.76 | 7.34 | 8.73 | 5.66 |
| | | CRT 03 | 12.31 | 9.33 | 26.86 | 9.27 | 9.44 | 10.61 | 7.94 | 11.79 | 9.27 |
| | | CRT 04 | 19.74 | 15.33 | 36.32 | 9.25 | 15.52 | 17.42 | 12.31 | 19.04 | 15.67 |
| | | CRT 05 | 11.30 | 8.13 | 26.31 | 10.24 | 8.60 | 9.66 | 6.86 | 11.11 | 9.03 |
| | | CRT 06 | 21.31 | 17.33 | 34.77 | 8.67 | 17.37 | 19.11 | 15.20 | 20.39 | 15.79 |
| | | CRT 07 | 17.58 | 13.69 | 30.96 | 7.57 | 13.81 | 15.45 | 11.72 | 16.77 | 12.21 |
| | | CRT 08 | 19.39 | 14.90 | 36.79 | 8.69 | 14.26 | 15.76 | 11.40 | 17.91 | 14.18 |
| | | CRT 09 | 15.86 | 11.46 | 33.04 | 8.25 | 11.30 | 12.52 | 8.67 | 14.67 | 11.12 |
| | | CRT 10 | 21.26 | 16.43 | 40.48 | 8.27 | 15.51 | 16.82 | 12.01 | 19.83 | 16.16 |
| | | CRT 11 | 17.67 | 13.19 | 36.33 | 10.84 | 12.78 | 13.59 | 9.50 | 16.68 | 13.61 |
| | R-VL | R-VL1 | 11.07 | 19.43 | 10.21 | 13.16 | 14.18 | 12.29 | 15.63 | 13.92 | 10.80 |
| | | R-VL2 | 14.15 | 15.57 | 12.11 | 11.86 | 12.52 | 11.30 | 14.31 | 10.88 | 8.66 |
| | | R-VL3 | 15.27 | 15.65 | 13.20 | 13.16 | 13.78 | 12.83 | 16.08 | 11.60 | 9.11 |
| | | R-VL4 | 15.95 | 12.62 | 13.66 | 11.00 | 11.55 | 10.91 | 14.57 | 9.40 | 9.21 |
| | | R-VL5 | 16.40 | 13.85 | 14.17 | 14.27 | 12.70 | 12.64 | 16.87 | 10.21 | 9.76 |
| | | R-VL6 | 22.85 | 16.53 | 20.86 | 19.17 | 16.72 | 17.71 | 21.46 | 15.35 | 15.01 |
| | | R-VL7 | N/A | N/A | N/A | N/A | N/A | N/A | N/A | N/A | N/A |
| | | R-VL8 | N/A | N/A | N/A | N/A | N/A | N/A | N/A | N/A | N/A |
| | | R-VL9 | N/A | N/A | N/A | N/A | N/A | N/A | N/A | N/A | N/A |
| | | R-VL10 | N/A | N/A | N/A | N/A | N/A | N/A | N/A | N/A | N/A |
| | | R-VL11 | N/A | N/A | N/A | N/A | N/A | N/A | N/A | N/A | N/A |
| | | R-VL12 | N/A | N/A | N/A | N/A | N/A | N/A | N/A | N/A | N/A |
| | R-H&LL | R-HL1 | 40.18 | 14.30 | 36.19 | 10.93 | 13.28 | 14.81 | 12.52 | 12.99 | 9.37 |
| | | R-HL2 | 12.95 | 7.71 | 10.63 | 8.11 | 8.15 | 9.05 | 8.28 | 8.13 | 6.63 |
| | | R-HL3 | 24.13 | 11.32 | 20.89 | 9.45 | 12.09 | 13.89 | 11.41 | 12.28 | 11.21 |
| | | R-HL4 | 20.19 | 13.15 | 17.20 | 7.61 | 11.97 | 12.59 | 12.63 | 11.43 | 9.38 |
| | | R-HL5 | 18.24 | 12.13 | 15.35 | 7.89 | 10.41 | 10.85 | 10.94 | 9.36 | 7.02 |
| | | R-HL6 | 18.34 | 12.04 | 15.51 | 7.78 | 10.25 | 10.58 | 10.79 | 9.62 | 8.97 |
| | | R-LL1 | 48.04 | 11.49 | 43.76 | 12.43 | 12.44 | 13.86 | 11.20 | 16.40 | 9.57 |
| | | R-LL2 | 18.99 | 10.35 | 16.10 | 9.00 | 10.76 | 11.96 | 9.36 | 11.91 | 8.91 |
| | | R-LL3 | 23.74 | 9.36 | 20.53 | 8.14 | 9.63 | 10.49 | 9.46 | 11.05 | 8.99 |
| | | R-LL4 | 20.87 | 10.30 | 17.76 | 7.76 | 9.61 | 9.85 | 10.86 | 10.03 | 7.69 |
| | | R-LL5 | 21.26 | 9.48 | 18.16 | 8.91 | 9.08 | 9.52 | 9.96 | 9.25 | 7.37 |
| | | R-LL6 | 21.63 | 10.04 | 18.41 | 8.12 | 9.17 | 9.76 | 9.93 | 9.48 | 8.29 |

# A2.3 Performance of Chroma Predictors

| | | Name | CLAB | LLAB | RLAB | H94 | 97s | FC | Fd | 02s | K03 |
|---|---|---|---|---|---|---|---|---|---|---|---|
| Cll-Kwak | P | P-Grey | 33.86 | 27.71 | 34.73 | 25.05 | 26.10 | 25.28 | 28.24 | 27.68 | 25.91 |
| | | P-Black | 28.92 | 21.50 | 28.89 | 22.92 | 25.21 | 24.74 | 28.83 | 19.33 | 17.99 |
| | | P-Filter | 29.67 | 23.76 | 30.37 | 23.08 | 25.09 | 24.16 | 26.78 | 25.51 | 24.47 |
| | M | M-Grey | 24.43 | 20.34 | 22.06 | 22.08 | 22.07 | 21.92 | 26.47 | 22.38 | 19.34 |
| | | M-Black | 26.05 | 18.46 | 21.13 | 26.58 | 25.07 | 24.63 | 28.75 | 23.24 | 19.70 |
| | | M-White | 26.59 | 19.30 | 25.68 | 21.77 | 23.22 | 23.26 | 36.45 | 21.73 | 19.12 |
| | C | C-Grey | 29.96 | 17.71 | 29.82 | 17.83 | 17.88 | 17.55 | 24.65 | 21.83 | 19.12 |
| | | C-White | 37.14 | 24.57 | 36.17 | 28.61 | 32.13 | 31.07 | 46.34 | 29.52 | 27.68 |
| | | C-Black | 30.61 | 19.59 | 29.86 | 21.53 | 32.33 | 33.40 | 42.74 | 20.34 | 17.45 |
| | | C-35mm | 24.06 | 26.15 | 32.68 | 21.41 | 19.64 | 19.84 | 21.53 | 22.22 | 21.85 |
| | A&F | A-Dark | 29.34 | 16.50 | 27.53 | 15.45 | 15.21 | 15.22 | 23.32 | 19.11 | 17.15 |
| | | A-Max | 32.22 | 19.87 | 34.53 | 16.53 | 16.27 | 16.15 | 24.94 | 24.70 | 21.99 |
| | | Filter0-02 | 30.58 | 17.56 | 28.37 | 17.44 | 17.10 | 16.88 | 24.31 | 21.38 | 19.76 |
| | | Filter0-10 | 32.35 | 18.01 | 29.75 | 18.31 | 17.59 | 17.47 | 25.95 | 22.28 | 19.04 |
| | | Filter1-02 | 27.51 | 20.00 | 27.19 | 17.90 | 19.53 | 18.91 | 23.97 | 19.90 | 18.55 |
| | | Filter1-10 | 27.38 | 19.53 | 26.44 | 18.02 | 19.37 | 18.82 | 23.91 | 19.44 | 17.63 |
| | | Filter2-02 | 32.38 | 21.55 | 31.96 | 25.00 | 23.67 | 23.74 | 31.09 | 25.24 | 24.54 |
| | | Filter2-10 | 29.10 | 20.36 | 27.45 | 21.39 | 19.00 | 18.97 | 25.81 | 20.14 | 19.02 |
| | | Filter3-02 | 40.74 | 42.36 | 43.36 | 39.63 | 34.44 | 33.96 | 35.68 | 37.14 | 33.94 |
| | | Filter3-10 | 43.11 | 39.51 | 42.37 | 42.04 | 33.90 | 34.12 | 38.06 | 35.43 | 34.70 |
| LUTCHI | 35 | 35mm 1 | 19.18 | 19.02 | 24.72 | 19.44 | 17.02 | 19.06 | 19.49 | 16.85 | 14.91 |
| | | 35mm 2 | 17.54 | 20.25 | 22.63 | 16.37 | 17.54 | 17.12 | 18.80 | 16.99 | 15.73 |
| | | 35mm 3 | 16.50 | 17.35 | 22.12 | 18.89 | 15.76 | 17.61 | 17.39 | 15.42 | 13.28 |
| | | 35mm 4 | 16.68 | 18.14 | 22.75 | 19.67 | 17.23 | 19.48 | 18.81 | 16.19 | 13.82 |
| | | 35mm 5 | 19.05 | 19.02 | 24.75 | 20.58 | 18.21 | 19.83 | 19.91 | 17.19 | 15.26 |
| | | 35mm 6 | 18.06 | 19.53 | 22.19 | 22.20 | 18.93 | 20.87 | 16.71 | 16.26 | 16.16 |
| | CRT | CRT 01 | 23.90 | 22.36 | 26.73 | 15.16 | 15.57 | 15.12 | 22.57 | 22.49 | 19.67 |
| | | CRT 02 | 17.64 | 16.46 | 18.42 | 15.19 | 13.13 | 13.63 | 16.87 | 12.94 | 12.19 |
| | | CRT 03 | 16.29 | 16.72 | 17.38 | 18.87 | 16.33 | 17.64 | 18.24 | 15.03 | 13.27 |
| | | CRT 04 | 16.29 | 15.69 | 18.05 | 18.42 | 16.68 | 17.71 | 20.46 | 16.80 | 14.15 |
| | | CRT 05 | 18.31 | 18.33 | 20.41 | 15.42 | 13.44 | 14.21 | 16.30 | 13.75 | 13.17 |
| | | CRT 06 | 25.02 | 18.03 | 24.13 | 14.24 | 15.60 | 14.81 | 19.87 | 16.76 | 15.14 |
| | | CRT 07 | 24.05 | 17.28 | 22.97 | 11.18 | 12.14 | 11.37 | 15.61 | 12.27 | 11.53 |
| | | CRT 08 | 23.16 | 17.51 | 21.96 | 23.20 | 15.88 | 18.20 | 19.83 | 16.69 | 16.39 |
| | | CRT 09 | 21.39 | 17.38 | 21.77 | 20.28 | 16.13 | 16.86 | 21.44 | 18.01 | 17.52 |
| | | CRT 10 | 35.92 | 18.89 | 20.39 | 34.66 | 18.87 | 21.61 | 23.61 | 21.05 | 20.00 |
| | | CRT 11 | 32.66 | 20.08 | 21.37 | 32.32 | 19.45 | 19.52 | 23.39 | 21.30 | 21.00 |
| | R-VL | R-VL1 | 18.63 | 16.78 | 23.15 | 15.74 | 15.96 | 18.39 | 17.93 | 11.78 | 11.72 |
| | | R-VL2 | 23.03 | 20.24 | 28.97 | 15.35 | 14.61 | 16.14 | 16.44 | 15.33 | 15.04 |
| | | R-VL3 | 21.05 | 18.66 | 26.19 | 16.14 | 15.38 | 16.19 | 16.73 | 14.48 | 14.33 |
| | | R-VL4 | 23.25 | 20.43 | 27.17 | 18.01 | 17.09 | 17.32 | 19.44 | 18.40 | 17.74 |
| | | R-VL5 | 29.71 | 28.22 | 35.46 | 20.69 | 21.83 | 20.92 | 20.97 | 23.37 | 23.90 |
| | | R-VL6 | 37.70 | 41.97 | 43.33 | 38.61 | 40.41 | 40.11 | 37.83 | 38.34 | 38.18 |
| | | R-VL7 | 22.16 | 18.15 | 26.18 | 14.59 | 14.82 | 17.03 | 18.19 | 13.12 | 13.19 |
| | | R-VL8 | 22.11 | 19.84 | 27.85 | 16.00 | 15.28 | 17.01 | 16.57 | 14.81 | 14.56 |
| | | R-VL9 | 18.53 | 16.89 | 23.38 | 15.54 | 14.58 | 15.77 | 15.05 | 12.89 | 12.43 |
| | | R-VL10 | 22.87 | 20.07 | 27.17 | 15.94 | 15.24 | 15.18 | 17.59 | 17.21 | 16.18 |
| | | R-VL11 | 27.08 | 24.72 | 32.74 | 19.99 | 20.98 | 20.22 | 21.67 | 22.16 | 22.11 |
| | | R-VL12 | 31.68 | 32.81 | 38.62 | 31.57 | 33.25 | 33.01 | 33.96 | 30.83 | 30.84 |
| | R-H&LL | R-HL1 | 28.86 | 22.90 | 29.44 | 19.94 | 24.09 | 23.59 | 31.78 | 19.85 | 21.21 |
| | | R-HL2 | 27.44 | 27.28 | 30.19 | 19.33 | 19.43 | 19.54 | 19.15 | 18.46 | 20.59 |
| | | R-HL3 | 27.45 | 24.69 | 29.76 | 14.21 | 14.11 | 14.21 | 15.40 | 16.80 | 17.97 |
| | | R-HL4 | 21.59 | 12.94 | 21.54 | 14.71 | 14.82 | 15.15 | 21.82 | 15.28 | 12.86 |
| | | R-HL5 | 31.69 | 20.32 | 32.44 | 17.32 | 16.46 | 16.58 | 22.60 | 21.93 | 20.21 |
| | | R-HL6 | 23.34 | 15.96 | 21.65 | 16.83 | 14.85 | 15.83 | 20.74 | 14.47 | 13.33 |
| | | R-LL1 | 29.97 | 23.81 | 30.37 | 21.21 | 25.86 | 25.47 | 34.68 | 22.19 | 22.96 |
| | | R-LL2 | 26.73 | 23.88 | 28.95 | 15.58 | 15.92 | 15.80 | 16.83 | 16.63 | 18.21 |
| | | R-LL3 | 27.44 | 23.39 | 28.63 | 15.99 | 16.57 | 16.46 | 19.16 | 18.13 | 19.07 |
| | | R-LL4 | 26.93 | 19.79 | 27.28 | 14.35 | 14.84 | 14.60 | 19.56 | 17.20 | 16.65 |
| | | R-LL5 | 33.11 | 22.95 | 33.67 | 15.91 | 17.03 | 15.97 | 22.12 | 23.15 | 23.13 |
| | | R-LL6 | 26.40 | 16.47 | 24.64 | 13.41 | 15.34 | 13.99 | 22.87 | 16.66 | 16.38 |

# A2.4 Performance of Colourfulness Predictors

| | | Name | CLAB | LLAB | RLAB | H94 | 97s | FC | Fd | 02s | K03 |
|---|---|---|---|---|---|---|---|---|---|---|---|
| CII-Kwak | P | P-Grey | | 29.58 | | 25.05 | 26.10 | 25.28 | 28.24 | 27.68 | 25.91 |
| | | P-Black | | 28.95 | | 26.01 | 32.29 | 31.90 | 46.67 | 51.91 | 22.67 |
| | | P-Filter | | 27.37 | | 24.27 | 25.54 | 24.71 | 27.91 | 27.16 | 26.58 |
| | M | M-Grey | | 21.45 | | 22.08 | 22.07 | 21.92 | 26.47 | 22.38 | 19.34 |
| | | M-Black | | 20.50 | | 26.69 | 25.34 | 24.80 | 31.66 | 42.25 | 19.87 |
| | | M-White | | 19.14 | | 23.63 | 27.89 | 27.55 | 40.98 | 21.83 | 19.13 |
| | C | C-Grey | | 23.03 | | 17.83 | 17.88 | 17.55 | 24.65 | 21.83 | 19.12 |
| | | C-White | | 24.92 | | 28.69 | 33.36 | 32.57 | 47.49 | 29.53 | 27.75 |
| | | C-Black | | 24.77 | | 46.48 | 28.12 | 27.58 | 30.80 | 24.25 | 18.06 |
| | | C-35mm | | 22.58 | | 21.75 | 21.86 | 21.16 | 26.56 | 27.55 | 26.77 |
| | A&F | A-Dark | | 18.53 | | 15.45 | 15.21 | 15.22 | 23.32 | 19.11 | 17.15 |
| | | A-Max | | 22.19 | | 28.76 | 18.95 | 18.94 | 27.59 | 25.94 | 22.88 |
| | | Filter0-02 | | 20.25 | | 18.40 | 18.08 | 17.85 | 25.04 | 22.20 | 20.61 |
| | | Filter0-10 | | 19.46 | | 18.34 | 17.63 | 17.52 | 26.14 | 22.35 | 19.88 |
| | | Filter1-02 | | 23.30 | | 21.14 | 21.70 | 21.30 | 27.05 | 23.63 | 23.34 |
| | | Filter1-10 | | 27.06 | | 26.49 | 26.48 | 26.31 | 32.85 | 29.32 | 24.88 |
| | | Filter2-02 | | 28.91 | | 30.43 | 24.10 | 24.30 | 32.91 | 26.10 | 26.37 |
| | | Filter2-10 | | 39.73 | | 40.81 | 30.26 | 30.64 | 40.04 | 33.19 | 30.77 |
| | | Filter3-02 | | 61.05 | | 61.86 | 43.69 | 44.72 | 58.46 | 38.05 | 37.07 |
| | | Filter3-10 | | 62.03 | | 68.76 | 48.48 | 50.00 | 64.28 | 41.32 | 34.91 |
| LUTCHI | 35 | 35mm 1 | | 18.26 | | 19.61 | 18.89 | 20.75 | 21.23 | 18.78 | 17.01 |
| | | 35mm 2 | | 18.83 | | 16.95 | 19.73 | 18.90 | 20.43 | 19.65 | 17.27 |
| | | 35mm 3 | | 16.48 | | 19.69 | 16.44 | 18.17 | 17.62 | 15.99 | 13.80 |
| | | 35mm 4 | | 18.52 | | 19.68 | 20.77 | 22.70 | 22.13 | 19.90 | 17.93 |
| | | 35mm 5 | | 18.85 | | 22.05 | 18.34 | 19.97 | 20.14 | 17.65 | 15.46 |
| | | 35mm 6 | | 17.81 | | 22.92 | 19.23 | 21.35 | 16.71 | 16.35 | 16.16 |
| | CRT | CRT 01 | | 19.25 | | 23.89 | 22.34 | 21.64 | 37.28 | 22.80 | 20.18 |
| | | CRT 02 | | 20.16 | | 32.79 | 24.15 | 24.63 | 30.93 | 22.31 | 22.12 |
| | | CRT 03 | | 19.33 | | 29.30 | 20.85 | 21.86 | 27.06 | 23.75 | 20.78 |
| | | CRT 04 | | 18.80 | | 28.61 | 20.77 | 21.60 | 27.92 | 24.30 | 20.86 |
| | | CRT 05 | | 20.83 | | 29.26 | 20.54 | 21.10 | 27.59 | 24.76 | 22.39 |
| | | CRT 06 | | 25.87 | | 32.11 | 24.79 | 24.71 | 32.07 | 28.15 | 26.06 |
| | | CRT 07 | | 22.36 | | 28.46 | 20.38 | 20.35 | 27.64 | 23.48 | 21.71 |
| | | CRT 08 | | 32.40 | | 42.81 | 34.61 | 35.46 | 45.80 | 42.01 | 38.08 |
| | | CRT 09 | | 30.93 | | 40.30 | 33.10 | 33.40 | 44.75 | 40.80 | 36.86 |
| | | CRT 10 | | 38.08 | | 47.48 | 34.92 | 36.99 | 44.55 | 42.61 | 39.13 |
| | | CRT 11 | | 32.57 | | 42.01 | 29.50 | 30.51 | 39.38 | 37.39 | 34.05 |
| | R-VL | R-VL1 | | 19.49 | | 25.51 | 25.29 | 27.11 | 26.10 | 22.18 | 21.50 |
| | | R-VL2 | | 19.98 | | 15.85 | 15.04 | 16.53 | 16.59 | 15.33 | 15.05 |
| | | R-VL3 | | 18.42 | | 18.86 | 18.31 | 18.78 | 18.44 | 15.21 | 14.87 |
| | | R-VL4 | | 16.39 | | 18.24 | 17.57 | 17.64 | 19.44 | 18.49 | 17.86 |
| | | R-VL5 | | 23.89 | | 20.86 | 22.77 | 21.55 | 20.97 | 23.44 | 23.94 |
| | | R-VL6 | | 37.03 | | 38.68 | 49.18 | 47.39 | 38.56 | 48.95 | 52.74 |
| | | R-VL7 | | 17.19 | | 16.56 | 16.58 | 18.68 | 19.51 | 14.84 | 14.60 |
| | | R-VL8 | | 18.47 | | 16.04 | 15.30 | 17.03 | 16.58 | 15.06 | 14.94 |
| | | R-VL9 | | 15.13 | | 18.03 | 17.28 | 18.12 | 16.59 | 13.47 | 12.84 |
| | | R-VL10 | | 17.45 | | 17.22 | 17.11 | 16.69 | 18.01 | 17.31 | 16.25 |
| | | R-VL11 | | 21.26 | | 20.01 | 21.17 | 20.29 | 21.92 | 22.23 | 22.24 |
| | | R-VL12 | | 28.34 | | 31.74 | 43.81 | 41.91 | 35.24 | 43.66 | 48.03 |
| | R-H&LL | R-HL1 | | 22.81 | | 20.05 | 27.64 | 26.61 | 38.84 | 19.87 | 21.25 |
| | | R-HL2 | | 24.61 | | 19.34 | 19.48 | 19.56 | 19.38 | 19.24 | 20.83 |
| | | R-HL3 | | 22.91 | | 14.21 | 14.11 | 14.21 | 15.40 | 16.80 | 17.97 |
| | | R-HL4 | | 12.75 | | 14.74 | 14.83 | 15.17 | 21.82 | 15.39 | 13.12 |
| | | R-HL5 | | 17.59 | | 17.78 | 17.37 | 17.73 | 24.34 | 23.03 | 21.09 |
| | | R-HL6 | | 14.02 | | 16.92 | 15.19 | 15.93 | 21.65 | 14.52 | 13.40 |
| | | R-LL1 | | 21.46 | | 21.27 | 29.01 | 28.28 | 41.30 | 22.37 | 23.09 |
| | | R-LL2 | | 19.71 | | 16.89 | 16.59 | 16.63 | 17.63 | 16.79 | 18.62 |
| | | R-LL3 | | 19.96 | | 16.09 | 16.61 | 16.51 | 19.30 | 18.73 | 19.57 |
| | | R-LL4 | | 17.45 | | 14.56 | 14.93 | 14.75 | 19.89 | 18.15 | 17.73 |
| | | R-LL5 | | 20.61 | | 16.21 | 17.41 | 16.68 | 23.61 | 24.42 | 23.86 |
| | | R-LL6 | | 15.28 | | 13.71 | 15.57 | 14.04 | 23.82 | 17.05 | 16.64 |

# A2.5 Performance of Hue Predictors

| | | Name | CLAB | LLAB | RLAB | H94 | 97s | FC | Fd | 02s | K03 |
|---|---|---|---|---|---|---|---|---|---|---|---|
| CII-Kwak | P | P-Grey | | 10.88 | 11.76 | 8.99 | 8.74 | 8.72 | 8.79 | 8.99 | 8.53 |
| | | P-Black | | 9.95 | 11.44 | 7.91 | 7.77 | 7.65 | 7.80 | 8.05 | 7.56 |
| | | P-Filter | | 11.61 | 12.48 | 10.01 | 9.65 | 9.58 | 9.70 | 9.80 | 9.08 |
| | M | M-Grey | | 10.17 | 12.88 | 11.86 | 9.71 | 10.72 | 9.76 | 9.21 | 8.75 |
| | | M-Black | | 9.41 | 11.24 | 10.72 | 9.07 | 8.83 | 9.07 | 8.05 | 7.31 |
| | | M-White | | 9.18 | 10.99 | 9.93 | 8.91 | 9.98 | 9.00 | 8.27 | 8.27 |
| | C | C-Grey | | 11.56 | 12.94 | 9.38 | 10.28 | 9.60 | 10.29 | 10.48 | 10.09 |
| | | C-White | | 13.41 | 14.36 | 11.54 | 11.73 | 11.10 | 11.76 | 12.29 | 11.41 |
| | | C-Black | | 11.71 | 13.47 | 9.87 | 11.36 | 11.17 | 11.36 | 10.35 | 10.06 |
| | | C-35mm | | 9.34 | 14.23 | 9.34 | 7.13 | 7.45 | 7.49 | 7.38 | 6.93 |
| | A&F | A-Dark | | 8.50 | 12.38 | 7.97 | 8.25 | 8.05 | 8.23 | 8.20 | 8.30 |
| | | A-Max | | 8.21 | 11.73 | 7.87 | 8.02 | 7.80 | 8.01 | 7.85 | 7.82 |
| | | Filter0-02 | | 9.90 | 14.04 | 9.32 | 9.51 | 9.34 | 9.49 | 9.50 | 9.49 |
| | | Filter0-10 | | 10.41 | 14.41 | 9.67 | 10.05 | 10.01 | 10.06 | 10.22 | 10.14 |
| | | Filter1-02 | | 10.67 | 14.11 | 9.82 | 9.96 | 9.85 | 9.94 | 9.71 | 9.46 |
| | | Filter1-10 | | 10.45 | 14.17 | 9.43 | 10.29 | 10.22 | 10.28 | 10.17 | 9.82 |
| | | Filter2-02 | | 10.13 | 12.19 | 8.72 | 8.86 | 8.76 | 8.84 | 9.20 | 8.77 |
| | | Filter2-10 | | 10.72 | 12.55 | 9.62 | 9.50 | 9.42 | 9.49 | 9.95 | 9.49 |
| | | Filter3-02 | | 10.53 | 12.32 | 8.66 | 8.98 | 8.91 | 8.94 | 9.08 | 8.40 |
| | | Filter3-10 | | 10.80 | 12.88 | 13.15 | 9.64 | 9.58 | 9.60 | 9.97 | 9.34 |
| LUTCHI | 35 | 35mm 1 | | 8.84 | 11.54 | 7.27 | 6.41 | 6.72 | 6.41 | 6.04 | 5.89 |
| | | 35mm 2 | | 8.52 | 10.04 | 6.78 | 6.33 | 6.38 | 6.29 | 6.17 | 6.46 |
| | | 35mm 3 | | 7.96 | 10.67 | 7.06 | 5.97 | 6.20 | 5.98 | 5.71 | 5.40 |
| | | 35mm 4 | | 8.39 | 11.27 | 7.36 | 6.45 | 6.77 | 6.46 | 6.07 | 5.94 |
| | | 35mm 5 | | 8.18 | 11.56 | 10.15 | 7.33 | 7.86 | 7.33 | 6.64 | 6.27 |
| | | 35mm 6 | | 13.26 | 13.04 | 11.56 | 10.25 | 10.71 | 10.12 | 9.97 | 9.26 |
| | CRT | CRT 01 | | 8.72 | 10.76 | 7.09 | 7.20 | 7.22 | 7.23 | 7.15 | 6.98 |
| | | CRT 02 | | 7.28 | 8.40 | 5.59 | 5.72 | 5.54 | 5.70 | 5.16 | 5.53 |
| | | CRT 03 | | 7.72 | 12.06 | 8.63 | 7.14 | 7.82 | 7.18 | 6.56 | 6.89 |
| | | CRT 04 | | 7.45 | 10.84 | 7.38 | 5.97 | 6.54 | 5.94 | 5.49 | 6.06 |
| | | CRT 05 | | 7.28 | 10.48 | 6.32 | 5.30 | 5.62 | 5.34 | 5.14 | 5.13 |
| | | CRT 06 | | 7.72 | 8.64 | 5.92 | 5.24 | 5.29 | 5.24 | 5.38 | 5.26 |
| | | CRT 07 | | 10.07 | 11.72 | 9.97 | 8.91 | 9.09 | 8.87 | 8.77 | 5.55 |
| | | CRT 08 | | 7.62 | 9.59 | 8.87 | 6.35 | 6.25 | 6.52 | 6.42 | 5.72 |
| | | CRT 09 | | 9.57 | 11.09 | 9.58 | 8.41 | 7.84 | 8.52 | 8.37 | 7.29 |
| | | CRT 10 | | 11.31 | 13.68 | 21.04 | 9.59 | 13.63 | 9.68 | 9.12 | 8.89 |
| | | CRT 11 | | 13.05 | 12.37 | 18.21 | 12.07 | 11.31 | 11.90 | 11.73 | 11.93 |
| | R-VL | R-VL1 | | 6.47 | 9.74 | 5.85 | 5.95 | 6.48 | 5.97 | 5.71 | 6.02 |
| | | R-VL2 | | 7.91 | 12.06 | 7.04 | 6.41 | 7.52 | 6.47 | 5.97 | 6.00 |
| | | R-VL3 | | 7.04 | 10.39 | 5.68 | 5.11 | 5.58 | 5.13 | 4.82 | 4.94 |
| | | R-VL4 | | 8.13 | 8.98 | 6.48 | 7.65 | 7.16 | 7.71 | 7.22 | 6.44 |
| | | R-VL5 | | 6.28 | 9.00 | 4.87 | 5.77 | 5.07 | 5.84 | 4.87 | 4.93 |
| | | R-VL6 | | 9.53 | 8.06 | 7.45 | 11.52 | 10.97 | 11.60 | 8.61 | 8.15 |
| | | R-VL7 | | 6.42 | 9.78 | 5.66 | 5.63 | 6.63 | 5.64 | 5.29 | 5.62 |
| | | R-VL8 | | 7.00 | 10.27 | 5.73 | 5.32 | 6.04 | 5.30 | 4.98 | 5.34 |
| | | R-VL9 | | 7.83 | 11.93 | 7.09 | 5.79 | 6.76 | 5.79 | 5.61 | 5.79 |
| | | R-VL10 | | 8.35 | 9.07 | 7.01 | 8.20 | 7.65 | 8.27 | 7.69 | 6.72 |
| | | R-VL11 | | 6.44 | 7.97 | 4.60 | 5.91 | 5.11 | 5.94 | 4.75 | 4.56 |
| | | R-VL12 | | 8.90 | 9.22 | 8.01 | 11.05 | 10.55 | 11.13 | 8.41 | 8.18 |
| | R-H&LL | R-HL1 | | 8.49 | 10.03 | 7.30 | 7.86 | 7.82 | 7.86 | 7.75 | 7.96 |
| | | R-HL2 | | 7.45 | 7.52 | 5.60 | 6.49 | 6.33 | 6.50 | 6.37 | 6.22 |
| | | R-HL3 | | 6.97 | 9.47 | 6.03 | 6.27 | 6.26 | 6.28 | 6.08 | 6.21 |
| | | R-HL4 | | 6.88 | 10.02 | 5.85 | 5.77 | 5.74 | 5.78 | 5.60 | 6.11 |
| | | R-HL5 | | 9.16 | 13.58 | 9.17 | 7.98 | 8.24 | 8.12 | 8.45 | 8.25 |
| | | R-HL6 | | 7.91 | 11.82 | 6.33 | 6.11 | 6.35 | 6.22 | 6.08 | 6.46 |
| | | R-LL1 | | 8.08 | 9.07 | 6.49 | 7.17 | 7.24 | 7.18 | 7.17 | 7.43 |
| | | R-LL2 | | 6.21 | 7.95 | 4.29 | 5.55 | 5.17 | 5.55 | 5.08 | 5.44 |
| | | R-LL3 | | 6.68 | 9.07 | 5.08 | 5.66 | 5.50 | 5.68 | 5.57 | 5.60 |
| | | R-LL4 | | 7.56 | 9.24 | 6.04 | 5.87 | 5.82 | 5.86 | 6.02 | 6.10 |
| | | R-LL5 | | 8.97 | 12.59 | 8.39 | 9.17 | 8.75 | 9.34 | 8.97 | 8.76 |
| | | R-LL6 | | 8.74 | 13.73 | 7.92 | 10.67 | 9.32 | 10.78 | 8.77 | 8.62 |

# Appendix 3

# Scaling Factors Applied to Colour Appearance Models

# A3.1 Scaling Factors for Brightness

| R-VL | CIELAB | LLAB | RLAB | Hunt94 | CIECAM 97s | FC | Fairchild | CIECAM 02 | Kwak03 |
|---|---|---|---|---|---|---|---|---|---|
| Brightness SF | N/A | N/A | N/A | 4.406 | 4.341 | 4.334 | 4.49 | 0.806 | 0.909 |

# A3.2 Scaling Factors for Colourfulness

| Group | CIELAB | LLAB | RLAB | Hunt94 | CIECAM 97s | FC | Fairchild | CIECAM 02 | Kwak03 |
|---|---|---|---|---|---|---|---|---|---|
| P | N/A | 0.841 | N/A | 0.971 | 0.874 | 0.878 | 0.711 | 1.046 | 1.207 |
| M | N/A | 0.956 | N/A | 1.059 | 0.962 | 0.955 | 0.861 | 1.312 | 1.465 |
| C | N/A | 0.909 | N/A | 1.086 | 0.945 | 0.955 | 0.792 | 1.160 | 1.341 |
| A&F | N/A | 0.858 | N/A | 0.989 | 0.884 | 0.887 | 0.732 | 1.102 | 1.270 |
| LUTCHI | N/A | 0.834 | N/A | 0.888 | 0.897 | 0.891 | 0.768 | 1.199 | 1.373 |

# A3.3 Scaling Factors for Chroma Predictors

| | | Name | CLAB | LLAB | RLAB | H94 | 97s | FC | Fd | 02s | K03 |
|---|---|---|---|---|---|---|---|---|---|---|---|
| CII-Kwak | P | P-Grey | 0.651 | 1.580 | 0.845 | 0.883 | 0.792 | 0.796 | 0.644 | 0.889 | 1.806 |
| | | P-Black | 0.565 | 1.391 | 0.730 | 0.655 | 0.553 | 0.556 | 0.397 | 0.450 | 1.602 |
| | | P-Filter | 0.605 | 1.439 | 0.779 | 0.854 | 0.747 | 0.753 | 0.627 | 0.818 | 1.706 |
| | M | M-Grey | 0.917 | 1.761 | 1.253 | 0.943 | 0.855 | 0.955 | 0.765 | 1.077 | 2.100 |
| | | M-Black | 0.877 | 1.693 | 1.201 | 0.788 | 0.676 | 0.676 | 0.556 | 0.581 | 2.049 |
| | | M-White | 0.973 | 1.872 | 1.332 | 1.124 | 1.082 | 1.066 | 1.013 | 1.204 | 2.093 |
| | C | C-Grey | 0.600 | 1.432 | 0.767 | 0.877 | 0.762 | 0.770 | 0.639 | 0.811 | 1.714 |
| | | C-White | 0.675 | 1.571 | 0.874 | 0.984 | 0.911 | 0.928 | 0.780 | 0.947 | 1.750 |
| | | C-Black | 0.605 | 1.471 | 0.772 | 1.145 | 0.726 | 0.729 | 0.568 | 0.485 | 1.787 |
| | | C-35mm | 0.831 | 1.610 | 0.980 | 0.917 | 0.850 | 0.840 | 0.760 | 0.978 | 2.012 |
| | A&F | A-Dark | 0.731 | 1.570 | 0.942 | 0.876 | 0.782 | 0.784 | 0.647 | 0.898 | 1.813 |
| | | A-Max | 0.775 | 1.462 | 0.750 | 0.723 | 0.723 | 0.724 | 0.587 | 0.850 | 1.714 |
| | | Filter0-02 | 0.693 | 1.503 | 0.892 | 0.832 | 0.742 | 0.744 | 0.613 | 0.851 | 1.721 |
| | | Filter0-10 | 0.768 | 1.594 | 0.991 | 0.890 | 0.794 | 0.797 | 0.671 | 0.921 | 1.849 |
| | | Filter1-02 | 0.686 | 1.465 | 0.873 | 0.873 | 0.763 | 0.768 | 0.653 | 0.841 | 1.757 |
| | | Filter1-10 | 0.782 | 1.603 | 0.998 | 0.957 | 0.838 | 0.843 | 0.731 | 0.933 | 1.938 |
| | | Filter2-02 | 0.534 | 1.149 | 0.677 | 0.834 | 0.656 | 0.662 | 0.580 | 0.665 | 1.429 |
| | | Filter2-10 | 0.684 | 1.395 | 0.872 | 1.034 | 0.806 | 0.814 | 0.732 | 0.832 | 1.767 |
| | | Filter3-02 | 0.344 | 0.721 | 0.429 | 0.918 | 0.631 | 0.649 | 0.672 | 0.434 | 0.965 |
| | | Filter3-10 | 0.406 | 0.825 | 0.514 | 1.072 | 0.707 | 0.726 | 0.759 | 0.506 | 1.107 |
| LUTCHI | 35 | 35mm 1 | 0.796 | 1.535 | 0.960 | 0.814 | 0.745 | 0.740 | 0.636 | 0.923 | 1.817 |
| | | 35mm 2 | 0.731 | 1.428 | 0.919 | 0.789 | 0.708 | 0.708 | 0.611 | 0.847 | 1.712 |
| | | 35mm 3 | 0.764 | 1.466 | 0.920 | 0.804 | 0.735 | 0.731 | 0.639 | 0.888 | 1.770 |
| | | 35mm 4 | 0.776 | 1.494 | 0.937 | 0.790 | 0.724 | 0.718 | 0.619 | 0.898 | 1.767 |
| | | 35mm 5 | 0.805 | 1.571 | 0.962 | 0.829 | 0.761 | 0.754 | 0.646 | 0.908 | 1.855 |
| | | 35mm 6 | 0.837 | 1.582 | 1.005 | 0.811 | 0.757 | 0.744 | 0.665 | 0.933 | 1.895 |
| | CRT | CRT 01 | 0.937 | 1.626 | 1.176 | 1.002 | 0.973 | 0.961 | 0.984 | 1.087 | 1.890 |
| | | CRT 02 | 0.982 | 1.742 | 1.252 | 0.967 | 0.880 | 0.877 | 0.806 | 0.989 | 2.195 |
| | | CRT 03 | 0.975 | 1.725 | 1.242 | 0.958 | 0.871 | 0.865 | 0.804 | 1.111 | 2.135 |
| | | CRT 04 | 0.971 | 1.721 | 1.236 | 0.955 | 0.867 | 0.861 | 0.798 | 1.104 | 2.124 |
| | | CRT 05 | 0.995 | 1.763 | 1.266 | 0.986 | 0.895 | 0.890 | 0.826 | 1.140 | 2.186 |
| | | CRT 06 | 0.979 | 1.825 | 1.290 | 1.039 | 0.935 | 0.934 | 0.860 | 1.171 | 2.258 |
| | | CRT 07 | 0.945 | 1.759 | 1.245 | 1.004 | 0.905 | 0.903 | 0.834 | 1.134 | 2.184 |
| | | CRT 08 | 1.213 | 1.960 | 1.461 | 1.128 | 1.054 | 1.044 | 1.048 | 1.395 | 2.588 |
| | | CRT 09 | 1.193 | 1.921 | 1.433 | 1.111 | 1.032 | 1.025 | 1.024 | 1.364 | 2.532 |
| | | CRT 10 | 1.257 | 2.051 | 1.565 | 1.063 | 1.014 | 1.018 | 0.975 | 1.323 | 2.489 |
| | | CRT 11 | 1.164 | 1.875 | 1.431 | 0.982 | 0.929 | 0.936 | 0.894 | 1.212 | 2.277 |
| | R-VL | R-VL1 | 0.976 | 1.613 | 1.001 | 0.749 | 0.759 | 0.752 | 0.653 | 1.018 | 1.960 |
| | | R-VL2 | 0.999 | 1.674 | 1.019 | 0.794 | 0.805 | 0.800 | 0.697 | 1.053 | 2.049 |
| | | R-VL3 | 0.880 | 1.473 | 0.896 | 0.713 | 0.720 | 0.717 | 0.627 | 0.919 | 1.806 |
| | | R-VL4 | 0.833 | 1.394 | 0.846 | 0.708 | 0.709 | 0.709 | 0.627 | 0.873 | 1.729 |
| | | R-VL5 | 0.730 | 1.240 | 0.750 | 0.674 | 0.659 | 0.662 | 0.598 | 0.776 | 1.553 |
| | | R-VL6 | 0.449 | 0.748 | 0.460 | 0.577 | 0.476 | 0.482 | 0.477 | 0.476 | 0.970 |
| | | R-VL7 | 1.068 | 1.771 | 1.094 | 0.825 | 0.837 | 0.830 | 0.718 | 1.119 | 2.154 |
| | | R-VL8 | 1.028 | 1.719 | 1.049 | 0.814 | 0.826 | 0.821 | 0.716 | 1.081 | 2.105 |
| | | R-VL9 | 0.887 | 1.483 | 0.905 | 0.717 | 0.724 | 0.721 | 0.631 | 0.925 | 1.818 |
| | | R-VL10 | 0.805 | 1.348 | 0.817 | 0.686 | 0.687 | 0.687 | 0.607 | 0.845 | 1.675 |
| | | R-VL11 | 0.757 | 1.287 | 0.778 | 0.695 | 0.680 | 0.683 | 0.615 | 0.801 | 1.605 |
| | | R-VL12 | 0.443 | 0.747 | 0.453 | 0.571 | 0.472 | 0.478 | 0.469 | 0.472 | 0.961 |
| | R-H&LL | R-HL1 | 1.096 | 1.754 | 1.105 | 0.925 | 1.043 | 1.022 | 0.991 | 1.217 | 2.060 |
| | | R-HL2 | 0.962 | 1.610 | 0.973 | 0.778 | 0.780 | 0.778 | 0.659 | 0.925 | 2.020 |
| | | R-HL3 | 1.000 | 1.684 | 1.013 | 0.834 | 0.841 | 0.835 | 0.720 | 1.076 | 2.078 |
| | | R-HL4 | 1.047 | 1.733 | 1.069 | 0.840 | 0.845 | 0.840 | 0.718 | 1.091 | 2.124 |
| | | R-HL5 | 1.013 | 1.706 | 1.003 | 0.867 | 0.887 | 0.888 | 0.788 | 1.153 | 2.204 |
| | | R-HL6 | 1.018 | 1.700 | 1.019 | 0.818 | 0.813 | 0.819 | 0.678 | 1.056 | 2.039 |
| | | R-LL1 | 0.982 | 1.574 | 0.991 | 0.844 | 0.950 | 0.934 | 0.908 | 1.085 | 1.865 |
| | | R-LL2 | 0.884 | 1.489 | 0.896 | 0.760 | 0.754 | 0.753 | 0.649 | 0.853 | 1.884 |
| | | R-LL3 | 0.903 | 1.524 | 0.916 | 0.775 | 0.776 | 0.773 | 0.672 | 0.968 | 1.893 |
| | | R-LL4 | 0.927 | 1.536 | 0.945 | 0.779 | 0.779 | 0.777 | 0.680 | 0.977 | 1.921 |
| | | R-LL5 | 0.882 | 1.483 | 0.874 | 0.785 | 0.795 | 0.799 | 0.713 | 1.000 | 1.924 |
| | | R-LL6 | 0.940 | 1.568 | 0.936 | 0.782 | 0.750 | 0.772 | 0.619 | 0.958 | 1.868 |

# Appendix 4
# The CII-Kwak Data Set

# A4.1 P-Grey

| No. | $X_L$ | $Y_L$ (cd/m$^2$) | $Z_L$ | Lightness | | Colourfulness | | | Hue | |
|---|---|---|---|---|---|---|---|---|---|---|
| | | | | Avg | Stdev | Avg | Max | Min | Avg | Stdev |
| Reference White | 128.2 | 154.0 | 153.7 | | | | | | | |
| Back-ground | 24.40 | 28.24 | 40.47 | | | | | | | |
| 1 | 6.21 | 6.51 | 17.15 | 25.1 | 7.0 | 27.4 | 50.2 | 15.0 | 293 | 12 |
| 2 | 8.71 | 10.97 | 19.12 | 37.4 | 7.4 | 29.7 | 54.2 | 16.3 | 257 | 21 |
| 3 | 7.09 | 12.79 | 2.58 | 45.3 | 10.5 | 53.3 | 71.7 | 39.6 | 190 | 11 |
| 4 | 12.66 | 6.05 | 57.89 | 30.5 | 9.9 | 59.0 | 78.2 | 44.5 | 305 | 9 |
| 5 | 28.00 | 11.51 | 142.84 | 51.7 | 16.2 | 76.0 | 96.8 | 59.7 | 301 | 5 |
| 6 | 20.51 | 38.75 | 6.61 | 48.6 | 12.5 | 46.1 | 59.3 | 35.9 | 184 | 12 |
| 7 | 30.50 | 41.64 | 60.34 | 44.4 | 11.2 | 32.1 | 45.6 | 22.5 | 258 | 13 |
| 8 | 45.84 | 47.23 | 144.76 | 63.8 | 12.7 | 46.1 | 64.3 | 33.0 | 301 | 11 |
| 9 | 61.93 | 119.43 | 9.91 | 87.4 | 11.1 | 68.9 | 104.1 | 45.6 | 175 | 16 |
| 10 | 71.67 | 121.87 | 63.11 | 88.7 | 8.0 | 52.9 | 80.4 | 34.8 | 179 | 16 |
| 11 | 87.16 | 127.66 | 147.90 | 88.6 | 7.9 | 33.2 | 61.1 | 18.1 | 251 | 23 |
| 12 | 7.58 | 8.51 | 14.39 | 24.3 | 8.5 | 2.6 | 10.1 | 0.7 | 308 | 40 |
| 13 | 4.72 | 4.46 | 2.15 | 30.8 | 9.7 | 43.4 | 67.9 | 27.7 | 16 | 38 |
| 14 | 11.54 | 8.02 | 4.78 | 39.2 | 9.7 | 55.8 | 78.9 | 39.4 | 1 | 12 |
| 15 | 21.38 | 10.76 | 57.90 | 45.8 | 12.5 | 63.7 | 78.5 | 51.7 | 352 | 8 |
| 16 | 36.89 | 16.31 | 143.10 | 47.4 | 13.1 | 60.9 | 74.7 | 49.6 | 335 | 14 |
| 17 | 29.29 | 43.51 | 6.60 | 53.6 | 8.2 | 40.1 | 51.7 | 31.1 | 160 | 15 |
| 18 | 54.70 | 51.97 | 145.07 | 66.0 | 11.7 | 27.2 | 49.8 | 14.9 | 316 | 17 |
| 19 | 70.73 | 124.16 | 9.89 | 91.0 | 6.1 | 67.2 | 100.9 | 44.8 | 156 | 21 |
| 20 | 80.53 | 126.83 | 62.71 | 80.4 | 13.8 | 40.9 | 65.0 | 25.7 | 180 | 20 |
| 21 | 96.29 | 132.94 | 148.51 | 92.3 | 5.7 | 30.4 | 57.1 | 16.2 | 272 | 19 |
| 22 | 68.08 | 75.81 | 134.57 | 67.2 | 12.9 | 6.6 | 19.7 | 2.2 | 308 | 15 |
| 23 | 60.85 | 72.18 | 88.60 | 68.6 | 16.0 | 2.6 | 7.6 | 0.9 | 297 | 13 |
| 24 | 65.80 | 61.50 | 140.47 | 61.7 | 12.6 | 32.3 | 50.3 | 20.7 | 344 | 12 |
| 25 | 39.08 | 22.81 | 4.95 | 65.5 | 14.7 | 86.5 | 111.8 | 66.9 | 6 | 9 |
| 26 | 49.20 | 25.73 | 57.94 | 63.8 | 15.6 | 88.5 | 109.7 | 71.5 | 377 | 22 |
| 27 | 64.47 | 31.12 | 142.60 | 63.6 | 12.7 | 81.0 | 108.9 | 60.2 | 371 | 20 |
| 28 | 56.92 | 58.32 | 6.61 | 67.2 | 10.7 | 62.8 | 85.5 | 46.0 | 65 | 16 |
| 29 | 66.74 | 61.10 | 59.81 | 65.1 | 8.6 | 39.2 | 57.9 | 26.6 | 10 | 18 |
| 30 | 82.24 | 66.76 | 144.53 | 68.8 | 14.2 | 39.2 | 60.9 | 25.2 | 384 | 20 |
| 31 | 98.45 | 139.00 | 10.13 | 91.9 | 7.8 | 69.0 | 104.9 | 45.4 | 101 | 4 |
| 32 | 108.75 | 142.24 | 63.67 | 86.5 | 10.1 | 36.3 | 73.1 | 18.0 | 101 | 4 |

# A4.2 P-Black

| No. | $X_L$ | $Y_L$ (cd/m$^2$) | $Z_L$ | Lightness | | Colourfulness | | | Hue | |
|---|---|---|---|---|---|---|---|---|---|---|
| | | | | Avg | Stdev | Avg | Max | Min | Avg | Stdev |
| Reference White | 127.1 | 152.7 | 152.8 | | | | | | | |
| Back-ground | 0.5118 | 0.6400 | 0.7051 | | | | | | | |
| 1 | 3.74 | 4.18 | 10.01 | 22.5 | 8.2 | 14.1 | 34.1 | 5.9 | 298 | 21 |
| 2 | 6.02 | 8.33 | 11.52 | 36.2 | 10.1 | 23.2 | 53.4 | 10.1 | 257 | 17 |
| 3 | 5.57 | 10.52 | 1.23 | 41.2 | 9.2 | 45.8 | 57.8 | 36.2 | 190 | 14 |
| 4 | 9.81 | 4.02 | 47.56 | 34.8 | 10.8 | 54.0 | 76.6 | 38.1 | 307 | 7 |
| 5 | 26.74 | 9.87 | 141.10 | 39.4 | 14.7 | 66.6 | 86.2 | 51.5 | 301 | 7 |
| 6 | 18.25 | 35.36 | 3.80 | 54.9 | 8.2 | 52.3 | 66.4 | 41.3 | 190 | 11 |
| 7 | 26.70 | 37.69 | 49.66 | 54.4 | 8.3 | 33.7 | 45.1 | 25.2 | 262 | 15 |
| 8 | 43.64 | 43.78 | 142.58 | 62.6 | 12.4 | 40.2 | 60.1 | 26.9 | 301 | 10 |
| 9 | 59.69 | 115.78 | 7.06 | 86.6 | 9.6 | 65.6 | 99.0 | 43.4 | 170 | 18 |
| 10 | 68.53 | 118.86 | 53.43 | 83.8 | 7.5 | 38.1 | 73.1 | 19.9 | 190 | 27 |
| 11 | 85.11 | 124.42 | 145.28 | 81.8 | 10.3 | 31.2 | 57.3 | 17.0 | 269 | 33 |
| 12 | 4.86 | 5.79 | 7.35 | 28.9 | 11.2 | 1.1 | 1.5 | 0.8 | | |
| 13 | 3.43 | 2.85 | 0.78 | 27.1 | 8.2 | 41.8 | 59.1 | 29.6 | 34 | 29 |
| 14 | 9.71 | 6.18 | 2.14 | 36.2 | 9.7 | 43.8 | 60.6 | 31.7 | 15 | 20 |
| 15 | 18.23 | 8.57 | 47.65 | 53.2 | 13.7 | 55.8 | 76.0 | 40.9 | 359 | 13 |
| 16 | 35.38 | 14.54 | 141.84 | 49.5 | 14.0 | 59.1 | 74.8 | 46.7 | 334 | 25 |
| 17 | 26.63 | 39.87 | 3.85 | 58.8 | 9.2 | 47.4 | 60.7 | 37.0 | 170 | 14 |
| 18 | 52.18 | 48.42 | 143.02 | 69.8 | 10.6 | 29.7 | 45.6 | 19.3 | 317 | 21 |
| 19 | 68.08 | 120.36 | 7.07 | 85.1 | 10.5 | 68.2 | 101.4 | 45.9 | 173 | 16 |
| 20 | 77.29 | 123.90 | 53.87 | 88.3 | 9.9 | 35.2 | 68.7 | 18.1 | 169 | 24 |
| 21 | 93.23 | 128.56 | 144.60 | 90.1 | 5.7 | 19.3 | 40.0 | 9.3 | 255 | 23 |
| 22 | 64.46 | 71.38 | 128.25 | 79.3 | 6.9 | 15.8 | 27.4 | 9.2 | 312 | 14 |
| 23 | 56.25 | 67.25 | 78.22 | 78.4 | 14.5 | 1.3 | 2.2 | 0.7 | | |
| 24 | 62.46 | 57.41 | 135.70 | 72.6 | 9.0 | 28.6 | 44.1 | 18.6 | 339 | 13 |
| 25 | 37.13 | 20.89 | 2.22 | 64.8 | 13.4 | 75.2 | 99.4 | 56.8 | 9 | 10 |
| 26 | 45.61 | 23.25 | 47.60 | 65.3 | 10.6 | 71.6 | 92.8 | 55.3 | 378 | 22 |
| 27 | 63.04 | 29.38 | 141.44 | 60.4 | 13.5 | 66.0 | 84.2 | 51.8 | 370 | 17 |
| 28 | 54.21 | 54.75 | 3.87 | 58.0 | 11.1 | 46.1 | 61.5 | 34.5 | 59 | 10 |
| 29 | 62.67 | 57.16 | 49.70 | 70.7 | 9.7 | 34.8 | 55.8 | 21.7 | 6 | 13 |
| 30 | 79.68 | 63.18 | 142.40 | 70.8 | 11.3 | 36.1 | 55.7 | 23.5 | 365 | 16 |
| 31 | 96.17 | 136.18 | 7.17 | 87.7 | 9.2 | 72.2 | 105.2 | 49.6 | 105 | 10 |
| 32 | 104.38 | 138.01 | 53.28 | 84.4 | 8.8 | 33.3 | 61.7 | 18.0 | 102 | 4 |

# A4.3 P-Filter

| No. | $X_L$ | $Y_L$ (cd/m$^2$) | $Z_L$ | Lightness | | Colourfulness | | | Hue | |
|---|---|---|---|---|---|---|---|---|---|---|
| | | | | Avg | Stdev | Avg | Max | Min | Avg | Stdev |
| Reference White | 15.87 | 18.77 | 19.00 | | | | | | | |
| Back-ground | 3.058 | 3.506 | 5.054 | | | | | | | |
| 1 | 0.86 | 0.90 | 2.27 | 18.8 | 7.1 | 17.9 | 38.1 | 8.4 | 290 | 14 |
| 2 | 1.17 | 1.44 | 2.50 | 23.6 | 9.1 | 18.0 | 42.8 | 7.6 | 246 | 31 |
| 3 | 0.96 | 1.65 | 0.46 | 31.3 | 10.0 | 41.6 | 70.9 | 24.4 | 194 | 9 |
| 4 | 1.63 | 0.83 | 7.15 | 31.9 | 11.0 | 66.7 | 90.8 | 49.0 | 304 | 7 |
| 5 | 3.50 | 1.47 | 17.44 | 41.0 | 9.8 | 72.5 | 96.1 | 54.7 | 301 | 4 |
| 6 | 2.56 | 4.63 | 0.95 | 45.7 | 12.7 | 42.4 | 55.0 | 32.7 | 193 | 12 |
| 7 | 3.77 | 4.99 | 7.38 | 43.0 | 12.0 | 29.8 | 40.9 | 21.8 | 250 | 14 |
| 8 | 5.63 | 5.63 | 17.55 | 53.2 | 13.9 | 34.5 | 49.6 | 24.0 | 298 | 12 |
| 9 | 7.61 | 14.15 | 1.31 | 82.9 | 11.5 | 63.0 | 94.1 | 42.2 | 181 | 15 |
| 10 | 8.80 | 14.46 | 7.80 | 76.4 | 14.5 | 45.2 | 69.9 | 29.2 | 186 | 18 |
| 11 | 10.67 | 15.12 | 18.04 | 81.0 | 11.7 | 29.9 | 56.7 | 15.8 | 263 | 20 |
| 12 | 0.99 | 1.12 | 1.81 | 14.2 | 6.1 | 2.1 | 5.6 | 0.8 | 305 | 24 |
| 13 | 0.66 | 0.66 | 0.40 | 17.4 | 11.7 | 24.7 | 62.3 | 9.8 | 22 | 30 |
| 14 | 1.48 | 1.10 | 0.77 | 36.3 | 9.3 | 55.0 | 71.6 | 42.3 | 9 | 12 |
| 15 | 2.65 | 1.40 | 7.16 | 38.8 | 11.9 | 60.8 | 78.7 | 47.0 | 354 | 13 |
| 16 | 4.53 | 2.04 | 17.45 | 38.0 | 13.6 | 63.4 | 80.7 | 49.8 | 341 | 17 |
| 17 | 3.61 | 5.25 | 0.95 | 47.9 | 10.4 | 36.2 | 46.2 | 28.4 | 169 | 21 |
| 18 | 6.64 | 6.19 | 17.54 | 55.9 | 11.3 | 30.3 | 44.0 | 20.9 | 323 | 19 |
| 19 | 8.59 | 14.64 | 1.33 | 82.0 | 12.4 | 56.0 | 88.2 | 35.6 | 173 | 15 |
| 20 | 9.86 | 15.08 | 7.82 | 78.0 | 12.1 | 35.1 | 61.4 | 20.1 | 180 | 21 |
| 21 | 11.74 | 15.74 | 18.11 | 82.1 | 15.6 | 27.2 | 50.1 | 14.7 | 253 | 19 |
| 22 | 8.28 | 9.01 | 16.40 | 64.9 | 12.4 | 14.4 | 35.3 | 5.9 | 322 | 18 |
| 23 | 7.40 | 8.60 | 10.86 | 62.1 | 16.6 | 1.2 | 1.9 | 0.7 | | |
| 24 | 7.98 | 7.35 | 17.07 | 54.3 | 10.4 | 31.8 | 47.0 | 21.5 | 342 | 14 |
| 25 | 4.73 | 2.88 | 0.78 | 56.9 | 14.0 | 69.8 | 90.4 | 53.8 | 6 | 9 |
| 26 | 5.94 | 3.21 | 7.28 | 50.5 | 12.8 | 65.4 | 88.0 | 48.6 | 377 | 13 |
| 27 | 7.73 | 3.80 | 17.37 | 58.3 | 12.5 | 64.2 | 84.3 | 48.8 | 367 | 17 |
| 28 | 6.88 | 7.05 | 0.96 | 55.4 | 10.5 | 50.7 | 72.7 | 35.4 | 64 | 15 |
| 29 | 8.03 | 7.34 | 7.41 | 58.9 | 11.7 | 35.6 | 53.6 | 23.6 | 7 | 17 |
| 30 | 9.92 | 7.99 | 17.62 | 60.7 | 13.6 | 37.9 | 46.5 | 31.0 | 376 | 22 |
| 31 | 11.91 | 16.55 | 1.32 | 86.3 | 10.5 | 66.5 | 94.7 | 46.7 | 103 | 7 |
| 32 | 13.10 | 16.86 | 7.81 | 85.2 | 9.9 | 33.6 | 61.9 | 18.2 | 103 | 11 |

# A4.4 M-Grey

| No. | $X_L$ | $Y_L$ (cd/m$^2$) | $Z_L$ | Lightness | | Colourfulness | | | Hue | |
|---|---|---|---|---|---|---|---|---|---|---|
| | | | | Avg | Stdev | Avg | Max | Min | Avg | Stdev |
| Reference White | 75.21 | 90.33 | 90.07 | | | | | | | |
| Back-ground | 16.12 | 18.65 | 26.85 | | | | | | | |
| 1 | 25.5 | 32.5 | 69.5 | 59.0 | 9.1 | 42.5 | 52.3 | 34.5 | 296 | 18 |
| 2 | 3.08 | 2.23 | 3.01 | 24.6 | 10.5 | 40.3 | 59.3 | 27.4 | 376 | 56 |
| 3 | 24.63 | 15.61 | 6.42 | 69.8 | 14.4 | 68.4 | 90.9 | 51.5 | 12 | 18 |
| 4 | 26.40 | 31.42 | 17.59 | 54.4 | 16.8 | 30.1 | 45.0 | 20.1 | 153 | 74 |
| 5 | 8.49 | 7.20 | 2.73 | 41.7 | 7.8 | 33.2 | 53.8 | 20.5 | 41 | 36 |
| 6 | 47.42 | 55.01 | 39.81 | 82.3 | 6.4 | 23.7 | 43.1 | 13.1 | 87 | 22 |
| 7 | 13.50 | 17.84 | 31.85 | 47.1 | 13.6 | 40.0 | 58.0 | 27.5 | 271 | 12 |
| 8 | 40.61 | 25.29 | 4.54 | 77.7 | 12.8 | 75.7 | 107.6 | 53.2 | 16 | 15 |
| 9 | 38.94 | 61.83 | 31.39 | 77.1 | 9.9 | 42.9 | 60.3 | 30.5 | 182 | 17 |
| 10 | 12.08 | 8.15 | 5.24 | 41.7 | 14.8 | 43.7 | 54.1 | 35.3 | 395 | 25 |
| 11 | 54.50 | 41.12 | 74.45 | 80.0 | 14.1 | 55.4 | 83.2 | 36.9 | 378 | 27 |
| 12 | 60.37 | 75.23 | 35.58 | 82.7 | 11.3 | 43.7 | 66.6 | 28.7 | 109 | 23 |
| 13 | 61.51 | 65.51 | 82.47 | 79.3 | 11.2 | 11.0 | 28.9 | 4.2 | 332 | 90 |
| 14 | 5.95 | 8.73 | 3.76 | 40.6 | 14.1 | 38.9 | 50.5 | 29.9 | 190 | 13 |
| 15 | 57.63 | 61.75 | 17.84 | 82.5 | 12.3 | 58.8 | 83.8 | 41.2 | 80 | 23 |
| 16 | 17.31 | 19.30 | 20.29 | 38.3 | 15.4 | 7.8 | 29.7 | 2.0 | 51 | 13 |
| 17 | 2.31 | 3.09 | 2.13 | 11.8 | 7.2 | 5.6 | 26.8 | 1.2 | 211 | 19 |
| 18 | 30.31 | 46.36 | 22.41 | 70.6 | 9.4 | 41.6 | 53.7 | 32.3 | 180 | 20 |
| 19 | 4.91 | 3.26 | 1.42 | 39.6 | 9.2 | 50.8 | 67.2 | 38.4 | 395 | 15 |
| 20 | 5.18 | 4.74 | 22.22 | 49.4 | 11.1 | 56.2 | 71.9 | 43.9 | 299 | 7 |
| 21 | 57.24 | 76.06 | 21.10 | 84.2 | 10.8 | 62.5 | 88.3 | 44.3 | 100 | 1 |
| 22 | 1.60 | 1.51 | 6.15 | 16.7 | 9.6 | 19.7 | 46.3 | 8.4 | 306 | 15 |
| 23 | 22.72 | 19.96 | 44.35 | 56.7 | 10.7 | 34.0 | 43.2 | 26.7 | 349 | 34 |
| 24 | 17.65 | 12.64 | 26.02 | 42.8 | 7.5 | 53.7 | 65.4 | 44.1 | 353 | 44 |
| 25 | 49.68 | 40.46 | 10.10 | 79.3 | 13.1 | 66.5 | 89.8 | 49.2 | 53 | 17 |
| 26 | 68.08 | 72.36 | 59.66 | 89.3 | 7.1 | 14.2 | 30.9 | 6.6 | 25 | 31 |
| 27 | 26.90 | 24.38 | 61.65 | 54.8 | 9.6 | 39.9 | 55.2 | 28.8 | 340 | 21 |
| 28 | 25.85 | 35.50 | 39.24 | 60.8 | 10.4 | 32.8 | 41.7 | 25.9 | 221 | 39 |
| 29 | 19.71 | 20.85 | 44.76 | 43.2 | 14.7 | 26.7 | 37.7 | 18.9 | 336 | 11 |
| 30 | 1.50 | 1.70 | 1.60 | 3.3 | 4.4 | 1.8 | 4.1 | 0.8 | | |
| 31 | 61.19 | 83.95 | 88.50 | 90.8 | 5.5 | 24.7 | 40.9 | 14.9 | 234 | 40 |
| 32 | 3.00 | 2.76 | 1.47 | 27.8 | 6.1 | 31.1 | 46.8 | 20.7 | 23 | 33 |
| 33 | 45.37 | 42.62 | 42.39 | 71.3 | 11.8 | 32.9 | 47.7 | 22.6 | 13 | 31 |
| 34 | 3.90 | 4.05 | 11.18 | 30.5 | 8.6 | 31.5 | 44.4 | 22.4 | 301 | 8 |
| 35 | 20.92 | 28.73 | 40.15 | 60.6 | 14.3 | 35.9 | 42.9 | 30.0 | 242 | 24 |
| 36 | 7.59 | 5.21 | 2.86 | 41.5 | 9.9 | 50.9 | 63.5 | 40.9 | 11 | 23 |
| 37 | 5.87 | 7.44 | 12.97 | 39.9 | 9.4 | 34.3 | 44.5 | 26.5 | 249 | 17 |
| 38 | 27.42 | 17.17 | 3.95 | 74.8 | 14.6 | 74.8 | 103.6 | 54.0 | 13 | 10 |
| 39 | 54.25 | 79.62 | 87.27 | 88.8 | 5.9 | 36.8 | 57.6 | 23.5 | 240 | 30 |
| 40 | 44.54 | 50.17 | 79.68 | 63.5 | 8.2 | 17.8 | 47.1 | 6.8 | 320 | 34 |

# A4.5 M-Black

| No. | $X_L$ | $Y_L$ (cd/m$^2$) | $Z_L$ | Lightness | | Colourfulness | | | Hue | |
|---|---|---|---|---|---|---|---|---|---|---|
| | | | | Avg | Stdev | Avg | Max | Min | Avg | Stdev |
| Reference White | 74.91 | 89.81 | 89.29 | | | | | | | |
| Back-ground | 0.299 | 0.324 | 0.558 | | | | | | | |
| 1 | 25.31 | 32.33 | 69.04 | 63.73 | 11.99 | 38.94 | 50.69 | 29.92 | 297.27 | 17.94 |
| 2 | 3.01 | 2.12 | 2.84 | 28.45 | 11.33 | 35.11 | 57.98 | 21.26 | 394.09 | 20.10 |
| 3 | 24.56 | 15.51 | 6.24 | 70.64 | 9.08 | 60.00 | 83.42 | 43.16 | 22.73 | 16.18 |
| 4 | 26.38 | 31.35 | 17.52 | 60.00 | 14.83 | 27.94 | 35.97 | 21.70 | 115.45 | 31.82 |
| 5 | 8.45 | 7.13 | 2.55 | 41.82 | 12.70 | 39.10 | 52.04 | 29.38 | 38.18 | 25.72 |
| 6 | 47.22 | 54.72 | 39.65 | 79.55 | 12.93 | 27.50 | 45.21 | 16.73 | 92.73 | 12.12 |
| 7 | 13.47 | 17.79 | 31.77 | 50.64 | 10.27 | 37.05 | 41.65 | 32.96 | 284.55 | 15.08 |
| 8 | 39.92 | 24.80 | 4.37 | 79.09 | 14.63 | 74.22 | 115.10 | 47.86 | 23.64 | 18.45 |
| 9 | 38.32 | 60.79 | 30.96 | 83.00 | 11.66 | 43.59 | 63.27 | 30.03 | 175.00 | 22.25 |
| 10 | 11.96 | 7.99 | 5.11 | 43.64 | 14.33 | 39.48 | 46.87 | 33.25 | 12.73 | 19.54 |
| 11 | 53.55 | 40.30 | 72.90 | 82.09 | 10.30 | 44.38 | 67.65 | 29.11 | 366.82 | 21.01 |
| 12 | 59.40 | 73.89 | 35.06 | 90.91 | 5.84 | 35.32 | 58.26 | 21.41 | 120.91 | 32.77 |
| 13 | 60.63 | 64.61 | 80.57 | 85.91 | 13.63 | 4.75 | 24.08 | 0.94 | 345.00 | 16.43 |
| 14 | 5.90 | 8.67 | 3.62 | 38.00 | 14.04 | 41.60 | 48.97 | 35.33 | 180.91 | 36.93 |
| 15 | 56.51 | 60.57 | 17.23 | 82.55 | 12.42 | 57.13 | 70.33 | 46.41 | 88.36 | 14.05 |
| 16 | 17.21 | 19.17 | 20.02 | 53.64 | 13.06 | 1.36 | 2.85 | 0.65 | | |
| 17 | 2.25 | 3.00 | 1.98 | 26.00 | 13.96 | 24.78 | 46.89 | 13.09 | 194.55 | 17.53 |
| 18 | 29.76 | 45.48 | 21.86 | 85.09 | 8.95 | 42.55 | 67.39 | 26.86 | 176.82 | 20.77 |
| 19 | 4.83 | 3.15 | 1.21 | 33.18 | 12.42 | 44.02 | 58.78 | 32.97 | 12.73 | 14.03 |
| 20 | 5.08 | 4.60 | 21.99 | 49.09 | 13.93 | 54.90 | 74.85 | 40.27 | 299.73 | 3.85 |
| 21 | 55.89 | 74.16 | 20.35 | 89.73 | 8.53 | 65.36 | 99.33 | 43.01 | 100.91 | 3.02 |
| 22 | 1.51 | 1.39 | 5.98 | 20.36 | 13.43 | 30.46 | 65.51 | 14.16 | 298.18 | 14.71 |
| 23 | 22.46 | 19.72 | 43.64 | 64.36 | 9.56 | 39.08 | 47.35 | 32.26 | 355.00 | 15.33 |
| 24 | 17.47 | 12.46 | 25.62 | 55.27 | 7.86 | 44.55 | 56.52 | 35.11 | 365.91 | 12.61 |
| 25 | 48.79 | 39.83 | 9.82 | 84.82 | 7.87 | 66.44 | 94.91 | 46.51 | 51.82 | 13.28 |
| 26 | 67.08 | 71.35 | 58.69 | 94.27 | 7.38 | 4.30 | 18.19 | 1.02 | | |
| 27 | 26.61 | 24.08 | 60.68 | 65.64 | 11.64 | 40.32 | 55.36 | 29.36 | 339.55 | 11.50 |
| 28 | 25.69 | 35.26 | 38.90 | 68.45 | 10.88 | 28.55 | 44.11 | 18.48 | 225.00 | 16.28 |
| 29 | 19.66 | 20.81 | 44.41 | 56.18 | 10.93 | 28.10 | 42.56 | 18.56 | 334.09 | 13.19 |
| 30 | 1.40 | 1.58 | 1.42 | 17.09 | 11.27 | 6.05 | 36.01 | 1.02 | | |
| 31 | 61.13 | 83.78 | 88.04 | 95.09 | 4.88 | 24.77 | 52.92 | 11.60 | 241.82 | 31.74 |
| 32 | 2.93 | 2.66 | 1.31 | 28.14 | 13.47 | 36.01 | 46.71 | 27.76 | 34.55 | 23.18 |
| 33 | 45.60 | 42.85 | 42.56 | 82.05 | 11.06 | 30.58 | 46.78 | 19.99 | 10.68 | 24.47 |
| 34 | 3.85 | 3.98 | 11.14 | 30.05 | 12.81 | 36.30 | 48.99 | 26.89 | 304.77 | 8.55 |
| 35 | 21.03 | 28.93 | 40.38 | 66.68 | 11.71 | 34.88 | 46.81 | 25.98 | 252.95 | 20.76 |
| 36 | 7.61 | 5.17 | 2.71 | 43.95 | 11.67 | 47.01 | 57.65 | 38.34 | 19.32 | 15.13 |
| 37 | 5.84 | 7.42 | 12.99 | 42.50 | 9.94 | 29.21 | 41.53 | 20.54 | 272.95 | 17.92 |
| 38 | 27.54 | 17.18 | 3.79 | 74.55 | 13.91 | 71.52 | 106.87 | 47.86 | 24.55 | 19.77 |
| 39 | 54.26 | 79.65 | 87.15 | 93.23 | 6.99 | 31.53 | 59.49 | 16.71 | 246.14 | 28.95 |
| 40 | 44.54 | 50.14 | 79.44 | 77.00 | 12.61 | 15.24 | 45.35 | 5.12 | 324.50 | 15.85 |

# A4.6 M-White

| No. | $X_L$ | $Y_L$ (cd/m$^2$) | $Z_L$ | Lightness | | Colourfulness | | | Hue | |
|---|---|---|---|---|---|---|---|---|---|---|
| | | | | Avg | Stdev | Avg | Max | Min | Avg | Stdev |
| Reference White | 75.09 | 90.22 | 90.32 | | | | | | | |
| Back-ground | 75.09 | 90.22 | 90.32 | | | | | | | |
| 1 | 25.55 | 32.56 | 69.33 | 46.5 | 7.2 | 47.5 | 54.6 | 41.3 | 294 | 14 |
| 2 | 3.504 | 2.816 | 3.606 | 13.3 | 6.4 | 31.4 | 53.7 | 18.3 | 9 | 14 |
| 3 | 24.75 | 16.02 | 6.981 | 56.8 | 8.9 | 62.1 | 78.0 | 49.5 | 0 | 9 |
| 4 | 26.38 | 31.42 | 18 | 51.3 | 9.2 | 38.5 | 51.1 | 29.1 | 156 | 28 |
| 5 | 8.786 | 7.679 | 3.3 | 24.9 | 6.7 | 35.8 | 51.2 | 25.0 | 28 | 29 |
| 6 | 47.04 | 54.66 | 39.78 | 74.6 | 8.6 | 19.1 | 34.3 | 10.7 | 89 | 32 |
| 7 | 13.71 | 18.09 | 31.78 | 39.1 | 8.4 | 43.1 | 52.8 | 35.2 | 283 | 17 |
| 8 | 40.54 | 25.58 | 5.164 | 64.2 | 14.3 | 71.8 | 104.3 | 49.4 | 6 | 9 |
| 9 | 38.75 | 61.31 | 31.41 | 67.0 | 9.7 | 45.0 | 79.2 | 25.6 | 180 | 31 |
| 10 | 12.25 | 8.559 | 5.748 | 30.8 | 12.3 | 47.9 | 63.2 | 36.3 | 388 | 12 |
| 11 | 53.89 | 40.9 | 73.65 | 66.7 | 8.6 | 64.4 | 80.1 | 51.7 | 370 | 19 |
| 12 | 59.44 | 74.14 | 35.54 | 80.5 | 8.3 | 33.1 | 57.3 | 19.2 | 114 | 31 |
| 13 | 60.29 | 64.28 | 80.91 | 70.5 | 7.0 | 29.3 | 46.3 | 18.6 | 353 | 16 |
| 14 | 6.239 | 9.057 | 4.31 | 26.5 | 9.9 | 44.9 | 66.0 | 30.6 | 198 | 11 |
| 15 | 56.32 | 60.37 | 17.75 | 65.4 | 9.2 | 62.2 | 80.9 | 47.9 | 79 | 17 |
| 16 | 17.23 | 19.29 | 20.13 | 35.0 | 9.7 | 2.6 | 9.4 | 0.7 | | |
| 17 | 2.754 | 3.63 | 2.701 | 3.5 | 5.2 | 1.9 | 6.5 | 0.5 | | |
| 18 | 29.8 | 45.43 | 22.27 | 60.9 | 7.1 | 48.0 | 62.3 | 36.9 | 190 | 11 |
| 19 | 5.23 | 3.776 | 1.976 | 23.6 | 10.9 | 39.3 | 65.2 | 23.7 | 388 | 14 |
| 20 | 5.459 | 5.167 | 21.98 | 34.8 | 13.1 | 51.3 | 76.6 | 34.3 | 301 | 4 |
| 21 | 56.93 | 75.69 | 21.19 | 73.5 | 12.6 | 42.0 | 63.9 | 27.7 | 108 | 9 |
| 22 | 2.052 | 2.089 | 6.621 | 12.3 | 7.7 | 24.7 | 54.3 | 11.2 | 303 | 7 |
| 23 | 22.69 | 20.12 | 43.97 | 50.0 | 6.0 | 47.5 | 56.0 | 40.3 | 342 | 14 |
| 24 | 17.72 | 12.96 | 25.99 | 36.4 | 9.2 | 50.5 | 59.9 | 42.6 | 361 | 14 |
| 25 | 49.34 | 40.33 | 10.46 | 61.8 | 7.7 | 67.4 | 86.3 | 52.7 | 53 | 15 |
| 26 | 67.22 | 71.49 | 58.9 | 80.1 | 6.1 | 29.6 | 55.7 | 15.7 | 14 | 21 |
| 27 | 26.84 | 24.48 | 61.14 | 47.0 | 6.6 | 55.0 | 71.0 | 42.7 | 331 | 13 |
| 28 | 25.76 | 35.34 | 38.94 | 49.7 | 8.3 | 35.8 | 51.8 | 24.7 | 236 | 19 |
| 29 | 19.74 | 20.98 | 44.35 | 38.9 | 7.8 | 39.6 | 52.0 | 30.1 | 318 | 21 |
| 30 | 1.914 | 2.258 | 2.177 | 1.3 | 2.3 | 1.3 | 3.0 | 0.5 | | |
| 31 | 60.89 | 83.58 | 88.09 | 88.8 | 5.5 | 39.2 | 77.9 | 19.7 | 249 | 19 |
| 32 | 3.41 | 3.307 | 2.063 | 13.7 | 10.0 | 12.8 | 46.3 | 3.5 | 23 | 24 |
| 33 | 45.08 | 42.47 | 42.15 | 57.5 | 4.7 | 41.5 | 49.7 | 34.7 | 385 | 21 |
| 34 | 4.288 | 4.569 | 11.54 | 16.6 | 8.6 | 22.9 | 49.0 | 10.7 | 294 | 15 |
| 35 | 20.96 | 28.78 | 40 | 50.3 | 5.8 | 40.4 | 52.7 | 30.9 | 253 | 25 |
| 36 | 7.936 | 5.735 | 3.436 | 28.9 | 6.7 | 48.1 | 66.5 | 34.8 | 5 | 15 |
| 37 | 6.228 | 7.909 | 13.35 | 28.8 | 10.8 | 27.9 | 43.6 | 17.8 | 259 | 30 |
| 38 | 27.66 | 17.63 | 4.606 | 57.0 | 7.9 | 72.8 | 89.2 | 59.4 | 4 | 8 |
| 39 | 54.63 | 80.21 | 87.95 | 83.5 | 6.6 | 48.4 | 87.9 | 26.7 | 251 | 20 |
| 40 | 44.69 | 50.37 | 80.29 | 57.2 | 9.9 | 43.4 | 60.4 | 31.2 | 328 | 14 |

# A4.7 C-Grey

| No. | $X_L$ | $Y_L$ (cd/m$^2$) | $Z_L$ | Lightness | | Colourfulness | | | Hue | |
|---|---|---|---|---|---|---|---|---|---|---|
| | | | | Avg | Stdev | Avg | Max | Min | Avg | Stdev |
| Reference White | 12.89 | 15.68 | 15.39 | | | | | | | |
| Back-ground | 2.304 | 2.724 | 3.655 | | | | | | | |
| 1 | 0.5011 | 0.3477 | 1.959 | 25.3 | 12.2 | 33.9 | 62.1 | 18.5 | 306 | 11 |
| 2 | 0.5427 | 0.5983 | 1.395 | 20.2 | 6.0 | 21.3 | 42.0 | 10.8 | 303 | 16 |
| 3 | 0.3172 | 0.4255 | 0.5377 | 9.3 | 4.8 | 2.7 | 11.8 | 0.6 | 258 | 56 |
| 4 | 0.8094 | 1.076 | 1.63 | 26.7 | 5.0 | 23.0 | 42.3 | 12.5 | 234 | 15 |
| 5 | 0.6847 | 1.252 | 0.22 | 37.4 | 8.5 | 41.3 | 56.8 | 30.0 | 191 | 13 |
| 6 | 2.749 | 1.078 | 14.14 | 51.7 | 17.0 | 69.4 | 107.0 | 45.0 | 301 | 6 |
| 7 | 1.986 | 3.833 | 0.5059 | 49.6 | 11.8 | 40.7 | 55.1 | 30.0 | 194 | 17 |
| 8 | 2.313 | 3.946 | 2.102 | 53.6 | 8.8 | 34.3 | 45.1 | 26.1 | 193 | 23 |
| 9 | 2.802 | 4.034 | 4.93 | 46.0 | 9.0 | 32.5 | 47.1 | 22.5 | 246 | 10 |
| 10 | 4.468 | 4.587 | 14.16 | 57.0 | 10.4 | 43.1 | 52.6 | 35.3 | 302 | 15 |
| 11 | 6.319 | 12.32 | 0.8764 | 80.7 | 9.5 | 62.1 | 97.3 | 39.7 | 176 | 21 |
| 12 | 8.73 | 12.93 | 14.54 | 83.7 | 6.9 | 37.2 | 69.0 | 20.0 | 262 | 13 |
| 13 | 0.3091 | 0.2241 | 0.733 | 15.6 | 7.7 | 23.8 | 62.0 | 9.1 | 331 | 20 |
| 14 | 4.392 | 6.842 | 5.455 | 64.8 | 9.0 | 36.1 | 44.9 | 29.0 | 196 | 23 |
| 15 | 1.242 | 1.938 | 0.866 | 41.4 | 9.2 | 33.8 | 46.5 | 24.5 | 186 | 17 |
| 16 | 1.93 | 0.9827 | 4.815 | 42.2 | 11.9 | 46.8 | 62.5 | 35.0 | 355 | 8 |
| 17 | 3.611 | 1.562 | 14.08 | 45.4 | 8.6 | 58.8 | 69.1 | 50.0 | 337 | 14 |
| 18 | 2.884 | 4.321 | 0.5252 | 42.6 | 7.9 | 35.3 | 44.9 | 27.8 | 158 | 25 |
| 19 | 5.347 | 5.054 | 14.23 | 63.3 | 11.5 | 41.6 | 51.3 | 33.7 | 328 | 21 |
| 20 | 8.174 | 13.21 | 5.396 | 84.0 | 6.7 | 51.5 | 75.3 | 35.3 | 173 | 15 |
| 21 | 9.981 | 13.91 | 14.87 | 88.9 | 3.8 | 32.1 | 59.7 | 17.3 | 268 | 17 |
| 22 | 6.754 | 7.65 | 12.89 | 67.8 | 11.6 | 28.7 | 44.9 | 18.4 | 311 | 20 |
| 23 | 6.416 | 6.055 | 13.4 | 60.2 | 12.0 | 37.6 | 48.6 | 29.0 | 333 | 29 |
| 24 | 10.44 | 14.05 | 11.01 | 87.2 | 10.6 | 12.6 | 27.6 | 5.7 | 179 | 45 |
| 25 | 8.87 | 10.72 | 7.668 | 78.2 | 14.0 | 21.8 | 41.0 | 11.6 | 83 | 23 |
| 26 | 4.693 | 2.465 | 4.859 | 49.1 | 8.4 | 54.9 | 73.0 | 41.3 | 378 | 9 |
| 27 | 6.321 | 3.018 | 14.03 | 65.4 | 10.0 | 69.2 | 85.4 | 56.0 | 363 | 17 |
| 28 | 8.096 | 6.546 | 14.17 | 67.8 | 4.9 | 49.1 | 63.2 | 38.2 | 370 | 14 |
| 29 | 10.07 | 14.38 | 0.8992 | 84.4 | 7.5 | 68.3 | 96.5 | 48.3 | 104 | 10 |
| 30 | 10.92 | 14.65 | 5.399 | 86.7 | 8.7 | 40.2 | 64.1 | 25.3 | 101 | 3 |
| 31 | 7.3145 | 12.69 | 5.526 | 78.3 | 4.1 | 47.6 | 72.4 | 31.3 | 177 | 13 |
| 32 | 0.4295 | 0.4029 | 0.1534 | 23.8 | 7.6 | 30.9 | 44.0 | 21.7 | 26 | 20 |
| 33 | 6.48 | 6.0475 | 5.0755 | 63.7 | 6.7 | 40.7 | 54.8 | 30.3 | 8 | 13 |
| 34 | 1.092 | 0.7519 | 0.3262 | 38.6 | 7.7 | 45.5 | 63.5 | 32.7 | 7 | 11 |
| 35 | 7.338 | 12.97 | 0.9015 | 85.2 | 7.0 | 62.0 | 83.5 | 46.1 | 162 | 26 |
| 36 | 0.1745 | 0.2015 | 0.168 | 4.2 | 4.8 | 2.2 | 5.1 | 0.9 | | |
| 37 | 8.989 | 10.955 | 5.2725 | 72.4 | 11.7 | 33.7 | 50.0 | 22.7 | 55 | 18 |
| 38 | 3.918 | 2.273 | 0.3602 | 56.5 | 11.6 | 71.1 | 94.3 | 53.6 | 7 | 10 |
| 39 | 1.058 | 0.521 | 4.787 | 37.7 | 13.8 | 63.0 | 92.8 | 42.8 | 304 | 6 |
| 40 | 5.6085 | 5.7665 | 0.5206 | 62.2 | 8.8 | 51.4 | 70.3 | 37.5 | 61 | 15 |

# A4.8 C-White

| No. | $X_L$ | $Y_L$ (cd/m$^2$) | $Z_L$ | Lightness | | Colourfulness | | | Hue | |
|---|---|---|---|---|---|---|---|---|---|---|
| | | | | Avg | Stdev | Avg | Max | Min | Avg | Stdev |
| Reference White | 13.40 | 16.28 | 15.70 | | | | | | | |
| Back-ground | 13.12 | 15.86 | 15.24 | | | | | | | |
| 1 | 1.094 | 0.9391 | 3.07 | 22.7 | 8.1 | 19.9 | 40.5 | 9.7 | 306 | 11 |
| 2 | 1.078 | 1.177 | 2.315 | 17.6 | 7.7 | 16.0 | 32.9 | 7.8 | 301 | 19 |
| 3 | 0.8309 | 0.9995 | 1.241 | 9.7 | 3.7 | 3.5 | 9.2 | 1.3 | 244 | 52 |
| 4 | 1.332 | 1.621 | 2.55 | 24.7 | 6.6 | 24.9 | 42.7 | 14.5 | 224 | 31 |
| 5 | 1.151 | 1.843 | 0.6184 | 28.7 | 9.4 | 31.8 | 56.5 | 17.9 | 189 | 16 |
| 6 | 3.208 | 1.642 | 14.51 | 47.9 | 13.9 | 71.8 | 95.4 | 54.1 | 304 | 7 |
| 7 | 2.517 | 4.53 | 1.072 | 50.9 | 8.6 | 56.0 | 77.0 | 40.8 | 188 | 12 |
| 8 | 2.962 | 4.701 | 3.253 | 54.4 | 11.8 | 48.9 | 65.3 | 36.6 | 196 | 20 |
| 9 | 3.627 | 4.936 | 6.726 | 53.9 | 9.8 | 43.8 | 59.5 | 32.2 | 265 | 16 |
| 10 | 5.018 | 5.376 | 14.6 | 58.3 | 9.8 | 49.1 | 64.2 | 37.6 | 297 | 11 |
| 11 | 6.673 | 12.72 | 1.416 | 75.1 | 6.3 | 56.1 | 71.5 | 43.9 | 184 | 18 |
| 12 | 9.178 | 13.59 | 15.02 | 78.4 | 7.4 | 52.9 | 69.9 | 40.1 | 259 | 13 |
| 13 | 0.8282 | 0.7833 | 1.505 | 9.7 | 8.0 | 6.1 | 20.3 | 1.8 | 348 | 27 |
| 14 | 5.164 | 7.77 | 7.07 | 60.7 | 7.5 | 41.0 | 55.4 | 30.3 | 226 | 25 |
| 15 | 1.763 | 2.537 | 1.596 | 38.0 | 9.3 | 40.7 | 55.4 | 29.9 | 194 | 15 |
| 16 | 2.679 | 1.648 | 6.411 | 41.1 | 9.6 | 56.5 | 72.5 | 44.1 | 345 | 12 |
| 17 | 4.142 | 2.161 | 14.49 | 45.6 | 9.4 | 63.3 | 73.4 | 54.5 | 338 | 14 |
| 18 | 3.46 | 5.063 | 1.089 | 51.6 | 9.6 | 40.8 | 53.9 | 31.0 | 171 | 29 |
| 19 | 5.896 | 5.819 | 14.47 | 57.3 | 7.4 | 45.3 | 56.4 | 36.5 | 312 | 22 |
| 20 | 8.793 | 13.75 | 7.099 | 76.8 | 7.1 | 42.5 | 59.5 | 30.4 | 182 | 22 |
| 21 | 10.18 | 14.16 | 15.05 | 80.7 | 8.8 | 40.7 | 60.3 | 27.5 | 271 | 16 |
| 22 | 7.349 | 8.435 | 13.42 | 54.4 | 11.0 | 24.4 | 48.5 | 12.3 | 300 | 13 |
| 23 | 7.096 | 6.926 | 13.96 | 59.9 | 7.9 | 42.0 | 56.2 | 31.4 | 332 | 12 |
| 24 | 11.11 | 14.68 | 12.19 | 85.8 | 4.7 | 22.3 | 41.9 | 11.9 | 201 | 33 |
| 25 | 9.788 | 11.71 | 9.199 | 71.6 | 12.0 | 23.0 | 29.3 | 18.1 | 65 | 41 |
| 26 | 5.596 | 3.224 | 6.547 | 53.7 | 6.0 | 63.5 | 79.6 | 50.6 | 375 | 10 |
| 27 | 6.947 | 3.681 | 14.42 | 58.1 | 8.9 | 69.6 | 82.6 | 58.7 | 365 | 15 |
| 28 | 8.894 | 7.525 | 14.73 | 60.6 | 6.3 | 46.3 | 54.6 | 39.3 | 362 | 15 |
| 29 | 10.63 | 15.03 | 1.468 | 85.8 | 6.1 | 57.4 | 92.6 | 35.5 | 103 | 7 |
| 30 | 11.56 | 15.16 | 7.023 | 89.1 | 2.6 | 33.6 | 57.4 | 19.7 | 101 | 9 |
| 31 | 7.7365 | 13.08 | 6.992 | 75.5 | 6.2 | 46.2 | 66.9 | 31.9 | 194 | 25 |
| 32 | 0.8997 | 0.9626 | 0.5583 | 15.3 | 6.2 | 17.9 | 32.1 | 10.0 | 39 | 30 |
| 33 | 7.43 | 7.0065 | 6.692 | 57.1 | 4.9 | 44.5 | 55.2 | 35.9 | 2 | 24 |
| 34 | 1.654 | 1.3635 | 0.8865 | 32.6 | 8.5 | 39.4 | 59.7 | 26.1 | 21 | 16 |
| 35 | 7.706 | 13.415 | 1.458 | 74.9 | 8.4 | 52.8 | 74.6 | 37.4 | 174 | 17 |
| 36 | 0.6231 | 0.7419 | 0.5656 | 5.1 | 5.2 | 2.1 | 4.9 | 0.9 | | |
| 37 | 9.7085 | 11.7 | 6.755 | 70.6 | 5.7 | 34.2 | 46.9 | 24.9 | 68 | 15 |
| 38 | 4.4695 | 2.8865 | 0.8808 | 53.8 | 9.7 | 70.8 | 100.4 | 49.9 | 4 | 7 |
| 39 | 1.744 | 1.13 | 6.3985 | 34.2 | 7.3 | 56.2 | 69.4 | 45.5 | 308 | 12 |
| 40 | 6.316 | 6.61 | 1.0925 | 56.2 | 5.8 | 53.9 | 63.9 | 45.4 | 63 | 11 |

# A4.9 C-Black

| No. | $X_L$ | $Y_L$ (cd/m$^2$) | $Z_L$ | Lightness | | Colourfulness | | | Hue | |
|---|---|---|---|---|---|---|---|---|---|---|
| | | | | Avg | Stdev | Avg | Max | Min | Avg | Stdev |
| Reference White | 12.38 | 15.00 | 14.74 | | | | | | | |
| Back-ground | 0.00 | 0.00 | 0.00 | | | | | | | |
| 1 | 0.3675 | 0.2209 | 1.554 | 16.5 | 4.9 | 29.7 | 58.4 | 15.2 | 309 | 9 |
| 2 | 0.3652 | 0.4053 | 1.011 | 24.9 | 8.3 | 11.9 | 22.0 | 6.4 | 275 | 42 |
| 3 | 0.1991 | 0.2696 | 0.3614 | 18.3 | 6.6 | 10.7 | 26.9 | 4.3 | 212 | 24 |
| 4 | 0.6153 | 0.8547 | 1.193 | 27.5 | 8.7 | 23.7 | 36.5 | 15.3 | 250 | 25 |
| 5 | 0.6079 | 1.133 | 0.1436 | 31.1 | 9.7 | 50.6 | 64.1 | 39.9 | 189 | 12 |
| 6 | 2.692 | 1.001 | 14.18 | 45.1 | 11.0 | 75.1 | 89.9 | 62.8 | 304 | 6 |
| 7 | 1.836 | 3.593 | 0.3516 | 59.9 | 4.8 | 53.2 | 63.0 | 44.9 | 178 | 15 |
| 8 | 2.108 | 3.682 | 1.76 | 58.5 | 9.2 | 45.7 | 54.6 | 38.2 | 190 | 15 |
| 9 | 2.698 | 3.848 | 4.938 | 61.6 | 8.4 | 29.2 | 39.7 | 21.4 | 257 | 23 |
| 10 | 4.396 | 4.441 | 14.27 | 66.7 | 8.7 | 54.1 | 66.5 | 44.1 | 298 | 8 |
| 11 | 6.278 | 12.09 | 0.7136 | 79.4 | 7.1 | 73.9 | 100.3 | 54.5 | 172 | 15 |
| 12 | 8.87 | 12.97 | 14.73 | 84.5 | 4.2 | 34.7 | 58.8 | 20.4 | 248 | 36 |
| 13 | 0.1952 | 0.114 | 0.5005 | 10.5 | 4.5 | 25.9 | 47.0 | 14.2 | 351 | 18 |
| 14 | 4.372 | 6.743 | 5.528 | 67.6 | 6.8 | 44.1 | 56.7 | 34.3 | 198 | 22 |
| 15 | 1.115 | 1.76 | 0.6077 | 42.9 | 6.8 | 44.3 | 55.7 | 35.3 | 185 | 15 |
| 16 | 1.814 | 0.8453 | 4.802 | 39.4 | 8.5 | 51.3 | 72.5 | 36.3 | 359 | 11 |
| 17 | 3.533 | 1.43 | 14.23 | 51.8 | 9.5 | 60.6 | 77.3 | 47.5 | 335 | 15 |
| 18 | 2.747 | 4.135 | 0.385 | 58.2 | 7.8 | 43.0 | 54.2 | 34.1 | 157 | 22 |
| 19 | 5.294 | 4.943 | 14.38 | 69.4 | 8.1 | 47.3 | 66.6 | 33.6 | 323 | 14 |
| 20 | 7.936 | 12.81 | 5.264 | 80.4 | 4.7 | 43.5 | 76.4 | 24.8 | 174 | 14 |
| 21 | 9.772 | 13.49 | 14.74 | 82.9 | 6.4 | 37.9 | 61.3 | 23.4 | 274 | 16 |
| 22 | 6.662 | 7.44 | 13.01 | 68.8 | 8.7 | 33.4 | 45.4 | 24.6 | 312 | 17 |
| 23 | 6.406 | 5.974 | 13.79 | 68.0 | 8.3 | 42.9 | 58.8 | 31.2 | 328 | 20 |
| 24 | 10.46 | 13.97 | 11.29 | 90.3 | 4.5 | 16.7 | 36.4 | 7.7 | 184 | 34 |
| 25 | 8.542 | 10.29 | 7.638 | 85.6 | 10.0 | 9.5 | 25.4 | 3.6 | 83 | 22 |
| 26 | 4.505 | 2.284 | 4.858 | 54.4 | 6.1 | 70.4 | 85.4 | 58.1 | 383 | 21 |
| 27 | 6.2 | 2.873 | 14.22 | 64.9 | 6.3 | 66.8 | 78.6 | 56.8 | 369 | 14 |
| 28 | 8.003 | 6.385 | 14.47 | 64.6 | 6.9 | 49.3 | 66.2 | 36.8 | 367 | 22 |
| 29 | 9.899 | 14.19 | 0.7 | 83.6 | 6.1 | 68.6 | 90.2 | 52.2 | 105 | 10 |
| 30 | 10.55 | 14.11 | 5.263 | 83.0 | 10.8 | 29.7 | 47.2 | 18.6 | 111 | 13 |
| 31 | 7.097 | 12.365 | 5.294 | 83.4 | 7.1 | 50.6 | 77.7 | 33.0 | 173 | 14 |
| 32 | 0.3341 | 0.2752 | 0.0528 | 23.3 | 6.4 | 38.8 | 54.8 | 27.5 | 22 | 36 |
| 33 | 6.212 | 5.717 | 4.961 | 63.4 | 7.3 | 40.4 | 54.8 | 29.8 | 13 | 15 |
| 34 | 0.9644 | 0.6084 | 0.1832 | 37.3 | 7.7 | 43.9 | 54.4 | 35.4 | 10 | 19 |
| 35 | 7.146 | 12.665 | 0.7179 | 81.4 | 6.1 | 72.3 | 90.4 | 57.8 | 169 | 19 |
| 36 | | | | | | | | | | |
| 37 | 8.677 | 10.525 | 5.1275 | 73.1 | 7.7 | 29.0 | 44.6 | 18.8 | 81 | 16 |
| 38 | 3.652 | 2.054 | 0.1985 | 57.0 | 6.2 | 75.2 | 98.0 | 57.8 | 6 | 9 |
| 39 | 0.9668 | 0.3867 | 4.726 | 27.6 | 5.9 | 46.8 | 78.0 | 28.1 | 309 | 8 |
| 40 | 5.3915 | 5.507 | 0.3666 | 59.7 | 9.8 | 51.6 | 62.6 | 42.6 | 70 | 13 |

# A4.10 C-35mm

| No. | $X_L$ | $Y_L$ (cd/m$^2$) | $Z_L$ | Lightness | | Colourfulness | | | Hue | |
|---|---|---|---|---|---|---|---|---|---|---|
| | | | | Avg | Stdev | Avg | Max | Min | Avg | Stdev |
| Reference White | 14.19 | 15.42 | 6.34 | | | | | | | |
| Back-ground | 2.768 | 3.141 | 1.352 | | | | | | | |
| 1 | 0.5846 | 0.5279 | 2.441 | 32.5 | 10.8 | 61.9 | 77.2 | 49.6 | 300 | 4 |
| 2 | 0.3832 | 0.5739 | 0.8101 | 23.9 | 5.4 | 33.8 | 45.6 | 25.0 | 267 | 30 |
| 3 | 3.232 | 5.333 | 0.601 | 62.8 | 10.2 | 51.7 | 66.9 | 39.9 | 185 | 16 |
| 4 | 10.82 | 12.32 | 1.288 | 83.9 | 9.6 | 44.7 | 63.9 | 31.2 | 104 | 11 |
| 5 | 8.141 | 10.17 | 1.188 | 75.1 | 8.7 | 45.2 | 58.1 | 35.2 | 162 | 20 |
| 6 | 1.083 | 2.475 | 1.231 | 42.6 | 4.6 | 58.6 | 73.4 | 46.7 | 211 | 14 |
| 7 | 1.59 | 3.418 | 0.9029 | 57.6 | 11.4 | 57.5 | 72.8 | 45.4 | 196 | 18 |
| 8 | 3.143 | 5.071 | 1.49 | 55.5 | 5.7 | 47.5 | 61.1 | 36.9 | 210 | 19 |
| 9 | 0.3036 | 0.6049 | 0.2742 | 21.5 | 9.8 | 41.1 | 63.8 | 26.4 | 213 | 16 |
| 10 | 3.971 | 6.178 | 5.228 | 65.6 | 6.7 | 50.6 | 63.4 | 40.3 | 279 | 18 |
| 11 | 1.074 | 1.619 | 3.553 | 42.0 | 6.6 | 58.6 | 73.5 | 46.8 | 291 | 11 |
| 12 | 2.091 | 1.666 | 0.7034 | 44.4 | 10.5 | 36.0 | 46.1 | 28.1 | 4 | 29 |
| 13 | 0.9466 | 0.8993 | 0.8164 | 21.5 | 9.3 | 33.5 | 62.0 | 18.1 | 336 | 14 |
| 14 | 1.453 | 1.15 | 2.885 | 36.0 | 13.2 | 52.9 | 63.3 | 44.2 | 337 | 19 |
| 15 | 9.957 | 9.493 | 1.155 | 64.6 | 12.4 | 44.3 | 60.3 | 32.5 | 72 | 16 |
| 16 | 5.079 | 4.967 | 1.162 | 60.1 | 8.9 | 35.5 | 54.1 | 23.3 | 50 | 25 |
| 17 | 1.185 | 1.135 | 0.5774 | 27.5 | 14.0 | 14.9 | 25.1 | 8.9 | 379 | 46 |
| 18 | 3.821 | 2.305 | 1.08 | 42.2 | 6.1 | 61.7 | 75.4 | 50.4 | 384 | 17 |
| 19 | 5.281 | 3.215 | 3.191 | 56.4 | 8.4 | 66.4 | 80.6 | 54.6 | 380 | 19 |
| 20 | 12.89 | 12.91 | 1.944 | 78.0 | 5.0 | 34.1 | 53.1 | 21.9 | 78 | 18 |
| 21 | 0.7522 | 0.6636 | 1.243 | 23.0 | 12.1 | 47.4 | 69.2 | 32.5 | 324 | 13 |
| 22 | 0.2194 | 0.3646 | 0.0929 | 1.8 | 2.5 | 1.2 | 2.1 | 0.7 | | |
| 23 | 0.8622 | 1.19 | 0.2348 | 29.5 | 13.3 | 15.8 | 67.1 | 3.7 | 187 | 13 |
| 24 | 0.4734 | 0.7899 | 1.209 | 28.6 | 9.1 | 40.4 | 61.6 | 26.6 | 260 | 27 |
| 25 | 1.167 | 2.651 | 1.098 | 50.1 | 8.6 | 59.5 | 72.8 | 48.6 | 210 | 12 |
| 26 | 5.465 | 3.421 | 0.3219 | 60.4 | 7.5 | 57.2 | 80.8 | 40.5 | 11 | 9 |
| 27 | 3.188 | 1.911 | 0.2832 | 47.2 | 9.3 | 60.9 | 75.9 | 48.8 | 2 | 11 |
| 28 | 2.129 | 1.55 | 0.4491 | 40.2 | 8.1 | 38.0 | 53.4 | 27.0 | 13 | 26 |
| 29 | 6.483 | 7.374 | 3.153 | 64.2 | 10.8 | 1.4 | 2.8 | 0.7 | | |
| 30 | 4.331 | 2.9895 | 2.5165 | 48.2 | 5.9 | 47.2 | 59.9 | 37.1 | 377 | 16 |
| 31 | 0.1719 | 0.1338 | 0.52 | 8.9 | 6.3 | 10.7 | 33.7 | 3.4 | 308 | 12 |
| 32 | 0.4969 | 1.0215 | 0.1411 | 39.0 | 9.2 | 53.1 | 66.9 | 42.1 | 200 | 5 |
| 33 | 1.6135 | 1.191 | 0.0803 | 39.5 | 10.1 | 44.4 | 65.7 | 30.0 | 21 | 33 |
| 34 | 0.8227 | 1.048 | 3.141 | 42.7 | 10.6 | 59.4 | 74.5 | 47.4 | 296 | 5 |
| 35 | 0.7774 | 1.501 | 1.738 | 39.8 | 5.6 | 48.3 | 61.5 | 37.9 | 259 | 21 |
| 36 | 3.0225 | 2.8765 | 3.94 | 42.5 | 11.3 | 30.8 | 47.2 | 20.0 | 333 | 29 |
| 37 | 5.3345 | 3.3295 | 0.4742 | 58.5 | 6.7 | 61.6 | 77.4 | 49.0 | 11 | 10 |
| 38 | 10.57 | 12.61 | 2.7145 | 79.3 | 10.2 | 32.1 | 56.0 | 18.4 | 148 | 25 |
| 39 | 1.8895 | 1.8045 | 0.4968 | 34.2 | 7.3 | 32.8 | 47.4 | 22.8 | 25 | 33 |
| 40 | | | | | | | | | | |

# A4.11 A-Dark

| No. | $X_L$ | $Y_L$ (cd/m$^2$) | $Z_L$ | Lightness | | Colourfulness | | | Hue | |
|---|---|---|---|---|---|---|---|---|---|---|
| | | | | Avg | Stdev | Avg | Max | Min | Avg | Stdev |
| Reference White | 82.60 | 85.77 | 99.46 | | | | | | | |
| Back-ground | 16.25 | 17.00 | 19.70 | | | | | | | |
| 1 | 54.55 | 70.12 | 96.16 | 81.4 | 8.4 | 35.4 | 67.4 | 18.5 | 272 | 26 |
| 2 | 4.22 | 6.03 | 8.74 | 39.1 | 8.6 | 45.2 | 51.0 | 40.0 | 222 | 21 |
| 3 | 38.15 | 38.36 | 66.06 | 67.3 | 12.3 | 27.0 | 44.5 | 16.4 | 324 | 20 |
| 4 | 2.91 | 3.69 | 7.61 | 33.6 | 8.7 | 38.7 | 55.5 | 27.0 | 232 | 35 |
| 5 | 54.95 | 29.03 | 88.21 | 75.0 | 12.8 | 70.4 | 83.8 | 59.2 | 377 | 19 |
| 6 | 2.85 | 2.53 | 10.71 | 33.2 | 9.6 | 41.0 | 58.4 | 28.8 | 292 | 23 |
| 7 | 20.78 | 30.29 | 32.10 | 57.3 | 7.9 | 40.4 | 47.9 | 34.0 | 198 | 28 |
| 8 | 28.39 | 15.07 | 86.91 | 58.2 | 14.5 | 56.6 | 69.6 | 45.9 | 344 | 12 |
| 9 | 43.57 | 23.79 | 28.26 | 70.5 | 15.1 | 69.9 | 83.5 | 58.6 | 390 | 17 |
| 10 | 8.81 | 11.63 | 6.07 | 46.8 | 7.5 | 37.8 | 48.0 | 29.8 | 185 | 14 |
| 11 | 11.24 | 18.82 | 13.37 | 56.8 | 7.8 | 46.9 | 59.4 | 37.1 | 195 | 16 |
| 12 | 70.05 | 79.38 | 37.73 | 80.5 | 8.8 | 40.4 | 66.1 | 24.7 | 101 | 3 |
| 13 | 17.05 | 9.82 | 27.13 | 49.5 | 7.9 | 51.2 | 60.2 | 43.5 | 363 | 14 |
| 14 | 53.16 | 52.92 | 43.97 | 71.4 | 11.2 | 23.5 | 38.7 | 14.3 | 67 | 32 |
| 15 | 14.26 | 20.21 | 29.29 | 52.3 | 8.5 | 42.3 | 57.3 | 31.1 | 251 | 23 |
| 16 | 41.02 | 35.31 | 72.07 | 66.8 | 8.1 | 43.7 | 56.7 | 33.6 | 350 | 12 |
| 17 | 43.20 | 64.95 | 36.46 | 77.7 | 12.7 | 47.2 | 63.5 | 35.1 | 174 | 20 |
| 18 | 20.01 | 23.58 | 5.64 | 49.1 | 8.9 | 36.0 | 48.9 | 26.5 | 131 | 18 |
| 19 | 2.84 | 1.67 | 4.36 | 28.6 | 15.5 | 33.8 | 66.5 | 17.2 | 355 | 21 |
| 20 | 65.65 | 77.33 | 13.21 | 80.5 | 9.6 | 61.1 | 78.3 | 47.6 | 102 | 6 |
| 21 | 9.71 | 18.11 | 5.27 | 50.5 | 8.2 | 45.6 | 58.0 | 35.8 | 193 | 16 |
| 22 | 28.35 | 57.48 | 11.93 | 76.8 | 10.1 | 60.8 | 76.9 | 48.0 | 182 | 16 |
| 23 | 18.12 | 9.68 | 86.49 | 58.2 | 12.1 | 65.8 | 84.6 | 51.1 | 304 | 7 |
| 24 | 59.00 | 73.09 | 61.86 | 78.8 | 13.4 | 18.5 | 46.9 | 7.3 | 182 | 30 |
| 25 | 4.17 | 7.12 | 1.55 | 45.9 | 8.6 | 50.2 | 60.1 | 41.9 | 190 | 10 |
| 26 | 35.93 | 30.92 | 89.47 | 65.0 | 5.9 | 40.4 | 51.0 | 32.0 | 334 | 12 |
| 27 | 44.21 | 64.69 | 95.70 | 75.5 | 10.8 | 49.9 | 80.5 | 31.0 | 268 | 26 |
| 28 | 25.66 | 25.54 | 89.08 | 56.8 | 6.4 | 49.1 | 63.1 | 38.2 | 306 | 9 |
| 29 | 62.55 | 44.94 | 90.89 | 67.7 | 6.5 | 53.0 | 65.4 | 42.9 | 375 | 16 |
| 30 | 1.95 | 2.77 | 3.80 | 28.6 | 12.1 | 31.8 | 64.4 | 15.7 | 213 | 13 |
| 31 | 32.87 | 59.49 | 36.09 | 72.3 | 8.4 | 50.8 | 68.2 | 37.8 | 184 | 11 |
| 32 | 5.22 | 3.92 | 0.83 | 39.8 | 11.5 | 40.9 | 49.7 | 33.6 | 23 | 24 |
| 33 | 51.19 | 39.71 | 30.88 | 64.5 | 11.5 | 46.2 | 56.3 | 37.9 | 10 | 14 |
| 34 | 12.43 | 7.68 | 3.00 | 43.6 | 8.2 | 45.0 | 52.1 | 38.9 | 5 | 11 |
| 35 | 38.62 | 62.83 | 12.30 | 79.7 | 11.0 | 53.8 | 71.5 | 40.5 | 177 | 16 |
| 36 | 1.71 | 1.47 | 0.76 | 6.4 | 5.4 | 2.6 | 7.7 | 0.9 | | |
| 37 | 59.05 | 56.23 | 33.77 | 72.3 | 7.9 | 32.6 | 49.2 | 21.6 | 55 | 18 |
| 38 | 38.80 | 21.55 | 3.95 | 65.2 | 14.2 | 69.7 | 84.7 | 57.4 | 7 | 10 |
| 39 | 6.73 | 4.39 | 26.67 | 47.0 | 10.0 | 59.6 | 74.7 | 47.6 | 304 | 6 |
| 40 | 46.58 | 37.61 | 6.62 | 62.7 | 7.1 | 52.1 | 59.1 | 46.0 | 61 | 15 |

# A4.12 A-Avg

| No. | $X_L$ | $Y_L$ (cd/m$^2$) | $Z_L$ | Lightness | | Colourfulness | | | Hue | |
|---|---|---|---|---|---|---|---|---|---|---|
| | | | | Avg | Stdev | Avg | Max | Min | Avg | Stdev |
| Reference White | 85.79 | 89.13 | 102.6 | | | | | | | |
| Back-ground | 20.34 | 21.39 | 24.48 | | | | | | | |
| 1 | 58.51 | 74.51 | 100.8 | 78.2 | 8.1 | 37.2 | 60.7 | 22.8 | 273 | 24 |
| 2 | 8.13 | 10.24 | 13.38 | 39.5 | 8.8 | 34.6 | 49.2 | 24.4 | 218 | 17 |
| 3 | 42.40 | 42.94 | 71.28 | 64.1 | 8.0 | 25.8 | 43.1 | 15.5 | 325 | 14 |
| 4 | 6.80 | 7.86 | 12.20 | 32.3 | 10.6 | 29.7 | 55.5 | 15.9 | 236 | 28 |
| 5 | 59.29 | 33.39 | 93.71 | 73.2 | 12.1 | 68.5 | 85.3 | 55.0 | 373 | 19 |
| 6 | 6.79 | 6.77 | 15.39 | 34.5 | 10.6 | 36.4 | 55.5 | 23.8 | 298 | 11 |
| 7 | 24.89 | 34.80 | 37.01 | 57.3 | 6.5 | 38.6 | 47.0 | 31.7 | 197 | 28 |
| 8 | 32.49 | 19.36 | 91.85 | 60.9 | 13.9 | 54.7 | 66.2 | 45.2 | 345 | 12 |
| 9 | 47.76 | 28.14 | 32.98 | 70.5 | 12.1 | 66.9 | 87.9 | 50.9 | 389 | 11 |
| 10 | 12.82 | 15.96 | 10.75 | 48.2 | 7.5 | 40.2 | 51.6 | 31.3 | 184 | 13 |
| 11 | 15.28 | 23.23 | 18.11 | 47.3 | 4.1 | 39.0 | 48.4 | 31.4 | 200 | 15 |
| 12 | 74.50 | 84.13 | 42.32 | 79.1 | 8.0 | 31.7 | 58.8 | 17.1 | 101 | 3 |
| 13 | 21.08 | 14.09 | 31.91 | 50.0 | 8.1 | 49.1 | 60.4 | 39.9 | 363 | 11 |
| 14 | 57.22 | 57.34 | 48.93 | 69.4 | 10.7 | 20.2 | 36.6 | 11.1 | 66 | 33 |
| 15 | 18.32 | 24.64 | 34.19 | 50.5 | 8.2 | 39.8 | 50.8 | 31.2 | 254 | 21 |
| 16 | 45.10 | 39.70 | 76.98 | 60.5 | 15.9 | 35.7 | 48.6 | 26.2 | 347 | 13 |
| 17 | 47.43 | 69.66 | 41.43 | 74.5 | 9.1 | 41.7 | 59.0 | 29.4 | 172 | 21 |
| 18 | 24.11 | 28.01 | 10.34 | 49.5 | 5.7 | 37.6 | 47.1 | 29.9 | 139 | 20 |
| 19 | 6.80 | 5.90 | 9.02 | 23.6 | 10.5 | 25.2 | 56.1 | 11.4 | 344 | 30 |
| 20 | 69.49 | 81.50 | 18.00 | 77.7 | 10.1 | 62.5 | 84.5 | 46.2 | 100 | 4 |
| 21 | 13.74 | 22.53 | 9.95 | 50.0 | 5.5 | 43.5 | 52.9 | 35.8 | 188 | 11 |
| 22 | 32.52 | 62.28 | 16.72 | 76.5 | 10.5 | 55.9 | 73.3 | 42.7 | 180 | 17 |
| 23 | 22.18 | 13.96 | 91.74 | 57.7 | 11.9 | 63.2 | 78.3 | 50.9 | 305 | 8 |
| 24 | 63.18 | 77.70 | 67.15 | 78.0 | 12.3 | 17.0 | 36.7 | 7.8 | 181 | 34 |
| 25 | 8.16 | 11.43 | 6.19 | 45.5 | 5.2 | 47.7 | 65.4 | 34.8 | 190 | 12 |
| 26 | 40.12 | 35.35 | 94.70 | 62.7 | 11.7 | 42.5 | 56.6 | 31.9 | 333 | 14 |
| 27 | 48.45 | 69.44 | 101.1 | 73.6 | 12.9 | 45.6 | 84.1 | 24.7 | 277 | 20 |
| 28 | 29.83 | 30.01 | 94.52 | 54.4 | 6.1 | 43.9 | 55.6 | 34.7 | 305 | 16 |
| 29 | 66.89 | 49.52 | 96.27 | 65.0 | 11.6 | 43.9 | 68.7 | 28.1 | 379 | 17 |
| 30 | 5.91 | 7.03 | 8.49 | 30.9 | 10.4 | 28.1 | 60.4 | 13.1 | 210 | 17 |
| 31 | 37.04 | 64.21 | 41.00 | 73.6 | 8.5 | 52.2 | 70.6 | 38.6 | 187 | 8 |
| 32 | 9.20 | 8.18 | 5.44 | 38.4 | 9.2 | 38.0 | 52.9 | 27.3 | 33 | 17 |
| 33 | 55.53 | 44.27 | 35.70 | 66.0 | 7.0 | 41.5 | 59.2 | 29.1 | 21 | 18 |
| 34 | 16.49 | 11.99 | 7.69 | 48.2 | 7.8 | 47.0 | 56.7 | 38.9 | 17 | 20 |
| 35 | 42.81 | 67.52 | 17.03 | 76.4 | 10.1 | 51.9 | 65.9 | 40.8 | 176 | 21 |
| 36 | 5.65 | 5.69 | 5.38 | 5.7 | 4.5 | 1.5 | 3.3 | 0.7 | | |
| 37 | 63.32 | 60.81 | 38.44 | 68.9 | 7.4 | 33.4 | 47.8 | 23.3 | 55 | 18 |
| 38 | 43.16 | 25.98 | 8.56 | 63.9 | 12.7 | 71.8 | 88.0 | 58.6 | 7 | 10 |
| 39 | 10.73 | 8.65 | 31.52 | 49.1 | 11.1 | 56.4 | 75.3 | 42.3 | 304 | 6 |
| 40 | 50.75 | 42.05 | 11.33 | 62.0 | 4.7 | 50.2 | 62.4 | 40.4 | 61 | 15 |

# A4.13 Filter0-02

| No. | $X_L$ | $Y_L$ (cd/m$^2$) | $Z_L$ | Lightness | | Colourfulness | | | Hue | |
|---|---|---|---|---|---|---|---|---|---|---|
| | | | | Avg | Stdev | Avg | Max | Min | Avg | Stdev |
| Reference White | 83.69 | 87.37 | 100.7 | | | | | | | |
| Back-ground | 16.49 | 17.26 | 20.15 | | | | | | | |
| 1 | 5.47 | 7.64 | 11.06 | 42.8 | 6.7 | 42.5 | 51.0 | 35.4 | 224 | 14 |
| 2 | 55.09 | 70.99 | 97.81 | 84.6 | 7.5 | 24.8 | 55.2 | 11.1 | 284 | 20 |
| 3 | 38.65 | 38.88 | 67.34 | 63.3 | 11.9 | 20.8 | 39.9 | 10.8 | 333 | 19 |
| 4 | 3.46 | 4.21 | 7.84 | 30.3 | 12.4 | 38.0 | 70.1 | 20.6 | 232 | 20 |
| 5 | 55.56 | 29.27 | 89.36 | 78.1 | 15.1 | 62.2 | 92.7 | 41.7 | 375 | 16 |
| 6 | 2.61 | 2.24 | 9.98 | 30.8 | 14.2 | 38.9 | 86.6 | 17.4 | 295 | 15 |
| 7 | 21.05 | 30.76 | 32.82 | 63.3 | 10.1 | 39.3 | 48.5 | 31.8 | 203 | 28 |
| 8 | 28.78 | 15.17 | 88.29 | 58.8 | 14.6 | 59.3 | 77.4 | 45.5 | 343 | 16 |
| 9 | 43.98 | 24.00 | 28.69 | 74.6 | 12.3 | 56.5 | 96.5 | 33.1 | 387 | 17 |
| 10 | 10.32 | 12.08 | 10.52 | 38.3 | 12.3 | 30.7 | 43.3 | 21.8 | 192 | 18 |
| 11 | 9.34 | 16.15 | 11.39 | 52.8 | 9.6 | 43.2 | 59.8 | 31.2 | 193 | 12 |
| 12 | 82.18 | 85.31 | 98.86 | 102.5 | 4.5 | 1.0 | 1.0 | 1.0 | | |
| 13 | 17.24 | 9.90 | 27.62 | 52.8 | 8.5 | 50.3 | 61.5 | 41.2 | 368 | 12 |
| 14 | 53.54 | 53.43 | 44.65 | 71.7 | 11.3 | 20.8 | 35.3 | 12.2 | 82 | 30 |
| 15 | 14.46 | 20.55 | 29.94 | 50.4 | 7.8 | 35.6 | 48.1 | 26.4 | 240 | 26 |
| 16 | 41.42 | 35.67 | 73.36 | 70.4 | 10.1 | 34.0 | 52.6 | 22.0 | 349 | 11 |
| 17 | 43.48 | 65.64 | 37.18 | 78.5 | 8.7 | 42.9 | 64.3 | 28.7 | 180 | 20 |
| 18 | 20.85 | 23.74 | 27.78 | 43.3 | 20.7 | 5.8 | 16.7 | 2.0 | 214 | 43 |
| 19 | 2.43 | 1.43 | 4.70 | 28.5 | 14.8 | 37.2 | 77.9 | 17.7 | 348 | 23 |
| 20 | 65.68 | 77.71 | 13.50 | 86.7 | 12.3 | 63.2 | 90.1 | 44.4 | 100 | 1 |
| 21 | 9.80 | 18.41 | 5.38 | 52.9 | 10.5 | 44.1 | 54.1 | 36.0 | 190 | 13 |
| 22 | 28.49 | 58.18 | 12.21 | 82.5 | 13.7 | 60.6 | 76.5 | 48.0 | 191 | 10 |
| 23 | 18.42 | 9.72 | 88.09 | 54.8 | 11.9 | 69.2 | 84.2 | 56.9 | 304 | 6 |
| 24 | 68.94 | 74.21 | 80.11 | 90.2 | 7.5 | 1.1 | 1.7 | 0.8 | | |
| 25 | 4.20 | 7.22 | 1.54 | 44.3 | 8.9 | 47.9 | 56.5 | 40.7 | 192 | 13 |
| 26 | 26.04 | 31.53 | 9.69 | 54.3 | 12.1 | 30.8 | 43.3 | 21.9 | 133 | 21 |
| 27 | 44.61 | 65.40 | 97.36 | 83.8 | 12.1 | 40.6 | 88.1 | 18.7 | 283 | 21 |
| 28 | 26.00 | 25.80 | 90.60 | 59.0 | 9.0 | 42.0 | 70.1 | 25.2 | 300 | 13 |
| 29 | 63.22 | 45.35 | 92.29 | 72.3 | 12.7 | 45.5 | 67.1 | 30.9 | 385 | 25 |
| 30 | 1.70 | 2.43 | 3.35 | 22.1 | 9.2 | 31.8 | 69.9 | 14.4 | 213 | 16 |
| 31 | 11.41 | 7.77 | 3.62 | 44.9 | 4.9 | 45.0 | 52.2 | 38.7 | 11 | 18 |
| 32 | 33.09 | 60.19 | 36.81 | 79.0 | 12.2 | 46.8 | 65.0 | 33.7 | 189 | 19 |
| 33 | 5.28 | 3.96 | 0.81 | 32.9 | 9.3 | 45.4 | 59.2 | 34.8 | 22 | 25 |
| 34 | 51.54 | 40.06 | 31.41 | 72.3 | 8.6 | 38.1 | 62.2 | 23.3 | 9 | 24 |
| 35 | 38.87 | 63.53 | 12.56 | 78.7 | 8.8 | 50.2 | 67.4 | 37.4 | 184 | 17 |
| 36 | 1.41 | 1.21 | 0.64 | 10.5 | 6.8 | 7.1 | 32.4 | 1.6 | 7 | 30 |
| 37 | 59.19 | 56.45 | 34.23 | 70.4 | 9.2 | 29.5 | 40.0 | 21.7 | 62 | 23 |
| 38 | 39.28 | 21.82 | 4.06 | 72.8 | 15.8 | 71.3 | 88.3 | 57.5 | 5 | 9 |
| 39 | 6.85 | 4.42 | 27.27 | 44.0 | 10.3 | 60.3 | 78.7 | 46.2 | 301 | 5 |
| 40 | 47.23 | 38.14 | 6.75 | 67.0 | 8.8 | 51.5 | 63.5 | 41.7 | 62 | 15 |

# A4.14 Filter0-10

| No. | $X_{L10}$ | $Y_{L10}$ (cd/m$^2$) | $Z_{L10}$ | Lightness | | Colourfulness | | | Hue | |
|---|---|---|---|---|---|---|---|---|---|---|
| | | | | Avg | Stdev | Avg | Max | Min | Avg | Stdev |
| Reference White | 91.43 | 96.24 | 108.3 | | | | | | | |
| Back-ground | 18.03 | 19.03 | 21.65 | | | | | | | |
| 1 | 6.08 | 8.35 | 11.70 | 50.4 | 5.8 | 41.4 | 50.3 | 34.0 | 225 | 15 |
| 2 | 62.67 | 79.66 | 106.5 | 87.5 | 8.4 | 23.3 | 50.2 | 10.9 | 275 | 35 |
| 3 | 42.73 | 44.22 | 73.47 | 61.7 | 11.7 | 29.8 | 44.8 | 19.8 | 338 | 11 |
| 4 | 3.69 | 4.55 | 8.20 | 34.3 | 11.2 | 34.4 | 55.2 | 21.4 | 241 | 29 |
| 5 | 58.88 | 35.59 | 99.18 | 79.8 | 12.4 | 59.2 | 85.1 | 41.2 | 379 | 19 |
| 6 | 2.70 | 2.59 | 10.62 | 32.5 | 16.0 | 45.0 | 64.5 | 31.3 | 298 | 6 |
| 7 | 24.04 | 33.83 | 35.16 | 63.3 | 11.5 | 40.1 | 49.2 | 32.7 | 194 | 21 |
| 8 | 31.14 | 20.39 | 97.47 | 62.1 | 11.2 | 52.1 | 79.1 | 34.3 | 346 | 16 |
| 9 | 46.06 | 26.99 | 31.79 | 76.7 | 15.7 | 55.6 | 88.0 | 35.1 | 389 | 14 |
| 10 | 11.27 | 13.03 | 11.06 | 44.0 | 12.7 | 31.0 | 37.7 | 25.4 | 193 | 18 |
| 11 | 10.73 | 17.33 | 11.81 | 46.7 | 9.1 | 41.5 | 49.4 | 34.9 | 200 | 14 |
| 12 | 90.71 | 95.07 | 108.2 | 102.7 | 4.8 | 1.0 | 1.0 | 1.0 | | |
| 13 | 18.20 | 11.73 | 30.34 | 48.2 | 8.3 | 50.8 | 61.4 | 42.1 | 361 | 14 |
| 14 | 58.44 | 58.61 | 48.39 | 71.8 | 9.0 | 19.5 | 33.9 | 11.2 | 70 | 25 |
| 15 | 16.52 | 22.92 | 32.24 | 51.0 | 6.7 | 38.9 | 51.7 | 29.2 | 251 | 16 |
| 16 | 45.33 | 41.30 | 80.06 | 71.3 | 10.5 | 35.1 | 51.6 | 23.8 | 348 | 16 |
| 17 | 49.71 | 70.94 | 39.23 | 78.3 | 9.1 | 40.2 | 61.2 | 26.4 | 188 | 16 |
| 18 | 23.11 | 26.27 | 29.98 | 45.0 | 18.2 | 8.4 | 22.6 | 3.1 | 228 | 29 |
| 19 | 2.36 | 1.48 | 4.87 | 33.3 | 15.3 | 46.7 | 87.0 | 25.1 | 350 | 21 |
| 20 | 72.22 | 82.77 | 13.56 | 85.3 | 10.0 | 63.6 | 87.9 | 46.0 | 101 | 3 |
| 21 | 11.30 | 19.40 | 5.09 | 48.8 | 5.7 | 51.0 | 66.9 | 38.8 | 196 | 11 |
| 22 | 33.60 | 61.44 | 11.43 | 76.2 | 11.7 | 54.4 | 72.6 | 40.7 | 190 | 12 |
| 23 | 20.26 | 14.44 | 96.52 | 58.2 | 14.0 | 63.7 | 87.9 | 46.1 | 303 | 5 |
| 24 | 75.95 | 82.05 | 86.77 | 86.0 | 11.9 | 1.4 | 2.9 | 0.6 | | |
| 25 | 4.61 | 7.41 | 1.19 | 45.0 | 12.4 | 50.8 | 65.6 | 39.3 | 192 | 13 |
| 26 | 28.58 | 33.47 | 9.84 | 58.3 | 10.1 | 34.8 | 46.4 | 26.1 | 119 | 20 |
| 27 | 51.88 | 73.78 | 105.9 | 82.5 | 8.1 | 42.7 | 77.7 | 23.4 | 289 | 18 |
| 28 | 29.44 | 31.58 | 99.26 | 62.5 | 9.2 | 42.7 | 62.5 | 29.2 | 301 | 9 |
| 29 | 68.09 | 52.69 | 101.4 | 71.8 | 10.0 | 48.9 | 72.8 | 32.9 | 388 | 19 |
| 30 | 1.71 | 2.45 | 3.29 | 25.7 | 12.3 | 35.3 | 66.6 | 18.7 | 213 | 19 |
| 31 | 11.81 | 8.20 | 3.72 | 47.6 | 6.4 | 48.5 | 55.8 | 42.2 | 14 | 12 |
| 32 | 38.87 | 65.06 | 38.68 | 79.7 | 9.7 | 43.3 | 60.7 | 30.9 | 191 | 16 |
| 33 | 5.35 | 3.98 | 0.57 | 37.2 | 10.7 | 44.4 | 55.2 | 35.7 | 37 | 27 |
| 34 | 55.12 | 44.05 | 34.37 | 70.8 | 9.0 | 34.2 | 58.9 | 19.8 | 6 | 28 |
| 35 | 44.38 | 67.32 | 11.98 | 79.1 | 10.0 | 55.2 | 71.7 | 42.5 | 185 | 18 |
| 36 | 1.27 | 1.03 | 0.36 | 16.7 | 9.2 | 15.6 | 68.6 | 3.6 | 31 | 30 |
| 37 | 64.49 | 61.74 | 37.07 | 73.3 | 9.1 | 27.1 | 43.4 | 17.0 | 61 | 19 |
| 38 | 40.77 | 23.43 | 4.58 | 73.0 | 17.1 | 73.9 | 93.1 | 58.7 | 3 | 11 |
| 39 | 7.38 | 5.79 | 29.71 | 49.0 | 9.5 | 62.2 | 76.7 | 50.5 | 304 | 6 |
| 40 | 49.80 | 40.47 | 7.11 | 68.2 | 9.2 | 56.0 | 70.9 | 44.2 | 61 | 15 |

# A4.15 Filter1-02

| No. | $X_L$ | $Y_L$ (cd/m$^2$) | $Z_L$ | Lightness | | Colourfulness | | | Hue | |
|---|---|---|---|---|---|---|---|---|---|---|
| | | | | Avg | Stdev | Avg | Max | Min | Avg | Stdev |
| Reference White | 8.436 | 8.856 | 9.929 | | | | | | | |
| Back-ground | 1.643 | 1.726 | 1.989 | | | | | | | |
| 1 | 0.580 | 0.803 | 1.121 | 37.3 | 9.0 | 38.9 | 54.5 | 27.8 | 213 | 20 |
| 2 | 5.460 | 7.058 | 9.569 | 85.9 | 12.4 | 27.0 | 49.8 | 14.7 | 288 | 17 |
| 3 | 3.826 | 3.873 | 6.593 | 54.5 | 18.4 | 19.5 | 43.6 | 8.8 | 318 | 19 |
| 4 | 0.385 | 0.460 | 0.799 | 23.8 | 11.2 | 31.1 | 58.4 | 16.6 | 222 | 22 |
| 5 | 5.460 | 2.877 | 8.741 | 75.4 | 12.6 | 66.3 | 86.6 | 50.8 | 383 | 19 |
| 6 | 0.292 | 0.265 | 1.020 | 15.4 | 8.3 | 20.0 | 50.5 | 7.9 | 298 | 6 |
| 7 | 2.116 | 3.077 | 3.223 | 57.7 | 14.1 | 29.9 | 45.2 | 19.8 | 220 | 26 |
| 8 | 2.824 | 1.506 | 8.646 | 56.8 | 12.9 | 59.1 | 72.4 | 48.3 | 343 | 12 |
| 9 | 4.342 | 2.369 | 2.798 | 68.9 | 14.7 | 65.1 | 81.0 | 52.2 | 392 | 14 |
| 10 | 1.051 | 1.225 | 1.072 | 36.2 | 7.7 | 27.4 | 41.8 | 18.0 | 195 | 15 |
| 11 | 0.969 | 1.638 | 1.169 | 40.8 | 10.4 | 34.4 | 56.7 | 20.9 | 200 | 8 |
| 12 | 4.961 | 5.136 | 6.618 | 67.1 | 20.8 | 2.0 | 6.4 | 0.6 | | |
| 13 | 1.683 | 0.986 | 2.682 | 48.5 | 7.7 | 48.7 | 69.2 | 34.3 | 370 | 14 |
| 14 | 5.275 | 5.253 | 4.353 | 65.4 | 12.5 | 19.1 | 38.0 | 9.6 | 58 | 25 |
| 15 | 1.470 | 2.086 | 2.947 | 45.8 | 10.2 | 34.0 | 52.0 | 22.2 | 245 | 21 |
| 16 | 4.064 | 3.512 | 7.162 | 54.0 | 16.1 | 27.8 | 47.8 | 16.2 | 333 | 27 |
| 17 | 4.313 | 6.506 | 3.661 | 80.8 | 12.4 | 39.9 | 67.0 | 23.7 | 181 | 21 |
| 18 | 2.089 | 2.392 | 2.742 | 40.0 | 17.1 | 5.4 | 20.6 | 1.4 | 217 | 25 |
| 19 | 0.278 | 0.187 | 0.511 | 14.8 | 7.9 | 19.0 | 52.7 | 6.8 | 353 | 27 |
| 20 | 6.492 | 7.669 | 1.349 | 77.5 | 15.9 | 57.8 | 88.8 | 37.6 | 100 | 0 |
| 21 | 1.016 | 1.861 | 0.588 | 43.8 | 9.6 | 38.3 | 58.2 | 25.2 | 192 | 17 |
| 22 | 2.883 | 5.824 | 1.269 | 78.5 | 13.4 | 60.8 | 83.9 | 44.0 | 184 | 18 |
| 23 | 1.831 | 0.994 | 8.603 | 52.2 | 21.6 | 67.0 | 84.7 | 53.0 | 304 | 6 |
| 24 | 6.799 | 7.324 | 7.830 | 89.1 | 13.4 | 1.1 | 1.5 | 0.8 | | |
| 25 | 0.461 | 0.755 | 0.205 | 39.7 | 7.8 | 45.0 | 66.4 | 30.4 | 191 | 17 |
| 26 | 2.599 | 3.155 | 0.987 | 52.2 | 9.9 | 32.9 | 49.7 | 21.7 | 141 | 22 |
| 27 | 4.453 | 6.518 | 9.541 | 77.5 | 14.7 | 41.6 | 76.0 | 22.8 | 284 | 19 |
| 28 | 2.607 | 2.592 | 8.931 | 68.3 | 15.4 | 53.2 | 73.9 | 38.3 | 302 | 9 |
| 29 | 6.231 | 4.468 | 8.962 | 64.8 | 13.0 | 46.3 | 64.1 | 33.5 | 385 | 24 |
| 30 | 0.213 | 0.287 | 0.384 | 17.3 | 8.1 | 23.4 | 61.3 | 8.9 | 212 | 17 |
| 31 | 1.138 | 0.788 | 0.400 | 44.2 | 8.6 | 41.3 | 61.1 | 28.0 | 15 | 20 |
| 32 | 3.323 | 6.007 | 3.630 | 73.1 | 17.9 | 39.9 | 65.8 | 24.2 | 195 | 19 |
| 33 | 0.552 | 0.429 | 0.129 | 29.2 | 7.9 | 39.8 | 64.9 | 24.5 | 22 | 25 |
| 34 | 5.100 | 3.968 | 3.078 | 66.2 | 13.1 | 40.4 | 56.0 | 29.2 | 14 | 31 |
| 35 | 3.873 | 6.318 | 1.294 | 76.6 | 9.9 | 55.3 | 80.4 | 38.0 | 182 | 19 |
| 36 | 0.185 | 0.170 | 0.119 | 9.3 | 6.8 | 6.2 | 29.7 | 1.3 | 9 | 39 |
| 37 | 5.833 | 5.553 | 3.308 | 70.9 | 12.7 | 33.5 | 50.5 | 22.2 | 64 | 14 |
| 38 | 3.889 | 2.158 | 0.425 | 69.2 | 19.3 | 71.7 | 95.0 | 54.1 | 5 | 11 |
| 39 | 0.704 | 0.471 | 2.694 | 29.8 | 10.9 | 47.8 | 73.5 | 31.1 | 301 | 3 |
| 40 | 4.670 | 3.760 | 0.690 | 64.0 | 6.3 | 53.3 | 69.7 | 40.8 | 60 | 15 |

# A4.16 Filter1-10

| No. | $X_{L10}$ | $Y_{L10}$ (cd/m$^2$) | $Z_{L10}$ | Lightness | | Colourfulness | | | Hue | |
|---|---|---|---|---|---|---|---|---|---|---|
| | | | | Avg | Stdev | Avg | Max | Min | Avg | Stdev |
| Reference White | 9.237 | 9.683 | 10.70 | | | | | | | |
| Back-ground | 1.748 | 1.836 | 2.092 | | | | | | | |
| 1 | 0.662 | 0.887 | 1.206 | 41.1 | 6.5 | 39.8 | 53.3 | 29.7 | 224 | 17 |
| 2 | 6.167 | 7.792 | 10.31 | 84.2 | 11.4 | 21.2 | 49.6 | 9.0 | 286 | 19 |
| 3 | 4.209 | 4.338 | 7.149 | 63.3 | 14.8 | 19.0 | 41.5 | 8.7 | 319 | 29 |
| 4 | 0.432 | 0.515 | 0.863 | 28.3 | 12.3 | 32.9 | 51.9 | 20.9 | 228 | 25 |
| 5 | 5.637 | 3.230 | 9.304 | 76.1 | 12.9 | 66.0 | 85.1 | 51.2 | 377 | 20 |
| 6 | 0.326 | 0.324 | 1.111 | 22.5 | 7.9 | 28.5 | 53.0 | 15.3 | 295 | 14 |
| 7 | 2.417 | 3.353 | 3.448 | 63.3 | 9.1 | 35.3 | 58.4 | 21.4 | 216 | 19 |
| 8 | 2.962 | 1.817 | 9.205 | 63.3 | 15.4 | 60.2 | 77.4 | 46.9 | 341 | 13 |
| 9 | 4.441 | 2.523 | 2.971 | 69.2 | 14.8 | 66.8 | 88.3 | 50.6 | 393 | 16 |
| 10 | 1.124 | 1.293 | 1.120 | 39.5 | 10.5 | 20.4 | 37.2 | 11.2 | 205 | 15 |
| 11 | 1.125 | 1.759 | 1.232 | 48.8 | 10.5 | 36.6 | 49.5 | 27.0 | 201 | 8 |
| 12 | 5.437 | 5.654 | 7.146 | 72.7 | 15.8 | 1.3 | 2.4 | 0.7 | | |
| 13 | 1.773 | 1.153 | 2.932 | 53.8 | 10.5 | 54.8 | 63.7 | 47.2 | 365 | 15 |
| 14 | 5.716 | 5.673 | 4.661 | 68.9 | 14.0 | 21.4 | 39.5 | 11.6 | 52 | 27 |
| 15 | 1.684 | 2.308 | 3.172 | 51.9 | 7.2 | 34.5 | 46.4 | 25.6 | 245 | 25 |
| 16 | 4.412 | 3.990 | 7.792 | 65.0 | 13.5 | 28.3 | 50.6 | 15.8 | 337 | 15 |
| 17 | 4.903 | 6.942 | 3.832 | 77.8 | 10.6 | 35.1 | 66.3 | 18.6 | 182 | 21 |
| 18 | 2.239 | 2.544 | 2.881 | 49.1 | 11.8 | 7.1 | 22.5 | 2.2 | 221 | 20 |
| 19 | 0.296 | 0.218 | 0.557 | 15.4 | 7.2 | 20.3 | 50.9 | 8.1 | 350 | 21 |
| 20 | 7.093 | 8.046 | 1.293 | 74.8 | 13.9 | 64.4 | 85.2 | 48.7 | 101 | 3 |
| 21 | 1.185 | 1.962 | 0.588 | 52.9 | 7.8 | 38.7 | 63.0 | 23.7 | 190 | 13 |
| 22 | 3.411 | 6.119 | 1.210 | 79.8 | 12.3 | 62.4 | 91.3 | 42.7 | 183 | 20 |
| 23 | 2.016 | 1.434 | 9.434 | 60.3 | 20.0 | 71.6 | 90.2 | 56.8 | 301 | 7 |
| 24 | 7.460 | 7.989 | 8.422 | 91.5 | 9.9 | 1.1 | 1.3 | 0.9 | | |
| 25 | 0.528 | 0.795 | 0.203 | 47.1 | 12.1 | 45.8 | 60.0 | 35.0 | 190 | 15 |
| 26 | 2.772 | 3.272 | 0.999 | 56.4 | 8.8 | 34.5 | 46.7 | 25.4 | 131 | 25 |
| 27 | 5.137 | 7.227 | 10.290 | 75.0 | 10.9 | 44.4 | 78.2 | 25.3 | 286 | 13 |
| 28 | 2.937 | 3.112 | 9.745 | 67.0 | 14.8 | 54.8 | 77.8 | 38.5 | 297 | 5 |
| 29 | 6.636 | 5.071 | 9.773 | 67.8 | 11.8 | 49.6 | 76.9 | 31.9 | 376 | 20 |
| 30 | 0.241 | 0.316 | 0.413 | 18.8 | 6.5 | 25.6 | 55.6 | 11.8 | 218 | 20 |
| 31 | 1.189 | 0.839 | 0.429 | 47.8 | 10.7 | 42.2 | 58.7 | 30.4 | 14 | 18 |
| 32 | 3.893 | 6.421 | 3.799 | 73.3 | 11.1 | 42.1 | 70.9 | 25.0 | 195 | 20 |
| 33 | 0.572 | 0.445 | 0.134 | 31.7 | 8.4 | 41.2 | 57.5 | 29.5 | 24 | 23 |
| 34 | 5.393 | 4.276 | 3.312 | 68.8 | 10.9 | 40.6 | 64.3 | 25.7 | 13 | 22 |
| 35 | 4.239 | 6.532 | 1.256 | 74.3 | 11.9 | 55.8 | 78.2 | 39.9 | 179 | 22 |
| 36 | 0.198 | 0.182 | 0.128 | 10.4 | 6.2 | 6.9 | 34.6 | 1.4 | 7 | 31 |
| 37 | 6.269 | 5.936 | 3.515 | 68.1 | 9.3 | 33.1 | 50.9 | 21.5 | 55 | 22 |
| 38 | 3.992 | 2.268 | 0.453 | 69.3 | 16.5 | 74.8 | 99.3 | 56.3 | 6 | 9 |
| 39 | 0.773 | 0.615 | 2.948 | 32.9 | 11.6 | 55.4 | 76.8 | 40.0 | 301 | 3 |
| 40 | 4.835 | 3.887 | 0.692 | 67.5 | 10.7 | 55.6 | 78.2 | 39.6 | 56 | 14 |

# A4.17 Filter2-02

| No. | $X_L$ | $Y_L$ (cd/m$^2$) | $Z_L$ | Lightness | | Colourfulness | | | Hue | |
|---|---|---|---|---|---|---|---|---|---|---|
| | | | | Avg | Stdev | Avg | Max | Min | Avg | Stdev |
| Reference White | 0.968 | 1.010 | 1.164 | | | | | | | |
| Back-ground | 0.202 | 0.211 | 0.248 | | | | | | | |
| 1 | 0.079 | 0.105 | 0.136 | 30.0 | 8.2 | 32.3 | 52.8 | 19.8 | 221 | 21 |
| 2 | 0.629 | 0.809 | 1.116 | 79.7 | 14.4 | 24.9 | 52.8 | 11.8 | 279 | 17 |
| 3 | 0.444 | 0.449 | 0.769 | 64.3 | 10.8 | 19.2 | 34.1 | 10.9 | 326 | 7 |
| 4 | 0.055 | 0.065 | 0.100 | 18.2 | 10.5 | 11.2 | 49.3 | 2.5 | 286 | 21 |
| 5 | 0.614 | 0.325 | 1.010 | 58.7 | 11.7 | 48.2 | 71.5 | 32.5 | 370 | 18 |
| 6 | 0.037 | 0.037 | 0.124 | 22.5 | 11.5 | 26.5 | 55.1 | 12.7 | 297 | 9 |
| 7 | 0.256 | 0.366 | 0.384 | 52.1 | 9.7 | 27.2 | 45.3 | 16.3 | 229 | 21 |
| 8 | 0.329 | 0.179 | 1.009 | 49.2 | 9.0 | 45.4 | 63.7 | 32.3 | 344 | 15 |
| 9 | 0.482 | 0.269 | 0.322 | 54.6 | 7.0 | 46.0 | 65.7 | 32.2 | 384 | 9 |
| 10 | 0.133 | 0.153 | 0.129 | 37.0 | 10.2 | 14.6 | 46.3 | 4.6 | 189 | 14 |
| 11 | 0.121 | 0.200 | 0.140 | 37.8 | 16.2 | 25.7 | 45.6 | 14.5 | 205 | 9 |
| 12 | 0.759 | 0.714 | 0.856 | 73.9 | 14.4 | 21.9 | 34.9 | 13.7 | 12 | 43 |
| 13 | 0.205 | 0.124 | 0.323 | 39.0 | 10.7 | 37.2 | 52.1 | 26.6 | 360 | 15 |
| 14 | 0.615 | 0.618 | 0.507 | 70.5 | 15.5 | 17.6 | 33.0 | 9.4 | 53 | 33 |
| 15 | 0.179 | 0.247 | 0.353 | 45.0 | 10.5 | 27.8 | 41.2 | 18.8 | 229 | 21 |
| 16 | 0.473 | 0.413 | 0.841 | 58.5 | 17.2 | 24.1 | 39.4 | 14.8 | 347 | 18 |
| 17 | 0.501 | 0.750 | 0.430 | 77.7 | 9.9 | 28.2 | 47.2 | 16.9 | 193 | 30 |
| 18 | 0.250 | 0.284 | 0.324 | 43.0 | 14.8 | 5.9 | 22.9 | 1.5 | 214 | 21 |
| 19 | 0.043 | 0.030 | 0.062 | 10.7 | 6.7 | 7.8 | 44.5 | 1.4 | 348 | 33 |
| 20 | 0.739 | 0.880 | 0.146 | 80.5 | 12.8 | 37.7 | 58.7 | 24.2 | 101 | 6 |
| 21 | 0.129 | 0.227 | 0.070 | 47.7 | 9.3 | 31.2 | 52.4 | 18.6 | 190 | 14 |
| 22 | 0.334 | 0.669 | 0.148 | 72.3 | 6.5 | 40.6 | 59.4 | 27.7 | 183 | 19 |
| 23 | 0.213 | 0.118 | 1.013 | 42.4 | 11.3 | 55.3 | 71.7 | 42.6 | 306 | 11 |
| 24 | 0.785 | 0.846 | 0.913 | 93.8 | 5.9 | 1.7 | 4.7 | 0.6 | 97 | 6 |
| 25 | 0.066 | 0.101 | 0.025 | 35.4 | 9.8 | 32.3 | 49.0 | 21.2 | 198 | 30 |
| 26 | 0.303 | 0.368 | 0.113 | 54.8 | 10.7 | 26.7 | 40.2 | 17.7 | 144 | 20 |
| 27 | 0.522 | 0.748 | 1.119 | 78.4 | 7.8 | 30.9 | 55.8 | 17.1 | 281 | 21 |
| 28 | 0.302 | 0.301 | 1.036 | 52.0 | 9.8 | 41.6 | 59.6 | 29.1 | 302 | 16 |
| 29 | 0.711 | 0.517 | 1.051 | 67.8 | 6.5 | 41.6 | 60.1 | 28.8 | 373 | 18 |
| 30 | 0.033 | 0.043 | 0.047 | 10.5 | 5.8 | 9.9 | 46.4 | 2.1 | 277 | 44 |
| 31 | 0.141 | 0.103 | 0.045 | 41.5 | 9.0 | 42.6 | 53.4 | 34.1 | 11 | 18 |
| 32 | 0.389 | 0.692 | 0.431 | 70.3 | 10.2 | 39.5 | 57.0 | 27.4 | 210 | 26 |
| 33 | 0.075 | 0.061 | 0.015 | 28.9 | 7.0 | 42.0 | 58.7 | 30.0 | 399 | 32 |
| 34 | 0.576 | 0.458 | 0.355 | 64.7 | 8.5 | 29.3 | 49.4 | 17.4 | 11 | 33 |
| 35 | 0.451 | 0.730 | 0.146 | 77.1 | 10.2 | 41.3 | 55.3 | 30.9 | 180 | 20 |
| 36 | 0.032 | 0.029 | 0.015 | 5.2 | 5.0 | 2.8 | 12.6 | 0.6 | | |
| 37 | 0.668 | 0.644 | 0.385 | 67.5 | 11.5 | 28.3 | 44.5 | 18.0 | 47 | 23 |
| 38 | 0.428 | 0.246 | 0.035 | 52.1 | 13.2 | 49.7 | 74.5 | 33.2 | 5 | 9 |
| 39 | 0.093 | 0.065 | 0.323 | 29.5 | 11.4 | 37.6 | 54.5 | 26.0 | 306 | 8 |
| 40 | 0.521 | 0.434 | 0.066 | 59.5 | 10.7 | 42.0 | 56.3 | 31.3 | 55 | 12 |

# A4.18 Filter2-10

| No. | $X_{L10}$ | $Y_{L10}$ (cd/m$^2$) | $Z_{L10}$ | Lightness | | Colourfulness | | | Hue | |
|---|---|---|---|---|---|---|---|---|---|---|
| | | | | Avg | Stdev | Avg | Max | Min | Avg | Stdev |
| Reference White | 1.057 | 1.099 | 1.254 | | | | | | | |
| Back-ground | 0.221 | 0.229 | 0.269 | | | | | | | |
| 1 | 0.089 | 0.115 | 0.146 | 32.7 | 11.0 | 32.8 | 50.1 | 21.4 | 216 | 21 |
| 2 | 0.710 | 0.887 | 1.199 | 85.0 | 16.4 | 30.0 | 65.3 | 13.8 | 275 | 34 |
| 3 | 0.487 | 0.499 | 0.831 | 67.9 | 12.0 | 25.8 | 50.5 | 13.2 | 320 | 17 |
| 4 | 0.062 | 0.071 | 0.107 | 15.7 | 9.9 | 8.9 | 40.0 | 2.0 | 253 | 52 |
| 5 | 0.641 | 0.382 | 1.104 | 68.5 | 22.3 | 54.4 | 72.1 | 41.1 | 375 | 15 |
| 6 | 0.042 | 0.043 | 0.134 | 21.9 | 11.4 | 29.2 | 54.9 | 15.5 | 298 | 7 |
| 7 | 0.291 | 0.395 | 0.409 | 52.9 | 15.1 | 32.3 | 57.7 | 18.1 | 221 | 17 |
| 8 | 0.352 | 0.230 | 1.100 | 60.0 | 21.1 | 51.9 | 77.8 | 34.7 | 348 | 13 |
| 9 | 0.496 | 0.292 | 0.353 | 51.1 | 12.3 | 51.9 | 70.1 | 38.4 | 386 | 15 |
| 10 | 0.146 | 0.164 | 0.138 | 32.9 | 15.2 | 17.0 | 34.7 | 8.3 | 188 | 32 |
| 11 | 0.140 | 0.213 | 0.147 | 39.1 | 17.0 | 26.7 | 40.2 | 17.7 | 199 | 20 |
| 12 | 0.820 | 0.778 | 0.924 | 78.0 | 11.3 | 24.0 | 48.8 | 11.8 | 395 | 35 |
| 13 | 0.215 | 0.143 | 0.351 | 41.4 | 9.5 | 43.0 | 64.1 | 28.9 | 360 | 18 |
| 14 | 0.664 | 0.660 | 0.544 | 75.0 | 12.8 | 20.4 | 42.8 | 9.7 | 63 | 28 |
| 15 | 0.204 | 0.271 | 0.379 | 49.1 | 10.9 | 31.4 | 47.4 | 20.7 | 221 | 19 |
| 16 | 0.512 | 0.465 | 0.911 | 63.6 | 13.6 | 33.5 | 51.2 | 21.9 | 341 | 18 |
| 17 | 0.569 | 0.795 | 0.450 | 82.3 | 15.9 | 31.9 | 58.8 | 17.3 | 183 | 28 |
| 18 | 0.275 | 0.307 | 0.348 | 40.6 | 21.5 | 11.4 | 23.1 | 5.6 | 202 | 31 |
| 19 | 0.046 | 0.034 | 0.067 | 11.8 | 9.6 | 11.5 | 61.9 | 2.1 | 371 | 34 |
| 20 | 0.805 | 0.915 | 0.140 | 75.7 | 10.2 | 52.4 | 73.1 | 37.6 | 99 | 3 |
| 21 | 0.149 | 0.237 | 0.070 | 46.4 | 11.9 | 38.6 | 60.7 | 24.6 | 192 | 15 |
| 22 | 0.396 | 0.698 | 0.142 | 79.1 | 18.4 | 55.4 | 77.5 | 39.6 | 189 | 17 |
| 23 | 0.234 | 0.167 | 1.106 | 57.0 | 21.4 | 66.4 | 85.8 | 51.3 | 305 | 8 |
| 24 | 0.859 | 0.915 | 0.980 | 95.6 | 9.1 | 1.5 | 2.9 | 0.7 | | |
| 25 | 0.075 | 0.105 | 0.025 | 31.5 | 13.4 | 42.4 | 64.2 | 28.0 | 186 | 19 |
| 26 | 0.333 | 0.386 | 0.116 | 48.9 | 17.1 | 28.4 | 40.4 | 20.0 | 138 | 26 |
| 27 | 0.600 | 0.823 | 1.204 | 84.2 | 19.1 | 40.2 | 76.0 | 21.3 | 260 | 42 |
| 28 | 0.340 | 0.357 | 1.126 | 55.8 | 11.9 | 46.0 | 70.6 | 29.9 | 300 | 15 |
| 29 | 0.757 | 0.582 | 1.142 | 74.5 | 9.6 | 31.1 | 55.3 | 17.5 | 375 | 19 |
| 30 | 0.037 | 0.047 | 0.050 | 9.9 | 8.2 | 6.3 | 36.6 | 1.1 | 223 | 37 |
| 31 | 0.147 | 0.109 | 0.049 | 38.2 | 11.7 | 44.0 | 63.7 | 30.5 | 12 | 16 |
| 32 | 0.455 | 0.734 | 0.451 | 80.0 | 15.2 | 42.7 | 64.7 | 28.2 | 197 | 20 |
| 33 | 0.078 | 0.063 | 0.015 | 29.0 | 12.2 | 33.7 | 73.4 | 15.5 | 12 | 18 |
| 34 | 0.608 | 0.491 | 0.381 | 65.7 | 10.2 | 31.5 | 54.1 | 18.3 | 20 | 20 |
| 35 | 0.513 | 0.761 | 0.141 | 82.1 | 18.9 | 48.9 | 69.4 | 34.4 | 179 | 22 |
| 36 | 0.034 | 0.031 | 0.015 | 7.5 | 5.8 | 4.8 | 19.0 | 1.2 | 371 | 56 |
| 37 | 0.716 | 0.683 | 0.408 | 68.2 | 10.6 | 33.1 | 51.0 | 21.5 | 46 | 23 |
| 38 | 0.436 | 0.256 | 0.037 | 55.0 | 13.2 | 62.6 | 86.9 | 45.1 | 7 | 6 |
| 39 | 0.101 | 0.082 | 0.351 | 34.1 | 8.0 | 52.0 | 70.1 | 38.5 | 304 | 8 |
| 40 | 0.547 | 0.452 | 0.067 | 65.9 | 11.4 | 40.9 | 67.3 | 24.9 | 47 | 19 |

# A4.19 Filter3-02

| No. | $X_L$ | $Y_L$ (cd/m$^2$) | $Z_L$ | Lightness | | Colourfulness | | | Hue | |
|---|---|---|---|---|---|---|---|---|---|---|
| | | | | Avg | Stdev | Avg | Max | Min | Avg | Stdev |
| Reference White | 0.0934 | 0.0972 | 0.1144 | | | | | | | |
| Back-ground | 0.0183 | 0.0193 | 0.0227 | | | | | | | |
| 1 | 0.0065 | 0.0089 | 0.0130 | 28.0 | 15.7 | 8.5 | 28.6 | 2.5 | 258 | 53 |
| 2 | 0.0616 | 0.0793 | 0.1109 | 80.3 | 12.6 | 21.2 | 43.7 | 10.3 | 280 | 31 |
| 3 | 0.0431 | 0.0431 | 0.0769 | 55.3 | 14.2 | 10.9 | 38.8 | 3.1 | 323 | 18 |
| 4 | 0.0043 | 0.0052 | 0.0094 | 13.3 | 12.7 | 3.1 | 13.0 | 0.7 | 275 | 42 |
| 5 | 0.0621 | 0.0326 | 0.1022 | 55.5 | 10.6 | 39.1 | 56.3 | 27.2 | 381 | 13 |
| 6 | 0.0033 | 0.0030 | 0.0117 | 8.0 | 7.3 | 2.4 | 5.8 | 1.0 | 300 | 0 |
| 7 | 0.0236 | 0.0342 | 0.0372 | 57.1 | 9.6 | 21.6 | 33.4 | 13.9 | 234 | 28 |
| 8 | 0.0322 | 0.0171 | 0.1000 | 44.5 | 9.1 | 26.6 | 40.5 | 17.5 | 343 | 16 |
| 9 | 0.0492 | 0.0269 | 0.0329 | 50.0 | 7.1 | 38.1 | 58.4 | 24.9 | 393 | 19 |
| 10 | 0.0116 | 0.0135 | 0.0123 | 29.5 | 14.4 | 3.6 | 12.8 | 1.0 | 204 | 11 |
| 11 | 0.0110 | 0.0183 | 0.0132 | 40.5 | 14.9 | 15.4 | 47.7 | 4.9 | 206 | 25 |
| 12 | 0.0545 | 0.0564 | 0.0742 | 74.1 | 12.2 | 4.9 | 20.1 | 1.2 | 331 | 20 |
| 13 | 0.0194 | 0.0113 | 0.0317 | 40.5 | 11.9 | 24.5 | 48.5 | 12.4 | 366 | 18 |
| 14 | 0.0597 | 0.0595 | 0.0508 | 76.8 | 8.7 | 13.7 | 28.1 | 6.7 | 38 | 49 |
| 15 | 0.0167 | 0.0234 | 0.0342 | 47.3 | 7.2 | 17.7 | 37.1 | 8.4 | 230 | 32 |
| 16 | 0.0463 | 0.0396 | 0.0838 | 63.0 | 9.9 | 16.0 | 30.4 | 8.4 | 346 | 16 |
| 17 | 0.0483 | 0.0731 | 0.0418 | 77.3 | 13.5 | 20.8 | 32.2 | 13.5 | 210 | 41 |
| 18 | 0.0233 | 0.0266 | 0.0313 | 44.3 | 15.7 | 3.1 | 10.3 | 0.9 | 207 | 16 |
| 19 | 0.0031 | 0.0021 | 0.0057 | 7.7 | 7.9 | 1.6 | 3.1 | 0.9 | | |
| 20 | 0.0735 | 0.0873 | 0.0153 | 80.2 | 13.4 | 22.3 | 39.7 | 12.5 | 104 | 11 |
| 21 | 0.0112 | 0.0208 | 0.0065 | 40.0 | 16.3 | 16.1 | 43.6 | 6.0 | 205 | 23 |
| 22 | 0.0339 | 0.0663 | 0.0120 | 76.2 | 13.6 | 26.9 | 37.3 | 19.4 | 194 | 20 |
| 23 | 0.0212 | 0.0114 | 0.1004 | 42.7 | 11.3 | 37.1 | 59.7 | 23.1 | 309 | 15 |
| 24 | 0.0769 | 0.0828 | 0.0910 | 96.7 | 6.6 | 1.4 | 3.0 | 0.7 | | |
| 25 | 0.0050 | 0.0084 | 0.0022 | 17.5 | 12.5 | 4.4 | 17.3 | 1.1 | | |
| 26 | 0.0291 | 0.0353 | 0.0112 | 54.9 | 10.7 | 14.2 | 21.0 | 9.6 | 129 | 27 |
| 27 | 0.0536 | 0.0752 | 0.1102 | 82.5 | 12.3 | 27.9 | 49.2 | 15.8 | 283 | 20 |
| 28 | 0.0303 | 0.0295 | 0.1025 | 50.6 | 11.2 | 27.0 | 36.8 | 19.9 | 300 | 11 |
| 29 | 0.0707 | 0.0505 | 0.1054 | 66.8 | 9.3 | 28.9 | 39.6 | 21.0 | 375 | 20 |
| 30 | 0.0023 | 0.0032 | 0.0043 | 7.5 | 9.3 | 1.5 | 3.4 | 0.7 | 267 | 58 |
| 31 | 0.0129 | 0.0090 | 0.0045 | 27.4 | 11.7 | 20.5 | 38.1 | 11.0 | 16 | 18 |
| 32 | 0.0399 | 0.0689 | 0.0421 | 76.3 | 11.6 | 25.6 | 44.1 | 14.8 | 231 | 48 |
| 33 | 0.0062 | 0.0049 | 0.0014 | 13.6 | 11.7 | 6.3 | 24.1 | 1.7 | 12 | 24 |
| 34 | 0.0574 | 0.0446 | 0.0360 | 59.8 | 6.8 | 26.1 | 33.5 | 20.3 | 12 | 24 |
| 35 | 0.0435 | 0.0711 | 0.0143 | 75.6 | 12.8 | 22.3 | 35.5 | 14.0 | 199 | 20 |
| 36 | 0.0020 | 0.0018 | 0.0012 | 7.6 | 10.8 | 1.5 | 3.1 | 0.7 | | |
| 37 | 0.0660 | 0.0631 | 0.0389 | 69.5 | 11.2 | 22.2 | 30.8 | 16.1 | 19 | 25 |
| 38 | 0.0436 | 0.0245 | 0.0048 | 46.9 | 7.9 | 48.1 | 69.2 | 33.4 | 8 | 12 |
| 39 | 0.0080 | 0.0053 | 0.0310 | 31.4 | 9.0 | 23.3 | 56.1 | 9.7 | 308 | 12 |
| 40 | 0.0524 | 0.0424 | 0.0078 | 59.4 | 7.6 | 32.2 | 44.2 | 23.4 | 47 | 8 |

# A4.20 Filter3-10

| No. | $X_{L10}$ | $Y_{L10}$ (cd/m$^2$) | $Z_{L10}$ | Lightness | | Colourfulness | | | Hue | |
|---|---|---|---|---|---|---|---|---|---|---|
| | | | | Avg | Stdev | Avg | Max | Min | Avg | Stdev |
| Reference White | 0.1011 | 0.1048 | 0.1240 | | | | | | | |
| Back-ground | 0.0199 | 0.0208 | 0.0246 | | | | | | | |
| 1 | 0.0074 | 0.0097 | 0.0141 | 40.5 | 8.6 | 11.5 | 40.1 | 3.3 | 241 | 47 |
| 2 | 0.0696 | 0.0865 | 0.1202 | 87.0 | 9.2 | 17.6 | 35.7 | 8.7 | 287 | 16 |
| 3 | 0.0470 | 0.0476 | 0.0837 | 61.5 | 9.4 | 17.2 | 36.8 | 8.0 | 335 | 18 |
| 4 | 0.0048 | 0.0057 | 0.0102 | 19.8 | 13.2 | 9.4 | 31.2 | 2.9 | 270 | 67 |
| 5 | 0.0636 | 0.0376 | 0.1122 | 64.5 | 9.8 | 38.4 | 55.3 | 26.7 | 387 | 24 |
| 6 | 0.0037 | 0.0036 | 0.0128 | 15.1 | 12.1 | 7.1 | 31.0 | 1.6 | 331 | 46 |
| 7 | 0.0270 | 0.0369 | 0.0401 | 61.0 | 8.1 | 21.1 | 28.5 | 15.6 | 237 | 23 |
| 8 | 0.0342 | 0.0218 | 0.1099 | 49.0 | 12.4 | 34.8 | 45.1 | 26.8 | 340 | 13 |
| 9 | 0.0492 | 0.0287 | 0.0360 | 51.0 | 7.0 | 40.7 | 56.5 | 29.3 | 4 | 18 |
| 10 | 0.0127 | 0.0144 | 0.0132 | 38.0 | 7.1 | 3.7 | 17.2 | 0.8 | 220 | 45 |
| 11 | 0.0128 | 0.0194 | 0.0140 | 39.3 | 18.0 | 16.7 | 38.1 | 7.4 | 219 | 25 |
| 12 | 0.0592 | 0.0612 | 0.0806 | 75.8 | 17.9 | 8.9 | 25.0 | 3.2 | 339 | 11 |
| 13 | 0.0200 | 0.0129 | 0.0347 | 40.5 | 7.4 | 28.2 | 42.8 | 18.6 | 357 | 16 |
| 14 | 0.0637 | 0.0633 | 0.0548 | 77.0 | 15.7 | 11.7 | 18.5 | 7.4 | 28 | 37 |
| 15 | 0.0192 | 0.0256 | 0.0371 | 50.0 | 10.0 | 20.3 | 38.8 | 10.6 | 239 | 28 |
| 16 | 0.0496 | 0.0443 | 0.0915 | 66.3 | 13.5 | 26.4 | 44.1 | 15.8 | 342 | 12 |
| 17 | 0.0549 | 0.0771 | 0.0443 | 81.5 | 12.5 | 16.1 | 30.5 | 8.5 | 201 | 33 |
| 18 | 0.0256 | 0.0287 | 0.0339 | 45.7 | 15.9 | 2.6 | 8.5 | 0.8 | 232 | 43 |
| 19 | 0.0032 | 0.0024 | 0.0063 | 6.5 | 7.8 | 3.5 | 13.2 | 0.9 | | |
| 20 | 0.0791 | 0.0903 | 0.0152 | 82.8 | 14.9 | 19.3 | 32.5 | 11.5 | 104 | 8 |
| 21 | 0.0132 | 0.0217 | 0.0066 | 38.5 | 17.0 | 17.6 | 42.1 | 7.3 | 205 | 27 |
| 22 | 0.0402 | 0.0689 | 0.0116 | 79.5 | 11.9 | 23.9 | 32.6 | 17.5 | 206 | 26 |
| 23 | 0.0235 | 0.0161 | 0.1103 | 53.8 | 11.6 | 38.4 | 56.7 | 26.0 | 310 | 11 |
| 24 | 0.0836 | 0.0890 | 0.0985 | 96.5 | 5.2 | 1.2 | 2.0 | 0.7 | | |
| 25 | 0.0057 | 0.0087 | 0.0023 | 21.2 | 12.5 | 14.6 | 37.5 | 5.7 | 233 | 45 |
| 26 | 0.0315 | 0.0368 | 0.0116 | 56.8 | 8.2 | 19.7 | 28.1 | 13.8 | 147 | 35 |
| 27 | 0.0617 | 0.0824 | 0.1195 | 82.0 | 13.4 | 28.7 | 46.8 | 17.6 | 286 | 16 |
| 28 | 0.0342 | 0.0348 | 0.1122 | 59.5 | 11.2 | 32.1 | 51.7 | 20.0 | 308 | 11 |
| 29 | 0.0739 | 0.0562 | 0.1153 | 71.0 | 9.7 | 31.7 | 46.9 | 21.5 | 376 | 22 |
| 30 | 0.0026 | 0.0035 | 0.0046 | 9.2 | 11.2 | 1.7 | 4.5 | 0.7 | 300 | 0 |
| 31 | 0.0130 | 0.0093 | 0.0048 | 27.8 | 10.0 | 24.2 | 46.5 | 12.7 | 13 | 18 |
| 32 | 0.0467 | 0.0729 | 0.0446 | 77.4 | 12.1 | 22.5 | 35.6 | 14.2 | 230 | 39 |
| 33 | 0.0063 | 0.0050 | 0.0015 | 11.4 | 9.2 | 6.4 | 20.7 | 2.0 | 10 | 32 |
| 34 | 0.0592 | 0.0472 | 0.0390 | 64.3 | 6.6 | 23.1 | 29.7 | 17.9 | 20 | 16 |
| 35 | 0.0495 | 0.0739 | 0.0141 | 77.4 | 13.4 | 20.9 | 31.3 | 13.9 | 193 | 19 |
| 36 | 0.0021 | 0.0019 | 0.0013 | 4.8 | 6.0 | 1.3 | 2.6 | 0.7 | | |
| 37 | 0.0696 | 0.0664 | 0.0417 | 71.4 | 16.5 | 19.2 | 25.6 | 14.4 | 21 | 22 |
| 38 | 0.0431 | 0.0251 | 0.0052 | 50.8 | 7.8 | 54.4 | 76.2 | 38.8 | 7 | 15 |
| 39 | 0.0088 | 0.0068 | 0.0340 | 40.9 | 8.0 | 28.2 | 54.6 | 14.6 | 306 | 11 |
| 40 | 0.0536 | 0.0436 | 0.0080 | 59.3 | 7.6 | 33.2 | 47.0 | 23.4 | 50 | 12 |